PB81-197873

Evaluation of Emissions and Control Technology for Industrial Stoker Boilers

Battelle Columbus Labs., OH

Prepared for

Industrial Environmental Research Lab.
Research Triangle Park, NC

May 81

U.S. Department of Commerce
National Technical Information Service
NTIS

PB81-157673

EPA 600/7-81-090
May 1981

EVALUATION OF EMISSIONS AND CONTROL TECHNOLOGY FOR INDUSTRIAL STOKER BOILERS

by

Robert D. Giammar, Russell H. Barnes, David R. Hopper,
Paul R. Webb, and Albert E. Weller

Battelle-Columbus Laboratories
505 King Avenue
Columbus, Ohio 43201

Contract No. 68-02-2627

EPA Project Officer: John H. Wasser

U.S. ENVIRONMENTAL PROTECTION AGENCY
Industrial Environmental Research Laboratory
Research Triangle Park, NC 27711

REPRODUCED BY:
NATIONAL TECHNICAL
INFORMATION SERVICE
U.S. DEPARTMENT OF COMMERCE
SPRINGFIELD, VA. 22161

IERL-RTP-1187

TECHNICAL REPORT DATA

(Please read Instructions on the reverse before completing)

1. REPORT NO. EPA 600/7-81-090	2.	3. RECIPIENT'S ACCESSION NO. PB81 19787 3
4. TITLE AND SUBTITLE Evaluation of Emissions and Control Technology for Industrial Stoker Boilers		5. REPORT DATE May 1981
		6. PERFORMING ORGANIZATION CODE
7. AUTHOR(S) R. D. Giammar, R. H. Barnes, D. R. Hopper, P. R. Webb, and A. E. Weller		8. PERFORMING ORGANIZATION REPORT NO.
9. PERFORMING ORGANIZATION NAME AND ADDRESS Battelle, Columbus Laboratories 505 King Avenue Columbus, Ohio 43201		10. PROGRAM ELEMENT NO. EHE624A
		11. CONTRACT/GRANT NO. 68-02-2627
12. SPONSORING AGENCY NAME AND ADDRESS EPA, Office of Research and Development Industrial Environmental Research Laboratory Research Triangle Park, NC 27711		13. TYPE OF REPORT AND PERIOD COVERED Final; 10/77-10/80
		14. SPONSORING AGENCY CODE EPA/600/13

15. SUPPLEMENTARY NOTES IERL-RTP project officer is John H. Wasser, Mail Drop 65, 919/541-2476.

16. ABSTRACT The report gives results of a three-phase program to evaluate emissions and control technology for industrial stoker boilers. In Phase I, emission characteristics were determined for a variety of coals fired in a 200-kW stoker boiler. It was observed that significant amounts of sulfur were retained in the lignite and western subbituminous coals. Fuel nitrogen conversion to NO was found to be between 10 and 20%. In addition, a limestone/coal fuel pellet was developed and found effective in capturing 80% of the fuel sulfur. Phase II focused on identifying and evaluating potential control concepts. Using an 8-MW spreader stoker boiler, it was found that improved control of combustion air (i.e., underfire and overfire air) resulted in lower excess air operation (improved efficiency), reduced particulate loading, smoke, CO and NO emissions, and no effect on SO2 levels. The limestone/coal pellet (Ca/S=7) was successfully fired, achieving 75% SO2 reduction. In Phase III, the limestone/coal fuel pellet was refined. A pellet was produced that had physical properties that could survive an industrial coal handling system. This pellet (Ca/S=3.5) was fired in the 8-MW boiler, achieving sulfur captures of 50%. The cost of this pellet would add approximately $1/million Btu to the cost of the raw high-sulfur coal.

17. KEY WORDS AND DOCUMENT ANALYSIS

a. DESCRIPTORS		b. IDENTIFIERS/OPEN ENDED TERMS	c. COSATI Field/Group	
Pollution	Polycyclic Compounds	Pollution Control	13B	07C
Boilers	Organic Compounds	Stationary Sources	13A	
Combustion	Limestone	Criteria Pollutants	21B	08G
Efficiency	Coal	POM	14G	
Flue Gases	Pelleting	Limestone/Coal Pellets		07A
Stokers		Treated Coals		

18. DISTRIBUTION STATEMENT Release to Public	19. SECURITY CLASS (This Report) Unclassified	21. NO. OF PAGES
	20. SECURITY CLASS (This page) Unclassified	22. PRICE

EPA Form 2220-1 (9-73)

DISCLAIMER

This report has been reviewed by the Industrial Environmental Research Laboratory (RTP), U.S. Environmental Protection Agency, and approved for publication. Approval does not signify that the contents necessarily reflect the views and policies of the Agency, nor does mention of trade names or commercial products constitute endorsement or recommendation for use.

FOREWORD

The coal-fired stoker boiler provides an option for industry to meet its energy needs. This option has not been exercised by a significant number of industries primarily because oil- and gas-fired equipment have been, and still are, more environmentally and economically attractive. However, with the dwindling supplies of oil and gas, the rising costs of these fuels, and increased attention given to coal utilization, industry once again is considering the coal-fired stoker boiler.

In support of our nation's commitments to maintain a clean environment and to utilize coal, EPA funded a research and development program to identify and demonstrate improvements in stoker-coal firing that can provide an incentive for greater industrial use of coal. The overall objectives of this program were to

- Characterize the spectrum of emissions from industrial coal-fired stoker boilers using several types of coal under various stoker-firing conditions
- Investigate control methods to reduce these emissions
- Determine the effect of these control methods and variations in stoker-boiler operation on the overall performance of the stoker boiler, and,
- Assess the environmental impact of new technology on the future acceptability of stoker boilers.

This program was divided into three phases. In Phase I, Alternative Fuels Evaluation, emission characteristics were determined for a variety of coals fired in a 200-kW stoker boiler. Emphasis was focused on identifying coals with low pollutant potential, including both physically and chemically treated coals. In Phase II, Control

Technology Evaluation, potential concepts for control of emissions for full-scale industrial stokers were evaluated. In Phase III, Limestone/Coal Pellet Development, a limestone/coal fuel pellet was developed and evaluated as a viable SO_2 control for industrial stoker boilers.

This report presents the results of the three phases of work. The report is organized into the following three parts corresponding to the three phases of work:

Phase I.	Alternative Fuels Evaluation
Phase II.	Control Technology Evaluation
Phase III.	Limestone/Coal Pellet Development

These parts actually represent separate reports but are included under one cover.

ACKNOWLEDGMENT

The research covered in this report was pursuant to Contract No. 68-02-2627 with the U.S. Environmental Protection Agency, Combustion Research Section. The authors wish to express their appreciation for the assistance and direction given the program by project monitor John H. Wasser.

We would also like to acknowledge Harold Johnson of Detroit Stoker, William Engelleitner of Mars-Mineral, Sam Spector of Banner Industries, and Donald Hansen of Alley-Cassetty Coal Company for providing advice and assistance to the program.

Finally, we would like to recognize Battelle-Columbus staff members--John Faught, Tom Lyons, Paul Strup, Don Hupp, Luis Kahn, and Andrew Skidmore, and acknowledge the cooperation of John Clayton and his Facilities staff who allowed us to use the Battelle steam plant boiler during the program.

BEGIN FIRST LINE OF TEXT HERE
TYPING GUIDE SHEET
CENTER OF PAGE
TOP OF IMAGE AREA
DROPPED HEAD: BEGIN SECTIONS HERE

CONTENTS

	Page
Foreword	**iii**
Acknowledgment	**iv**
Phase I. Alternative Fuels Evaluation	**I-i**
Phase II. Control Technology Evaluation	**II-i**
Phase III. Limestone/Coal Pellet Development	**III-i**

6-1/2"
9-1/8"
BEGIN LAST LINE OF TEXT
BOTTOM OF IMAGE AREA; OUTSIDE DIMENSION FOR TABLES AND ILLUSTRATIONS
3/8"
PAGE NUMBER
EPA-287 (Cin.)
(4-76)

Phase I. Alternative Fuels Evaluation

CONTENTS

Page

FIGURES . . . . . I- iii
TABLES . . . . . I- iv
EXECUTIVE SUMMARY . . . . . I- v

I. BACKGROUND I-1

II. OBJECTIVE AND SCOPE. I-2

III. EXPERIMENTAL PLAN. I-3

Underfeed Stoker I-6
Model Spreader I-6

Coal Selection and Preparation. I-7

Coal Selection I-7
Coal Preparation I-8
Coal Analyses. I-9

Experimental Procedures I-9

Model Spreader Simulation. I-9
Sampling and Analytical Procedures I-10
Coal Sampling. I-10

IV. EXPERIMENTAL RESULTS I-13

Underfeed Stoker Results. I-13

Gaseous Emissions. I-15
Particulate Loadings I-16
POM Loadings I-16

Model Spreader Stoker Results I-18

Gaseous Emissions. I-18
Particulate Loadings I-20
POM Loadings I-20
Particle Size Distribution I-22
Gas Probing Observations I-22
Bed Temperature Profiles I-24
Observations of Suspension and Fixed Bed Combustion I-28

PHASE I

CONTENTS (Continued)

Page

V. ALTERNATIVE FUELS FOR STOKERS--PELLETIZATION APPLICATIONS . I-33

VI. CONCLUSIONS. I-34

REFERENCES I-35

APPENDIX A - BINDER IDENTIFICATION AND RESTRUCTURING TECHNIQUE REVIEW

PHASE I

LIST OF FIGURES

Page

Figure I-1. 200 kW Stoker-Boiler Facility I-4

Figure I-2. Spreader Feed Mechanism I-5

Figure I-3. Particle Size Distrubution of Fly Ash for Runs a) MS-72, b) MS-73, c) MS-5 and d) MS-103 . . . . I-23

Figure I-4. Bed Temperature Profiles for a High Volatile Coal . . I-26

Figure I-5. Bed Temperature Profiles for a Low Volatile Coal. . . I-27

Figure I-6. Fuel Bed Isotherms for a 27 Percent Volatile Australian Coal I-29

PHASE I

LIST OF TABLES

Page

Table I-1. Analysis of Selected Untreated Coals I-10

Table I-2. Analysis of Selected Treated Coals I-11

Table I-3. Summary of Emissions for Selected Coals Fired in The Underfeed and Modal Spreader Stokers I-14

Table I-4. POM Quantification for Underfeed Stoker Experiments. . I-17

Table I-5. POM Quantification for Model Stoker Experiments. . . . I-21

Table I-6. Bed Temperatures I-25

Table I-7. Proximate and Ultimate Analyses (In Weight Percent) of 4 Coal Samples Obtained During Combustion. I-31

EXECUTIVE SUMMARY

A 200-kW stoker-boiler facility was used to evaluate characteristics of emissions from combustion of a variety of coals, including coals that could not be conveniently or economically evaluated in larger industrial systems. The stoker was initially operated in an underfeed mode to expand the data base developed in an earlier EPA program(I-1). This facility was modified to accommodate a model spreader stoker more typical of an industrial boiler.

Raw coals with low pollution potential and treated coals were evaluated. Because there was only one treated coal available during the time framework of the program, Battelle developed, as part of this program, a limestone/high sulfur coal fuel pellet.

Results of the Phase I emission characterization were as follows.

NO

For the underfeed stoker, less than 10 percent of the fuel nitrogen was converted to NO, assuming no thermal NO. For the model spreader-stoker, between 10 and 20 percent of the fuel nitrogen was converted to NO.

SO_2

Coals naturally high in calcium and sodium and those treated with these elements retained significant percentages of the sulfur in the ash. For the eastern bituminous coals, with relatively small amounts of calcium and sodium but significant amounts of iron, sulfur retention in the ash was as high as 20 percent. Note that bed temperatures in these laboratory stokers are significantly lower than these measured in an industrial stoker.

CO

CO levels can be controlled by the use of overfire air and were generally less than 100 ppm.

Particulate Loading

Particulate loadings did not correlate consistently with either the ash content of the coal nor its size consist prior to feeding. It appears that the friability and inherent moisture content of the coal may affect particulate loading since these properties influence the amount of fines generated.

POM Loadings

POM loadings for continuous operation of the underfeed stoker were significantly less than those reported earlier(I-1) for intermittent operation.

Particle-Size Distribution

For the model spreader, the average stack particle size ranged between 15 and 30 micrometers.

Treated Coals

No commercially available, chemically treated coals were identified. Treated coals required pelletization for firing in stokers.

The Battelle Hydrothermally Treated (HTT) coal was available for laboratory evaluation. The treatment reduced the fuel sulfur from 2.6 percent to 1.1 percent. Because of the relatively high calcium and sodium residual from the treatment, only 28 percent of the remaining sulfur was emitted as SO_2.

Also, the limestone/coal fuel pellet, with a Ca/S molar ratio of 7, reduced SO_2 emissions by over 70 percent. Even at the elevated fuel-bed temperatures (> 1100 C), the calcium reacts with the coal sulfur and retains it as a sulfide/sulfate as part of the fuel ash.

PHASE I ALTERNATIVE FUELS EVALUATION

SECTION I

BACKGROUND

The overall performance of a stoker-boiler system and the emissions that it generates depend on several factors, including stoker-boiler system design, combustion operating parameters, and coal properties. Generally, for a given stoker-boiler system, the overall boiler performance and combustion-generated emissions can be controlled to a limited extent by optimizing stoker-boiler operating parameters. In contrast, the type of coal fired in system has the most dominant effect on both emission levels and system performance.

Unfortunately, coals in major U.S. reserves located near the industrial sector contain relatively high levels of sulfur. Firing these coals in an environmentally acceptable manner, requires either pretreatment to remove the sulfur or burning in systems with flue-gas desulfurization (FGD) equipment. Industrial boiler owners/operators have resisted FGD because of the high cost and low reliability. As a result, there has been increased interest in coal treatment processes. In addition, as an alternative to high-sulfur eastern bituminous coals, consideration has been given to increased industrial utilization of low-sulfur coals such as lignite, western subbituminous, and western bituminous coals. Because the treated coals have not been available and the western coals have not been used extensively, there is relatively little combustion generated emission data on these fuels to assess their impact on the acceptability of stoker boilers.

SECTION II

OBJECTIVE AND SCOPE

The overall objective of the Phase I research program was to evaluate the emission characteristics resulting from the combustion of a representative number of raw coals and available treated coals. Because of the limited availability of treated coals and the logistics problems and high costs of procuring large quantities of western coals, the combustion tests were conducted in a 200-kW (20-bhp) stoker-boiler facility used on an earlier EPA stoker program(I-1). This facility was initially designed and operated with an underfeed stoker. A limited number of coals were fired in this operational mode primarily to extend the data base developed from the earlier program. However, because the spreader stoker is the type preferred by industry, a "model spreader" was designed to simulate that mode of operation. The majority of experiments were conducted with the model spreader. In addition, as part of Phase I activities, limited emission measurements were made in the Battelle (8 MW) (25,000 lb steam/hr) steam plant spreader stoker for comparison with those of the model spreader.

As first conceived, this program was to focus primarily on evaluating the emission characteristics of treated coals. However, this scope was altered because the various processes to treat coals did not develop sufficiently within the time framework of the program. As a consequence, the development of a limestone/high sulfur coal pellet, conceived by the Battelle staff, was pursued as part of Phase I activities.

SECTION III

EXPERIMENTAL PLAN

Phase I experiments focused on assessing emission characteristics for a variety of coals for both the underfeed and model spreader operations. The effects of system operating variables for relatively small systems are difficult to scale to larger systems because wall effects, heat losses, and particle dynamics are more pronounced. Accordingly, these variables were of secondary interest. Nine raw coals and two treated coals were evaluated using particulate loading, CO, SO_2, and NO emission levels as the primary basis for evaluation; a limited number of POM emission measurements were also made.

FACILITY

Figure I-1 is a photograph of the stoker research facility used in the Phase I experiments. The basic element of this facility is a Kewanee 3R-5 200 kw (20 bhp), fire-tube, hot water boiler capable of firing coal at rates up to 34 kg/hr. Coal was fed to the boiler by either a Will Burt 34 kg/hr underfeed stoker or a "model" spreader stoker. The "model" spreader, shown in Figure I-2, was designed and constructed by the Battelle-Columbus staff. This spreader can distribute coal uniformly over a 0.6-m wide by 1-m deep grate at rates ranging from 13.6 to 68 kg/hr. The "model" spreader was installed through the firebox door of the boiler, the normal location of a burner for oil or gas firing. These two types of stokers provide radically different burning methods -- suspension plus bed burner for the spreader and entirely bed burning for the underfeed. They even have opposite combustion air flow patterns -- counter flow for the spreader and parallel flow for the underfeed.

FIGURE I-1. 200 KW STOKER-BOILER FACILITY

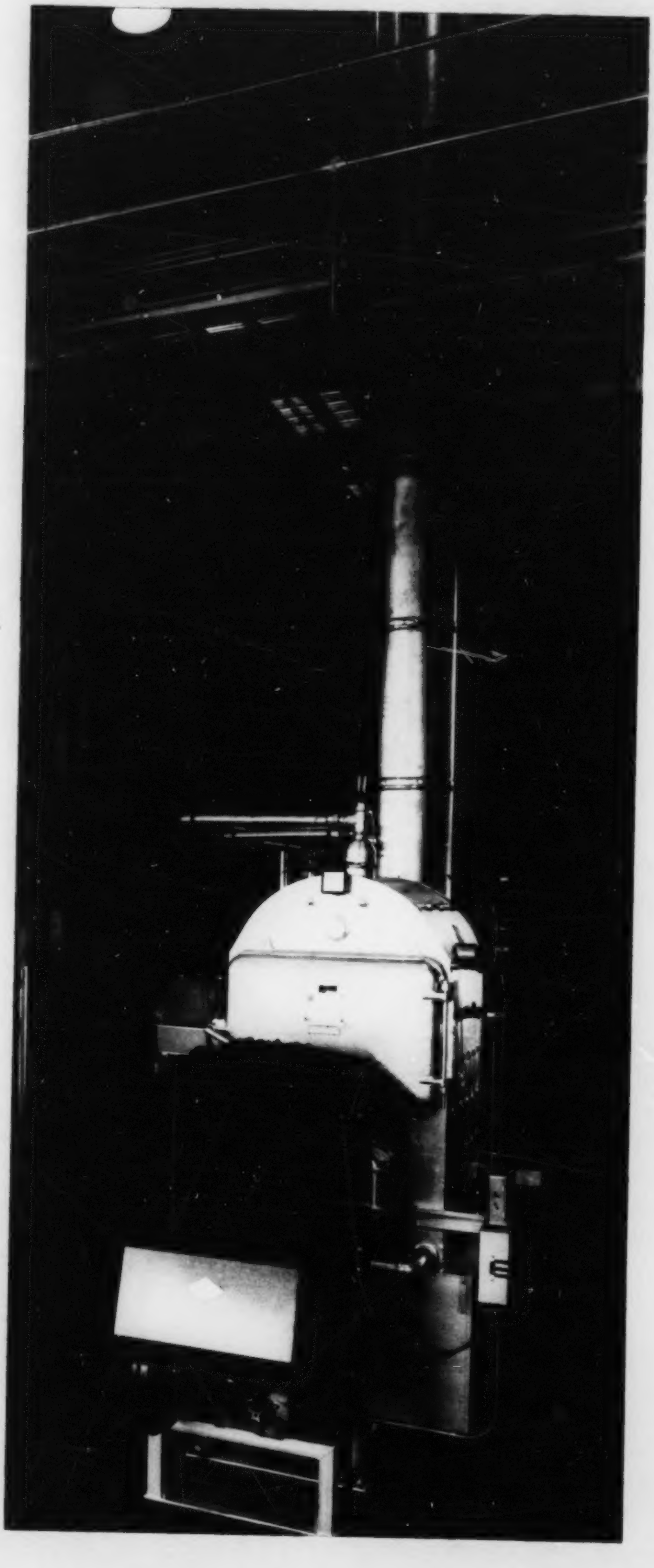

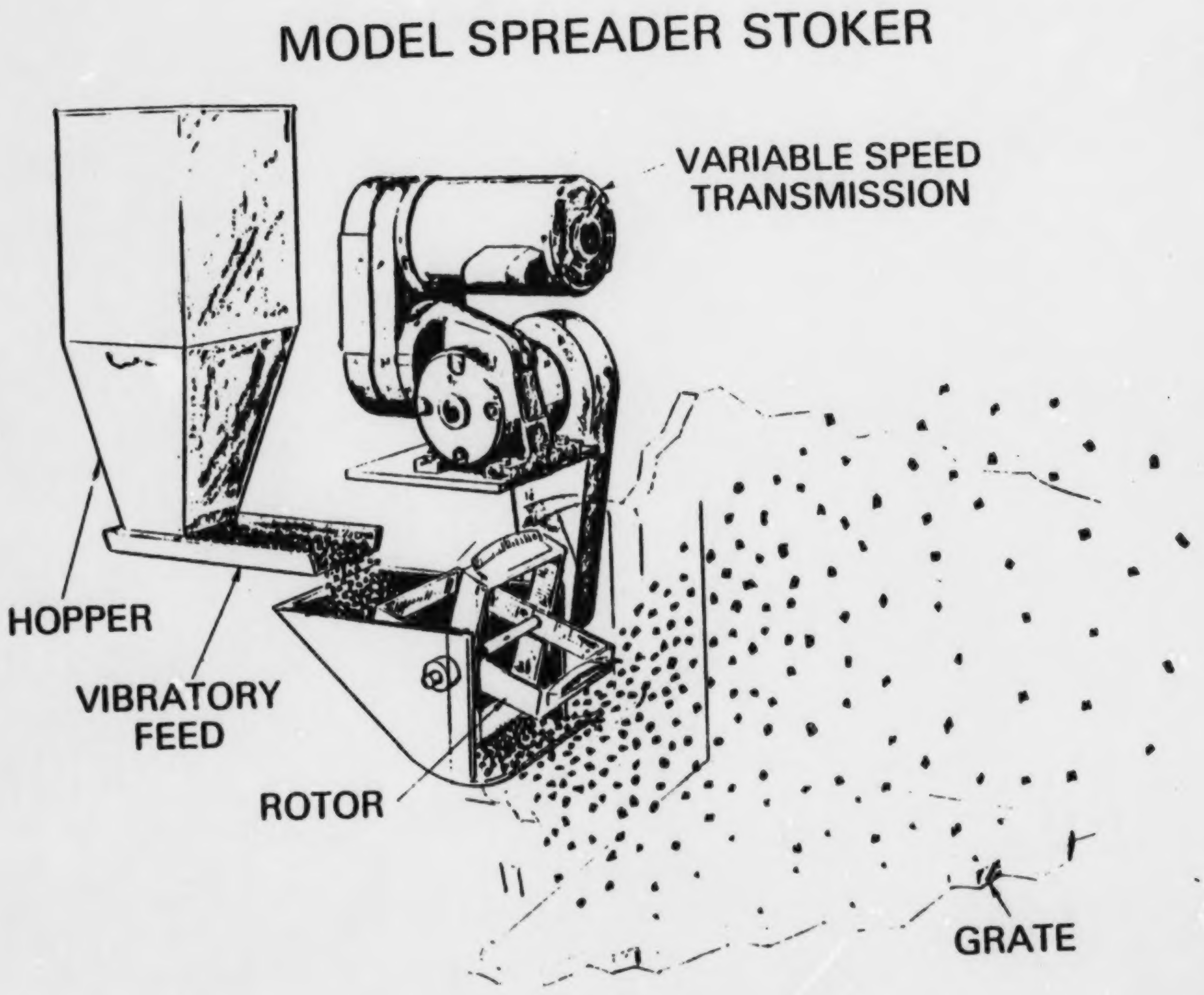
MODEL SPREADER STOKER
VARIABLE SPEED TRANSMISSION
HOPPER
VIBRATORY FEED
ROTOR
GRATE

FIGURE I-2. SPREADER FEED MECHANISM

These units have fixed beds with no provision for automatic ash removal. The combustion zone is surrounded by the water wall of the boiler.

Combustion gases were vented through a 0.35-m diameter, insulated stack that included provision for sampling at a location 10-stack diameters downstream of the boiler outlet. A damper (approximately 1.5 m above the sampling port) provided a control at the boiler outlet. Ports for smoke and gaseous-emission sampling and for temperature and pressure measurements were provided at the base of the stck.

Underfeed Stoker

The Will-Burt stoker is a conventional bituminous underfeed stoker. The majority of coal is burned in the retort with the remaining coal being burned on a ceramic hearth surrounding the retort. Normally, the primary combustion air would be supplied by a fan; however, to provide for a greater range of flow rates, laboratory compressed air was used for these experiments. The flow rate was measured with a standard ASME orifice.

Four overfire air jets, 150 mm on centers and 7 mm in diameter, were installed approximately 300 mm above the retort. The overfire or secondary air was measured with a laminar flow element.

Model Spreader

This spreader mechanism introduced coal into the boiler through the fire door. The spreader mechanism was installed on the boiler in much the same way as a gas or oil burner. Seals were used to minimize leakage. Pitch of the four rotor baldes on this spreader mechanism was varied by cold flow tests to provide uniform fuel distribution. However, there was still some tendency for the coal to build up slightly in the center of the grate. Coal was fed to the rotors from the coal hopper by a vibrating feeder. The flow rate was controlled by the vibration of the feeder.

The stationary grate was designed with a free flow area of 4 percent to provide for a uniform distribution of the air through 6-mm holes.

To compensate for the slight build up of coal in the center of the grate, the 6-mm holes along the outer edge were plugged.

The water-cooled walls of the boiler firebox were lined with high-temperature (1400 C) blanket-type insulation. This insulation reduced the heat loss the from the burning zone and improved combustion in the suspension zone above the bed.

Sampling ports located 25 mm, 100 mm, and 200 mm above the grate were used to measured bed temperature. Bed temperature was extremely sensitive to the bed structure. Accordingly, procedures were developed and coal feeding apparatus was modified to establish and maintain a reasonably uniform fuel bed. This was accomplished with continuous scrutiny and adjustment of the feed mechanism.

COAL SELECTION AND PREPARATION

Coals considered for this program were categorized as

- Untreated -- naturally occurring raw coals
- Reconstituted -- physically treated/clean coals that require restructuring
- Processed -- chemically treated coals that may require restructuring.

Selection was based primarily on availability and the low pollution potential of the coal. Coal preparation ranged from crushing and screening the untreated coals to pelletizing the treated coals.

Coal Selection

The untreated coals were to be representative stoker fuels and/or have low pollution potential based upon chemical analyses. The reconstituted and processed coals were to be coals treated to obtain the desired properties of low emission fuels. Additionally, the availability and cost of procuring and preparing the coal was considered.

The untreated coals were commercially available. The costs of these coals at the mine were nominal and the transportation costs were reasonable for the 5 ton lots. In the case of the processed coals, only one (Battelle Hydrothermally Treated) was available for this program. This coal also required pelletization for stoker firing. Likewise, the reconstituted coals or coals that were physically treated to "deep clean" were not available. Because of the unavailability of treated coals, Battelle developed a reconstituted fuel by physically mixing finely ground limestone with pulverized high-sulfur coal. This limestone/coal mixture was restructured by pelletization producing a pellet approximately 12 mm in diameter by 18-mm long that was suitable for stoker firing.

Coal Preparation

For reasons discussed later, the untreated coals were crushed and screened to a top size of 15 mm, with about 20 percent fines (less than 5 mm but greater than 1-mm diameter). The reconstituted fuels and processed fuels required restructuring.

Each of the initial fuels evaluation experiments required 100 kg to 150 kg of fuel pellets. To prepare this quantity of pellets, Battelle used a California Laboratory Pellet Mill capable of producing about 5 kg of pellets per hour. For the limestone/coal pellets, the base coal, Illinois No. 6, was pulverized to 100 percent through -20 mesh and 50 percent through -100 mesh with a hammer mill. A -50 mesh limestone (>90 percent $CaCO_3$) was used. This limestone, the Illinois No. 6 coal, and appropriate binders were then mixed in either (1) a Hobart mixer for small batch quantities of pellets for mechanical strength evaluation or (2) a portable cement mixer for larger quantities for combustion tests. For the Battelle Hydrothermally Treated Coal, similar procedures were used except that limestone was not added.

Restructuring of these fuels required a binder that provided enough mechanical strength that the resultant fuel pellet could be handled without serious physical deterioration. Thus, an effort was undertaken to identify and evaluate binders. In addition, different restructuring techniques were reviewed. These efforts are described in Appendix I-A.

Coal Analyses

Tables I-1 and I-2 present the ultimate and proximate analyses and the free-swelling index for the untreated and treated coals fired in Phase I. The free-swelling index is a measure of caking tendency of coal and is applicable to the underfeed stokers rather than the model spreader. The nitrogen content of the washed Western Kentucky coal appears low at 0.75 percent in comparison to the unwashed western coal at 1.38. Washing coal does not reduce the nitrogen content (as is the case for the ash and sulfur content) but rather increases the fuel N percentage because of the removal of ash.

EXPERIMENTAL PROCEDURES

For the underfeed stoker experiments, procedures previously developed on the earlier EPA stoker program(I-1)* were used. For the model spreader experiments, procedures were developed to simulate the operating characteristics of an industrial spreader stoker. Proven analytical techniques were used to determine the criteria pollutants.

Model Spreader Simulation

Spreader stokers burn up to 50 percent of the coal in suspension in the combustion zone above the fuel bed. The remaining coal is burned in the fuel bed. The amount of coal burned in suspension depends on the percentage of coal fines and the stoker boiler design (residence time above the bed). The model spreader was designed to provide for both suspension and bed burning. To compensate for the decreased residence time in the freeboard of the model spreader (residence time could not be "scaled" in the model spreader), the as-received stoker coal was crushed to reduce the overall particle size distribution to a top size of about 15 mm. The bottom size could not be reduced substantially as particles less than 0.5 mm to 1 mm would be transported by the combustion gases to the stack without reaching the burning regime. Also, it was observed that if the coal feed contained more than 20 percent fines, the fuel bed tended to mat. Evidently, these coal fines did not burn to completion in suspension and accumulated on the fuel bed. Accordingly, the percentage of coal fines was controlled to about 20 percent of the total feed.

---

* References on page I-35

TABLE I-1. ANALYSIS OF SELECTED UNTREATED COALS

Fuel Type	Proximate Analysis, % (as run)				Ultimate Analysis, % (dry)					High Heating Value KJ/g	Free Swelling Index
	Volatiles	Fixed Carbon	Moisture	Ash	C	H	N	S	Oxygen (difference)		
SE Kentucky	36.94	54.01	3.89	5.37	79.9	5.5	1.53	1.27	6.3	33.3	6-1/2
Illinois No. 6	39.31	46.90	11.07	13.79	66.9	4.7	1.04	4.94	8.5	28.1	3-1/2
Western Ky. (unwashed)	39.7	49.8	6.88	10.46	70.4	4.6	1.38	4.57	8.5	29.1	2
E. Kentucky	40.0	53.5	2.35	4.7	78.2	5.1	1.3	1.22	9.5	32.8	2
W. Virginia (Bishop mine)	21.4	70.8	0.9	6.9	84.7	4.7	(1.5)	0.61	1.6	34.1	7-1/2
Western Sub-bituminous	28.4	35.6	26.1	9.86	50.6	3.2	0.8	0.67	34.8	24.1	Non-Agglom.
Lignite	29.1	28.3	32.6	9.57	62.2	3.8	0.9	1.57	21.6	21.9	Non-Agglom.
Western Ky. (washed)	41.76	52.6	7.48	5.62	74.64	5.41	.75	3.53	10.01	31.6	2-1/2

TABLE I-2. ANALYSIS OF SELECTED TREATED COALS

Fuel Type	Proximate Analysis, % (as run)				Ultimate Analysis, % (dry)					High Heating Value, KJ/g
	Volatiles	Fixed Carbon	Moisture	Ash	C	H	N	S	Oxygen (difference)	
Battelle (Hydrothermally Treated	34.17	46.42	7.15	19.41	65.3	4.3	1.17	1.16	8.55	26.5
L/C 50/50 Latex Bound[a]	46.01	9.72	7.06	44.3	37.6	2.2	0.63	2.21	13.0	12.8
L/C 50/50 Cement Bound	44.9	2.96	12.60	52.1	34.0	1.8	0.55	2.24	9.3	11.3
L/C 50/100 Cement Bound	43.9	19.82	6.99	36.3	46.5	2.9	0.78	2.87	10.5	17.4

(a) L/C = limestone/coal, fuel pellets

Spreader stokers have relatively thin, fast-burning beds. In the model spreader there was no provision for continuous ash disposal and the fuel bed became progressively deeper. High ash fuels, such as the limestone/coal pellet, accentuated this problem. Deep beds generally resulted in a nonuniform burning of the bed. Accordingly, to provide some measure of control of the fuel bed when making emission measurements before emission sampling was began, the stoker was operated long enough to establish a stable fuel bed, but not so long that ash build-up would significantly interfere with the stoker performance.

Sampling and Analytical Procedures

Particulate and POM levels were determined by a modified EPA Method 5 procedure with the probe wash and filter catch being used to determine the filterable particulate loadings and an absorbent column being used to determine POM loadings.(I-2) The extract from the column was analyzed by GC/MS techniques.

Gaseous emissions were determined by: paramagnetic analysis for oxygen; nondispersive infrared (NDIR) analysis for carbon monoxide, carbon dioxide, and nitrogen oxide; and a dry electrochemical analyzer for sulfur dioxide. Gas samples from the stack first passed through a heated filter that was coupled close to the stack, and then through an ice trap to reduce the dewpoint. After this trap, the sample gas was conveyed through teflon tubing to a manifold and then distributed to each instrument. For the NO measurement, a dry ice trap was located between the manifold and the NDIR instrument to eliminate all moisture in the stack gas.

Coal Sampling

Because coal is not a homogeneous fuel, its composition can vary substantially. An accurate determination of the coal composition is needed for combustion calculations. In the model spreader experiments, coal samples were collected from the feed system through the run. These aggregate samples were then ground and analyzed. In addition to this procedure, coal was sampled from each drum in which it was stored and then ground for analysis. Generally, there were some minor discrepancies that were attributed to the difficulty of obtaining representative samples. For the combustion calculations, coal analyses were based on those samples collected during the experiment.

SECTION 4

EXPERIMENTAL RESULTS

The emissions of a stoker-boiler system depend on its design as well as its operation and the coal being burned. Accordingly, these factors must be considered when comparing emission and performance data from several systems.

Phase I experiments were designed to provide a relative measure of emissions from a variety of coals, including coals that could not be conveniently evaluated in larger industrial systems. The majority of the gaseous emission data correlate primarily with coal properties and to a lesser extent with system design parameters. As a consequence, these data would be representative of a variety of industrial units, including underfeed and spreader stokers. In fact, gaseous emission levels obtained from firing the same coal in both the model and industrial spreader stoker were similar. On the other hand, particulate emission levels depend on system design. Thus, particulate emission data from the laboratory-size stoker-boiler may not be representative of data for industrial-size units.

UNDERFEED STOKER RESULTS

The underfeed stoker experiments were designed to extend the data base of the earlier EPA stoker program(I-1) to cover additional coal types and operating conditions. In the earlier program, the underfeed stoker was most often operated under cyclic conditions (on/off mode), while in this program, the stoker was operated continuously.

Table I-3 summarizes the results of these underfeed stoker experiments for the coals fired and the operating conditions listed.

TABLE I-3. SUMMARY OF EMISSIONS FOR SELECTED COALS FIRED IN THE UNDERFEED AND MODEL SPREADER STOKERS

		Average Flue Gas Composition						SO_2 at 3%O, ppm		Fuel Sulfur emitted	NO at 3%O_2, ppm		Fuel N Converted to NO	Particulate Loading	POM Loading
Run No.	Coal Type	O_2 %	CO_2 %	CO ppm	SO_2 ppm	NO ppm	CO 3%O_2 ppm	Calculated	Measured	%	Calculated	Measured	%	mg/SM^3	µg/SM^3
a. Underfeed															
UF-1	E.Kentucky Bit.	7.5	12.4	40	720	160	54	940	970	(103)	2280	220	9.6	64	.5
UF-2	Lignite	8.5	11.2	70	350	120	100	1570	510	32	2030	160	8.0	338	.9
UF-3	Western Subbit.	7.4	12.4	60	560	160	81	1270	760	60	2530	220	8.7	160	.7
UF-4	Illinois No. 6	6.0	13.0	80	3800	160	97	4700	4630	98	2220	190	8.6	120	.3
UF-5	Illinois No. 6 w/limestone	6.0	13.2	240	3200	190	290	4700	3880	83	2220	230	10	--	--
b. Model Spreader															
MS-1	Lo-vol W. Va.	7.2	11.8	20	--	120	26	390	--	--	2400	160	6.7	290	
MS-2	E Kentucky Bit.,TP Mine	6.8	12.0	24	--	250	31	940	--	--	2280	320	7.1	400	
MS-3	SE Kentucky Bit.	7.5	11.0	50	--	360	67	940	--	--	2710	480	18	1360	37
MS-4	SE Kentucky Bit.	8.2	11.1	40	--	225	56	940	--	--	2710	320	12	700	9
MS-5	Illinois No. 6	8.8	10.2	30	--	220	44	4700	--	--	2220	330	15	360	60
MS-6	Illinois No. 6	8.6	10.2	20	--	200	39	4700	--	--	2220	300	14	330	37
MS-7	Lignite	10.2	10.4	10	--	170	17	1570	--	--	2030	290	14	500	
MS-8	Western Bit. Col	9.1	11.0	10	--	170	15	590	--	--	3400	260	7.6	380	
MS-9	Western Bit. Col	8.8	10.5	15	--	200	23	590	--	--	3400	310	9.1	170	
MS-10	Pellets, Ca/S = 7,Latex binder	9.5	11.5	70	1200	180	110	3830	--	--	2560	280	11	780	
MS-11	Pellets, Ca/S = 7, Latex binder	10.2	11.0	50	1300	200	84	3830	--	--	2560	340	7.5	430	
MS-12	Pellets, Ca/S = 3.5,Latex	8.8	10.5	250	2200	150	370	3840	--	--	1690	220	13.	1020	
MS-13	Illinois No. 6	7.9	10.4	30	--	270	42	4700	--	--	2220	380	17.	390	
MS-14	Lo-vol W. Va.	6.8	12.9	20	--	190	26	390	--	--	2400	240	10.	170	
MS-15	SE Kentucky, Bit.	6.8	11.5	40	--	240	51	940	--	--	2710	310	11.	340	
MS-16	W. Kentucky, unwashed	7.7	11.1	10	--	150	14	3500	--	--	2490	210	8.4	200	
MS-17	W Kentucky, washed	8.2	10.6	50	--	230	70	2760	--	--		320		160	
MS-18	E Kentucky, Bit.	7.6	13.4	30	--	170	40	940	--	--	2280	230	10.	180	
MS-19	Lignite	9.6	--	15	--	--	20	1570	--	--	2030	--	--	310	
MS-20	Pellets, Ca/S=3.5 Latex	10.7	9.7	24	790	310	42	3840	1370	36	2020	540	27		
MS-21	Illinois No 6	9.4	10.4	50	3100	320	78	4700	4852	(103)	2200	500	23		
MS-22	Pellets, Ca/S = 7, Cement binder	9.3	10.9	20	560	180	31	4020	880	22	2250	280	12		
MS-23	Pellets, Ca/S = 7, Cement binder	9.7	11.0	--	700	160	--	4020	1160	29	2250	260	12		
MS-24	HTT Pellets	7.5	11.1	11	220	180	15	1090	300	28	2510	240	9.6		
MS-25	Lo-vol W. Va.	7.5	12.0	20	210	220	27	390	280	72	2400	300	13		
MS-26	Lignite	7.0	12.8	20	380	320	26	1570	490	31	2070	410	20		
MS-27	SE Kentucky	7.0	17.0	20	640	300	26	940	830	88	2710	390	14		
MS-28	E Kentucky	5.0	14.8	20	760	300	23	940	860	91	2280	340	15		
MS-29	Illinois No. 6	8.3	11.0	28	2800	280	41	4700	4090	87	2220	410	18		
MS-30	Western Bituminous	7.5	12.8	15	400	290	18	590	540	92	3400	390	11		
MS-31	Pellets, Ca/S = 7.0	11.0	10	30	600	230	55	4020	1100	27	2250	420	19		

Gaseous Emissions

NO. Table I-3 indicates that a small fraction, less than 10 percent, of the fuel nitrogen is converted to NO (assuming no thermal NO). In comparison to pulverized coal combustion, where as much as 30 to 40 percent of fuel nitrogen is converted to NO, the fuel nitrogen conversion is relatively low for stoker firing. This low conversion may be attributed to the inherent "staged combustion" of stoker firing and/or low excess air combustion occurring within the stoker bed. Additionally, as suggested in Reference I-3, the relatively high levels of CO that are present in the fuel bed may serve to reduce the NO to N_2.

SO_2. Table I-3 shows the percent fuel sulfur emitted as SO_2 for selected coals. It is well recognized (References I-4 and I-5) that the alkaline content in the coal can be effective in retaining a portion of the fuel sulfur as sulfate in the ash. Thus, when firing coals with naturally high calcium and sodium content and those treated with these elements, only a portion of the fuel sulfur is emitted as SO_2 as evidenced in Table I-3.

The measured values of SO_2 were exceptionally low for the lignite and the western subbituminous coals -- coals with relative high sodium and calcium contents. Maloney(I-5) suggests that lime is more effective in capturing fuel sulfur as sulfide in fuel-rich regions. It was observed in the underfeed stoker that when firing lignite and subbituminous coals, combustion was nonuniform in the fuel bed -- a condition that often leads to unburned carbon in the bottom ash.

In Run UF-5, -50 mesh limestone was fed at a rate equivalent to a Ca/S molar ratio of 7 along with the stoker-sized coal. SO_2 emissions were reduced by 17 percent, a considerably lower reduction than for coals with naturally occurring alkaline content and lower Ca/S ratios. This result suggests that the manner in which the alkaline material contacts the sulfur and the conditions (oxygen level, temperature) at which this contact occurs are important.

CO. CO levels can generally be controlled with the overfire or secondary air. For the coals fired, overfire air rates of 10 to 20 percent of the total air were required to minimize CO emissions as well as to achieve near smokeless operation. CO levels varied between 50 and 100 ppm, except when limestone was added to the Illinois No. 6 coal (Run UF-5). The addition of limestone appeared to flux the ash resulting in clinkering. The clinkering caused nonuniform bed burning, increasing the CO levels to 290 ppm.

Particulate Loadings

In comparison to the high volatile Eastern coal, and to a lesser extent the Illinois No. 6, the lignite and western subbituminous coals generated higher particulate loadings. Generally in underfeed firing, there is very little fly-ash carryover. However, because of the friability of the lignite and western subbituminous coals, an excessive amount of fines were produced while conveying the coal to the retort. A rough measure indicated about 50 percent fines were introduced into the retort. Also, because of the high sodium content of the lignite, it appears that some portion of the particulate loading may be attributed to condensed sodium vapor.

POM Loadings

Previously reported POM data indicated that loadings varied by an order of magnitude for essentially identical runs firing fuel oils under controlled laboratory conditions. The mechanisms involved in the formation of POM are not fully understood and thus it is difficult to explain these apparent discrepancies. Thus, in reviewing the POM loadings presented in Table I-3, there appears to be no significant difference in the levels that could be attributed to coal type or the combustion conditions. Of greater significance is the fact that the POM levels generated during continuous firing of this unit were at least 1000 less than those measured from the same unit operating under cyclic conditions. Table I-4 presents POM species quantification.

TABLE I-4. POM QUANTIFICATION FOR UNDERFEED STOKER EXPERIMENTS

Component	Notation	UF-1, ng	UF-2, ng	UF-3, ng	UF-4, ng
Anthracene/Phenanthrene		384	863	527	169
Methyl anthracenes		98.4	257	123	22.7
Fluoranthere		380	385	405	281
Pyrene		30.2	88.8	0.1	4.8
Methyl Pyrene/Fluoranthene		0.1	0.1	0.1	0.1
Benzo(c)phenanthrene	***	5.2	4.0	2.4	3.7
Chrysene/Benz(a)anthracene	*	10.4	12.7/ 2.4	7.4	11.8
Methyl chrysenes	*	0.1	0.1	0.1	0.1
7,12-Dimethylbenz(a)anthracene	****	ND(a)	0.1		
Benzo fluoranthenes	**	ND	5.5		
Benz(a)pyrene	***		2.7		
Benz(e)pyrene			2.2		
Perylene			0.1		
Methylbenzopyrenes					
3-Methylcholanthrene	****				
Indeno(1,2,3,-cd)pyrene	*				
Benzo(ghi)perylene					
Dibenzo(a,h)anthracene	***				
Diebenzo(c,g)carbazole	***				
Dibenz(ai and ah)pyrenes	***				
Coronene					
Total		910ng	1620ng	1070ng	490ng

(a) None detected.

The POM loadings in Runs UF-1 through UF-4 are very low. These levels are about an order of magnitude lower than those measured from firing a 500-kw package boiler on oil and gas.(I-6) This is a somewhat surprising result when coal is believed to generate higher levels than oil or gas for similar combustion condition. A review of the sampling and analysis procedures indicated identifiable changes in technique occurred that could have resulted in the POM levels being altered. Because the levels are extremely low, the data are considered suspect.

MODEL SPREADER STOKER RESULTS

Table I-3 summarizes the results of the model spreader stoker experiments for the coals fired and the operating conditions listed.

Gaseous Emissions

NO. For the most part, 10 to 20 percent of the fuel nitrogen is converted to NO (assuming no thermal NO). This percent conversion is somewhat higher than that observed in the underfeed runs and may be attributed to two factors. First, in the model spreader stoker some portion of the coal is burned in suspension. (In industrial spreader stokers as much as 50 percent of the coal is burned in suspension.) In suspension burning, the coal particles are surrounded by an oxidizing atmosphere, which can contribute to a higher percentage of fuel nitrogen conversion to NO than in bed burning alone. The other factor is that in spreader stoker firing, the fuel bed is thinner and there is more surface burning than in underfeed firing. This condition results in a greater portion of the combustion occurring in an oxidizing atmosphere.

SO_2. The percent fuel sulfur emitted as SO_2 for selected conventional coals fired in the model spreader stoker was similar to that observed during the underfeed stoker runs. In Run MS-24, because of the relatively high alkaline content in the lignite, only about 31 percent of the fuel sulfur was emitted as SO_2. Likewise for the bituminous coals that have lower alkaline contents, between 72 and 100 percent of the fuel sulfur was emitted as SO_2. Unfortunately, due to degradation of an electrolytic cell, the Faristor analyzer used to measure SO_2 was found to give inconsistent results during Runs MS-1 through MS-19. As a consequence, the data are not reported. The problem was corrected after Run MS-19.

Hydrothermally Treated Coal. The hydrothermal treatment of coal removes approximately 50 percent of the fuel sulfur depending on whether the sulfur is organic or inorganic.(I-7) The process results in some alkali residuals (7 percent Ca and 0.5 percent Na by weight) that are effective in capturing a portion of the remaining fuel sulfur. As indicated by Run MS-24 in Table I-3, only 28 percent of the fuel sulfur contained in the HTT coal was emitted as SO_2.

Limestone/Coal Pellets. The most significant finding of the model spreader stoker experiments was that the limestone/high-sulfur coal pellet was effective in capturing as much as 78 percent of the fuel sulfur. For a Ca/S molar ratio of 7, as indicated in Runs MS-22, MS-23, and MS-31, only 22, 29, and 27 percent, respectively, of the fuel sulfur was emitted as SO_2. Similarly, for a Ca/S molar ratio of 3-1/2 in Run MS-20, only 36 percent of the fuel sulfur was emitted as SO_2. Illinois No. 6 coal was used as the base coal (Runs MS-21 and MS-29).

In comparison to Run UF-5, where limestone was simply introduced into the feed system along with stoker-size coal, the data indicate that the limestone/coal pellets were significantly more effective in capturing sulfur. This increased sulfur capture may be attributed to the intimate contact of the limestone with the coal particle in the pellets and possibly to the more reactive surface of the pellet.

CO. As in the underfeed stoker experiments, during the model spreader runs CO levels were controlled with overfire air. CO levels were generally less than 100 ppm. CO levels were noticeably high for two of the pellet runs (MS-10 and MS-12), which may be attributed to several factors. Observation of the fuel bed during these runs indicated nonuniform burning and a general appearance of low heat release rate. Temperatures in and above the bed for these runs, as well as for other pellet runs, were less than 1000 C while those for the conventional coal runs were greater than 1000 C as indicated in Table I-5.

Particulate Loading

The model spreader stoker, as expected, generates significantly higher particulate loadings than does the underfeed stoker firing the same coals. The higher particulate loadings are attributed to the suspension burning that occurs in spreader stoker firing that results in a greater amount of fly-ash (carbon) carryover than is observed in either underfeed or overfeed stokers. Another significant, but expected, finding was that particulate loadings from the limestone/coal pellet runs were significantly higher than those from the conventional coal runs. These higher loadings of the limestone/coal pellet are attributed to the high ash content of the pellet (about 50 percent for Ca/S = 7) and the fines fed into boiler.

The particulate loadings do not correlate with either the ash content of the coal nor its size prior to feeding. It was observed that the feed system would often crush the coal and reduce its size. The amount of crushing and size reduction appears to be dependent on the initial coal size and, also, the friability of the coal. Unlike a large industrial stoker, the model spreader does not provide sufficiently long residence times at elevated temperatures to burn coal fines in suspension. As a consequence, an unusually high amount of fly carbon, in addition to the fly ash, is emitted to the stack. Thus, the particulate loadings of the model spreader experiments were affected by factors other than ash content of the coal that are not easily quantified.

POM Loadings

POM loadings were measured for Runs MS-3, MS-4, MS-5, and MS-6. There does not appear to be any relationship between coal type and POM

TABLE I-5. POM QUANTIFICATION FOR MODEL STOKER EXPERIMENTS

Component	NAS Notation	MS-2 ng	MS-3, ng	MS-5, ng	MS-6, ng
Anthracene/Phenanthrene		15,013	5,313	20,955	17,417
Methyl anthracenes		2,648	1,553	3,210	4,125
Fluoranthene		10,927	2,516	42,340	13,405
Pyrene		2,591	1,409	7,142	4,542
Methyl Pyrene/Fluoranthene		1,528	ND	ND	2,677
Benzo(c)phenanthrene	***	921	911	1,034	1,099
Chrysene/Benz (a)anthracene	*	1,242	972	2,027	2,716
Methyl chrysenes	*			1,041	1,677
7,12-Dimethylbenz(a)anthracene	****				
Benxo fluoranthenes	**			1,329	2,207
Benz(a)pyrene	***			1,137	1,286
Benz(e)pyrene					
Perylene					
Methylbenzopyrenes					
3-Methylcholanthrene	****				
Indeno(1,2,3,-cd)pyrene	*	1,062		1,076	1,161
Benzo(ghi)perylene		1,035		1,047	1,024
Dibenzo(a,h)anthracene	***				
Diebenzo(c,g)carbazole	***				
Dibenz(ai and ah)pyrenes	***				
Coronene					
TOTAL		36,000	12,700	82,000	53,300

ND = None Detected

levels nor do the POM levels correlate with CO levels or particulate loadings. The POM levels are, as expected, somewhat higher than those measured in the oil/gas 500 kW packaged boiler.(I-6) Table I-5 gives the POM specie quantification.

Particle Size Distribution

Particle size distribution, as determined by the Coulter Counter method using the filter catch, was similar for Runs MS-2, MS-3, MS-5, and MS-10. The range was from about 5 to 100 micrometers with an average particle size between 15 and 30 micrometers, about the same as that observed for pulverized coal firing. The upper cutoff limit could be attributed to the probe collecting particles larger than 100 micrometers while the lower limit is attributed to the particular Coulter Counter procedure used. Figure I-3 shows these distribution curves.

Gas Probing Observations

In an attempt to determine the combustion phenomena occuring in the stoker boiler, the furnace environment was sampled for gaseous constituents at various locations within the firebox in a plane 0.3 m above the bed using a watercooled stainless steel probe. Evidently, the overfire air jets and the combustion generated sufficient turbulence that consistent data could not be collected. Gaseous constituents varied significantly. For example, O_2 varied from 3 percent to 20 percent and CO from 40 ppm to 1000 ppm. The sample ports were located in approximately the same plane as the overfire air jets and, as a result, measurements were significantly affected. Gas probing 0.6 m above the bed showed that the levels of gaseous constituents in this region were similar to those in the stack.

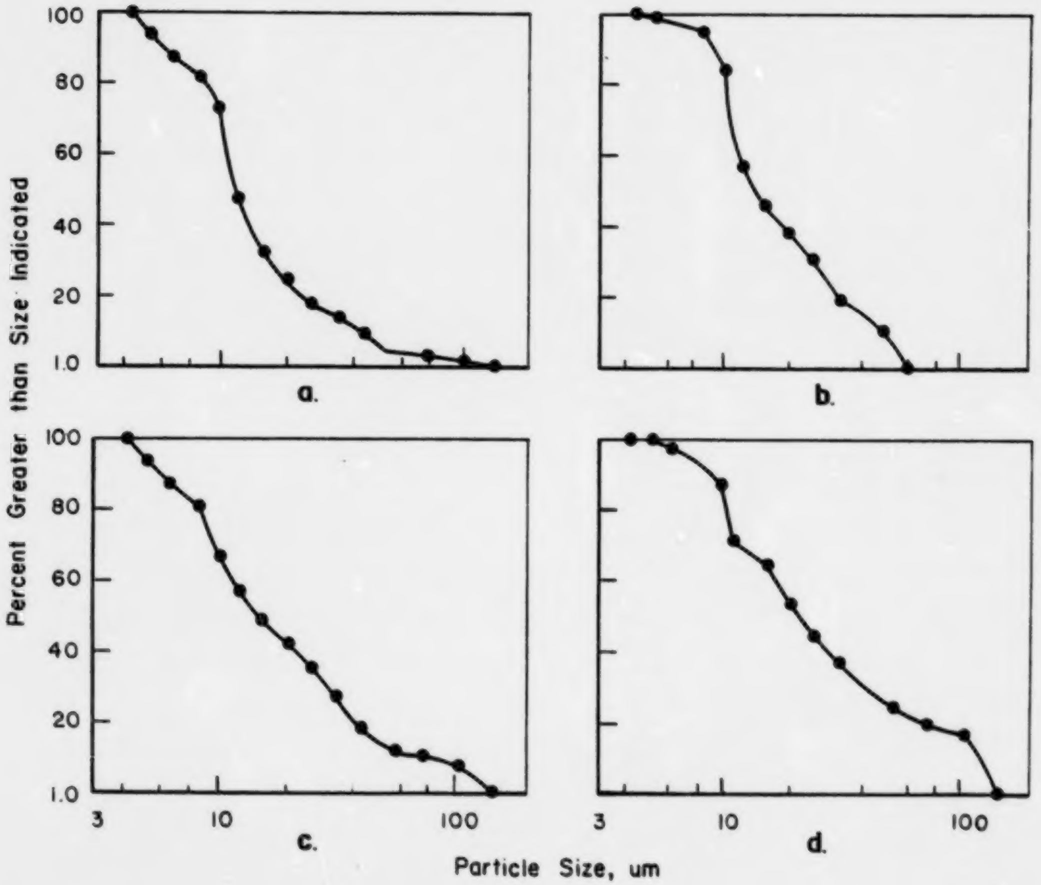

FIGURE I-3. PARTICLE SIZE DISTRIBUTION OF FLY ASH FOR RUNS a) MS-72, b) MS-73, c) MS-5 and d) MS-103

Bed Temperature Profiles

Temperatures were measured at three points within the furnace -- at 25 mm above the grate, well within the bed; at 100 mm above the grate, close to the surface of a well-established bed; and at 200 mm above the grate definitely in the freeboard (suspension burning zone) for most of the run. Because the fuel bed is fixed and there are no provisions for removing ash, the bed increases in depth and the flame front continually changes relative to the location of the thermocouples. These temperature measurements were made over a period of time and were used to estimate relative burning rates for several coals. Stack temperatures at the outlet of the furnace were also recorded. The average values for these temperatures during each run are reported in Table I-6, along with the feed rates and the final bed depth.

Figures I-4 and I-5 show bed temperature profiles for high (40 percent) and low (21 percent) volatile bituminous coals. Since both the combustion conditions and stack temperatures of these runs (MS-1 and MS-4) were essentially the same, overall or total heat releases from the combustion of these coals can be assumed to be essentially equivalent. Thus, a comparison of bed temperature (25 mm location) and freeboard temperature (200 mm location) provides an indication of the relative differences in heat release between these two regions. For example, the low volatile coal produces a higher bed temperature than freeboard temperature indicating a higher heat release within the bed than in the combustion zone above the bed. On the other hand, the high volatile coal produces a higher freeboard temperature than bed temperature indicating a relatively higher heat release in the freeboard region than in the fuel bed. Toward the end of a run, as the bed becomes deeper, the temperatures at the 200 mm point for each approach each other. Temperature at the 25 mm point drops as this zone becomes buried in the ash and is cooled by underfire air. With high ash coals and deep beds, for example with the limestone/coal pellets, this dropoff becomes quite dramatic as the combustion zone moves above this point. Profiles of this type are a

TABLE I-6. BED TEMPERATURES

Run No.	Coal	Average Temperatures, C				Final Bed Dept., mm	Coal Feed, kg/hr	Total Air, kg/hr
		25mm	100mm	200mm	Stack			
--	SE Kentucky	1200	1180	1450	350	100	27	300
--	SE Kentucky	950	1230	1150	360	100	22	300
--	SE Kentucky	--	--	--	--	250	22	250
--	SE Kentucky	1430	1320	1320	370	550	22	340
--	SE Kentucky	1450	1260	1230	400	--	32	300
--	E Kentucky	1180	1320	1200	340	150	27	300
MS-1	Lo-Vol West Virginia	1430	1480	1340	340	330	27	300
MS-2	E Kentucky	--	1230	--	350	100	25	300
MS-3	SE Kentucky	--	1260	1230	350	180	28	300
MS-4	SE Kentucky	1290	1040	1200	360	90	27	300
MS-5	Illinois No. 6	1180	1260	1150	330	100	28	300
MS-6	Illinois No. 6	1200	1260	1150	320	150	27	300
--	Lignite	1150	820	820	270	130	27	220
MS-7	Lignite	1200	1120	870	280	510	50	220
--	Lo-Vol West Virginia	1400	1290	1320	360	--	25	310
MS-8	West Bituminous	420	830	1100	330	150	28	300
MS-9	West Bituminous	800	1270	1220	350	200	30	300
MS-10	L/C Pellets Ca/S=7	800	890	970	310	460	61	220
--	SE Kentucky	1220	1210	1210	380	<100	32	360
—	SE Kentucky	1220	1370	1280	360	180	25	300
MS-11	L/C Pellets Ca/S=7	610	660	1130	300	280	43	250
MS-12	L/C Pellets Ca/S=3-1/2	520	760	1120	290	280	46	250
MS-13	Illinois No. 6	890	1300	1120	330	130	31	300
MS-14	Lo-Vol West Virginia	1400	1420	1210	350	90	23	300
MS-15	SE Kentucky	1000	1090	1000	340	50	24	300
MS-16	W Kentucky, unwashed	980	960	800	300	80	26	300
MS-17	W Kentucky, washed	--	1200	1180	340	50	25	300
MS-18	E Kentucky	1310	1220	1130	360	50	25	300
MS-19	Lignite	--	1040	1050	300	150	42	200
--	Western Bituminous	680	1100	1140	320	100	27	300
MS-20	L/C Pellets Ca/S=3.5	820	--	720	330	150	37	270
MS-21	Illinois No. 6	--	1200	1240	370	250	29	270
MS-22	L/C Pellets Ca/S=7	200	870	860	330	--	43	260
MS-23	L/C Pellet Ca/S=3-1/2	—	290	1050	300	330	36	250
MS-24	HTT Pellets	1190	1250	1080	300	250	45	250

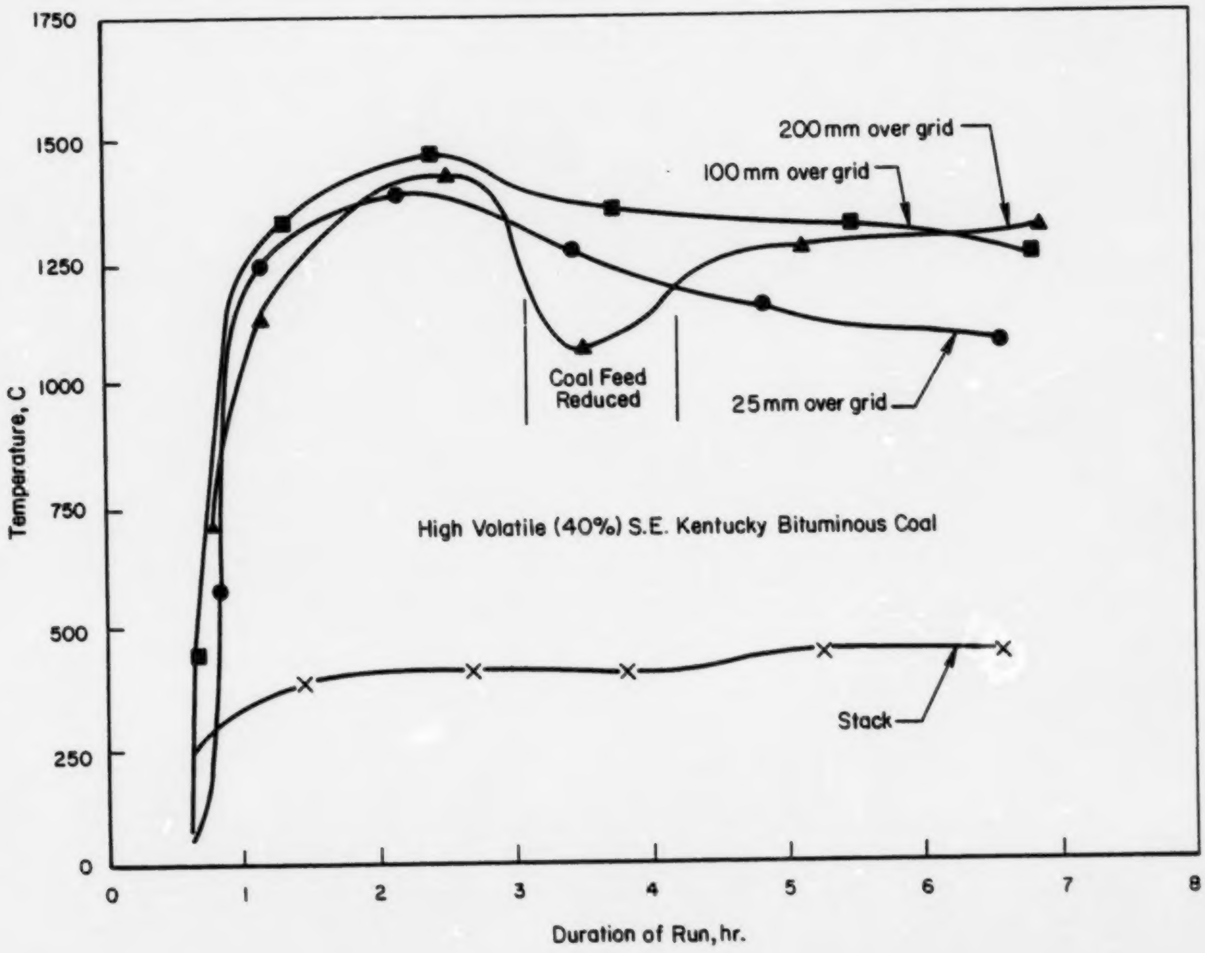

FIGURE I-4. BED TEMPERATURE PROFILES FOR A HIGH VOLATILE COAL

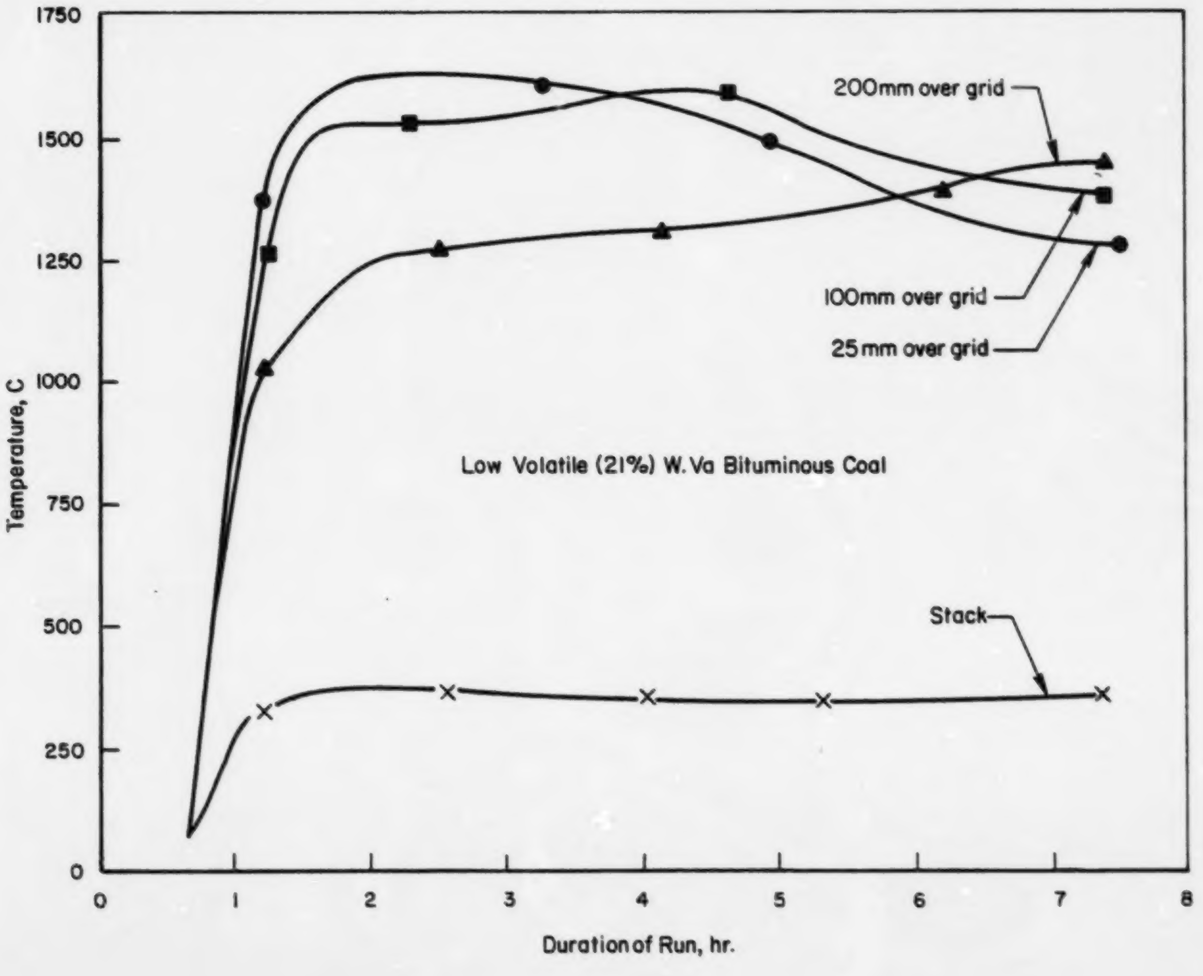

FIGURE I-5. BED TEMPERATURE PROFILES FOR A LOW VOLATILE COAL

graphical indication of the relative amounts of suspension burning. These results relating bed temperatures to coal volatility confirm those of Marskell, et al.(I-8)

Marskell conducted pilot scale testing of a variety of coals under spreader firing conditions. His studies are relevant in that the fuel-bed isotherms that were generated provide some insight as to regions in which the calcium-sulfur reactions may occur. His studies indicate that fuel-bed temperatures can be as high as 1480 C to 1590 C depending on the type of coal. Moreover, his data indicate that there are significant regions within the fuel bed where temperatures are below 1370 C. It is in these regions that we suspect Ca/S reactions will occur. Figure I-6 is an isotherm for a 27 percent volatile Australian coal.(I-8)

Observations of Suspension and Fixed-Bed Combustion

Suspension Burning. In addition to the bed temperature profiles, several observations support a conclusion that suspension burning is significant in the model spreader stoker. After a uniform bed was established in these experiments, the coal feed was stopped. CO levels then increased from 50 ppm to greater than 1250 ppm. (The same phenomenon was observed in the 8-MW spreader stoker.) Evidently, the combustion of the coal in flight provided a sufficiently high temperature to burn out the CO evolving from the bed. Also, the combustion zone above the bed provided a thermal barrier between the fuel bed and the heat transfer surface. Without this combustion zone, the fuel-bed temperature dropped quickly resulting in a reduced burning rate. Thus, when the coal feed was stopped, while maintaining the combustion air flow rate, O_2 concentration in the stack increased significantly, suggesting that significant suspension burning occurred and that bed burning was reduced. Apparently volatile matter was driven off above and immediately at the surface of the bed and provided a region of intense burning. The coal remaining in the bed appeared to be essentially all char. To support this observation, four samples were collected during various phases of stoker combustion. Table

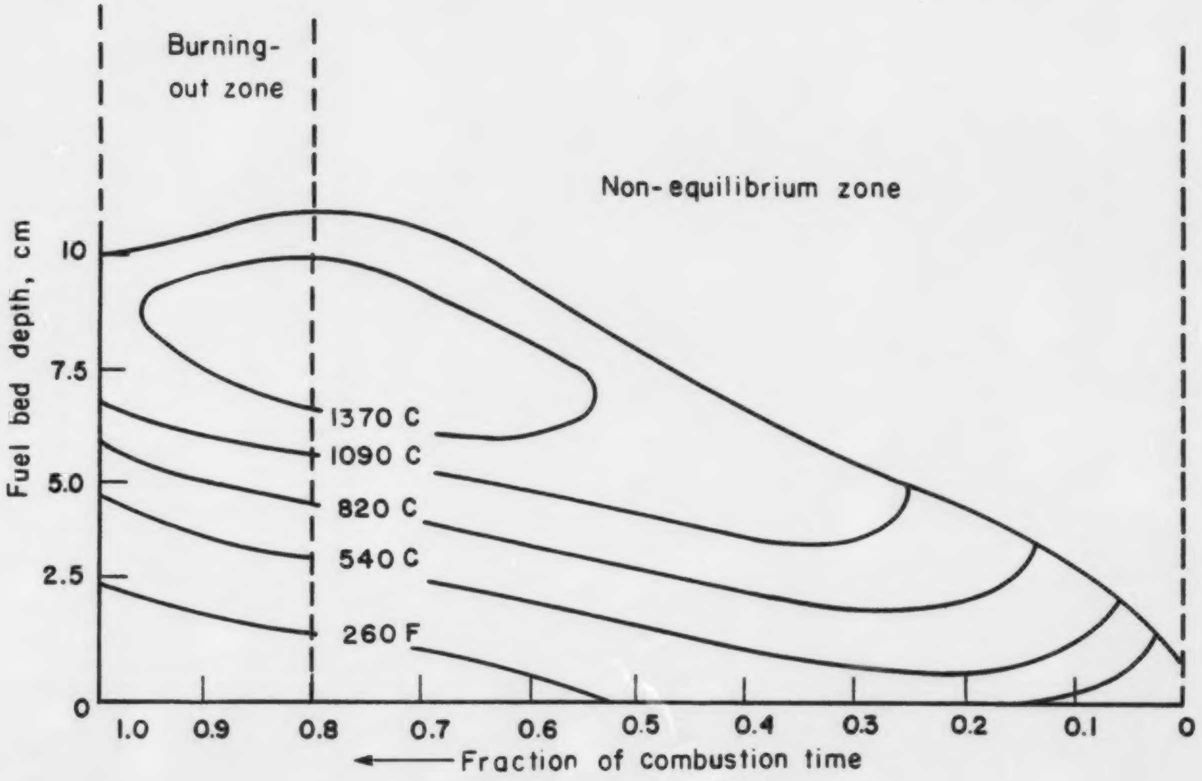

FIGURE I-6. FUEL BED ISOTHERMS FOR A 27 PERCENT VOLATILE AUSTRALIAN COAL (I-8)

I-7 lists the ultimate and proximate analyses of these samples. Sample No. 1 is the raw coal, Sample No. 2 is a lump of coal that was extracted from the stoker after about 4 minutes of burning, Sample No. 3 was extracted from the burning bed, and Sample No. 4 was removed from the bed after combustion was completed. These data indicate that the coal devolatilizes readily while carbon burnout proceeds more slowly. In addition, analysis of Sample Nos. 2 and 3 on a mass basis suggests that sulfur is burning at about the same rate as the carbon.

Fixed Bed Combustion. In another set of experiments with the southeastern Kentucky coal, bed depth was varied (1) to determine the optimum depth and (2) to optimize excess air. Thermocouples were located in the fuel bed and a gas sample probe and thermocouple were located above the bed. Measurements from these instruments along with visual observations were used in characterizing the stoker combustion. Maximum bed temperatures of 1370 C were observed for shallow beds (50 to 100 mm). Temperatures decreased with increasing bed depth. For bed depth of 200 mm or more, the average bed temperature was about 820 C with the higher temperatures occurring near the surface of the bed. Surface temperatures of 1260 C to 1370 C were measured for shallow beds and dropped to about 1100 C for the deeper beds.

These results were somewhat confusing in that classical fixed bed combustion indicates that the maximum flame temperature should occur at the flame front near the incoming air. However, this classical approach deals with a homogeneous bed. This is not the case for our model spreader as the coal continually devolatilizes, the rate decreasing for increasing bed depth. The maximum bed temperature occurs in the region of maximum reactivity. In the case of our model spreader stoker, this appears at or near the surface of the bed.

These results indicate that if limestone were to be effective in capturing SO_2, the stoker should be operated with a deep bed. (This would not be the case if most of the SO_2 comes off in suspension burning.) Temperatures are lower and there is more reactive surface. This supports

TABLE 7. PROXIMATE AND ULTIMATE ANALYSES (IN WEIGHT PERCENT) OF 4 COAL SAMPLES OBTAINED DURING COMBUSTION

	No. 1 Raw Coal	No. 2 Devolatized Coal Lump	No. 3 "Burning Bed"	No. 4 "Dead" Bed
Moisture	3.89	1.27	0.48	0.18
C	76.74	73.59	87.28	7.59
H	5.24	1.45	0.38	0.11
N	1.53	1.17	0.84	0.06
Cl	0.12	0.04	0.08	0.02
S	1.22	0.55	1.06	0.10
Ash	5.16	21.48	11.56	92.54
O_2	6.10	0.45	-1.68	-0.60
Vol.	36.94	5.62	2.68	1.41
Fixed carbon	54.01	71.63	85.70	5.87

our observations on the underfeed effort in which the limestone captured up to 70 percent of the sulfur in a deep bed. The effectiveness of the limestone in capturing sulfur that comes off with the volatiles remains questionable, however.

These results also suggest that the ratio of the overfire to underfire air should be a function of bed depth. If the coal (containing up to 40 percent volatiles and a somewhat lower percentage of the heating value) devolatilizes at or above the bed then, perhaps, an amount of air sufficient to burn these volatiles should be introduced in this region rather than through the underfire grate. An excess amount of air passing through the grate will cool the coal and retard the burnout of the carbon in the bed.

SECTION V

ALTERNATIVE FUELS FOR STOKERS--PELLETIZATION APPLICATIONS

During Phase I, no candidate "treated" industrial stoker-boiler fuels were identified that would be commercially available in the near future. However, some alternative fuels that have potential to become stoker fuels include:

- Most chemically cleaned coals
- "Deep" physically cleaned coals
- Limestone/coal mixtures
- Waste coal fines
- Refuse-derived fuels
- Wood wastes.

These fuels may require restructuring before they can be handled and fed properly into a stoker-boiler. Restructuring consists of a technique to upgrade fuel particle size. Such a technique must provide a restructured product that has:

- Variable particle size
- Mechanical strength, durability and weatherability similar to raw coals without the addition of large amounts of binder
- Controlled density
- No undesirable combustion characteristics
- Acceptable production concepts.

Some of the pelletization processes that were briefly explored show promise of meeting these requirements. Pelletization is not a new technology but the application of it to restructuring alternative stoker boiler fuels is. Consequently, some research effort will be required before techniques are fully developed. Prior to that, some potential market area must be created. The development of the limestone/coal pellet as a viable industrial boiler fuel may help create that market.

SECTION VI

CONCLUSIONS

Phase I experiments indicated that

- The conversion of fuel No to NO was less than 20 percent for stokers, somewhat less than pulverized coal firing
- POM levels for continuous combustion were significantly lower than for intermittment combustion
- Coals containing alkaline material retain significant amounts of sulfur in the ash. Intimate contact of the sulfur and alkaline material is essential to achieve substantial sulfur retention.

Additionally, no treated or modified coals were identified that could be evaluated during Phase I. As a result, a limestone/coal fuel pellet was developed. This pellet offers a potentially new means of sulfur control for industrial boilers. Further refinement of the pellet and evaluation in larger-scale equipment are needed to assess its full potential.

REFERENCES

I-1. Giammar, R. D., R. B. Engdahl, and R. E. Barrett. Emissions from Residential and Small Commercial Stoker-Coal-Fired Boilers Under Smokeless Operation. EPA-600/7-76-029, U.S. Environmental Protection Agency, Washington, D.C. 20460, October, 1976.

I-2. Jones, P. W., et al. Improved Measurement Techniques for Polycyclic Aromatic Hydrocarbons from Combustion Effluents. In: Carcinogenesis--A Comprehensive Survey, Vol 1, Polynuclear Aromatic Hydrocarbons, Chemistry, Metabolism, and Carcinogenesis, Raven Press, NY, 1976.

I-3. Merryman, E. L., S. E. Miller, and A. Levy. Reduction of NO in the Presence of Fly Ash. Combustion and Science Technology, 20, 160-163, 1973.

I-4. Gronhovd, G. H., P. H. Tufte, and S. J. Selle. Some Studies on Stack Emissions from Lignite-Fired Power Plants. Presented at the 1973 Lignite Symposium, Grand Forks, ND, May 9-10, 1973.

I-5. Maloney, K. L., P. K. Engel, and S. S. Cherry. Sulfur Retention in Coal Ash. KVB 8810-482-b, EPA Contract No. 68-02-1863, Industrial Environmental Research Laboratory, EPA, Research Triangle Park, NC, Nov, 1978.

I-6. Giammar, R. D., Weller, A. E., Locklin, D. W., and Krause, H. H., Experimental Evaluation of Fuel Oil Additives for Reducing Emissions and Increasing Efficiency of Boilers, U.S. Environmental Protection Agency Report No. 600/2-77-008b, Jan, 1977.

I-7. Stambaugh, E. P., et al., Combustion of Hydrothermally Treated Coals, EPA-600/7-78-068, U.S. Environmental Protection Agency, Washington, D.C., 20460, April, 1978.

I-8. Marskell, W. G., and C. W. Pratt, J. Inst. Fuel, 28, 212-21, 1952.

APPENDIX I-A

BINDER IDENTIFICATION AND RESTRUCTURING TECHNIQUE REVIEW

Binder Identification

A cursory review of the literature indicated that a number of binders could be used to pelletize the finely ground limestone and coal. Table I-A-1 lists those binders that were evaluated during this phase to produce pellets. Of these, cement and a latex emulsion were found to be the most desirable binders for the initial combustion tests because they were readily available, relatively inexpensive, easy to handle, and produced a pellet that remained intact during feeding and handling. No sophisticated test procedures were used to evaluate the mechanical strength properties of these pellets in this phase of the program. The pellet was dropped from 6 m, and if it remained intact, the pellet was considered satisfactory for the combustion evaluation experiments.

A review of the literature indicated that binders improve the strength of compacts and generally are classified as matrix type, film type, or chemical[*]. They usually take advantage of combinations of the forces due to solid bridges and/or immobile liquid bridges. Table I-A-1 lists some of the important characteristics of the binders tested. Highly viscous materials such as asphalt and pitch form immobile liquid bridges. These bridges between the compacted particles more fully exploit available adhesion and/or cohesion forces producing greater binding ability than the mobile bridges. This results in significantly stronger pellets. These immobile bridges fail by tearing apart the weakest bond, leaving the remainder intact. Such pellets tend to be maleable and deform rather than powder. However, many of these binders can be difficult to handle due to their viscous nature. A tempering process is frequently required during pellet production. Pitch for example is normally kept within a few degrees of its softening point during the entire operation.

---

[*] Komarek, Chem. Eng., 74 (25), 154 (1967).

As the initial thrust was to pelletize coals which have the potential to generate less SO_2, some potentially good binders containing high amounts of sulfur were not included. The tests of HTT coal and the initial limestone/coal (L/C) pellet tests in the model spreader were all performed with pellets utilizing a latex emulsion (Du Pont Hycal-S83) as a binder. This binder is a room temperature film former that utilizes both immobile liquid bridges and solid bridges to increase pellet strength. Pellets produced with this binder had sufficient mechanical strength for the model spreader, but were crushed severely when encountering the severe mechanical stresses of the underfeed stoker. Additionally, the pellets deteriorated when fed through the Battelle steam plant boiler coal-handling system.

Common cement as a binder produced a pellet with sufficient strength to survive the steam plant boiler system. Cement is a matrix-type binder which relies mostly on solid bridges formed when this "gel" sets to produce additional strength. Cement normally contains approximately 4 percent sulfur which would not effect SO_2 levels if used in small quantities. Pellets utilizing this binder exhibit excellent weathering characteristics as might be expected.

Though many potential binders were not tested, this investigation was terminated at this point as the primary objective of mechanical strength had been met. Many interesting aspects remain to be explored. What role could the binder or other additions play during combustion was virtually ignored in this work. Cement is an inert that increases the ash content, while polyvinyl alcohols are ash free and contain appreciable heating value. Substances as or in addition to the binder which volatilize readily in the combustion zone could alleviate this potential problem. For example fuel oils and motor oils do not produce strong pellets, but their addition with cement binder would increase the volatility and weatherability of the fuel. Disposal of used crankcase oil is a problem area due to its heavy metal content. When added to the L/C pellets these metals might be trapped in the ash, while significantly increasing the volatility of the fuel.

TABLE I-A-1. BINDERS TESTED FOR USE IN RECONSTITUTING FUELS

Binder	Type	Bonding Mechanisms	Comments
Water	Film	Mobile liquid bridges	Present in all pellets. Some fuels such as BTC produce very hard pellets with water alone.
Pitch-asphaltum	Film	Forms immobile liquid bridges hard pitch can form solid bridges	A high percentage is usually required. Also needs tempering but exhibits good weathering. Rejected due to handling problems and the amount of sulfur contained.
Lignin sulfonates	Film	Immobile liquid bridges	Readily available from papermills. Tends to produce maleable pellets. Rejected due to high sulfur content.
Starches (corn, potatoe)	Matrix	Solid bridges formed during crystallization	Inadequate pellet strength - brittle
Sugar	Matrix	Solid bridges formed during crystallization	Inadequate pellet strength - brittle
Sterotex (hydrogenated cottonseed oil)	Matrix	Solid bridges formed as oil recrystallizes	Relies on heat of pelleting process to melt the oil. Exhibits good weatherproofing as well as lubrication of the die. Combustible. Rejected - brittle pellets.
Fuel oil	Film	Mobile liquid bridges	Add heating valve and volatility . Good weatherproofing. Pellets too soft.
Motor oil	Film	Mobile liquid bridges	Add heating valve and volatility. Good weather proofing. Soft pellets.
Hycar 2800 (latex resin) X 138	Film	Immobile liquid and solid bridges	Required curing. Combustible, ash free strong pellet.
X 83	Film	Immobile liquid and solid bridges	Room temperature. Film former. Easier to handle and somewhat stronger than X 138. The binder used in the majority of model tests.
Elvanol (polyvinyl alcohol)	Film Matrix	Solid bridges during crystallization	Binder difficult to handle-moisture becomes critical. Ash free with significant heating value. Tests not conclusive.
Methyl Cellulose	Film Matrix	Solid bridges during crystallization	Similar to elvanol
Bentonite	Matrix Chemical	Solid bridges	No heating value - 100 percent ash. Produces a strong pellet but softens badly when wet. For final strength and weatherproofing it must be fired.
Cement	Matrix Chemical	Solid bridges formed when "gel" sets	No heating value - 100 percent ash. Produces a very strong pellet with excellent weatherability. Binder selected for Phase II experiments. Crushes when excess force applied.

Phase II. Control Technology Evaluation

CONTENTS

Page

LIST OF FIGURES . . . . .II- iii
LIST OF TABLES . . . . .II- iv
EXECUTIVE SUMMARY . . . . .II- v

I. BACKGROUND II-1

II. OBJECTIVE AND SCOPE. II-2

III. PLAN OF EXPERIMENTAL INVESTIGATION II-3

Facility. II-3

Stoker II-3
Fly Ash Reinjection System II-5
Overfire Air Jets. II-6
Boiler II-6
Sampling Ports II-6
Coal Handling System II-7

Coal Properties II-7

Pellet Production II-9

Material Preparation II-9
Processing Operations. II-9
Sampling Equipment and Procedures. II-11
Mass-Rate Determinations II-12

IV. EXPERIMENTAL RESULTS II-14

Stoker-Boiler Emissions II-14

Nitrogen Oxides. II-14
Sulfur Oxides. II-16
CO II-22
Particulate Loading. II-22
POM. II-22

Effect of Operating Variables on Emissions and Boiler Performance II-25

Excess Air II-25
Overfire Air II-34
Fuel-Bed Depth II-35
Boiler Load. II-36

PHASE II

CONTENTS (Continued)

Page

Fly Ash Reinjection. II-41
Coal Types II-42

Combustion System Design Modifications. II-44

Feed System. II-45
Grate Design II-45
Overfire Air II-46
Fly Ash Reinjection. II-47

SUMMARY. II-48
REFERENCES II-49
APPENDIX A - OVERFIRE AIR JETS

PHASE II

List of Figures

Page

Figure II-1. Schematic of the 8-MW Stoker-Boiler Facility. . . . II-4

Figure II-2. Pellet Procuction Process Flow Diagram. II-10

Figure II-3. NO Emission Levels as a Function of Excess Air For Washed, Run-Of-The-Mine Ohio Coal II-30

Figure II-4. NO Emission Levels as a Function of Excess Air For Unwashed Ohio Coal. II-31

Figure II-5. NO Emission Levels as a Function of Excess Air For Washed, Stoker Ohio Coal. II-32

Figure II-6. NO Emission Levels as a Function of Excess Air For LOW-Sulfur Kentucky Coal. II-33

Figure II-7. Fuel-Bed Temperature Distribution II-40

PHASE II

List of Tables

Page

Table II-1. Properties of Coals Fired in Phase II. II-8

Table II-2. Operating Variables Studied for System Characterization in Phase II II-13

Table II-3. Emission Summary Data of 8 MW_{th} Boiler Experiments II-15

Table II-4. Conversion of Fuel Nitrogen to NO for Coals Fired In Phases I and II II-17

Table II-5. Sulfur Balances for Steamplang Stoker Runs II-19

Table II-6. Distribution of Coal Ash Within The Stoker-Boiler System II-20

Table II-7. CHNS and Ash Analyses of Bes Ash, Reinjected Fly Ash, Cyclone Catch, and Filler Catch, Wt Percent. II-21

Table II-8. Coal Properties Affecting Particulate Loading. . . . II-23

Table II-9. Listing of POM Loadings, Particulate Loadings Carbon Particulate, CO Emission Level, and Smoke Opacity For Selected Runs. II-24

Table II-10. POM Quantification II-26

Table II-11. PAH Quantification µg Total Sample II-27

Table II-12. Comparison of Particulate Loading Between Optimal And Normal Stoker Operation Firing the Medium Sulfur Kentucky Coal. II-29

Table II-13. Smoke, CO, and Particulate Emissions for Two Overfire/Total Air Ratios II-35

Table II-14. The Effect of Boiler Load on Performance and Emission Levels II-37

Table II-15. SO_2 Levels As A Function of Boiler Load and Fuel Bed Temperature. II-39

Table II-16. Effect of Fly Ash Reinjection II-42

Table II-17. Boiler Efficiencies for Selected Coals. II-43

EXECUTIVE SUMMARY

Potential control concepts were identified and evaluated in the Battelle 8 MW_{th} (25,000 lb steam/hr) spreader stoker boiler. Control strategies were limited to:

- Use of compliance coals
- Combustion-system operational modifications
- Minor combustion-system design modification
- Use of treated coal (limestone/coal fuel pellet).

Flue-gas clean-up techniques were not considered. Criteria pollutants were used as the basis for evaluation.

The Phase II experiments have demonstrated that emission levels can be reduced by proper control of the stoker operating variables. In addition, the limestone/coal pellets have been demonstrated to offer potential for SO_2 control. In summary, the major findings are:

- The limestone/high-sulfur coal pellet showed a sulfur capture of about 75 percent for a Ca/S molar ratio of 7.
- Sulfur capture efficiencies of around 25 percent were noticed with some eastern bituminous coals.
- High excess air rates at low loads result in increased sulfur retention in the bed ash.
- CO and smoke levels can be controlled by providing adequate excess air. CO levels were low for all fuels tested except the limestone/coal pellet.
- Clinker formation may be a limiting factor in determining the minimum excess air rate.
- NO levels increase slightly with increase in excess air.
- Conversion of fuel nitrogen to NO was between 12 to 20 percent, assuming no thermal NO.

- An increase in overfire air/total air flow rate ratio reduces CO and smoke, the latter more significantly. Particulate loadings are also reduced with increased overfire air.
- NO is lower for inactive overfire air jets.
- Clinker formation occurs readily if bed depths become excessive, while the danger of burning the grates exists for operation with very shallow beds. Bed depths around 6.3 to 7.6 cm appear to be optimum for low ash coals.
- POM levels ranged from 13 to 24 $\mu g/Nm^3$. They were somewhat lower than those of the model spreader and only slightly higher than those from a 500 kW packaged boiler firing natural gas and fuel oil.
- A higher excess air rate is required for low-load than for partial- or full-load operation. A greater percentage of overfire air is required at low load. Low-load smoke can be reduced by a reduction in underfire air, coupled with attentive boiler operation.
- At full load, fly-ash reinjection increase boiler efficiency by 1.5 percent. However, particulate loadings were reduced by 10 to 25 percent by operating without fly-ash reinjection.
- The high-sulfur Ohio coals had to be fired at higher excess air rates than did the low-sulfur Ohio and Kentucky coals. The high-ash unwashed stoker coal and high moisture Illinois No. 6 coal could not be fired satisfactorily.

PHASE II. CONTROL TECHNOLOGY EVALUATION

SECTION 1

BACKGROUND

Industrial utilization of coal could be enhanced provided technology is made available to control air pollution emissions in an economically and environmentally acceptable manner. Control technologies to consider for industrial boilers include:

- Use of compliance coals
- Flue-gas cleanup
- Combustion-system operational modifications
- Combustion-system design modifications
- Use of treated or modified coals.

Depending on the specific stoker-boiler design and local air pollution regulation, one or more of these control technologies may be required to operate a boiler within the standards.

Data collected from industrial stoker boilers to evaluate the effect of these control technologies on their performance and emissions are limited. Before improvements in stoker firing can be achieved, baseline performance and emission level data must be generated so that pollution control potential can be accurately assessed.

SECTION 2

OBJECTIVE AND SCOPE

The overall objective of the Phase II program was to identify and evaluate potential concepts for control of emissions for full-scale industrial stoker boilers. For this phase of the program, control strategies were limited to operational and minor design modification of the Battelle 8 MW_{th} steamplant (25,000 lb steam/hr) spreader stoker boiler and to firing of low pollution coals (either naturally occuring or those that had been chemically or physically treated). Research on flue gas clean-up equipment was not within the scope of this program.

The operating variables that were investigated for system characterization studies included:

- excess air levels
- overfire air rate
- fuel-bed depth
- boiler load
- fly ash reinjection
- coal types (including treated coals).

Combustion design modifications were considered where the system characterization studies identified a need and extensive modification of the boiler was not necessary.

SECTION 3

PLAN OF EXPERIMENTAL INVESTIGATION

Phase II experiments focused on assessing emissions for a variety of stoker-boiler system operating variables. The experiments were conducted in a Battelle steam plant 8 MW_{th} spreader-stoker, boiler. Seven coals were fired in addition to the limestone/coal fuel pellets. Particulate loading, SO_2, NO, CO, particulate, and smoke emission levels, plus a limited number of POM measurements, were obtained.

FACILITY

The heating plant facility includes a coal-fired stoker utilizing balanced induced draft and forced draft fans for combustion air and a boiler for generating steam. This boiler was designed for a traveling-grate stoker and initially fired on gas and oil. During conversion to coal, the boiler was modified for spreader-stoker firing. The combustion particulate control system consists of two cyclone dust collectors. The ash from the grate discharge, grate siftings, and cyclone dust collectors is discharged into a hopper, which is periodically emptied into dump trucks. Figure II-1 is a schematic showing the relative locations of the system components.

Stoker

The stoker is a 2A-Hoffman "Firite" Pulsating Ash Discharge (PAD) type with a nominal feed-rate of about 910 kg/hr. This spreader stoker spreads coal uniformly on a level, specially designed, high-resistance grate. The coal is burned in a thin layer on top of the ashes and in suspension.

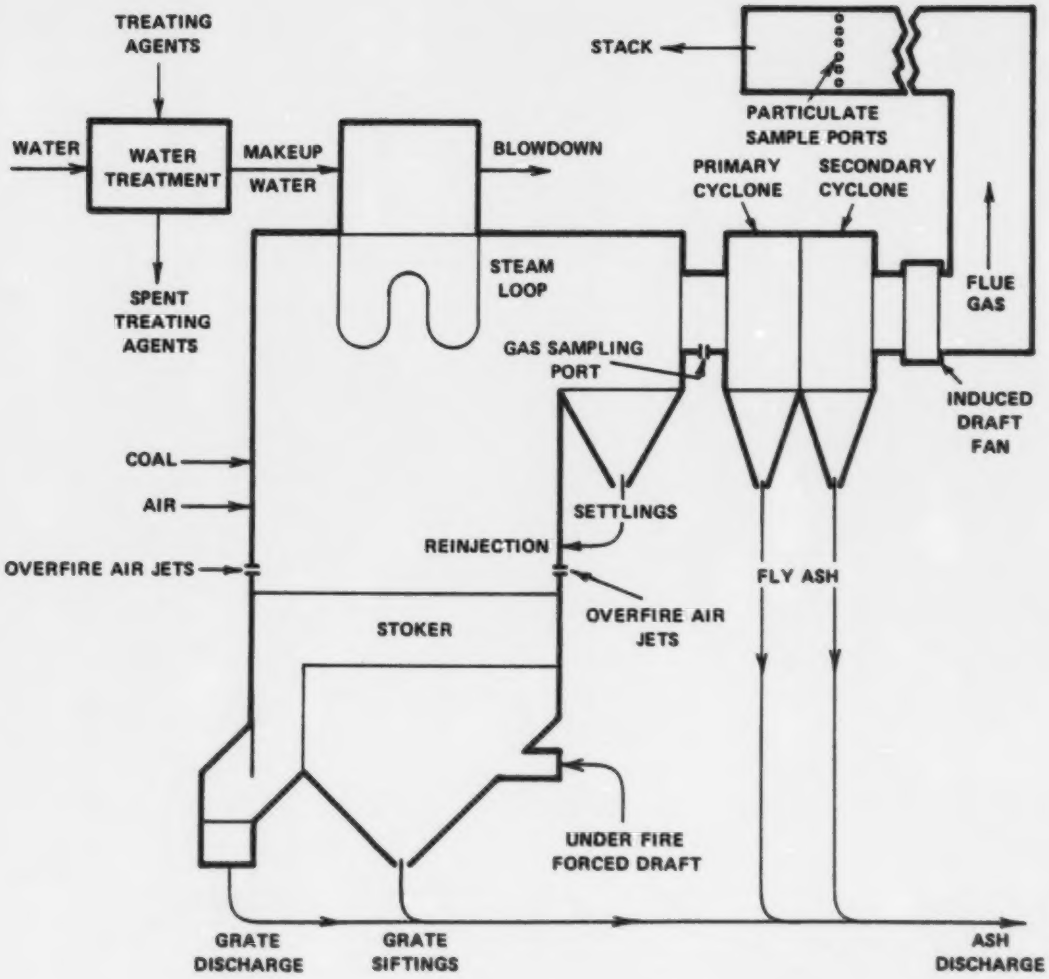
TREATING AGENTS
WATER
WATER TREATMENT
MAKEUP WATER
BLOWDOWN
SPENT TREATING AGENTS
STACK
PARTICULATE SAMPLE PORTS
PRIMARY CYCLONE
SECONDARY CYCLONE
STEAM LOOP
FLUE GAS
GAS SAMPLING PORT
INDUCED DRAFT FAN
COAL
AIR
SETTLINGS
REINJECTION
OVERFIRE AIR JETS
FLY ASH
STOKER
OVERFIRE AIR JETS
UNDER FIRE FORCED DRAFT
GRATE DISCHARGE
GRATE SIFTINGS
ASH DISCHARGE

FIGURE II-1. SCHEMATIC OF THE 8-MW STOKER-BOILER FACILITY

Coal feed is regulated by changing the length of stroke of the reciprocating feed plates. Length of throw is regulated by the speed of the distributor blades. Uniformity of distribution is a natural consequence of the underthrow principle used exclusively by Hoffman. Distribution is modified by changing the pitch angle of the circular tray.

The grate surface area is 5 m^2 (2.4 m by 2.1 m). Incorporated in this area are 18 individual grates. The six grated positioned in the center are 23 cm by 99 cm, while the remaining twelve grates located on the sides of the boiler are 30 cm by 99 cm in dimension. The 30 cm-wide grates have four rows of tubes (16 in each row) and each tube has five 0.635 cm flower-like openings on the grate surface to distribute the air. The 23 cm grates have three rows of tubes (16 in each row) with similar holes.

The grate is activated periodically to discharge ashes according to a predetermined time cycle. The time interval between discharge periods is varied manually or automatically. The amount of ash discharged per cycle is adjusted manually to suit the particular type of coal and usually requires no further adjustment for load change.

The grate assembly is energized by a revolving eccentric weight in such a manner that the resulting reciprocating motion or pulsations move the ash bed toward the discharge end. The rotating eccentric weight shaft is driven through speed changing devices either from the line shaft or by a separate motor. The speed changer adjusts for the optimum speed, after which the speed setting remains fixed. This adjustment determines the distance the grate moves in each pulsation.

Fly Ash Reinjection System

Fly ash is collected in hoppers under the boiler passes and is reinjected to the furnace to complete its burning. Venturi type nozzles (Hoffman design) entrain the fly ash using air discharged from the overfire air blower. The fly ash nozzles do not need any special attention except to keep the nozzle piping free and clear. During operation, the minimum air pressure that will insure continuous trouble-free operation is used.

Fly ash is reinjected through two nozzles located at the rear of the boiler. These nozzles are approximately 30 cm from the sidewalls and 25 cm above the grate.

Overfire Air Jets

There are four overfire air jets in the rear and five in the front of the furnace. These are located approximately 25 cm above the grate. The maximum overfire air pressure attainable is approximately 40 cm. W. G. The various overfire air jets have individual and branch dampers adjustable by hand. The minimum air pressure that will provide turbulence in the furnace is selected.

Boiler

The water tube gas/oil fired boiler is a Keeler Type MKB manufactured by E. Keeler Company, Williamsport, Pennsylvania. The boiler was installed at Battelle-Columbus in 1964 and altered for coal firing in 1976. It has an operating pressure of 860 kPa (125 psig) with an ASME Power Test Code heating surface of 383 m^2 utilizing a furnace volume of 40 m^3. The boiler can operate at a capacity of 8 MW_{th}, continuous, with a heat release rate of 845,615 $kJ/m^3/hr$ (22,700 $Btu/ft^3/hr$).

Sampling Ports

Figure II-1 shows the relative location of the particulate and gas emissions sampling ports. Particulate sampling ports were located in the breaching between the induced draft fan and the stack. This specific location of the breaching is common to the three Battelle boilers, the other two of which fire gas only. Most tests were conducted when only the stoker-boiler was on-line. On occasion, one of the gas-fired boilers was in operation, but the particulate loading contribution from this boiler is negligible in comparison to that of the stoker-boiler.

The gas sampling port was located at the boiler outlet immediately upstream of the dust collector and induced-draft fan.

Coal Handling System

Coal is initially fed into a concrete pit from a front-end loader or dumped by truck. A vibrating feeder inside the pit delivers coal to the bottom of a bucket elevator. A flop-gate at the top of the 15-m bucket elevator diverts the coal into a silo (for storage) or onto a screw conveyor. The screw conveyor empties into a day hopper located directly above the stoker. Coal is gravity fed through a conical chute to the two stokers.

Throughout the coal-handling system, the coal can encounter significant mechanical stresses that may create an excessive amount of fines.

COAL PROPERTIES

Eight coals were fired in the steamplant boiler during Phase II experiments, including the limestone/coal fuel pellet (Ca/S molar ratio of 7). Table II-1 lists ultimate and proximate analyses, heating values, ash-fusion temperature, and size consist for these coals. The size consist was determined before the coal was introduced into the handling system. These coals were selected to provide a range of fuels suitable for industrial stoker-boiler firing. Based on Phase I, the fuel pellet was selected as the treated fuel with the greatest potential to become a viable SO_2 control in the near future.

The Ca/S molar ratio of 7 was selected to assess whether the concept of a limestone/pellet had any potential as an SO_2 control in an industrial system without optimizing the pellet. Phase I development of the fuel pellet concept indicated that optimization of the pellet in terms of

- binder selection
- coal and limestone size distribution
- size and shape

may allow for the reduction of Ca/S ratio without significant reduction in SO_2 retention. Program plans were to optimize the pellet as part of Phase III, provided the firing of the Ca/S = 7 pellet showed promise.

TABLE II-1. PROPERTIES OF COALS FIRED IN PHASE II

Coal Type	Proximate Analysis (As Received), %			Ultimate Analysis (As-Received), %							Heating Value, KJ/g	Ash-Fusion Temperature, F (Initial Deformation)		Fuel Size Consist, % less than 3mm
	Volatiles	Fixed Carbon	Ash	Moisture	Carbon	Hydrogen	Nitrogen	Chlorine	Sulfur	Oxygen (Difference)		Reducing	Oxidizing	
Low-S Ohio	33.12	47.59	9.60	9.69	64.81	4.26	1.26	0.05	0.70	9.63	26.7	NA*	1480+	7
Medium-S Kentucky	38.20	53.15	4.95	3.70	76.96	5.15	1.26	0.14	1.38	6.46	32.1	1160	1340	12
Stoker-grade, washed Ohio	37.84	42.58	10.34	9.24	63.40	4.54	1.21	0.06	3.00	8.21	26.6	1120	1350	6
Stoker-grade, unwashed Ohio	36.34	40.95	18.50	4.21	59.98	4.23	1.09	0.06	3.94	7.99	25.6	1140	1360	17
Run-of-the Mine, washed Ohio	38.89	43.47	8.60	9.04	65.02	4.56	0.98	0.04	3.19	8.57	27.3	1100	1320	16
Low-S Kentucky	36.87	52.83	7.71	2.59	75.42	5.03	1.53	0.11	0.89	6.72	31.3	1360	1480	12
Illinois No. 6	37.30	39.97	8.63	14.10	60.52	4.23	1.10	0.14	3.46	7.82	25.3	1100	1270	6
Limestone/high-Sulfur coal pellet	39.20	NA	45.60	12.60	29.70	1.54	0.48	--	1.96	8.64	9.9	NA	NA	NA

* NA - Not Available.

PELLET PRODUCTION

Approximately 100 tons of limestone/coal pellets with a Ca/S molar ratio of 7 were produced for evaluation in the steamplant spreader stoker boiler. Figure II-2 is a flow diagram for the pellet production process. There are many components in this process with the major element being the pellet mill.

Pellet formulation was the same as in Phase I, namely

- Illinois No. 6 coal (48 percent)
- Piqua limestone (47 percent)
- Cement binder (5 percent)

Material Preparation

As received, the limestone and cement required no further preparation. The coal required size reduction from -2.5 cm to -20 mesh which was accomplished in a Model 2W Mikropulverizer hammermill. (This mill processed about 400 kg/hr of raw coal and was operated about 12 hrs/day.)

Processing Operations

In addition to coal grinding and materials handling, the pellet process consisted of the following four separate operations:

(1) Blending
(2) Pelleting
(3) Size Classification
(4) Drying

Blending. The coal, limestone, cement, and water were thoroughly blended prior to introduction into the pellet mill. A 0.2 m^3 Voeller batch mixer, typically used for batch mixing in the glass industry, was used. The capacity of this mixer, 800 kg/hr, was the limiting factor in the pellet production process.

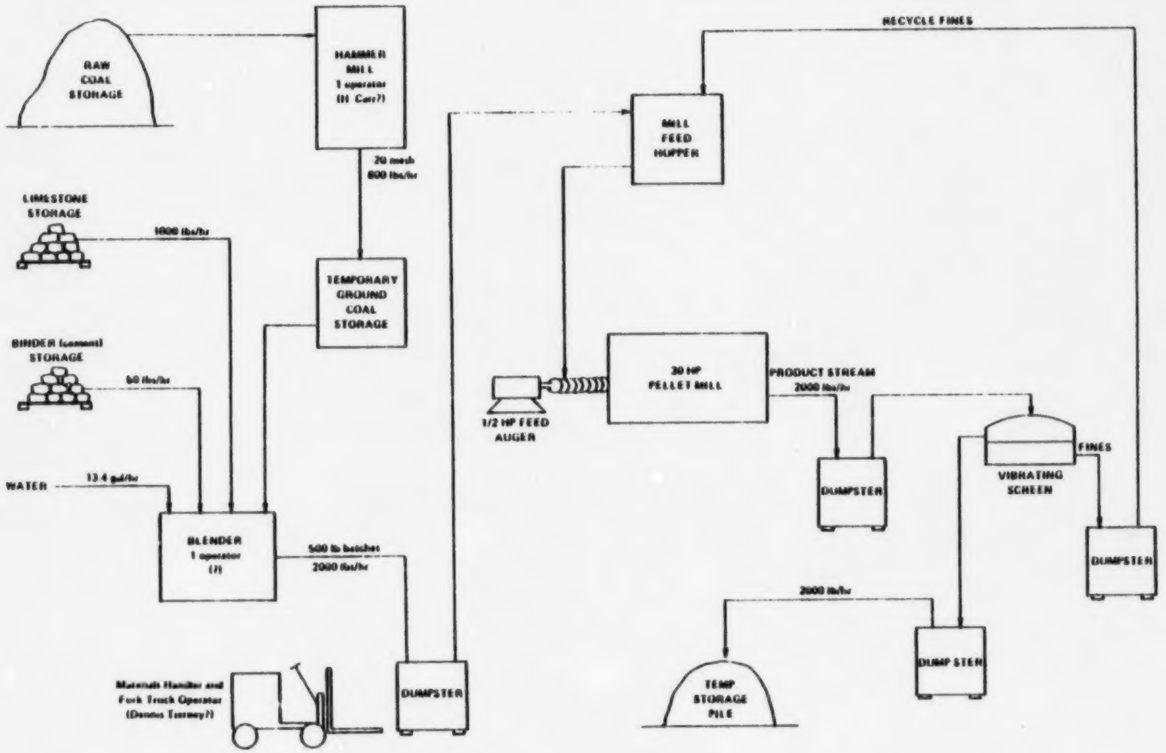
RAW COAL STORAGE
HAMMER MILL 1 operator (H Carr?)
20 mesh
800 lbs/hr
LIMESTONE STORAGE
1000 lbs/hr
TEMPORARY GROUND COAL STORAGE
BINDER (cement) STORAGE
50 lbs/hr
WATER
13.4 gal/hr
BLENDER 1 operator (?)
500 lb batches
2000 lbs/hr
Materials Handler and Fork Truck Operator (Dennis Tierney?)
DUMPSTER
MILL FEED HOPPER
RECYCLE FINES
1/2 HP FEED AUGER
30 HP PELLET MILL
PRODUCT STREAM
2000 lbs/hr
DUMPSTER
VIBRATING SCREEN
FINES
DUMPSTER
2000 lb/hr
DUMP STER
TEMP STORAGE PILE

FIGURE II-2. PELLET PRODUCTION PROCESS FLOW DIAGRAM

Pelleting. Pellets, nominally 1.3 cm in diameter and 1.9 cm long, were produced with a California Pellet Mill (22 kW Master Model). There were a number of operational problems with this mill, primarily associated with roller damage due to coal influx into the bearing lubricant. Once these were resolved, the mill produced pellets at a rate of about 1200 Kg/hr.

Size Classification. The mill output contained about 10 percent fines along with the pellets. These fines were removed with a model ME 38 Midwestern Screen Separator and recycled back to the mill.

Drying. After separation, the pellets required drying, which, because of the relatively small batch quantities could be done in air. However, on a larger scale production or during inclement weather, air drying might be inadequate and another method of drying would be required.

Materials Handling. The pellet production operation was highly labor intensive requiring six men for operation. Most of this labor was associated with materials handling, especially in the blending operation. Larger scale operations with automation would significantly reduce the labor intensity.

Summary. The 100 tons of pellets were produced for about $600/ton. A large-scale, mine-mouth operation would reduce these costs significantly to about $15/ton. However, we experienced significant maintenance and "downtime" that must be minimized for this operation to be economically attractive.

Sampling Equipment and Procedures

Sampling equipment and procedures were similar to those of the Phase I experiments with one exception. Stack gases were transported through a heated sampling line, about 6-m long, before filtering and moisture removal rather than filtering the particulate and condensing the moisture in a trap adjacent to the stack. Analysis procedures were also similar.

Mass-Rate Determinations

Bell mouth orifices were installed on inlets of both force-draft fans, one supplying the undergrate air and the other supplying overfire air. These orifices provided a measure of the total air-flow rate into the boiler. Steamflow rates were also determined from an orifice. The coal feed rate was determined by measuring the time required to displaced a fixed volume of coal (in the day hopper). Fly ash reinjection rates were determined by collecting the reinjection fly ash in drums and weighing the contents for a specific collection time.

SECTION 4

EXPERIMENTAL RESULTS

The performance of the stoker boiler and the emissions that it generates depend on a number of factors, including the combustion operating parameters and the properties of the coal. Table II-2 outlines the operating variables investigated during this Phase II effort. Table II-3 summarizes the gaseous and particulate emissions generated during the firing of the eight different coals for the conditions listed. Because there are few measurements to characterize the fuel bed other than visual observations, qualitative observations are necessary to describe the fuel-bed combustion. Accordingly, such observations are included with the experimental measurements to interpret the data.

In the subsections below, a general discussion of the emissions generated from the steam plant stoker is given first. Then, the effect of stoker boiler operating variables on emissions and boiler performance is discussed. Finally, based upon observations of the stoker-boiler system and analysis of the data, combustion modifications that have the potential to reduce emissions and improve boiler performance are identified.

STOKER-BOILER EMISSIONS

The criteria emissions are discussed in terms of coal properties.

Nitrogen Oxides

Nitrogen oxide emissions are largely a function of the nitrogen content of the coal. Unfortunately, coal cleaning or treatment techniques do not remove nitrogen; in fact as a result of reducing the ash content, the percentage of nitrogen in the coal appears to be increased. This emission can be controlled by operating a low excess air levels.

TABLE II-2. OPERATING VARIABLES STUDIED FOR SYSTEM CHARACTERIZATION IN PHASE II

- EXCESS AIR
  - Minimum levels
  - Optimum operating levels from both an emissions and efficiency viewpoint

- OVERFIRE AIR RATE
  - Jets inactive
  - Optimum rate from an emissions viewpoint

- FUEL BED DEPTH
  - Maximum
  - Minimum
  - Optimum

- BOILER LOADS
  - Low load (30 to 40 percent of full load)
  - Partial load
  - Full load

- FLY ASH REINJECTION
  - Maximum
  - Partial
  - None

- COAL TYPES
  - Size distribution
  - Ash content
  - Ash-fusion properties
  - Sulfur levels
  - Treated coal: limestone/coal pellet

TABLE II-3. EMISSION SUMMARY DATA OF 8 MW_{th} BOILER EXPERIMENTS

No.	Coal Type	% Full-Load	Overfire Air / Total Air Ratio	Flue Gas Composition						CO at 3% O_2, ppm	SO_2 at 3% O_2, ppm		Fuel S Emitted, %	NO at 3% O_2, ppm		% Conversion of Fuel N to NO	Particulates ng/J	POM g/Nm3
				O_2, %	CO_2, %	CO, ppm	SO_2, ppm	NO, ppm	Smoke Opacity, %		Computed into System	Measured Emissions		Computed into System	Measured Emissions			
SP-1	Low-S Ohio	86	0.14	8.0	11.0	50	360	--	10	70	625	505	80.8	2565	—	--	110	--
SP-2	Low-S Ohio	58	0.23	7.5	11.4	60	350	--	4-5	80	625	470	75.2	2565	—	--	77	—
SP-3	Medium-S Kentucky	84	0.16	7.0	12.4	34	700	--	7	44	1010	910	90.1	2110	--	--	110	—
SP-4	Low-S Ohio	84	0.18	7.7	13.0	25-30	320	230	4	34-41	625	440	70.4	2565	320	12.5	73	—
SP-5	Low-S Ohio	38	0.32	11.8	8.4	70	190	185	5	140	625	375	60.0	2565	365	14.2	65	--
SP-6	Stoker-grade, washed Ohio	86	0.17	8.0	11.2	28-44	1800	280	6	38-60	2635	2475	93.9	2430	385	15.8	190	--
SP-7	Stoker-grade, unwashed Ohio	84	0.15	10.8	9.0	32-72	2200	250	7-11	52-120	3650	3635	99.6	2310	413	17.9	—	—
SP-8	Run-of-the-mine, washed Ohio	84	0.17	9.0	10.5	40-72	1800	230	6-9	60-80	2750	2740	99.6	1930	350	18.1	240	—
SP-9	Stoker-grade washed Ohio	90	0.16	9.4	10.1	40-68	1400	240	6	63-107	2635	2192	83.2	2430	375	15.4	220	14
SP-10	Run-of-the-mine, washed Ohio	88	0.18	9.0	10.8	35-50	1900	245	6	52-75	2750	2825	(102.7)	1930	365	18.9	290	13
SP-11	Low-S Kentucky	90	0.18	8.5	10.4	35-45	340	250	4	50-65	665	490	73.7	2615	360	13.8	73	22
SP-12	Low-S Kentucky	88	0.16	8.8	10.4	25-35	330	235	2	37-52	665	488	73.4	2615	350	13.4	56	26
SP-13	Run-of-the-mine, washed Ohio	80	0.17	9.3	9.8	30-45	1500	250	3	60-70	2750	2310	84.0	1930	385	19.9	150	22
SP-14	Run-of-the-mine, washed Ohio	82	0.19	9.8	9.4	40-68	1300	240	4	65-110	2750	2092	76.1	1930	386	20.0	170	--
SP-15	Stoker-grade, washed Ohio	80	0.18	10.0	9.8	20-35	1350	230	2	33-58	2635	2230	84.6	2430	380	15.6	160	22
SP-16	Stoker-grade, washed Ohio	84	0.19	9.2	10.2	20	1700	260	3	31	2635	2602	98.7	2430	398	16.4	180	12
SP-17	Illinois No. 6	68	0.19	9.5	10.2	36-40	1900	230	5	57-63	3190	2974	93.2	2320	360	15.5	--	--
SP-18	Limestone/high-S coal pellet	64	0.13	11.2	10.0	420-600	560	145	22	792-1132	4035	1057	26.2	2255	274	12.2	610	21
SP-19	Limestone/high-S coal pellet	60	0.16	11.8	9.5	1000	515	140	25	2010	4035	1035	25.6	2255	281	12.5	960	174

Table II-4 gives the conversion of fuel nitrogen to NO for coals fired in both Phases I and II. The conversion was based on the assumption that no thermal NO was present. For the steamplant boiler, the fuel nitrogen conversion ranged from 12 to 20 percent with an average of 15 percent. The rate of fuel N conversion for the model spreader runs ranged from 8 to 20 percent with an average of about 12 percent. This is a somewhat lower rate of fuel N conversion than observed in the steamplant stoker. This difference may be attributable to the higher percentage of bed burning in the model spreader than in steamplant stoker and also to the higher bed temperatures in the steamplant stoker.

The rate of fuel nitrogen conversion for the underfeed stoker is even lower, averaging about 9 percent. This extremely low rate of fuel N conversion may be attributed to the inherent staged combustion in the operation of an underfeed stoker and the low excess air combustion occurring in the bed.

Sulfur Oxides

Sulfur oxide emissions are largely a function of the sulfur content of the fuel. Sulfur is captured in the ash as a sulfate or emitted from the stack as SO_2, plus some small fraction (generally only a few percent) as SO_3. Because the fate of sulfur within a stoker boiler system is fairly well bounded, one might expect reasonable complete sulfur balances. However, review of data in Table II-5, and earlier work by BCL(II-1), Gronhovd(II-2), and Maloney(III-3), indicates that good sulfur balances from coal combustion are difficult to achieve. This is because accurate mass balances must be made throughout the entire system. From a practical sense, only estimates of mass balances can be reasonably achieved. Furthermore, sulfur balances are determined from analysis of relatively small samples that may not be representative of the total mass in question.

The scatter of the stoker data, as shown in Table II-5, is similar to that obtained by other researchers and reflects a general problem of achieving sulfur balances. Of primary interest is determining the amount of sulfur that can be retained with the ash, thus reducing the amount of SO_2 emitted. Phase I results, and those of Gronhovd and

TABLE II-4. CONVERSION OF FUEL NITROGEN TO NO FOR COALS FIRED IN PHASES I AND II

Coal	Nitrogen Content MAF, %	Fuel N Conversion, %
(a) Steamplant Stoker		
Low-S Kentucky	1.7	13.4
Low-S Kentucky	1.7	13.8
Low-S Ohio	1.6	12.5
Low-S Ohio	1.6	14.2
Stoker Grade, Washed, Ohio	1.5	15.8
Stoker Grade, Washed, Ohio		15.4
Stoker Grade, Washed, Ohio		15.6
Stoker Grade, Washed, Ohio		16.4
Stoker Grade, Unwashed, Ohio	1.4	17.9
Medium-S Kentucky	1.4	10
Illinois No. 6	1.4	15.5
ROM washed, Ohio	1.2	18.1
ROM washed, Ohio	1.2	18.1
ROM washed, Ohio	1.2	20.0
L/C Pellet, Ca/S=7	1.1	12.5
L/C Pellet, Ca/S=7	1.1	12.2

TABLE II-4. (continued)

(b) Model Spreader		
Western Bituminous	1.6	11
Western Bituminous	1.6	9
Western Bituminous	1.6	8
Low-S Kentucky	1.6	18
Low-S Kentucky	1.6	12
Low-S Kentucky	1.6	11
Low Volatile W. Virginia	1.6	13
Low Volatile W. Virginia	1.6	10
Western Kentucky, Unwashed	1.5	8
Hydrothermal	1.4	10
Eastern Kentucky	1.4	15
Eastern Kentucky	1.4	10
Eastern Kentucky	1.4	7
Illinois No. 6	1.2	15
Illinois No. 6	1.2	14
Illinois No. 6	1.2	17
L/C Pellets, Ca/S=4	1.2	13
L/C Pellets, Ca/S=7	1.1	12
L/C Pellets, Ca/S=7	1.1	12
L/C Pellets, Ca/S=7	1.1	8
L/C Pellets, Ca/S=7	1.1	11
Lignite	1.0	14
Lignite	1.0	20
(c) Underfeed Stoker		
E. Kentucky	1.4	10
Illinois No. 6	1.2	9
Lignite	1.0	8
Western Subbituminous	.9	9

Maloney, indicate that significant amounts of sulfur can be retained in the ash because of the presence of alkaline mineral compounds in the coal. However, Maloney's data, as well as data generated in Phases I and II, suggest that lesser amounts of sulfur may be retained in the ash, even without the presence of alkaline material.

As indicated in Table II-5, for Runs SP-1 through SP-17, all eastern coals, the fuel sulfur emitted as SO_2 ranged from 60 to 103 percent, with an average of 85 percent. This compares with Maloney's data, which indicated that for stoker firing eastern coals, the average fuel sulfur emitted was 90 percent.(II-3) Furthermore, the data in Table II-5 indicate the lowest value of fuel sulfur emitted as SO_2 occurred at low load operation while higher values occurred at higher boiler loads, confirming Maloney's observation.

However, for these same runs, the average amount of fuel sulfur retained in the ash was about 2 percent. The sulfur retention in the ash was based on the sulfur content of the bottom ash. The bottom ash provides a fairly accurate indication of the residual ash constituents as it accounts for about 80 percent of the coal ash input, as shown in Table II-6. Table II-6 indicates that the other major deposit of ash is from the fly ash reinjection hopper. A comparison of the CHNS and ash analyses from the ash discharge (bottom ash) and fly ash reinjection hoppers, shown in Table II-7, indicates a reasonably close agreement; sufficiently close, that using the bottom ash as representative of all the coal is reasonably accurate. Intuitively, it would appear that the sulfur analysis of the bed ash would be reasonably accurate making the SO_2 measurement either from the monitor or the procedure suspect. Calibration of the SO_2 measurement against Method 6 wet chemistry techniques, indicate that the SO_2 monitor did provide reasonably accurate results.

The data in Table II-5 indicate sulfur balances for runs with higher sulfur coals were superior to those of runs with the lower sulfur coals. This observation suggests that there may be some fixed amount of sulfur that cannot be accounted for; for example, fuel sulfur in the coal analyses or some fixed amount of SO_2 that is removed in the sampling system.

TABLE II- 5. SULFUR BALANCES FOR STEAM-PLANT STOKER RUNS

	SO_2 (ng/J)			
Run No.	Computed As Fuel S	Measured As SO_2	Retained in Bedash	Unaccounted, %
SP-1	524.6	425.7	8.6	17
SP-2	524.6	395.6	4.3	23
SP-3	860	774	5.59	9
SP-4	524.6	369.8	--	29
SP-5	524.6	318.2	4.3	39
SP-6	2253.2	2115.6	25.8	5
SP-7	3078.8	3065.9	--	1
SP-8	2339.2	2330.6	21.5	0
SP-9	2253.2	1874.8	8.6	17
SP-10	2339.2	2403.7	73.1	-6
SP-11	567.6	421.4	4.3	25
SP-12	567.6	417.1	4.3	25
SP-13	2339.2	1965.1	90.3	12
SP-14	2339.2	1780.2	12.9	23
SP-15	2253.2	1909.2	86	12
SP-16	2253.2	2223.1	--	0
SP-17	2730.5	2008.1	430	10
SP-18	3956	946	2365	16
SP-19	3956	1032	2021	23

TABLE II-6. DISTRIBUTION OF COAL ASH WITHIN THE STOKER-BOILER SYSTEM

	RUN SP-12					RUN SP-13				
Ash Sample Location	Sample Collection Rate, Kg/hr	Analysis of Sample, %		Ash Rate, Kg/hr	Distribution of Ash, %	Sample Collection Rate, Kg/hr	Analysis of Sample, %		Ash Rate Kg/hr	Distribution of Ash, %
		C	Ash				C	Ash		
Ash Hopper	52.16	7.1	93	48.08	89	109.8	17.1	80	87.54	79
Grate Siftings	0.32	7.0	93	0.32	1	0.45	6.4	95	0.45	0
Flyash Reinjection	12.7	59	25	3.2	6	31.75	29	71	22.68	20
Cyclone	1.27	44.4	55	0.68	1	0.18	24	74	0.136	0
Method 5 Catch	1.81	12.1	84	1.54	3	4.63	10	24	1.13	1
Total Measured	68.5			53.5	100	146.97			112.04	
Calc. From Coal Feed Rate and Analysis				77.1					95.26	

	RUN SP-15					RUN SP-17					RUN SP-18				
Ash Sample Location	Sample Collection Rate, Kg/hr	Analysis of Sample, %		Ash Rate Kg/hr	Distribution of Ash, %	Sample Collection Rate, Kg/hr	Analysis of Sample, %		Ash Rate Kg/hr	Distribution of Ash, %	Sample Collection Rate, Kg/hr	Analysis of Sample, %		Ash Rate Kg/hr	Distribution of Ash, %
		C	Ash				C	Ash				C	Ash		
Ash Hopper	56.25	3.2	98	55.34	83	94.35	--	70	66.23	85	884.52	6.4	86	762.5	78
Grate Siftings	0.41	2.1	99	0.41	1	0.91	--	95	0.91	1	1.36	5.1	93	1.36	--
Flyash Reinjection	11.8	30.2	71	8.16	13	14.52	--	70	9.53	14	228.16	6.1	88	201.85	21
Cyclone	0.45	18.8	76	0.36	1	0.68	--	70	0.45	1	0.59	9.2	83	0.45	--
Method 5 Catch	4.99	8.8	23	1.09	2	NA	--	--	--	--	13.61	6.8	85	11.34	1
Total Measured	73.94			65.32		110.68	--		78.02	--	1128.1			972.97	
Calc. From Coal Feed Rate and Analysis				108.86					85.73					1011.53	

TABLE II-7. CHNS AND ASH ANALYSES OF BED ASH, REINJECTED FLY ASH, CYCLONE CATCH, AND FILLER CATCH, WT PERCENT

Run No.	Bed Ash					Reinjected Flyash					Cyclone Catch					Filter Catch				
	C	H	N	S	Ash	C	H	N	S	Ash	C	H	N	S	Ash	C	H	N	S	Ash
SP-1	22.7	0.2	0.1	0.1	75.3	31.6	0.2	<0.1	0.21	69.5	40.2	0.4	0.2	0.23	61.4	11.3	2.2	0.28	3.1	66
SP-2	10.1	0.1	<0.1	0.04	88.8	48.5	0.4	0.1	0.19	49.2	30.9	0.3	0.1	0.28	64.1	18.7	2.9	0.43	3.5	12
SP-3	1.7	0.1	<0.1	0.17	98.6	41.3	0.6	0.2	5.32	46.6	33.7	0.3	0.1	0.53	59.9	16.1	2.3	0.37	7.4	49
SP-4	--	--	--	--	--	65.2	0.3	0.2	0.88	21.5	--	--	--	--	--	16.0	2.3	0.30	4.11	54
SP-5	7.7	0.1	0.1	0.03	90.9	46.3	0.5	0.3	0.53	39.0	26.9	0.6	0.1	0.28	62.2	37.6	4.05	0.87	3.76	35
SP-6	10.5	0.2	0.1	0.32	90.3	51.7	0.7	0.3	1.29	37.9	25.9	0.3	0.1	0.61	71.9	4.83	1.7	0.12	12.1	28
SP-7	--	--	--	--	--	--	--	--	--	--	--	--	--	--	--	--	--	--	--	--
SP-8	3.9	0.1	<0.1	0.37	96.3	48.8	0.5	0.2	1.45	42.9	23.3	0.3	0.1	0.95	70.9	10.3	4.32	0.31	12.2	24
SP-9	1.7	0.1	<0.1	0.10	98.6	50.7	0.6	0.2	1.33	37.6	31.5	0.3	0.1	0.84	62.8	8.73	6.07	0.21	12.33	23
SP-10	9.2	0.4	0.1	1.14	90.6	50.9	0.7	0.2	1.26	41.6	34.2	0.7	0.1	1.07	56.6	5.1	3.4	<0.1	15.0	22.4
SP-11	10.6	0.2	0.1	0.07	89.9	--	--	--	--	--	47.3	0.4	0.3	0.41	52.4	14.6	1.6	<0.1	7.2	81.6
SP-12	7.1	0.1	<0.1	0.1	92.6	59.0	0.3	0.1	0.4	24.9	44.4	0.3	0.1	0.5	54.8	12.1	1.9	<0.1	11.9	83.7
SP-13	17.1	0.2	0.1	1.40	79.8	29.4	0.3	0.2	0.72	71.4	20.9	0.2	0.1	0.95	70.9	2.26	2.44	<0.1	17.4	*
SP-14	3.7	0.4	0.1	0.17	96.8	--	--	--	--	--	--	--	--	--	--	3.23	3.4	<0.1	7.7	*
SP-15	19.2	0.2	0.1	1.09	82.4	30.2	0.2	0.1	0.68	71.4	18.8	0.2	0.1	0.77	76.2	3.06	2.2	<0.1	8.1	*
SP-16	1.8	0.2	<0.1	0.18	98.5	--	--	--	--	--	--	--	--	--	--	3.08	1.6	<0.1	6.1	*
SP-17	27.6	0.2	0.2	6.34	70.0	--	--	--	--	--	--	--	--	--	--	--	--	--	--	--
SP-18	6.1	0.3	0.1	2.33	86.4	6.1	0.1	<0.1	2.42	88.4	9.2	0.2	0.1	2.81	82.5	6.8	0.3	0.1	7.7	85.4
SP-19	7.6	0.1	0.2	2.16	93.5	13.7	0.5	0.1	2.45	77.1	11.7	0.3	0.1	2.82	78.3	9.4	0.4	0.2	15.9	81.8

* Deposit could not be removed from filter.

CO

CO levels were less than 70 ppm for all the conventional coals fired. The use of overfire air provided an adequate control.

Particulate Loading

The data in Table II-8 suggest that for conventional coals, the ash content of the coal is not the only, or even the dominant, factor contributing to the particulate load for industrial stoker boilers, as was suggested by the EPA emission factor publication.(II-4) This observation was also made in an earlier EPA study on underfeed stokers.(II-5) It appears that the amount of coal fines introduced into the boiler system would be a superior indicator of particulate loading than ash content. At least it should be considered along with the ash content as an indicator of particulate loading.

As seen in Table II-8, the limestone/coal fuel pellet generated the highest particulate loading. This fuel contained a relatively high amount of ash. Although the pellets contained small amounts of fines as produced, they degraded when transported through the fuel-handling system. As a result, 50 percent fines were introduced into the boiler. This, coupled with the high ash content, resulted in the unusually high particulate loading.

POM

POM were collected for those selected runs listed in Table II-1. POM are related to unburned carbonaceous materials, particulate loadings, percent of carbon deposited on Method 5 filters, CO levels, and smoke opacity; these data are included in Table II-9. For the conventional coals (Runs SP 9-16), POM levels were similar even though carbon and particulate loadings were not. POM levels ranged from 13 to 24 $\mu g/Nm^3$ and were somewhat lower than levels generated by the model spreader. Also, the levels of POM generaged by the steamplant stoker were only somewhat higher than those observed from firing a 500 kW packaged boiler on natural gas, distillate oil, and residual oil.(II-6) This was a rather surprising result in that coal combustion generates higher POM levels than oil or gas combuation.(II-7) Other factors must

TABLE II-8. COAL PROPERTIES AFFECTING PARTICULATE LOADING

Coal Type	Optimum O_2, %	Particulate Loading ng/J	Ash	Ash-Fusion Temperature Initial Deformation, Oxidizing	Fuel Size Consist (percent less than 3 mm)
Low-Sulfur, Ohio	7.7	73	9.6	1480	7
Medium-Sulfur, Kentucky	7.0	110	5.0	1315	12
Stoker-Grade Washed, Ohio	8.0	190	10.3	1370	6
Stoker-Grade Unwashed, Ohio	10.8	--	18.5	1370	17
Run of the Mine, Washed, Ohio	9.0	240	8.6	1315	16
Low-Sulfur, Kentucky	8.5	73	7.7	1480	12
Illinois No. 6	9.5	--	8.6	1260	6
Limestone/Coal Pellet	11.2	610	45.6	1480	50 (entering boiler)

TABLE II-9. LISTING OF POM LOADINGS, PARTICULATE LOADINGS CARBON PARTICULATE, CO EMISSION LEVEL, AND SMOKE OPACITY FOR SELECTED RUNS

Run No.	Coal	POM_ Loading, µg/Nm	Particulate Loading, ng/J	Percent C on filter	CO, ppm	Smoke Opacity, %
SP-9	Stoker-grade, washed Ohio	14	220	10.3	80	6
SP-10	Run-of-the-Mine washed Ohio	13	290	9.2	60	6
SP-11	Low-S Kentucky	22	73	--	60	4
SP-12	Low-S Kentucky	24	56	14.6	40	2
SP-13	Run-of-the-Mine, washed Ohio	22	150	12.1	60	3
SP-15	Stoker-grade, washed Ohio	22	160	3.6	50	2
SP-16	Stoker-grade, washed Ohio	12	180	4.8	30	3
SP-18	Limestone/high-S coal pellet	21	610	6.8	950	22
SP-19	Limestone/high-S coal pellet	174	960	9.4	2000	25

be considered, however, such as size, design, and operation of the equipment. The POM loading of Run SP-19 was significantly higher than those of the other runs. With the exception of Run SP-18, the CO level, smoke opacity and carbon and particulate loading of Run SP-19 were significantly higher than the other runs, as expected. In Run SP-18, the CO level, smoke opacity, carbon and particulate loading were not appreciably different than those in Run SP-19, yet the POM levels are significantly less. These results suggest that perhaps another factor may have a dominant effect on POM levels. It is difficult to generalize becuase the formation of POM is not fully understood nor are the sampling and analytical techniques completely developed. This creates some difficulties in interpreting the data.

Tables II-10 and II-11 give POM species quantification. The differences in species identification in the two quantification tables represent changes in analytical procedures. The total POM levels are not affected by these changes. The procedure used to generate data in Table II-11 improves the resolution of high-molecular weight species.

EFFECT OF OPERATING VARIABLES ON EMISSIONS AND BOILER PERFORMANCE

In general, those modifications in the operation of the stoker-boiler system that reduce emissions also improve boiler efficiency. Those modifications that improve the overall combustion, tend to decrease emissions by improved control of the air and fuel distribution throughout the stoker-boiler system. The operating variables that were investigated were listed in Table II-2 and are discussed below.

Excess Air

Operation. The limiting factor in determining the minimum excess air level at which the stoker boiler could be fired was not high emission levels but clinker formation on the fuel bed. This observation is verified by other researchers.(II-3, II-8) Infiltration into the boilers and leakage around stoker grates may be significant, hence the excess air level (generally measured in the stack) at which clinkers are formed depends on the specific design and condition of the stoker-boiler system, as well as the coal type and size.

TABLE II-10. POM QUANTIFICATION

Component	NAS Notation	SP-9	SP-10	SP-11	SP-12
Anthracene/Phenanthrene	•	23.17	19.77	24.51	24.30
Methyl anthracenes		2.83	1.84	3.20	3.56
Fluoranthene		5.92	4.10	12.66	15.12
Pyrene		1.79	1.11	2.35	4.45
Methyl Pyrene/Fluoranthene		0.427	0.291	0.747	1.58
Benzo(c)phenanthrene	***	ND	ND	0.079	0.258
Chrysene/Benz(a)anthracene	*	0.247	0.313	0.371	1.04
Methyl chrysenes	*	ND	ND	ND	ND
7,12-Dimethylbenz(a)anthracene	****	ND	ND	ND	ND
Benzo Fluoranthenes	**	ND	ND	ND	ND
Benz(a)pyrene	***	ND	ND	ND	ND
Benz(e)pyrene					
Perylene		ND	ND	ND	ND
Methylbenzopyrenes		ND	ND	ND	ND
3-Methylcholanthrene	****	ND	ND	ND	ND
Indeno(1,2,3,-cd)pyrene	*	ND	ND	ND	ND
Benzo(ghi)perylene		ND	ND	ND	ND
Dibenzo(a,h)anthracene	***	ND	ND	ND	ND
Diebenzo(c,g)carbazole	***	ND	ND	ND	ND
Dibenz(ai and ah)pyrenes	***	ND	ND	ND	ND
Coronene		ND	ND	ND	ND
TOTAL		34	27	44	50

TABLE II-11. PAH QUANTIFICATION
µg Total Sample

PAH	SP-13	SP-15	SP-16	SP-18	SP-19
Naphthalene	12.6	16.3	5.27	14.1	77.1
Acenaphthylene	0.946	0.811	0.088	0.236	3.61
Acenaphthene	2.51	1.86	0.647	3.71	37.3
Fluorene	1.31	1.28	0.342	0.888	14.8
Anthracene	0.717	0.785	0.165	0.566	5.79
Phenanthrene	18.1	21.7	5.90	13.4	113
Methyl Anthracenes	3.75	3.40	1.45	1.93	15.5
Fluoranthene	6.04	4.92	3.04	5.04	8.00
Pyrene	3.24	2.43	1.36	1.36	3.76
Methyl Pyrene/Fluoranthene	0.135	0.102	0.072	0.069	0.223
Benzo(c)phenanthrene	0.261	0.112	0.106	0.125	0.298
Chrysene	0.399	0.098	0.164	0.254	0.669
Benz(a)anthracne	0.154	0.074	0.078	0.070	0.218
Benzofluoranthenes	ND	ND	ND	ND	0.165
Benz(a)pyrene	ND	ND	ND	ND	0.077
Benz(e)pyrene	ND	ND	ND	ND	0.133
Perylene	ND	ND	ND	ND	0.224
Indeno-pyrene	ND	ND	ND	ND	ND
Benzo(ghi)perylene	ND	ND	ND	ND	ND
Total	50	54	18	42	280

Table II-8 indicates the optimum levels of excess air that were determined for the various coals fired in the Battelle stoker boiler at the same load. Optimum is defined as the lowest excess air that could be continually maintained while providing an adequate margin of safety before clinkers formed. For example, the low sulfur Ohio coal could be fired as low as 6 percent O_2 before clinkers formed. From Table II-8, it appears that the minimum excess air level that can be achieved depends on more than one of the coal properties given and/or others not included in the Table. For example, mineral analysis of the ash is used to predict the slagging potential of ash for pulverized coal firing but not for stoker firing. It appears that this analysis would be useful in determining the clinkering tendency. Table II-8 does suggest a weak relationship between minimum excess air and ash content. This may be attributed to the fact that higher ash coals form deeper beds than lower ash coals. Bed ash is a thermal insulator between the burning bed and the significantly cooler grate. Increasing the bed depth reduces heat losses from the bed, allowing an increase in bed temperature and clinker formation. In addition, because of the higher resistance of deeper beds, more air is bypassed around the grate. Though the indicated level of excess air in the stack may be the same, the amount of excess air in the bed may be significantly less for deeper beds.

The Illinois No. 6 coal could not be fired at full load without clinker formation even with the forced draft fan operating wide open. The high excess air of the limestone/coal pellet firing can be attributed to the abnormally deep and compact bed causing a significant amount of air to leak around the grate bypassing the fuel bed. The compact bed was caused both by the excessive amount of fines (50 percent) and the vibratory action of the grate tending to pack the bed.

Emissions. Data from the Battelle steamplant boiler indicate that low excess air operation can effectively control particulate loading and NO. Particulate loadings were measured at 1) a baseline condition in which the Battelle stoker operator established the normal operating condition, and 2) the optimum excess air condition established by the Battelle laboratory team. Both runs were made at approximately the same boiler load firing the medium-sulfur Kentucky coal. The results of the runs are tabulated below in Table II-12.

TABLE II-12. COMPARISON OF PARTICULATE LOADING BETWEEN OPTIMAL AND NORMAL STOKER OPERATION FIRING THE MEDIUM SULFUR KENTUCKY COAL

Conditions	O_2, %	Excess Air, %	Particulate Loading ng/J	CO, (@3% O_2), ppm
Baseline	9	78	150	60
Optimum	7	49	110	44

Reduction of excess air from 78 to 49 percent resulted in about a 30 percent reduction in particulate loading and about the same reduction in CO level. The lower particulate loading can be attributed to the higher fly-ash carryover. Also, the reduction of excess air increased boiler efficiency by about 3 percent.

NO. Figures II-3 through II-6 show that reduction in excess air from 100 percent to 60 percent can result in as much as a 20 to 25 percent reduction in NO levels. These observations are in general agreement with data reported by KVB researchers.(II-8) In pulverized coal firing, low excess air is also used as an NO_x control, but the excess air levels are considerably less than those from stoker firing. However, the air availability to the stoker fuel bed may be similar to that of the pulverized coal particle.

Two features stand out in examining the NO emissions: 1) NO levels in stoker firing are substantially less than those in pulverized coal firing and 2) the NO emissions are directly related to excess air levels in and above the bed. Both of these observations are corroborated by other investigators.(II-9)

Figures II-3 through II-6 show a range of NO levels (3 percent O_2, dry) of 340-460 ppm at excess air levels of 55-110 percent for coals of 1 to 1.5 percent nitrogen. These NO levels compare with levels of 300-1000 ppm NO_x (3 percent O_2, dry) at excess air levels of 5-25 percent for firing of pulverized coals ranging from 0.8 to 1.4 percent nitrogen. The marked difference in the NO emissions from the two systems reflects

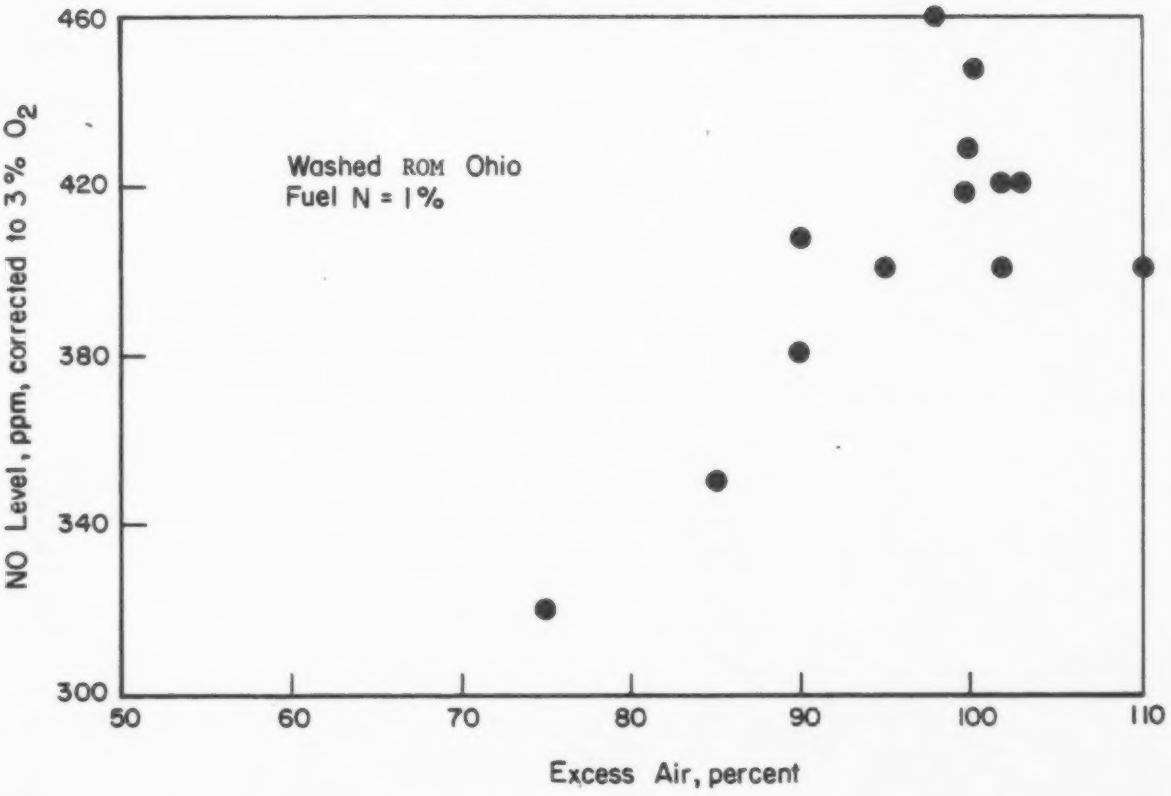

FIGURE II-3. NO EMISSION LEVELS AS A FUNCTION OF EXCESS AIR FOR WASHED, RUN-OF-THE-MINE OHIO COAL

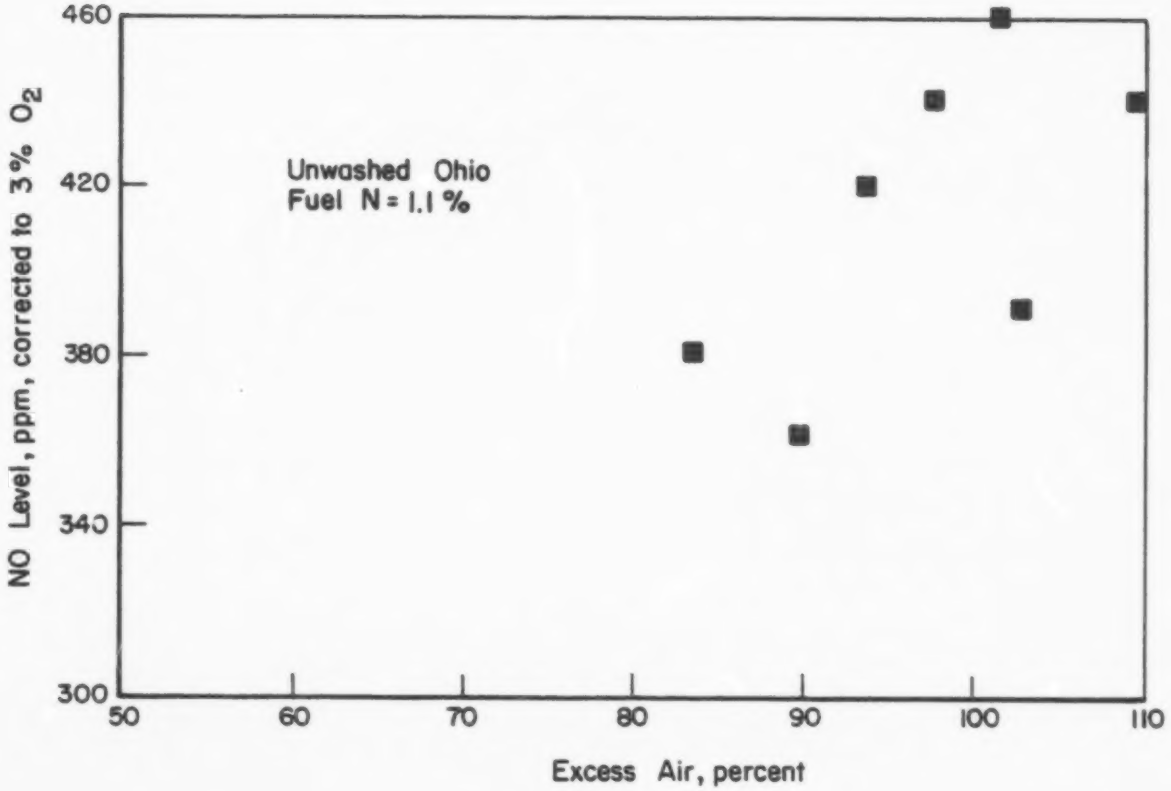

FIGURE II-4. NO EMISSION LEVELS AS A FUNCTION OF EXCESS AIR FOR UNWASHED OHIO COAL

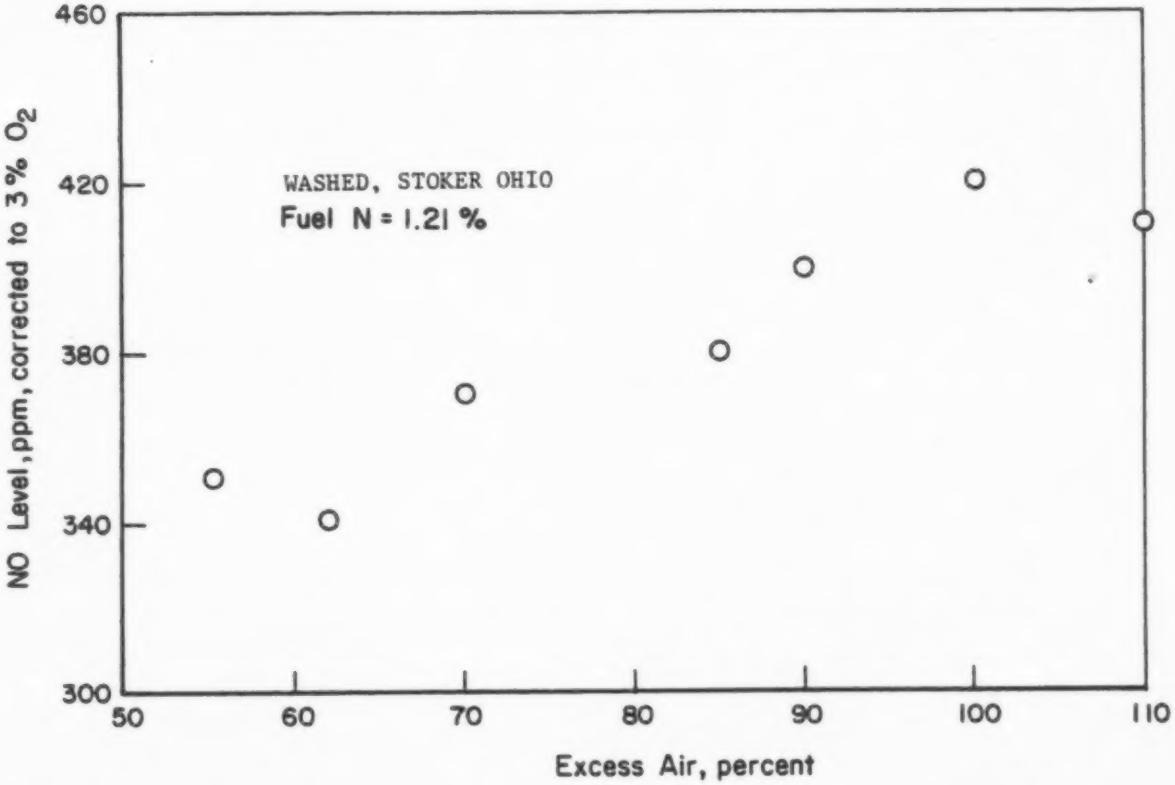

FIGURE II-5. NO EMISSION LEVELS AS A FUNCTION OF EXCESS AIR FOR WASHED, STOKER OHIO COAL

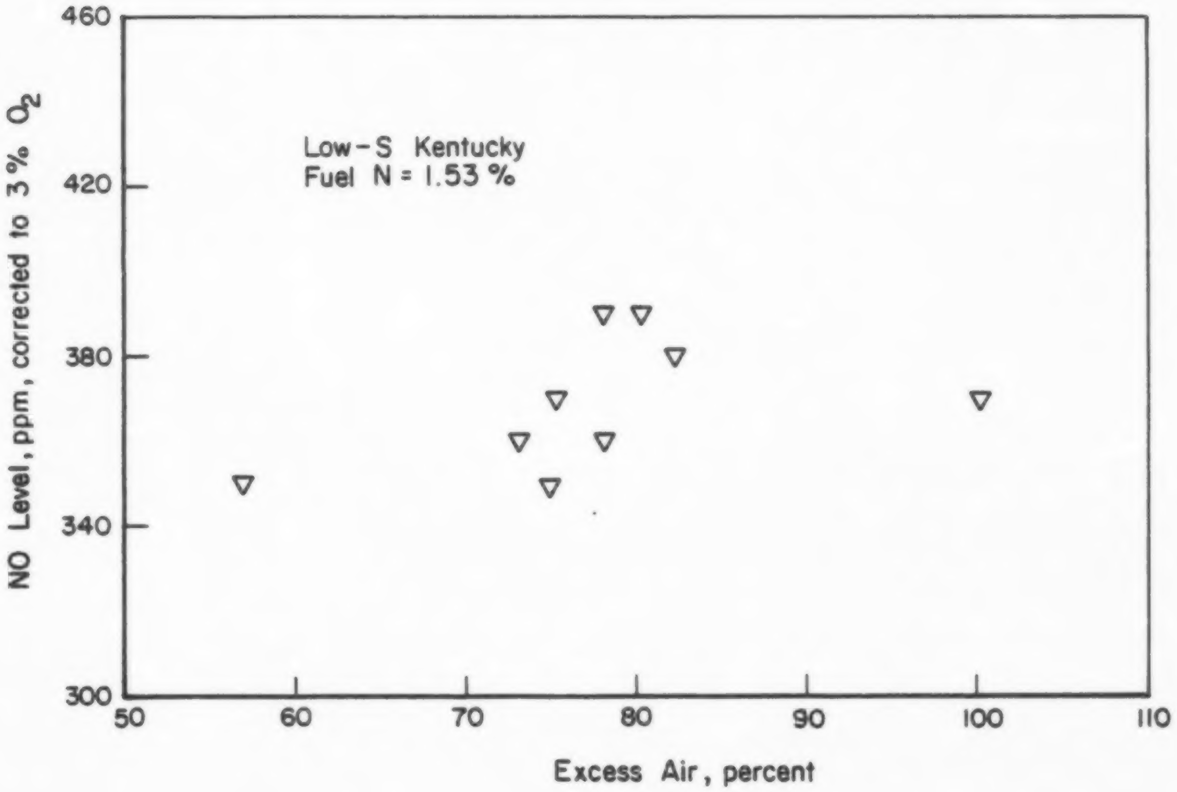

FIGURE II-6. NO EMISSION LEVELS AS A FUNCTION OF EXCESS AIR FOR LOW-SULFUR KENTUCKY COAL

the nautre of stoker combustion. Stoker combustion is primarily bed combustion and as such is similar (to a degree) to fluidized bed combustion. NO levels are lower in bed combustion (stoker or FBC) because of the significant reduction that occurs in the bed in spite of the overall lean stoichiometry.(I-10)

The relationships between NO_x and excess air are generally similar for all coal firing--stoker, FBC, pulverized coal, i.e., NO_x increases with increasing fuel-N and with increasing excess air. Our results corroborate the trend for increasing excess air but are not as obvious relative to fuel-N content. This is in part due to the fact that bed heights, bed temperatures, and overfire/bed air levels were not controlled as closely as desired.

$\underline{SO_2}$. No appreciable influence on SO_2 emission levels was observed for variations in excess air at full load operation. Maloney's data indicated that there was a tendency for SO_2 levels to be reduced for higher excess air levels.(II-13) This reduction was not significant and there was sufficient scatter in the data to suggest a very weak relationship between SO_2 and excess air levels.

Overfire Air

A variety of overfire air/total air flow rate ratios (0 to 0.25) were investigated at full-load operation for test firing of the low-sulfur Ohio coal. The total air flow rate was held constant. Changes in this ratio affected smoke and CO levels. The reduction in smoke levels was much more significant than that in CO at increased overfire air rates.

During the test period, both the rear and front overfire air jets were deactivated. Smoke levels increased to unacceptable levels (about 30 percent opacity) while CO increased from 30 ppm to 50 ppm. NO levels decreased slightly (less than 20 ppm) upon deactivating the jets. This can be attributed to several factors including lower above bed temperatures, reduced oxygen levels, and perhaps heterogeneous reduction reactions with smoke particles.

The optimum overfire air rate was about 18.0 percent of the total combustion air, corresponding to 7.5 to 7.7 percent O_2 in the flue gas. For a constant total air flow rate, an increase in the overfire air/total air flow rate ratio above 0.18 would further reduce smoke, but the reduction of underfire air through the bed would create severe clinkering.

For constant total combustion air, increased overfire air has two effects that can be illustrated by comparison of data of Runs SP-1 and SP-4 in Table II-13.

TABLE II-13. SMOKE, CO, AND PARTICULATE EMISSIONS FOR TWO OVERFIRE/TOTAL AIR RATIOS

Run	Overfire Air / Total Air Ratio	Smoke Opacity, percent	CO, ppm	Total Particulate Loading, ng/J	Carbon Particulate Loading, ng/J
SP-1	0.14	10	70	110	12.1
SP-4	0.18	4	40	73	11.7

The increased overfire air improved aerodynamic mixing above the bed resulting in decreased emissions and smoke opacity. Furthermore increased overfire air allows for decreased undergrate air. Decreasing undergrate air reduces the amout of fly ash carryover, as evidenced by the 30 percent reduction in particulate loading. It is interesting to note carbon loading remained virtually unchanged.

Fuel-Bed Depth

Experiments to explore the effects of different bed depths at full load were conducted for test firing with several coals. It was observed that for most coals, the stoker boiler could be fired only over a narrow range of fuel bed depths and still maintain satisfactory combustion. The stoker boiler was designed for about 8 to 10 cm deep ash bed at the front end of the grate for a 5 to 10 percent ash coal.

For ash bed depths less than 8 cm, full-load operation with complete carbon burnout could not be achieved. Additionally, if the bed becomes to shallow, there is danger of blowing the insulating ash layer off the grate and exposing grate metal to the heat of the furnace. In ash beds deeper than 15 to 20 cm, clinkers would form. Clinker formation in deeper beds is attributed to 1) increased bed resistance allowing more air to bypass the fuel bed and effectively lowering the air/fuel ratio in the bed, and 2) the insulating effect of the ash resulting in higher bed surface temperatures.

The medium sulfur Kentucky coal, because of its low ash content and high heating value, could be more satisfactorily fired over a range fuel bed depths than the other coals investigated. A shallow bed of about 6 cm was found to be optimum for this coal in terms of responsiveness to load swings and low excess air firing. Run SP-3 was made at this optimum condition, indicating that the medium sulfur coal could be fired at 7 percent O_2--the lowest O_2 level of any of the coals for continuous satisfactory operation. Even though this coal had lower ash content, the particulate loading was comparable to that of the low sulfur Ohio coal in Run SP-1. This may be attributed to factors that include a shallower more active bed, the friable nature of the Kentucky coal, the greater amount of fines, and the higher sulfur content, leading to condensible sulfate formation in the fly ash.

As discussed earlier, increased bed depths require increased excess air levels.

Boiler Load

The effect of boiler load on stoker performance and emission levels was investigated in Runs SP-1, and SP-5, firing low sulfur Ohio coal. The data are summarized in Table II-14.

TABLE II-14. THE EFFECT OF BOILER LOAD ON PERFORMANCE AND EMISSION LEVELS

Run	Load, %	Overfire Air Total Air Ratio	O_2, %	CO, ppm	SO_2, ppm	Smoke Opacity, ppm	Particulate Loading, ng/J	Boiler Efficiency, %
SP-1	86	14	8.0	50	505	10	110	78
SP-2	58	23	7.5	60	470	5	77	76
SP-5	38	32	11.8	70	375	5	65	75

Performance. The excess O_2 required at 58 and 86 percent loads was about the same, but was significantly higher at 38 percent load. The higher O_2 level at low load was required for two reasons: (1) to avoid clinker formation and (2) to reduce CO and smoke. Observations indicated that the amount of undergrate air required for satisfactory operation was somewhat independent of boiler load. A certain level of air flow through the grate had to be maintained to avoid clinker formation. Fow low loads, this resulted in reduced temperatures in the combustion zone above the bed. To compensate for this effect, the overfire air/total air flow ratio was increased to improve mixing to control CO and smoke levels. For example, the overfire/total air ratio of 0.15, CO levels were 150 ppm while smoke opacity was about 15 percent. Increasing this ratio to 0.32 decreased CO levels to about 70 ppm and smoke opacity to less than 10.

Boiler Efficiency. As indicated in Table II-14 boiler efficiencies were not significantly different for the various boiler loads.

Particulate Loading. A comparison of the particulate loadings in Runs SP-1, SP-2, and SP-5 shows a trend of increasing particulates with increasing boiler loads. This increase was attributed to the increased rate of fly ash carryover because of increased velocities (higher total flow rate and higher furnace temperature) at higher loads.

Smoke. A significant achievement of the low-load experiments was the alleviation of the low-load smoke problem. This was achieved by supplying a controlled amount of underfire air to the bed. At high underfire air settings, smoke formation occurs due to incomplete combustion resulting from local quenching of the flame by the combustion air. However, there is a minimum level of excess air that is required to avoid clinker formation. Smoke levels below 5 percent opacity were achieved for low-load operation at excess air levels around 12.0 percent oxygen (Run SP-5). It must be pointed out that the attention and skill of the boiler operator are important factors in controlling low-load smoke, as smoke levels can increase suddenly and drastically for any changes in boiler load or operation.

$\underline{SO_2}$. Bed temperatures, measured with an optical pyrometer about 5 cm above the bed in the central region of the grate, were around 1410 C at full load, 1340 C at partial load, and 1200 C at low load. The reduction in bed temperature would seem to account for the decrease in SO_2 emissions, that is greater sulfur capture for decreasing load, as shown in Table II-15.

TABLE II-15. SO_2 LEVELS AS A FUNCTION OF BOILER LOAD AND FUEL BED TEMPERATURE

Run	Load, %	SO_2 (@3% O_2), ppm	Fuel S Retained in Bed, percent	Bed Temperature, C
SP-1	86	505	19	1410
SP-2	58	470	25	1340
SP-5	38	375	40	1200

Analysis of the bed ash, however, does not verify the reduction in SO_2 observed in the stack gases.

In order to examine the relationsihp of bed temperature to sulfur retention in the ash, the fuel bed was probed with a thermocouple, 2.5 cm below the surface. Figure II-7 is a plan view of the grate, indicating the approximate location of the temperature measurements and the recorded temperatures for washed Ohio coal fired at 9.3 percent excess O_2 and 80 percent load. (There was not sufficient room in front of the boiler to insert a probe the full length of the grate.) Furnace temperatures about 5 cm above the bed in the central region of the grate, measured with an optical pyrometer, were around 1250 C to 1300 C and were in reasonably good agreement with the thermocouple measurements. The region of lower temperature (1040 C) about 1.2 m from the front wall was attributed to a cracked section of the grate that admitted an additional amount of underfire air. It is expected that bed temperatures would increase if the excess O_2 were reduced, the boiler load increased, or if a higher heating value coal was fired.

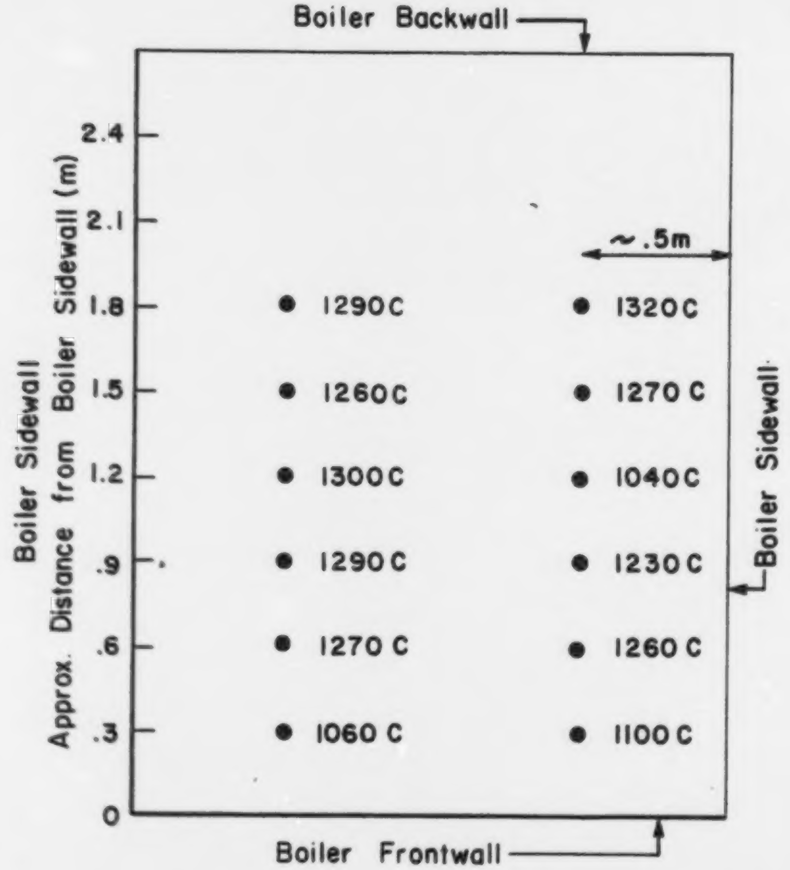
Boiler Backwall
Boiler Sidewall
Approx. Distance from Boiler Sidewall (m)
2.4
2.1
1.8
1.5
1.2
.9
.6
.3
0
~.5m
1290 C
1320 C
1260 C
1270 C
1300 C
1040 C
1290 C
1230 C
1270 C
1260 C
1060 C
1100 C
Boiler Sidewall
Boiler Frontwall

FIGURE II-7. FUEL-BED TEMPERATURE DISTRIBUTION

Fly Ash Reinjection

The effect of fly ash reinjection on particulate emissions and combustion efficiency was investigated for test firing with the following coals:

- Low-sulfur, washed Kentucky coal (Runs SP-11 and SP-12)
- High sulfur, washed run-of-the-mine Ohio Coal (Runs SP-13 and SP-14)
- High-sulfur, washed stoker-grade Ohio coal (Runs SP-15 and SP-16)

Fly ash was reinjected during Runs SP-11, SP-14, and SP-16, while no fly ash was reinjected during Runs SP-12, SP-13, and SP-15. Furthermore, only about 65 percent of the total fly ash was reinjected during the fly ash reinjection runs for the high-sulfur Ohio coals. Each coal was fired with and without fly ash reinjection under approximately the same boiler operating conditions--full load (9525.6 to 9979.2 Kg/hr) was maintained during these runs.

No significant trend in gaseous emissions was observed, while a reduction in smoke was observed for runs made without fly ash reinjection. The effect on smoke is, however, difficult to determine as smoke levels under all conditions were below 5 percent opacity.

The most significant effect was the reduction in particulate loadings without fly ash reinjection, as shown in Table II-16. These results suggest that particulate loadings may be reduced by 10 to 25 percent by operating the spreader-stoker boiler without fly ash reinjection. This table also shows that carbon loss by not reintroducing the fly ash is less than 1-1/2 percent of the total carbon input. With fly ash reinjection, the carbon loss is about 3 percent of the total carbon input for those coals investigated.

The fly ash carbon loss measured as high as 5 percent for the Battelle stoker-boiler facility. Although the potential existed to increase boiler efficiency by reinjecting fly ash, the fly ash reinjection system was not sufficiently effective to justify the increased maintenance. Portions of the system have to be replaced periodically due to erosion and higher particulate loading. Consequently, it was removed.

TABLE II-16. EFFECT OF FLY ASH REINJECTION

	Particulate Loading, ng/Nm^3		Percent Reduction in Particulate Loadings	Percent Increase in C Loss
Type of Coal	w/ Fly Ash Reinjection	w/o Fly Ash Reinjection		
Kentucky	73.1	55.9	23.5	1.0
Run-of-the-Mine Ohio	172	154.8	10.0*	1.3
Stoker-Grade Ohio	176.3	159.1	9.8*	0.5

* About 65 percent of total fly ash was reinjected during the fly ash reinjection runs.

Particulate emissions were significantly higher for the higher sulfur coals. Analysis of the filter catch for these high-sulfur runs indicates that as much as 25 percent of the particulate loading can be attributed to condensible sulfates compared to less than 10 percent for the low-sulfur coals. Dust collectors are ineffective in capturing condensible sulfates, which pass through the collector as SO_2 and then condense in the presence of water below 180 C.

The unwashed, stoker-grade, Ohio coal could not be fired satisfactorily in the Battelle steam plant boiler. When firing this coal, the boiler could not follow load swings. Additionally, clinkers were formed at loads above 50 percent. This unsatisfactory performance is attributed to the high ash content and high amount of coal fines. Similarly, the Illinois No. 6 coal could not be fired above 60 percent load without severe clinkering. This severe clinkering was attributed to the excessive amount of fines, which caused the bed to mat, as well as to the lower ash-fusion temperature.

Coal Types

The type of coal fired has a significant effect on the stoker-boiler emissions and performance. The characterization of emissions generated by the combustion of various coals provides a basis for selecting coals to meet emission standards. With the exception of the unwashed, stoker grade, Ohio coal, and to a certain extent the Illinois coal, all coals listed in Table II-3, including the limestone/coal fuel pellet, could be fired satisfactorily in the Battelle steamplant boiler.

Conventional Coals. The Kentucky and low-sulfur Ohio coals were superior to the high-sulfur, stoker-grade and run-of-the mine coals in terms of SO_2, NO, and particulate emissions, as previously discussed. Furthermore, these coals could be fired under a wider range of operating conditions. As shown in Table II-17, the highest boiler efficiencies were achieved with these coals.

TABLE II-17. BOILER EFFICIENCIES FOR SELECTED COALS

Coal	Boiler Efficiency
Medium-S Kentucky	84
Low-S Ohio	76
Stoker-grade Ohio washed	74
ROM washed Ohio	71
Stoker-grade Ohio unwashed	68

Limestone/High Sulfur Coal Fuel Pellet. The results of the Phase I study indicated that the limestone/high-sulfur coal fuel pellet showed excellent potential for sulfur capture. To test the concept further and to identify any operational problems, 90 Mg of pellets were fired in the Battelle steamplant boiler in Runs SP-18 and SP-19.

In these runs, sulfur captures of better than 70 percent were achieved, based on SO_2 emission levels in the stack. However, as indicated in Table II-5, only 84 and 77 percent of the fuel sulfur was accounted for in Runs SP-18 and 19, respectively, based upon a mass balance.

Several operational problems were encountered. These were attributed to the low-heating value, high ash content, and excessive amount of fines of the fuel product. The deep bed of compact fuel and ash significantly increased the resistance through the bed. As a result, there was noticeable air leakage around the grate. Consequently, it would appear that the air/fuel ratio in or just above the grate was substantially less than that indicated in the stack. Additionally, because of the excessive amount of fines and lack of a consistent size distribution, the fuel could not be fed uniformly to the bed. This may have been a factor in the relatively high CO emissions.

The limestone/coal pellet developed for this study offers a potentially interesting and exciting new means of sulfur control for industrial boilers. The use of limestone for capturing sulfur is by no means new. Exactly how and why limestone should be effective in capturing sulfur in a stoker bed is not well established at this time. Thermodynamically, one would guess that the coal bed is much too hot to retain sulfur as calcium sulfate. On the other hand, it is possible that the stoker bed is a very nonuniform combustion mixture. In such a state, one might anticipate significant lean air regions or areas. It is conceivable that reduced conditions (by insufficient combustion air diffusing into the pellet) exist in the fuel bed, ultimately leading to sulfur capture via sulfide formation. This is also an explanation offered by Maloney.(II-3)

COMBUSTION SYSTEM DESIGN MODIFICATIONS

As part of Phase II, combustion modifications with the potential to reduce emissions and improve overall boiler performance were to be identified. Experiments with the Battelle boiler indicated that those modifications that would improve air/fuel ratio control in the fuel bed and the combustion zone above the bed would provide optimum stoker-boiler performance from an emissions and performance viewpoint. This air/fuel ratio is dependent on the design of a number of system design components that include:

- feed system
- grate design
- overfire
- fly-ash reinjection.

Feed System

Although not a primary combustion modification technique, improvements in the coal feed system will increase the control of fuel distribution within the stoker boiler. This includes the rotor-feed mechanism, as well as the transport system to the feeders. The feeder must spread the coal uniformly on the grate and avoid regions of coal buildup. Many of the feed problems encountered are caused by the coal transport system segregating the coal size by distributing a disproportionate amount of fines to certain feeders. For example, in the Battelle stoker, one feeder received a disproportionate amount of fines while the other received a disproportionate amount of top sizes; the result was nonuniform combustion and excessive fly ash carryover.

Grate Design

The grate not only supports the fuel bed but also serves as a distributor plate providing a uniform flow of air through the bed. The pressure drop across the grate is only about 25 mm to 50 mm H_2O at full load. As a result, any maldistribution of the coal on the bed will result in a nonuniform flow of air. The shallower portions of the bed receive more air than the deeper portions. Increasing the pressure drop across the grate would tend to compensate for maldistribution of the coal. However, increased pressure drop would require improved air seals around the stoker grate.

Air leakage around the grate, or infiltration of air into the boiler, creates problems in controlling the air/fuel ratio. The excess air level of a stoker-boiler system is generally measured in the stack. With significant amounts of air infiltration, it is difficult, if not impossible, to determine the air/fuel ratio in the combustion zone. In the Battelle stoker, during cold flow tests on a bare grate, 14 percent of the air bypassed the grate through leakage around the grate. This percentage would increase during stoker operation. As a result, the stoker boiler is often operated with significantly more excess air than is required to ensure that there is sufficient undergrate air to burn the coal and keep the bed from clinkering. This additional amount of air acts only as a diluent and does directly enter into the combustion of the fuel. It does, however, reduce boiler efficiency, increase fly ash carryover, and perhaps increase NO levels.

Overfire Air

The overfire air jet system is designed to provide effective aerodynamic mixing above the bed. To accomplish this, the overfire air jet system must effectively mix fuel fragments and air above the bed without disrupting the fuel bed.

The overfire air systems is one of the more promising combustion modification techniques in terms of reduced emissions and improved performance. For this reason, and because modifying the overfire air jet system on a large system is expensive and difficult, it was decided to analytically investigate overfire air jet systems.

Analysis of the operation of such jet systems shows that the individual jets, which can be round or rectangular with a low aspect ratio, can be treated as simple round jets for the initial part of their trajectory. However, consideration must be given to the difference in density of the jet and its surrounding medium, which both affects the aspiration rate of the surrounding gases and imposes a negative buoyancy effect on the jet. Furthermore, the jet is in a cross-wind of the rising gases from the fuel bed.

As the jet approaches the opposite wall (or, for directly opposed jets, the mid-plane), two further effects occur. First, the jet is affected by the aspiration of adjacent jets. Second, the presence of a barrier wall forces the jet to turn upward away from the bed. These complications, plus the fact that the system is three-dimensional, make physical studies, physical modeling studies, and mathematical modeling studies quite difficult. This situation is discussed in more detail in Appendix II-A. As a result of these difficulties, we fine both a paucity of data in the literature on all but single jets in the open, and an overabundance of empirical rules of design. In fact, using all the empirical results that seem logical, one arrives at an overspecified system with no indication of which rules to drop. On the experimental side, even the most recent treatments(II-11) can refer only to very early work(II-12) for experimental results on overfire air jets.

The review in Appendix II-A shows that a water-salt water model can be used satisfactorily to develop either general rules for the optimization of overfire air jets or to optimize conditions for overfire air jets in any specific application. For most ranges of operation, it is expected that buoyancy effects can be ignored. In this case, air models can be used. Finally, techniques are now available that make three-dimensional mathematical modeling of the overfire air system economically feasible.

Fly-Ash Reinjection

Fly ash reinjection systems are used to return the carryover back into the high-temperature zone above the grate for burning. The manner and location in which the fly ash is reinjected can have a significant effect on particulate loadings. Ideally, the fly ash should be reinjected into the furnace in a region in which the carbon is burned out and the reinjected fly ash remains on the grate for disposal rather than being recirculated. Gravity flow systems, in which the fly ash is fed by gravity from the collecting hoppers to the rear end of a forward moving grate, have been used. In systems in which the fly ash is pneumatically conveyed back to furnace, the reinjection nozzle should be located between the overfire air jets to insure complete burnout of the fly carbon. In the Battelle steamplant, the fly ash from collecting hoppers was reinjected through nozzles along the boiler sidewalls. Because of the high amount of air leakage around the grate, much of this reinjected fly ash was carried to cooler regions of the boiler before the fly carbon could be burned.

SUMMARY

Of the criteria pollutants, the most troublesome emission to control in an industrial stoker-boiler system is SO_2. The level of SO_2 emission is related to the quantity of sulfur in the coal and is essentially independent of the combustion conditions. Thus, a modified or treated fuel, such as the limestone/coal fuel pellet, offers an option to flue-gas scrubbing. Treated or modified coals to control SO_2 are still in the development stage and must be shown to be economically viable before commercialization. NO_x emissions from stokers are lower than those from conventional pulverized-coal burners and until standards become more stringent, this emission does not appear to be a major deterrent to the use of stoker coal. Furthermore, NO_x emissions can be effectively controlled by combustion design or operating modifications. CO and unburned hydrocarbon emissions are related to the design and operation of the stoker-boiler system and can be controlled by careful regulation of the air and fuel distribution. Similarly, particulate loading is dependent on the design and operation of the stoker boiler system and can be controlled accordingly. In addition, particulate control devices, such as mechanical collectors or baghouses, have been found to be effective control devices.

The results of the Phase II program indicate that environmentally the lack of a viable SO_2 control is a deterrent to increased coal utilization. As a result, and because limestone/coal fuel pellet data are encouraging, it is recommended that the fuel pellet be refined further.

REFERENCES

II-1. Stambaugh, E. P., et al., Combustion of Hydrothermally Treated Coals. EPA-600/7-78-068, U.S. Environmental Protection Agency, Washington, D.C. 20460, April, 1978.

II-2. Gronhovd, G. H., P. H. Tufte, and S. J. Selle. Some Studies on Stack Emissions from Lignite-Fired Power Plants. Presented at the 1973 Lignite Symposium, Grand Forks, ND, May 9-10, 1973.

II-3. Maloney, F. L., P. K. Engel, and S. S. Cherry. Sulfur Retention in Coal Ash. KVB 8810-482-b, EPA Contract No. 68-02-1863, Industrial Environmental Research Laboratory, EPA, Research Triangle Park, NC, Nov, 1978.

II-4. Compilation of Air Pollution Emission Factors. AP-42. U.S. Environmental Protection Agency, 1973.

II-5. Giammar, R. D., et al., Emissions from Residential and Small Commercial Stoker-Coal-Fired Boilers under Smokeless Operation. EPA-600/7-76-029, U.S. Environmental Protection Agency, IERL, Office of Energy, Minerals, and Industry, Research Triangle Park, NC 27711, Oct, 1976.

II-6. Giammer, R. D., et al., Experimental Evaluation of Fuel Oil Additives for Reducing Emissions and Increasing Efficiency of Boilers. EPA-600/2/77-008b. US Environmental Protection Agency, Research Triangle Park, NC. Jan, 1977.

II-7. Jones, P. W., et al., "Efficient Collection of Polycyclic Organic Compounds from Combustion Effluents", presented at the 68th Annual Meeting of the Air Pollution Control Association, Paper No. 75-33.3, Boston, June 15-20, 1975.

II-8. Gabrielson, J. E. and P. L. Langsjoen. Field Tests of Industrial Stoker Fired Boilers for Emission Control. EPA-600/7-79-050a, Proceedings of the Third Stationary Source Combustion Symposium; Vol 1. Utility, Industrial, Commercial, and Residential Systems, Feb, 1979.

II-9. Heap, M. P. and R. Gershman. Pollutant Formation During Coal Combustion. EPA-600/7-78, Proceedings of the Engineering Foundation Conference on Clean Combustion of Coal. April, 1978.

REFERENCES
(continued)

II-10. Pereira, F. J., J. M. Beér, B. Gibbs, and A. B. Hedley, NO_x Emissions from Fluidized-Bed Coal Combustors. Fifteenth Symposium (Int'l) on Combustion, Tokyo, Aug, 1974.

II-11. Niessen, W. R. Combustion and Incineration Processes. Marcel Dekker, Inc., NYC, p 129-170, 1977.

II-12. Davis, R. F., The Mechanics of Flame and Air Jets. Proc. Inst. Mech. Eng., 137 (11-72) 1937.

APPENDIX II-A

OVERFIRE AIR JETS

INTRODUCTION

Overfire air jets are used in a stoker-fired furnace to produce a uniform composition of gases a short distance above the burning fuel surface. This not only prevents cold streams of air from passing completely through the combustion region above the fuel surface, but produces a uniform flux of heat back to the surface. This heat flux tends to level out variations in the surface combustion rate.

In this discussion, following certain general comments, the performance of the simple turbulent jet and then the turning effects on such jets are discussed. This is followed by comments on physical and mathematical modeling problems, and suggestions for their use in specific research programs.

GENERAL COMMENTS

Simple turbulent jets are characterized by a jet core of about 6 diameters in length, with a uniform velocity on the axis. This is followed by a decay of the velocity on the axis. Axially directed velocities off the axis are related to the maximum velocity on the axis by a distribution curve that is approximately Gaussion in nature. For round jets, the decay rate of velocity (and the jet component of the mixture) is inversely proportional to the distance, starting at the end of the core region. The aspiration of the surrounding gas is directly proportional to the distance. Slot jets follow a similar, but more complex relationship.

Recent emphasis in jet turbulence and mixing studies has been related to the large vortices that are formed and move along the interaction surface between the jet and the surrounding environment. This results in an unmixedness of a considerably different character than is usually ascribed to phenomena associated with Gaussion-type curves.

Jets used in overfire air systems are subjected to transverse buoyancy effects and to cross winds. In a cross wind or with transverse buoyancy effects, the jet tends to maintain its original character but is bent. For cross winds, the path shape in terms of jet characteristics becomes a function of the momentum ratio of the cross wind fluid to the jet fluid. The higher the ratio, the more the jet is bent. With severe bending, the jet cross section distorts from a circle to a bean shape.

The buoyancy effects enter in the form of a Froude number, $V^2\rho/gD\,\Delta\rho$. The larger the inverse value of this dimensionless group, the more the jet is deflected.

Since an overfire jet, even using recirculated products rather than air, is more dense than the surrounding medium composed of the hot gases coming off the fuel bed, the upward flow of gases from the burning fuel surface and the buoyancy act in opposite directions on the jet.

The multiple jets of an overfire system will interact, but for many situations, the effects can be predicted by a simple addition of the effects of the individual jets.

SIMPLE JET PERFORMANCE

Jet Size

The parameters involved in jet phenomena are taken from Schlichting(II-A-1)*. Other sources are equally acceptable, with little difference in the characteristic values. The equation assumes a point source, ignoring the potential core. The radius of the jet at the distance where the velocity is half the velocity on the axis, b, as a function of distance from the source x, is

$$b = .0848\ x.$$

The total volume flow rate, Q, is given by

$$Q = 0.404 \sqrt{K}\, x,$$

where

$$K = 2\pi \int_0^\infty u^2 r\,dr.$$

---

* References are listed on p II-A-13.

The value of the axial velocity, u, on the axis, U, is given by

$$1.59\ Ub = \sqrt{K}.$$

If the jet gas is assumed to be at the furnace gas temperature, so the performance can be compared with that of a jet in an environment of the same properties, the value of K based on the true jet entrance conditions must be multiplied by (ρ_o/ρ_f) to preserve the momentum. Thus,

$$K = (\rho_o/\rho_f)(\dot{M}/d\rho_o)^2\ (4/\Pi)\ .$$

where $\dot{M}$ is the mass flow rate, and subscripts o and f refer to jet and furnace gas conditions.

Aspiration of Furnace Gas by Jet

If we assume an active length of jet, L, equal to the distance across the furnace, it would seem reasonable that one would want to aspirate into the jet a volume produced by that portion of the burning bed assigned to that particular jet. For more intensive mixing, one might want to aspirate in n times the volume of gas produced. If the mass supply rate of gas per unit of the bed area is $\dot{m}$, then

$$nWL\dot{m}/\rho_f = .404\ \sqrt{K}\ L,$$

where W is the width of the area served by one jet. Since $\dot{m}$ and ρ_f are known, this specifies the jet momentum as a function of the width, W, of the area served by the jet. For a given air temperature relative to the furnace gas temperature, the product of jet velocity and diameter (or ratio of jet mass flow rate to diameter) is thus proportional to $nW\dot{m}$. For a constant ratio of the jet to the fuel bed mass velocity, n is therefore proportional to d/W.

Ratio of Overfire Air to Total Air

If the ratio of the overfire air to total air, A, is specified, another design relation can be established. Similarly, if recirculated products are used for overfiring, a design relationship can be established.

If $\dot{M}$ is the mass flow rate of air per jet serving an area of WL, then

$$\dot{M}/(\dot{M} + WL\dot{m}_a) = A$$

where $\dot{m}_a$ is the gas flow rate per unit area. If $\dot{m}_c$ is the fuel consumption rate per unit area,

$$\dot{m} = \dot{m}_c + \dot{m}_a \ .$$

If recirculated products are used, $\dot{M}$ in the denomination is set equal to zero.

For design purposes, $\dot{m}_c$ is 20 to 40 lb/hr ft^2, $\dot{m}_a/\dot{m}_c$ is 14 to 20, and A is 0.1 to 0.2.

Rewriting the equation for A,

$$\dot{M} = A\ \dot{m}_a\ WL/(1 - A).$$

Since $\dot{m}_a$ and A are specified, $\dot{M}/WL$ is a constant. Furthermore, L/d becomes a simple function of n. Specifically,

$$L/d = (2.194\ n)(\dot{m}/\dot{m}_a)(\rho_o/\rho_f)^{1/2}\ [(1 - A)/A)]$$

For $A = .15$, $\dot{m}_a/\dot{m}_c = 17$, $T_o = 600$ R and $T_f = 2860$ R, $L/D = 28.8\ n$.

If $L = 10$ ft and $n = 1$, $d = 4.18$ in. For $n = 2$, $d = 2.09$ in.

JET SPACING

The simple jet was shown to expand with a radius to the half axial velocity of

$$b = .0848\ x.$$

One might assume that

$$W = 2mb_{(L)}$$

where $b_{(L)}$ is evaluated at the distance, L.

Thus,

$$W = .1696\ mL.$$

The sample computation then gives

$$W = 5.73\ mnd;$$

for $m = n = 1$, this would result in 24-in. spacing of jets

TURNING EFFECTS ON JETS

Cross Flow and Buoyancy

Abramovich(II-A-2) suggests, in terms of the parameters defined above, the relationship

$$\frac{y}{d} = \left(\frac{\rho_f}{\rho_o}\right) \left(\frac{\dot{m}/\rho f}{4\ M/\rho_o \pi d^2}\right)^2 \left(\frac{x}{d}\right)^{2.55}$$

for the deflection of a jet by cross flow. This simplifies to

$$y/d = (\rho_o/\rho_f)\ (\pi d^2\ \dot{m}/4\dot{M})^2\ (x/d)^{2.55}$$

Gray and Robertson(II-A-3) suggest for the effect of buoyancy,

$$y/d = .0460 \left(\frac{T_o - T_f}{T_f}\right) \left(\frac{gx^3}{(4\dot{M}/\pi d^2 \rho_o)^2 d^2}\right)$$

(Note that the coefficient in the reference is in error.) Thring(II-A-4) suggests a more complex relation, but it is not worth the trouble to use at this point. As a result the total deflection is

$$y/d = (\rho_o/\rho_f) \left(\frac{\pi d^2 \dot{m}}{4\dot{M}}\right)^2 \left(\frac{x}{d}\right)^{2.55}$$

$$- .046\ (1 - \frac{\rho_f}{\rho_o}) \left(\frac{\pi d^2 \rho_o}{4\ \dot{M}}\right)^2\ gd \left(\frac{x}{d}\right)^3$$

Now considering the condition where y/d comes back to 0 after the original deflection,

$$(x_o/d)^{.45} = 21.7\ [(\rho_t/(\rho_o - \rho_f)]\ \left(\frac{\dot{m}}{\rho_f^{\ 2}\ gd}\right)^2$$

As a sample computation, using the same values as before, and assuming that $\dot{m}_c = 30$ lb/ft^2 hr, and d = 4.18 inches,

$$(x_o/d)^{.45} = 66.17$$

Thus, $x_o = 3846$ ft. This seems ridiculous. Calculating the cross wind effect separately, leads to a lift of 8.65 ft in 10 ft. However, the gravity fall will only be 7.1 in. at 10 ft for these particular conditions. If for some condition, the jet did fall to the surface rapidly or impact the surface, the aspiration effect would change as the jet spread out over the hot surface.

Wall Effect

We note that in the above computation, the impinging wall was neglected. If jets are directed out from one wall, or are directly opposite each other so there is a virtual wall in the center, then the aspirated gas plus the jet gas must turn upward as they approach the impinging wall. This phenomenon has nothing to do with either cross-wind effects or buoyancy effects. Some estimates can be made from impingement studies. One might assume that the jets are tipped down slightly and impinge on the floor and are evenly distributed. Then treating the problem as a two-dimensional potential flow problem, or using available experimental data, one can produce the velocity profiles. The upward velocity of the hot gases would then be superimposed.

When jets are staggered on opposite walls, they interlace. It would appear that the gross recirculation pattern described above for jets on only one wall would disappear.

Length of Throw

One may assume that the jet is ineffective when the velocity on the jet axis is equal to some multiple, p, of the upward velocity at the fuel surface. Thus, combining previous equations,

$$pu_c L_p = 6.57\ (\rho_o/\rho_f)^{1/2}\ u_j$$

where L_p is the penetration distance. Stephens and Mohr(II-A-5) assume a value of 4 for p. Engdahl(II-A-6) assumed a value of the order of 2. An alternate form is

$$L_p = 6.57\ (\rho_f/\rho_o)^{1/2}\ (4\ \dot{M}/\pi dmp).$$

For the assumed values of the various terms

$$L_p/L = 0.2925\ (W/pd)\ .$$

Removing W/d by use of previously derived relations,

$$L_p/L = 1.676\ mn/p.$$

If $m = n = 1$, $L_p = L$ at $p = 1.676$, close to the value used by Engdahl.

COMMENTS ON MODEL STUDIES

Mathematical Modeling

The above discussion indicates that the jets should probably be fairly close together. They might be from one side, opposed from two sides, or staggered. The plan view of possibilities resolves into two cases, as follows:

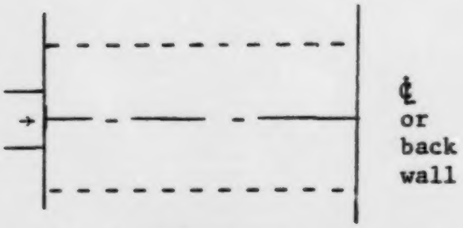

a. Jets from one side, or opposed

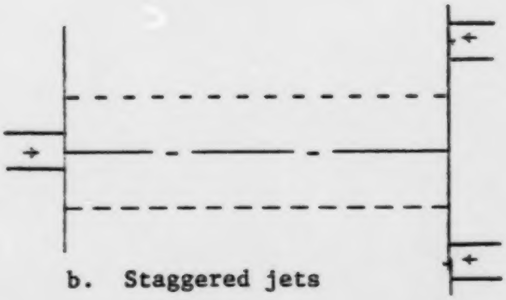

b. Staggered jets

In Case a, there is a surface of symmetry through the jet axis and between each pair of jets. In Case b, the same situation occurs, but the conditions on the surface between jets have to have a reflective character.

The sketch indicates that the region for which a solution is required is long and thin; in the vertical direction, the plane extends from somewhat below the jet to far above the jet. The jet may be directed in other than a horizontal manner. In any case, boundary layer type assumptions (uniform pressures through the narrow dimension) can be used.

Since the jets are controlling the mixing, another simplification may be made. Round jet flow equations can be based on a constant turbulent kinematic viscosity assumption. In fact, the character of turbulence can probably be considered uniform throughout the system.

It therefore appears that primitive 3-dimensional equations can be used in a simplified form to solve the flow problem. Small cold regions in the reaction surface can be considered, comparing the uniformity of temperature at higher levels as a function of the different variables.

In the long run, more sophisticated mixing equations and reactions above the bed can be included, but the simple approach outlined above should answer major questions as to optimum design, and the variations obtained by using air, steam, steam injected air, recirculated products, and steam injected recirculation products, with various jet sizes, velocities, and angles, for different fuel consumption rates, air supply rates, and overfire air rates.

Dimensional Analyses for Physical Modeling

If one were to investigate only the flow pattern with no temperature variation and no cross flow, and in a highly turbulent situation, the vector velocity at any point would be given by

$$\vec{u} = f(x, y, z, W, L, H, \alpha, U_j, d_j)$$

where H is the heigth of the jet above the grate, and α is the direction of the jet, zero when horizontal and positive upward. All measurements x, y, z are from the orifice center. This obviously can be simplified to

$$\vec{u}/u_j = f\left(\frac{x}{L}, \frac{y}{H}, \frac{z}{W}, \frac{W}{d_j}, \frac{L}{d_j}, \frac{H}{d_j}, \alpha\right)$$

If C is the concentration of the jet material,

$$C/C_j = \left(\frac{x}{L}, \frac{y}{H}, \frac{z}{N}, \frac{W}{d_j}, \frac{L}{d_j}, \frac{H}{d_j}, \alpha\right)$$

where

$$0 \leq \frac{x}{L} \leq 1, \ -1 \leq \frac{z}{W} \leq 1, \ -1 \leq \frac{y}{H}$$

Note that f indicates function, but not necessarily the same function. For

$$\frac{x}{L}, \frac{y}{H}, \frac{z}{W} \sim 1/2,$$

the data should correlate in the form

$$\vec{u}/u_j, \ C/C_j = f\left(\frac{x}{d_j}, \frac{y}{d_j}, \frac{z}{d_j}, \alpha\right)$$

This can be modified to

$$u/u_j, \ C/C_j = f\left(\left(\frac{x \cos \alpha + y \sin d}{d_j}\right), \left(\frac{(y \cos \alpha - x \sin \alpha)^2}{d_j^2} + z^2\right)^{1/2} \right)$$

If the flow velocity from the grate, U_g, is now added as a variable, the additional parameter, U_g/U_j, must be added to the independent variables, and α must be reinserted as a variable.

We next consider the case where there is a difference in temperature between the jet and the upward flow. Not considering gravity effects, the relation ρ_j/ρ_g must be added, or T_g/T_j. Since momentum effects are the key to the flow pattern, one would expect to change the ratio U_g/U_j to $(U_g/U_j)(T_j/T_g)^{1/2}$. For the regions some distance from the jet exit, one can follow through with the Thring criteria based on constancy of momentum in modeling, $\rho_j d_j^2 U_j^2 = \rho_g \bar{d}^2 \bar{U}_j^2$ and constancy of mass flow $\rho_j d_j^2 U_j = \rho_g \bar{d}^2 \bar{U}_j$. Thus, $U_j = \bar{U}_j$, and $\rho_j d_j^2 = \rho_g \bar{d}^2$, or $d = d_j(\rho_j/\rho_g)^{1/2}$ $= d_j(T_g/T_j)^{1/2}$, This indicates the substitution of $\bar{d}$ for d_j in the correlation relations.

The last factor to be considered is the effect of gravity. It is expected that the Froude number will enter at this point, in the form

$$U_j^2\, T_j/(gd_j)(T_g - T_j).$$

The final correlation relation, therefore, is

$$\vec{u}/u_j,\ C/C_j,\ \text{and}\ (T_g-T)/(T_g-T_j) =$$

$$f\left(\frac{x}{L}, \frac{y}{H}, \frac{z}{W}, \alpha, \left(\frac{W, L, H}{d_j\ (T_g/T_j)^{1/2}}\right), \left(\frac{U_g}{U_j}\right)\left(\frac{T_j}{T_g}\right)^{1/2},\right.$$
$$\left.\left(\frac{U_j^2\ T_j}{gd_j\ (T_g-T_j)}\right)\right)$$

A refinement which can be made later is to alter the terms on the LHS so they all go from 1 at the jet to zero at $\frac{y}{H} \to \infty$.

ADDITIONAL RESEARCH CONSIDERATIONS

Mixing data are required for the two basic overfire jet configurations as a function of jet size, jet angle, spacing, and heigth, relative to the furnace width. Three possibilities suggest themselves, namely water modeling, air modeling, and mathematical modeling. Each is discussed in turn.

Water Model

A water model can be used to simulate the entire system, including the buoyance effect. Salt water is used to simulate the overfire jets and pure water the gas flowing from the bed. A movable salt water source in the bed can be used to simulate a cold spot and determine the mixing. Concentration is determined by a measure of the local conductivity. Coloring matter can be used to trace flow paths and determine dispersion effects. While the density difference is not as great as that for the combustion process, 1.2:1 being about the most that can be obtained, there is a large gain in Reynolds number, of the order of 20. A size reduction of about 4 is possible with no change in Reynolds number of the jet, while simulating buoyance effects.

One visualized model would consist of a square stack, open at the top and with a perforated plate that could be moved up from the bottom. Part way up on two opposite sides would be slots where nozzle bars could be sealed in. These would contain the desired number and size of nozzles, at the desired angle, and with a feed supply. Salt water flow would be balanced to each nozzle bar and measured. Flow of fresh water through the perforated plate would also be measured.

Air Model

If the effects of gravity can be ignored, air modeling can be used. The nozzle size is increased to compensate for the higher density of the jet fluid relative to the surroundings and the modeling proceeds in the manner used in many investigations.

The effect of gravity, which involves the Froude number $\rho U^2/dg\Delta\rho$, may pose a problem. Even using a small model furnace, so that $\Delta\rho/\rho$ is the same as in the prototype, U^2/d must be held constant. Now considering the Reynolds number of the model jet compared to the full-scale jet, $Re_m/Re_p = (d_m/d_p)^{3/2}$. If $d_m/d_p = 1/5$, then $Re_m/Re_p = 1/11.2$. For large diameter jets, at low overfire air ratios and low firing rates, this puts the model Re in a questionably low range. However, it should be possible to ignore this effect when the full-scale Re is sufficiently large. The next item to consider, though, is that the jet velocity in the model would have to be reduced by 2.25. Since there is a definite relationship between jet velocity and bed velocity, the bed velocity would have to be reduced accordingly. The velocity would no longer correspond to that from a hot bed, and thus the hot gas would have to be generated separately and supplied through a simulated bed.

In an air model, a cold jet or tracer gas up through various spots in the simulated bed can be used to determine the degree of mixing. Both colored traces and temperature measurements could be used.

The model visualized would be similar to that described above for water.

Mathematical Model

The third possibility is to set up a mathematical model of the flow system. This would have to be three-dimensional, which complicates the problem considerably. However, programs are available in primitive variables (pressure and velocity) that can be used for this purpose. Since no chemical reactions are considered, the kinetic aspects are not involved; this simplifies the problem immensely. Depending on the size of the modules, the round jets can be simulated by square jets, or multiple square jets. At a reasonable distance from orifice, this would have no effect on the results.

From such a program, once could easily check the importance of certain factors in the analysis, such as the inclusion or exclusion of buoyance effects, the substitution of a larger diameter jet with a uniform gas temperature (momentum and volume flow rate matched) and the exclusion of flow from the bed in the computation. It is important to note, however, that certain parameters entering into the mathematical analyses would require experimental determination.

REFERENCES

II-A-1. Schlichting, H.. Boundary Layer Theory. McGraw Hill, 607-609, 1960.

II-A-2. Abramovich, G. N. The Theory of Turbulent Jets. M.I.T. Press, 1963. Equation 12.127.

II-A-3. Gray, F. A., and Robertson. The Deflection of Hot Jets Due to Buoyancy. J. Inst. Fuel, 29, 424-427, 1956.

II-A-4. Thring, M. W. The Science of Flames and Furnaces, Wm Clowes & Sons, 1962.

II-A-5. Stephens, R. H. and C. M. Mohr. Reduction of Combustible Emissions in Municipal Incinerators Using Overfire Jets. AIChE Symposium Series No. 147, 71, Air I. Pollution Control and Clean Energy, 134-140, 1975.

II-A-6. Engdahl, R. B. Design Data for Overfire Jets. Combustion, March, 1944.

Phase III. Limestone/Coal Pellet Development

CONTENTS

Page

List of Figures . . . . .III- i
List of Tables. . . . . .III- iii
Executive Summary . . . . .III- vi

I. BACKGROUND. III-1

II. OBJECTIVE AND SCOPE III-2

III. PELLET DEVELOPMENT. III-3

  Binder Selection III-4
  Mechanical Properties. III-7

    Pellet Durability Index (PDI) III-7
    Fuel Pellet Strength Test III-7
    Stoker Fuel Pellet Weatherability Index (WI). III-9
    Postweathering Test III-9
    Laboratory Test Results III-9
    Baseline Data III-11
    Effect of Production Technique. III-11
    Effect of Binder. III-12
    Discussion of Experimental Results. III-20
    Binder. III-23
    Conclusions from Fixed Bed Reactor Study. . . III-27

IV. PROCESS VARIABLES SELECTION III-28

  Pellet Details III-29

    Experimental Results. III-33

  Pellet Characterization Studies. III-42

    Scanning Electron Microscopy. III-49
    X-Ray Diffraction III-54
    Description of Mathematical Model III-54

  Modeling Analysis of Pellet Combustion Data. . . . III-59

    Determination of Rate Constants III-64
    Transient Heat-Transfer Analysis. III-74

CONTENTS (Continued)

Page

Detailed Modeling Calculations. III-77

Modeling and Characterization Summary and Conclusions III-84

V. LABORATORY EVALUATION III-85

Model Spreader Experiment. III-85

Sampling System III-87
Ca/S Ratio. III-87
Production Technique. III-87
Binder Type III-89

Pellet Preparation and Properties. III-90
Experimental Procedures. III-94

Checkout Runs III-96
Demonstration Test. III-99

Summary. III-103

VI. LIMESTONE/COAL FUEL PELLET PROCESS COST SUMMARY. . . . III-104

Basic Assumptions. III-104
Process Flowsheet. III-106
Sources of Information III-106
Capital Cost Estimates III-110

References. III-114

PHASE III

List of Figures

Page

Figure III-1. Apparatus for Testing Fuel Pellet Strength. III-8

Figure III-2. Fixed-Bed Reactor III-15

Figure III-3. CO_2 Concentration Measured in the Gas Stream from the Fixed-Bed Reactor for the Limestone Pellets in Run 110. . . . . III-37

Figure III-4. Concentrations of CO_2, SO_2, O_2, and CO Measured in Gas Stream from the Fixed Bed Reactor for the 50 Weight Percent Coal/50 Weight Percent Limestone Pellets in Run 104 . . . . III-38

Figure III-5. Concentrations of CO_2, SO_2, O_2, and CO Measured in Gas Stream from the Fixed Bed Reactor for the 70 Weight Percent Coal/30 Weight Percent Limestone Pellets in Run 101. . . . . III-39

Figure III-6. Release Rates for CO_2 and SO_2 from 50 Weight Percent Coal/50 Weight Percent Limestone Pellets During Run 104. III-43

Figure III-7. Release Rates for CO_2 and SO_2 from 70 Weight Percent Coal/30 Weight Percent Limestone Pellets During Run 101 . . . . III-44

Figure III-8. Thermocouple Measurements for Fixed Bed Reactor Run 101 with 70 Weight Percent Coal/30 Weight Percent Limestone Pellet. III-45

Figure III-9. Metallographic Cross Sections of 50 Weight Percent Coal/50 Weight Percent Limestone Pellets as a Function of Burning Time. III-46A

Figure III-10. Scanning Electron Micrographs and Elemental X-Ray Maps for Unburned 50 Weight Percent Coal/50 Weight Percent Limestone Pellet (Pellet 72). III-50a

Figure III-11. Scanning Electron Micrographs and Elemental X-Ray Maps for Outer Ash Zone in 50 Weight Percent Coal/ 50 Weight Percent Limestone Pellet (Pellet 65) Burned for 12 Minutes in the Fixed Bed Reactor. . III-51a

Figure III-12. Scanning Electron Micrographs and Elemental X-Ray Maps for White Reaction Zone in 50 Weight Percent Coal/50 Weight Percent Limestone Pellet (Pellet 65) Burned for 12 Minutes in the Fixed Bed Reactor. . . III-52a

List of Figures (continued)

Page

Figure III-13. Scanning Electron Micrographs and Elemental X-Ray Maps for Inner Core in 50 Weight Percent Coal/50 Weight Percent Limestone Pellet (Pellet 65) Burned for 12 Minutes in the Fixed-Bed Reactor III-53a

Figure III-14. CuKα Radiation Scatter of Unburned Coal III-55

Figure III-15. CuKα Radiation Scatter of Unheated Limestone. III-55

Figure III-16. CuKα Radiation Scatter of Unburned 70/30 Mixture. . . III-55

Figure III-17. CuKα Radiation Scatter of 70/30 Limestone/Coal Burned Pellet. Major Identified Constituents CaO (Lime), $CaSO_4$ (Anhydrite) III-55

Figure III-18. Summary of Results of the Chemical Analyses on 50 Weight Percent Coal/60 Weight Percent Limestone Pellets from Fixed Bed Reactor Experiments (Data from Table 8). III-62

Figure III-19 Summary of Results of the Chemical Analyses on 70 Weight Percent Coal/30 Weight Percent Limestone Pellets from Fixed Bed Reactor Experiments (Data from Table 9). III-63

Figure III-20. Unburned Core Radius as a Function of Burning Time Calculated Using Simplified Model (Data Points Represent Measurements on 50/50 Pellets) III-65

Figure III-21. SO_2 Release Rate and Calculated ECO Analyzers Based on the Simplified Model (Equation 7) for 50 Weight Percent Coal/50 Weight Percent Limestone Pellet III-70

Figure III-22. Oxygen Consumption Rates Calculated Using Simplified Model III-71

Figure III-23 Sulfur Retention and Burning Time for 50 Weight Percent Coal/50 Weight Percent Limestone Pellet Calculated as a Function of Pellet Diameter Using the Simplified Model III-72

Figure III-24. Burning Time for 50 Weight Percent Coal/50 Weight Percent Limestone Pellet Calculated as a Function of Temperature Using the Simplified Model. III-73

Figure III-25. Transient Heat Transfer Calculations for a 70 Weight Percent Coal/30 Weight Percent Limestone 13.7 mm Diameter Spherical Pellet. III-75

List of Figures (continued)

Page

Figure III-26. Transient Heat Transfer Calculations for a 50 Weight Percent Coal/50 Weight Percent 13.7 mm Diameter Limestone Spherical Pellet. III-76

Figure III-27. Calculated Combustion Rate for 70 Weight Percent Coal/30 Weight Percent Limestone Pellet. III-78

Figure III-28. Calculated SO_2 Release Rate for 70 Weight Percent Coal/30 Weight Percent Limestone Pellet. III-79

Figure III-29. Calculated O_2 Consumption Rate for 70 Weight Percent Coal/30 Weight Percent Limestone Pellet. . III-80

Figure III-30. Calculated CaO Distribution at 35.10 sec in 70 Weight Percent Coal/30 Weight Percent Limestone Pellet III-81

Figure III-31. Calculated SO_2 Distribution at 35.10 sec in 70 Weight Percent Coal/30 Weight Percent Limestone Pellet III-82

Figure III-32. Calculated O_2 Distribution at 35.10 sec for 70 Weight Percent Coal/30 Weight Percent Limestone Pellet III-83

Figure III-33. Model Spreader Sampling System III-88

Figure III-34. Location and Orientation of Gas Sample Probe . . . III-95

Figure III-35. Coal/Limestone/Cement Pelletizing Process Flowsheet. III-107

PHASE III

List Of Tables

Page

Table III-1. Agglomeration Methods. III-5

Table III-2. Binders Evaluated During the Phase III Program . III-6

Table III-3. Pellet Optimization Data III-10a

Table III-4. Comparison of Test Results By Production Technique III-12

Table III-5. Reproducibility Series with 50/50 Pellets, Furnace Temperature 1040 C, with 33% Overfire Air . III-18

Table III-6. Fixed-Bed Experiment Runs. III-19

Table III-7. The Effect of Ca/S Ratio on Sulfur Capture . . . III-21

Table III-8. The Effect of Sorbent on Sulfur Capture. III-22

Table III-9. Comparison of the Effect of Limestone and Lime on Sulfur Capture. III-23

Table III-10. The Effect of Binder Type on Sulfur Capture. . . III-24

Table III-11. The Effect of Production Method on Sulfur Capture III-25

Table III-12. The Effect of Production Technique on Reactivity III-26

Table III-13. The Effect of Additives on Sulfur Capture. . . . III-26

Table III-14. Typical Pellet Densities and Porosities. III-31

Table III-15. Summary of Chemical Analyses on Raw Coal and Pellets. III-32

Table III-16. Summary of Fixed-Bed Reactor Experiments Performed in Support of the Modeling Studies III-34

Table III-17. Results from Chemical Analyses of Pellets From Fixed Bed Reactor Experiments. III-36

Table III-18. Response Parameters for Gas Analyzers. III-41

Table III-19. Results from Gas Analyzer Measurements III-47

List of Tables (Continued)

		Page
Table III-20.	Comparison of Gas Analyzer Measurements for Coal/Limestone Pellets.	III-48
Table III-21.	Summary of Results of the Chemical Analyses on 50 Weight Percent Coal/50 Weight Percent Limestone Pellets from Fixed Bed Reactor Experiments	III-60
Table III-22.	Summary of Results of the Chemical Analyses on 70 Weight Percent Coal/30 Weight Percent Limestone Pellets from Fixed Bed Reactor Experiments.	III-61
Table III-23.	Summary of Chemical Analyses and Physical Measurements on the Limestone Pellets from the Fixed Bed Reactor Experiments.	III-66
Table III-24.	Summary of Burning Rate Measurements for 50 Weight Percent Coal/50 Weight Percent Limestone Pellets Based on Metallographic Studies.	III-67
Table III-25.	Summary of Calculations Using Simplified Model	III-68
Table III-26.	Model-Spreader Studies	III-86
Table III-27.	Potential Tolling Companies for Large Quantities of Pellets	III-91
Table III-28.	Ultimate, Proximate, and Ash-Fusion Temperature Analyses for Limestone/Coal Fuel Pellet Ca/S=3.5	III-92
Table III-29.	Mineral Analysis of Ash.	III-93
Table III-30.	Comparison of Emissions From Combustion of a Low Sulfur Coal and Limestone/Coal Pellet.	III-98
Table III-31.	Emission Data Summary for Fuel Pellet Demonstration	III-100
Table III-32.	Analysis of Method 5 Filter Catch (Weight Percent)	III-101
Table III-33.	Analysis of Grate Discharge (Weight Percent)	III-101
Table III-34.	Sulfur Balance	III-101
Table III-35.	Summary of Limestone/coal Pelletizing Process Costs.	III-105
Table III-36.	Coal/Limestone/Cement Pelletizing Process. . . .	III-
Table III-37.	Capital Cost Estimates	III-

EXECUTIVE SUMMARY

The Phase III program focused on refinement of the limestone/coal fuel pellet and evaluation of its suitability as an industrial stoker-boiler fuel. This program consisted of four major tasks.

1. Pellet Development aimed at developing a fuel pellet with mechanical strength characteristics that can withstand weathering and the severe stresses of an industrial stoker coal-handling and feeding system, burns at reasonable rates, and captures sufficient sulfur to be competitive with other control strategies. Mechanical strength characteristics were evaluated with standard laboratory tests. Burning characteristics and sulfur capture were determined in a fixed-bed reactor simulating the fuel bed of a spreader stoker.

2. Process Variables Selection combining a mathematical model analysis with a series of experimental studies to develop a more comprehensive understanding of the processes that influence the combustion of the fuel pellet and control the capture of sulfur.

3. Laboratory Evaluations conducted in both the 200 kW_{th} model-spreader stoker and the 8 MW_{th} Battelle steam plant boiler to evaluate the most promising candidate pellets.

4. Economic Analysis aimed at developing pellet process costs.

The major results and conclusions of the four tasks are:

Pellet Development

- A fuel pellet was produced that, according to laboratory tests, has mechanical strength and durability characteristics similar to those of conventional coals.

- Pellets produced by auger extrusion or pellet mill processes had better mechanical strength than those produced by disc pelleting or briquetting.

- Binders that provide some resistance to the weather were identified. However, no binder was identified that provided complete weather proofing.

- The fixed-bed reactor experiments indicated a weak dependency between Ca/S ratio and sulfur capture for Ca/S ratios above 2.

- Calcium oxide is a superior absorbent to limestone, but is not economically competitive with limestone.

- Additives do not appear to enhance sulfur capture.

Process Variables Selection

- The mathematical model predicts an optimum coal size (35-40 mm diameter) for maximum sulfur retention.

- The model indicates a weak dependency on the calcium/sulfur ratio.

- Scanning electron microscopy and x-ray diffusion are powerful tools for the study of solid-state reactions in the pellets. Results indicate that sulfur is retained predominantly as $CaSO_4$.

- Sulfur may react directly with limestone by solid-state processes without involving the formation of SO_2.

Laboratory Evaluations

- Auger-extruded and milled pellets burned better than briquets and disc-agglomerated pellets.

- Sulfur capture of about 65 percent was achieved at Ca/S molar ratios of 3.5.

- Sulfur capture of about 50 percent was achieved in the steam-plant stoker. In comparison to the model spreader, this lower SO_2 capture was attributed to higher temperatures (in excess of 1300 C).

- Sulfur capture appeared to be weakly dependent on fuel-bed temperature.

- In the Battelle steam power plant, the fuel pellets burned as well as low-sulfur coal.

Economic Analysis

- It is estimated that limestone/coal fuel pellets can be produced for about \$15.40/Mg (\$14/ton) of pellets above the costs of the high-sulfur coal.

PHASE III. LIMESTONE/COAL PELLET DEVELOPMENT

SECTION III-1

BACKGROUND

During Phase II of this program, Control Technology Evaluation, SO_2 was considered as the most troublesome emission to control in an industrial stoker-boiler system. The other criteria emissions could be controlled with existing technology or were within the current emissions requirements. As a result, and because the limestone/coal fuel pellet offers a means for environmentally acceptable burning of high-sulfur coal in existing boilers, EPA continued the development of the fuel pellet as part of this program.

From an industrial point of view, the possibilities of using limestone/coal pellets for removing SO_2 in situ via a dry process is more acceptable than the use of scrubbers. The additional costs for pelletizing the coal/limestone mixture and for the removal of 3 to 4 times as much ash is far more attractive than the high cost of operating and maintaining wet scrubbers.

SECTION III-2

OBJECTIVE AND SCOPE

The overall objective of the Phase III program was to refine the limestone/coal fuel pellet and evaluate its suitability as an industrial stoker boiler fuel. Phase III focused on the following major tasks:

- Pellet Development aimed at producing a limestone/coal fuel pellet that is economically competitive with other control technologies, has sufficient mechanical strength, durability, and weatherability characteristics, and burns like ordinary coal.

- Process Variables Selection aimed at developing a coal pellet combustion model to be used as: (1) a predictive tool to support pellet development and (2) an interpretive tool to provide information on the burning time and sulfur capture behavior of coal/limestone pellets.

- Laboratory Evaluations focused on evaluating the most promising candidate pellets in the model-spreader stoker boiler. In addition, a limited number of pellet tests were conducted in the steam plant stoker.

- Economic Analysis aimed at estimating costs for the manufacture of limestone/coal fuel pellets.

SECTION III-3

PELLET DEVELOPMENT

The results of the Phase II short-term steam plant demonstration indicated that the physical properties of pellets had to be improved if they were to be a viable industrial-stoker boiler fuel. Cement-bound pellets used in Phase II did not have adequate strength or durability. They broke on handling so that up to 50 percent fines was introduced into the boiler. Furthermore, both from an economical and operational standpoint, the amount of limestone required to capture the target goal of 70 percent sulfur had to be limited to stay within a Ca/S molal ratio of 3 to 4. Accordingly, an experimental research and development effort was undertaken to provide an improved pellet over that evaluated in Phase II.

PELLET PRODUCTION TECHNIQUES

The concept of agglomerating coal particles is not new. The Institute for Briquetting and Agglomeration (IBA) was formed originally as the International Briquetting Association in 1949 and has held biannual conferences since. Initially, these conferences focused on coal briquetting but have more recently expanded to include all types of agglomeration. Agglomeration, in the general sense, is any process where smaller particles are brought together and formed into larger masses of compacted material. Agglomeration processes include pelleting, briquetting, and pelletizing.

Pelleting is described as an extrusion of small, particle-sized material through a die, the material being forced by an auger or a ring mill. Briquetting involves high-pressure compaction of material, often between rolls that contain pockets to form the desired size and shape. Pelletizing is a particle agitation process that involves rolling of fine, moist powders in a disc or drum causing the particles to coalesce and form spheres

All of these methods have advantages and disadvantages that affect their suitability for coal agglomeration. They have all been used on at least a laboratory scale for coal agglomeration, but no clearcut advantage has been cited in the literature for any of them. Relative processing characteristics for different agglomeration methods are summarized in Table III-1, based on a review of IBA proceedings.

BINDER SELECTION

The binder is an essential element in fuel-pellet formulations. With the right binder, a pellet will have the mechanical strength, durability, and weatherability needed for a stoker-boiler fuel. Accordingly, an extensive search was conducted to identify candidate binders. Table III-2 lists the more promising binders evaluated during this phase of the work.

A review of the literature indicated that while extensive work has been done on coal briquets, there has been little work on disc pelletizing, mill pelleting, or auger extrusion of coal fines. Further, most of the coal briquets were produced using a hard pitch binder, which requires an extensive tempering process. This prior research, however, was useful in producing a list of candidate binders to be investigated further.

Komarek(III-1)* provides a very useful discussion on binders used during pressure compaction of various materials. From this source, as well as data from Pennwalt Chemicals Corporation reproduced in the Chemical Engineer's Handbook(III-2), candidate binders were identified. This list was expanded during discussions with members of the ceramic and polymer chemistry groups at Battelle, as well as technical representatives of companies manufacturing agglomerating equipment. Most of the major chemical companies were also consulted as were companies in the pulp-paper industry. Late in the program, unpublished data from a study on pelletizing fines were made available to this program. This study, performed by Babcock Contractors for the U.S. Department of Energy, Pittsburgh Mining Technology Center, concentrated only on disc pelletizing but the data should still extrapolate well to other processes. All binders that Babcock Contractors found promising were already included in the candidate list.

---

* References are listed on page III-114.

TABLE III-1. AGGLOMERATION METHODS

Comments	Mill Pelleting	Briquetting	Disc Pelletizing	Auger Extrusion
Moisture Required (w/o)	10-20	4-10	10-20	10-20
Lubricant Required	Desirable	Desirable	No	Yes
Binder Required	Yes	Not Necessarily	Yes	Yes
Maintenance	High	High	Low	Moderate
Power Costs	Moderate	High	Low	High
Die Wear Costs	High	High	N/A	High
Labor Required	Moderate	Low	Moderate	Moderate
Operational Problems	Possible	Few	Possible	Possible
Agglomerate Size	Small Cylinders	Assorted Shapes and Sizes	Spheres 1/4-1 in. dia.	Continuous Ribbons or Cylinders
Relative Size Distribution of Feed Material	Moderate	Large	Small	Moderate
Relative Agglomerate Density	Moderate	High	Low	Moderate
Relative Output	Small	High	Moderate	High
Drying Required	Yes	Possibly	Yes	Yes
Relative Strength	Moderate	High	Low	Moderate
Other	Generates Heat	Feed Screw Wear Possible	Longer Start Up and Waste	Mixing May not be Required

TABLE III-2. BINDERS EVALUATED DURING THE PHASE III PROGRAM

Inorganics

Cement
Epsom salt
Magnesium sand
Magnesium hydroxide
Phosphoric acid
Sulfuric acid
Bentonite clay
Calcium borate

Natural Organics

Potato starch
Corn starch
Parafin
Asphalt emulsion (5)
Lignin
Ligno sulfonate
Waxes
Dextrose
Creosol
Anthracene oil
Coal tars
Pitches
Fuel oil
Sawdust
Wheat flour

Processed Organics

Dowell M-107.01 latex resin
Dowell M-166 latex resin
Goodrich X-183 latex resin
Goodrich X-83 latex resin
Dow methocel F (methyl cellulose gum)
Dow methocel A (methyl cellulose gum)
Borden polyco (3) vinylacetate copolymers
Dow P-4000 polyethylene glyco copolymer
Dow E-8000 polyethylene glyco copolymer
Union Carbide PEG-100, polyethylene glyco copolymer
Union Carbide PEG-200, polyethylene glyco copolymer
Epon G-15 epoxy resin
Sterotex, hydrogenated cottonseed oil
Allbond 200, pregeletanized corn starch

MECHANICAL PROPERTIES

Limestone/coal fuel pellets must have sufficient mechanical strength, durability, and weatherability to survive the severe tumbling, crushing, and weathering actions associated with typical fuel handling and storage for industrial stoker firing. The following laboratory test procedures were developed to evaluate different formulations for mechanical properties.

Pellet Durability Index (PDI)

The PDI is determined using the equipment and procedure specified by ASAE (Reference S-269.1). This test, similar to the ASTM tumbling index test, simulates the tumbling action and impact forces encountered in handling operations. The PDI indicates the percentage of pellets that remain intact after such handling. In this test, a 500-gram sample is placed in a 0.6 m square, 127 mm wide test bin, which is rotated at 50 rpm for 10 minutes. The contents are then screened (4 mesh) and the +4 mesh fraction weighed. The PDI is defined as:

$$\text{PDI} = \frac{\text{weight of +4 mesh fraction (grams)}}{500} \times 100.$$

Fuel Pellet Strength Test

This test and the associated equipment (Figure III-1) were designed to simulate the crushing forces a pellet might experience during storage in a pile, transportation by truck or railroad car, and feeding and handling. The pellet is placed between two 25-mm diameter circular plates so that radial forces are applied. (Cylindrical pellets are usually capable of withstanding greater axial forces than radial forces.) The top plate is attached to an air-driven plunger. The pressure on the 775-mm^2 plunger is increased until the pellet fractures. The compressive force required to crush the pellet is obtained by multiplying the air pressure by the plunger area, i.e.,

$$F \text{ lbs} = \text{psi} \times 1.2$$

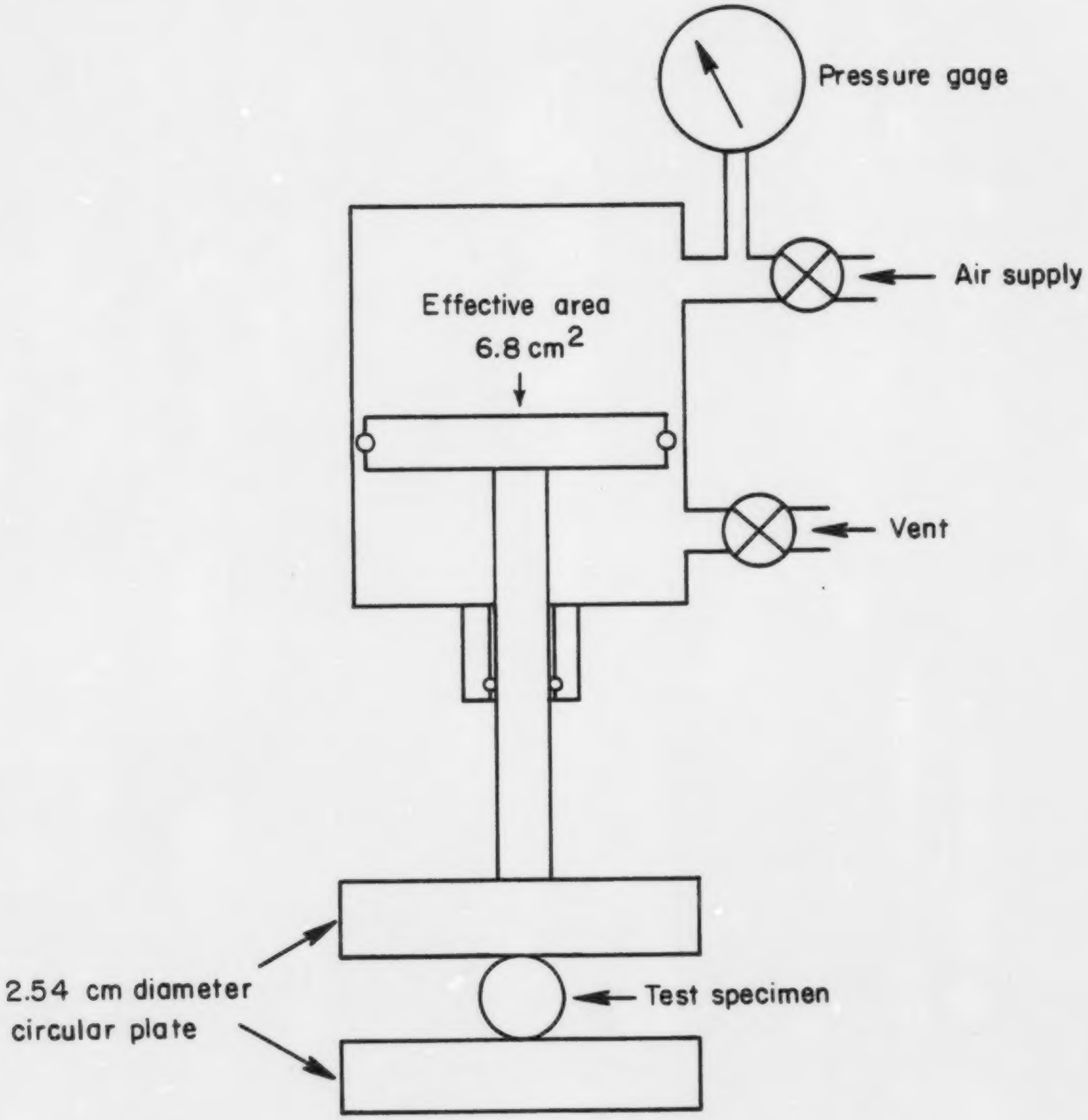
Pressure gage
Air supply
Effective area
6.8 cm^2
Vent
2.54 cm diameter
circular plate
Test specimen

FIGURE III-1. APPARATUS FOR TESTING FUEL PELLET STRENGTH

Stoker Fuel Pellet Weatherability Index (WI)

This test is designed to simulate the severe weathering conditions a fuel pellet may encounter during outdoor winter storage. It has been derived from ANSI/ASTM Test No. C666, "Resistance of Concrete to Rapid Freezing and Thawing". The test consists of four freeze/thaw cycles of 4 hours each.

A 0.45 Kg sample of pellets is alternately placed in 4 C water for 2 hours, then frozen in -18 C air for 2 hours. After four such cycles, the pellets are drained and exposed to ambient room conditions overnight. After the fuel pellets reach equilibrium with the room conditions, a screen analysis (4 mesh) is run and the weatherability index is reported as the percentage of whole pellets:

$$\text{WI} = \frac{\text{lbs } (+4 \text{ mesh})}{1.0} \times 100 \quad .$$

Postweathering Test

Since coal that is exposed to severe weathering conditions during storage must retain its mechanical strength and durability characteristics, the whole pellet samples were retested for durability and strength after the weatherability tests. These retests are referred to as postweathering tests.

Laboratory Test Results

During the pellet development work, the four production techniques referred to earlier were used to produce 166 test samples. These samples were evaluated for durability, strength, weatherability, and postweathering durability and strength. The data from these tests are presented in Table III-3. To provide a baseline for comparison and a target goal, four different coal types and the 50/50 pellet from Phase II were evaluated using the same test procedures. These are listed as the first five tests in Table III-3.

TABLE III-3. PELLET OPTIMIZATION DATA

Test No.	Production Method	Pellet Formulation(a) Coal Type	Coal %	Limestone Type	Limestone %	Binder Type	Binder %	Remarks	Durability Index(b)	Compression Strength, lb *	Weather Index(b)	Post Weathering Durability(b) Index	Post Weathering Strength,* lb
1	Raw Coal	Illinois #6	100	--	--	--	--	Baseline Data	85 ± 2	74 ± 12	89 ± 1	75	58 ± 34
2	Raw Coal	E. Kentucky	100	--	--	--	--	Baseline Data	85 ± 2	83 ± 22	94 ± 1	83	94 ± 16
3	Raw Coal	Lignite	100	--	--	--	--	Baseline Data	77 ± 4	92 ± 22	80 ± 4	34	45 ± 12
4	Raw Coal	Rosebud	100	--	--	--	--	Baseline Data	84 ± 2	50 ± 15	79 ± 2	20	68 ± 29
5	20 Hp CPM Mill	Illinois #6	50	Piqua	50	Cement	5	Baseline Data	37 ± 10	42 ± 1	59 ± 2	40	24
6	Mars-Disk	Illinois #6	50	Piqua	50	"Super"	10	Air Dried	-- --	24 ± 8	-- -	--	--
7	Mars Disk	Illinois #6	50	Piqua	50	"Super"	10	Oven Dried	-- --	19	-- -	--	--
8	CPM Lab Mill	Illinois #6	70	Piqua	30	Epon 815#	4	Epoxy Resin	15 ± 2	10 ± 1	-- -	--	--
9	CPM Lab Mill	Illinois #6	70	Piqua	30	#6 Fuel Oil	5		17 ± 2	8 ± 2	-- -	--	--
10	CPM Lab Mill	Illinois #6	70	Piqua	30	#6 Fuel Oil	2		8 ± 2	17 ± 5	-- -	--	--
11	CPM Lab Mill	Illinois #6	70	Piqua	30	Sawdust	5		1 ± 1	6 ± 1	-- -	--	--
12	CPM Lab Mill	Illinois #6	70	Piqua	30	Sawdust + Oil	7	(5 Sawdust -2 #6 Oil)	7 ± 2	4 ± 1	-- -	--	--
13	CPM Lab Mill	Illinois #6	70	Piqua	30	Epan 815#	5	Oven Cured	0	3 ± 2	-- -	--	--
14	CPM Lab Mill	Illinois #6	70	Piqua	30	Coal Tar	5	Mixed & Run	25 ± 5	24 ± 3	-- -	--	--
15	CPM Lab Mill	Illinois #6	70	Piqua	30	Cresol	5	Mixed & Run	2 ± 1	21 ± 7	-- -	--	--
16	CPM Lab Mill	Illinois #6	70	Piqua	30	Anthracene Oil	5	Mixed & Run	15 ± 1	38 ± 10	-- -	--	--
17	CPM Lab Mill	Illinois #6	70	Piqua	30	Indolinat Oil	5	Lignin	3 ± 2	17 ± 5	-- -	--	--
18	CPM Lab Mill	Lignite	100	---	0	None	-	Pelletized Lignite Fines	18 ± 2	12 ± 4	-- -	--	--
19	CPM Lab Mill	Illinois #6	70	Piqua	30	M-167.01	5	Dowell Latex	79 ± 1	88 ± 15	-- -	--	--
20	CPM Lab Mill	Illinois #6	70	Piqua	30	M-166	5	Dowell Latex	61 ± 1	49 ± 15	-- -	--	--
21	CPM Lab Mill	Illinois #6	70	Piqua	30	Coal Tar	5	Mix to Heat Treat - 1 hour @ 160 C	23 ± 7	33 ± 5	-- -	--	--
22	CPM Lab Mill	Illinois #6	70	Piqua	30	Cresol	5	Mix to Heat Treat - 1 hour @ 160 C	7 ± 2	29 ± 17	-- -	--	--
23	CPM Lab Mill	Illinois #6	70	Piqua	30	Anthracene	5	Mix to Heat Treat - 1 hour @ 160 C	21 ± 2	5 ± 1	-- -	--	--
24	CPM Lab Mill	Illinois #6	70	Piqua	30	Koppers Solvent	5	Mix to Heat Treat - 1 hour @ 160 C	25 ± 5	29 ± 1	-- -	--	--
25	CPM Lab Mill	Illinois #6	70	Piqua	30	Asphalt - E65	5	Emulsion from Armak	13 ± 2	19 ± 5	-- -	--	--
26	CPM Lab Mill	Illinois #6	70	Piqua	30	Asphalt - E4868	5	Emulsion from Armak	9 ± 3	25 ± 4	-- -	--	--
27	CPM Lab Mill	Illinois #6	70	Piqua	30	Asphalt - 13GR	5	Emulsion from Armak	4 ± 2	14 ± 2	-- -	--	--
28	CPM Lab Mill	Illinois #6	70	Piqua	30	Anthracene Oil	5	Test #16 Used - 19 days	28	~34	-- -	--	--
29	CPM Lab Mill	Illinois #6	50	Piqua	50	Cement	5	Ca/S Ratio Series	49 ± 2	38 ± 3	-- -	--	--
30	CPM Lab Mill	Illinois #6	60	Piqua	40	Cement	5	Ca/S Ratio Series	43 ± 3	39 ± 5	-- -	--	--
31	CPM Lab Mill	Illinois #6	70	Piqua	30	Cement	5	Ca/S Ratio Series	45 ± 2	36 ± 4	-- -	--	--
32	CPM Lab Mill	Illinois #6	80	Piqua	20	Cement	5	Ca/S Ratio Series	26 ± 0	32 ± 3	-- -	--	--
33	CPM Lab Mill	Illinois #6	70	Piqua	30	Cement	5	Production Run	44 ± 0.5	49 ± 9	-- -	--	--
34	CPM Lab Mill	Illinois #6	80	Lime (CaO)	20	Cement	5	Reagent Grade CaO	49 ± 4	46 ± 11	-- -	--	--
35	CPM Lab Mill	Illinois #6	70	Piqua	30	M-167.01	1	Dowell Latex	9 ± 3	22 ± 3	-- -	--	--
36	CPM Lab Mill	Illinois #6	70	Piqua	30	M-166	1	Dowell Latex	4 ± 1	19 ± 5	-- -	--	--
37	CPM Lab Mill	Illinois #6	70	Fedonia	30	Cement	5	Limestone Type Series	25 ± 1	26 ± 3	-- -	--	--
38	CPM Lab Mill	Illinois #6	70	Basic Lime	30	Cement	5	Limestone Type Series	32 ± 3	32 ± 7	-- -	--	--
39	CPM Lab Mill	Illinois #6	70	Howard	30	Cement	5	Limestone Type Series	19 ± 1	36 ± 2	-- -	--	--
40	Disk by Coalmet	Illinois #6	70	Piqua	30	Coalmet	?	Proprietary Organic	96	92 ± 19	100(c) -	--	53 ± 15
41	Disk	Illinois #6	83	Piqua	17	Asphalt 4868	8.3	Coarse Coal - 8 mesh	86	22 ± 1	0 -	--	--
42	Disk	Illinois #6	71	Piqua	29	Asphalt 4868	8.5	Coarse Coal - 8 mesh	28	8 ± 3	0 -	--	--
43	Disk	Illinois #6	71	Piqua	29	Asphalt 4868	8.5	Fine Coal - 100 mesh	15	~ 1	0 -	--	--
44	Disk	Illinois #6	70	Piqua	30	M-167.01	2.5	Dowell Latex	2	~ 1	0 -	--	--
45	Disk	Illinois #6	70	Piqua	30	M-167.01	1.2	Dowell Latex	3	~ 1	0 -	--	--

(a) Water added as needed.
(b) Percent survival = 100 - percent fines.
(c) Some evidence of fracturing
* 1 lb = 4.448 N

TABLE III-3. (continued)

Test No.	Production Method	Pellet Formulation[(a)] Coal Type	Coal %	Limestone Type	Limestone %	Binder Type	Binder %	Remarks	Durability Index[(b)]	Compression Strength, lb *	Weather Index[(b)]	Post Weathering Durability[(b)] Index	Post Weathering Strength, lb *
46	Disc	Illinois #6	70	Piqua	30	M-167.01	0.5	Dowell Latex	17	1	0	--	--
47	Disc	Illinois #6	70	Piqua	30	Norleg 11	10	Lignin Powder	65	11	0	--	--
48	Disc	Illinois #6	70	Piqua	30	Norleg 41	5	Lignin Liquor	0	1	--	--	--
49	Disc	Illinois #6	70	Piqua	30	Norleg 41	10	Lignin Liquor	0	3	--	--	--
50	CPM Lab Mill	Illinois #6	70	Piqua	30	Norleg 11	10	Lignin Powder	0	22 ± 8	0	--	--
51	CPM Lab Mill	Illinois #6	70	Piqua	30	Methocell F	5	Methyl Cellulose Gum by Dow	97	>110	0	--	--
52	CPM Lab Mill	Illinois #6	70	Piqua	30	Epsom Salt	5		22	22 ± 4	--	--	--
53	CPM Lab Mill	Illinois #6	70	Piqua	30	Mag. Sand	5	Magnesium salts	4	18 ± 1	--	--	--
54	CPM Lab Mill	Illinois #6	70	Piqua	30		5	Magnesium Hydroxide	4	18 ± 4	--	--	--
55	CPM Lab Mill	Illinois #6	70	Piqua	30	M-166	2.5	Dowell Latex	22	30 ± 10	--	--	--
56	CPM Lab Mill	Illinois #6	70	Piqua	30	M-166	5.0	Dowell Latex	29	35 ± 8	--	--	--
57	CPM Lab Mill	Illinois #6	70	Piqua	30	M-167.01	2.5	Dowell Latex	31	38 ± 10			
58	CPM Lab Mill	Illinois #6	70	Piqua	30	M-167.01	5	Dowell Latex	31	29 ± 5			
59	CPM Lab Mill	Illinois #6	70	Piqua	30	H_3PO_4	5		17	22 ± 9			
60	CPM Lab Mill	Illinois #6	70	Piqua	30	H_3PO_4	5	Cured 1 hour after mixing	28	38 ± 15			
61	CPM Lab Mill	Illinois #6	70	Piqua	30	H_2SO_4	5		6	31 ± 4			
62	CPM Lab Mill	Illinois #6	70	Piqua	30	H_2SO_4	5	Cured 1 hour after mixing	19	35 ± 9			
63	CPM Lab Mill	Illinois #6	70	Piqua	30	M-167.01	1	Dowell Latex	6	34 ± 4			
64	CPM Lab Mill	Illinois #6	70	Piqua	30	M-166	1	Dowell Latex	6	32 ± 3			
65	CPM Lab Mill	Illinois #6	70	Piqua	30	Norleg 41	15	Lignin Liquor	6	18 ± 9			
66	CPM Lab Mill	Lignite	100	--	--	--	--	Raw Lignite Fines	8	5			
67	CPM Lab Mill	Lignite	100	--	--	Methocell F	5	Methyl Cellulose Gum by Dow	95	>113			
68	CPM Lab Mill	Lignite	100	--	--	M-167.01	5	Dowell Latex	37	23			
69	CPM Lab Mill	Lignite	100	--	--	Asphalt 4868	5	Asphalt Emulsion	25	8			
70	CPM Lab Mill	Lignite	100	--	--	Methocell F	1	Methyl Cellulose Gum by Dow	42	18			
71	Disc	Illinois #6	70	Piqua	30	Methocell F	5	Air dried - 3 days	99.6	60 ± 24	0		
72	Disc	Illinois #6	70	Piqua	30	Methocell F	5	Oven dried - 3 hours 100° C	100	84 ± 12	0		
73	Disc	Illinois #6	70	Piqua	30	M-167.01	10	Air dried - 3 days	7	1	0		
74	Disc	Illinois #6	70	Piqua	30	Asphalt 4868	10	Air dried - 3 days	13	3	0		
75	CPM Lab Mill	Illinois #6	70	Piqua	30	M-167.01	2.5	Test 57 aged 32 days	52	56 ± 9	--	--	--
76	CPM Lab Mill	Illinois #6	70	Piqua	30	M-167.01	5	Aged 17 days	88	110 ± 2	85	62	106
77	CPM Lab Mill	Illinois #6	70	Piqua	30	M-167.01	2.5	Aged 17 days	40	53 ± 18	--	--	--
78	CPM Lab Mill	Illinois #6	70	Piqua	30	M-167.01	1.0	Aged 17 days	37	23 ± 1	--	--	--
79	CPM Lab Mill	Illinois #6	70	Piqua	30	M-167.01	5	Test 58 aged 32 days	55	32 ± 8	85	96	--
80	CPM Lab Mill	Illinois #6	70	Piqua	30	Methocell F	10	Methyl Cellulose Gum	99.6	>112	--	--	--
81	CPM Lab Mill	Illinois #6	70	Piqua	30	Methocell F	5	Methyl Cellulose Gum	93	>112	0	--	--
82	CPM Lab Mill	Illinois #6	70	Piqua	30	Methocell F	5	Methyl Cellulose Gum	98	>112	--	--	--
83	CPM Lab Mill	Illinois #6	70	Piqua	30	Methocell F	1	Methyl Cellulose Gum	96	112	--	--	--
84	CPM Lab Mill	Illinois #6	70	Piqua	30	Methocell F	0.5	Methyl Cellulose Gum	88	68 ± 18	0	--	--
85	CPM Lab Mill	Illinois #6	70	Piqua	30	Methocell F	0.1	Methyl Cellulose Gum	29	28 ± 6	--	--	--
86	CPM Lab Mill	Illinois #6	70	Piqua	30	Methocell A	33	Methyl Cellulose Gum	99.1	>112	--	--	--
87	CPM Lab Mill	Illinois #6	70	Piqua	30	Methocell A	10	Methyl Cellulose Gum	99.1	>112	--	--	--
88	CPM Lab Mill	Illinois #6	70	Piqua	30	Methocell A	5	Methyl Cellulose Gum	93	88 ± 30	0	--	--
89	CPM Lab Mill	Illinois #6	70	Piqua	30	Methocell A	1	Methyl Cellulose Gum	81	85 ± 18	--	--	--
90	CPM Lab Mill	Illinois #6	70	Piqua	30	Methocell A	0.5	Methyl Cellulose Gum	73	65 ± 9	--	--	--
91	CPM Lab Mill	Illinois #6	70	Piqua	30	Methocell A	0.1	Methyl Cellulose Gum	9	33 ± 11	--	--	--
92	CPM Lab Mill	Illinois #6	70	Piqua	30	Blend M-1	5	4% Methocell F - 1% M-167.01	97	>112	--	--	--
93	CPM Lab Mill	Illinois #6	70	Piqua	30	Blend M-2	5	2.5% Methocell F - 2.5% M-167.01	99	>112	92	90	>112
94	CPM Lab Mill	Illinois #6	70	Piqua	30	Blend M-3	5	1% Methocell F - 4% M-167.01	96	106 ± 2	--	--	--
95	CPM Lab Mill	Illinois #6	70	Piqua	30	Blend M-4	4.5	0.5% Methocell F - 4% M-167.01	94	>112	--	--	--
96	CPM Lab Mill	Illinois #6	70	Piqua	30	Blend M-5	5.5	0.5% Methocell F - 5% H_3PO_4	81	72 ± 12	0	--	--
97	Briquet	Unknown	100	--	--	?		Supplied by Evergreen - Sample #1	84	54 ± 2	0	--	--
98	Briquet	Unknown	100	--	--	?		Supplied by Evergreen - Sample #11	63	37	34	0	--
99	Briquet	Unknown	100	--	--	(Acid)		Supplied by Evergreen - Sample #12	29	24	14	0	--
100	Briquet	Unknown	100	--	--	?		Supplied by Evergreen - Sample #14	39	24	36	0	--
101	Briquet	Unknown	100	--	--	?		Supplidd by Evergreen - Sample #16	36	18	60	25	--
102	CPM Lab Mill	Illinois #6	70	Piqua 1	30	Methocell F	5	Test 82 Coated with Laquer	98	>112	96	93	>112
103	CPM Lab Mill	Illinois #6	70	Piqua	30	M-167.01	5	Test 76 Coated with Laquer	88	110	94	63	--
104	Disc	Illinois #6	70	Piqua	30	Methocell F	1		--	20	--	--	--
105	Disc	Illinois #6	70	Piqua	30	Methocell F	0.5		--	12	--	--	--
106	Disc	Illinois #6	70	Piqua	30	M-167.01	1		--	1	--	--	--

TABLE III-3. (continued)

Test No.	Production Method	Pellet Formulation[a]						Remarks	Durability Index[b]	Compression Strength, lb *	Weather Index[b]	Post Weathering	
		Coal		Limestone		Binder							
		Type	%	Type	%	Type	%					Durability[b] Index	Strength, lb *
107	CPM Lab Mill	Illinois #6	70	Piqua	30	P-4000	5	Dow polyethylene glycol	14	26	--	--	--
108	CPM Lab Mill	Illinois #6	70	Piqua	30	E-8000	5	Dow polyethylene glycol	1	5	--	--	--
109	CPM Lab Mill	Illinois #6	70	Piqua	30	PEG-100	5	Union Carbide polyethylene glycol	6	18	--	--	--
110	Briquetts	Ohio	70	(?)	30	Unknown	--	Supplied by Evergreen	25	30	100	24	43
111	Briquetts	Ohio	70	(?)	10	Unknown	--	Supplied by Evergreen	96	36	100	80	53
112	Briquetts	Illinois #6	70	Piqua	30	Methocel F	1	Methyl cellulose gum	60	28	0	--	--
113	Briquetts	Illinois #6	70	Piqua	30	Cement	5	Bentonite added	9	8	0	--	--
114	CPM Lab Mill	Illinois #6	70	Piqua	30	PEG-200	5	Union Carbide polyethylene glycol	7	10	--	--	--
115	CPM Lab Mill	Illinois #6	70	Piqua	30	Polyco 11755	5	Bordon-vinyl acetate latex	71	73	94	66	90
116	CPM Lab Mill	Illinois #6	70	Piqua	30	Polyco 2140	5	Bordon-vinyl acetate latex	51	71	--	--	--
117	CPM Lab Mill	Illinois #6	70	Piqua	30	Polyco 2136	5	Bordon-vinyl acetate latex	78	72	89	53	90
118	Banner Extrusion	Illinois #6	70	Piqua	30	Cement	5	M-167.01 added for plasticity	--	43	0	--	--
119	Banner Extrusion	Illinois #6	70	Piqua	30	Methocel F	1	Methyl cellulose gum	--	> 113	--	--	--
120	Banner Extrusion	Unknown	100	--	--	Allbond 200	1	Pregellatinized corn starch	--	80	--	--	--
121	CPM Lab Mill	Illinois #6	70	Piqua	30	Polyco 2136	1	Bordon-vinyl acetate latex	59	40	--	--	--
122	CPM Lab Mill	Illinois #6	70	Piqua	30	Polyco 2136	0.5	Borden-vinyl acetate latex	45	33	--	--	--
123	CPM Lab Mill	Illinois #6	70	Piqua	30	Polyco 11755	1	Borden-vinyl acetate latex	46	20	--	--	--
124	CPM Lab Mill	Illinois #6	70	Piqua	30	Polyco 11755	0.5	Borden-vinyl acetate latex	46	23	--	--	--
125													
126	CPM Lab Mill	Illinois #6	70	Piqua	30	Allbond 200	5	Pregellatinized corn starch	78	96	98	89	.111
127	CPM Lab Mill	Illinois #6	70	Piqua	30	Allbond 200	1	Pregellatinized corn starch	92	85	--	--	--
128	CPM Lab Mill	Illinois #6	70	Piqua	30	Cement	5	0.1% NaCl added as catalyst	--	--	--	--	--
129													
130	CPM Lab Mill	Illinois #6	70	Piqua	30	Cement	5	0.1% Fe_2O_3 added as catalyst	--	--	--	--	--
131	CPM Lab Mill	Illinois #6	89	CaO	11	Cement	5	Would not pelletize	--	--	--	--	--
132	CPM Lab Mill	Illinois #6	94	CaO	6	Cement	5		46	35	--	--	--
133	CPM Lab Mill	Illinois #6	71	Piqua	27	Cement	5	1.2% CaO added	62	41	62	32	--
134	CPM Lab Mill	Illinois #6	73	Piqua	23	Cement	5	3.1% CaO added	57	47	64	38	--
135	CPM Lab Mill	Illinois #6	70	Piqua	30	Blend M-6	1.5	0.5% Methocol + 1.0% M-167.01	91	109	40	36	--
136	Banner Extrusion	Illinois #6	70	Piqua	30	Methocel	1	Methycellulose gum	92	101	0	--	--
137	CPM Lab Mill	Illinois #6	70	Piqua	30	Blend F-1	3	2% Allbond 200 + 1% M-167.01	95	111	87	--	112

TABLE III-3. (continued)

Test No.	Production Method	Pellet Formulation[(a)]						Remarks	Durability Index[(b)]	Compression Strength, lb *	Weather Index[(b)]	Post Weathering	
		Coal		Limestone		Binder						Durability Index[(b)]	Strength, lb *
		Type	%	Type	%	Type	%						
138	CPM Lab Mill	Illinois #6	70	Piqua	30	Blend F-2	3	2% Allbond 200 + 1% Polyco 11755	92	82	93	84	> 112
139	CPM Lab Mill	Illinois #6	70	Piqua	30	Blend M-7	1.5	0.5% methocel + 1% Polyco 11755	55	74	62	30	--
140	CPM Lab Mill	Illinois #6	70	Piqua	30	Blend M-8	1.5	0.5% methocel + 1% Polyco 2136	52	98	62	27	--
141	CPM Lab Mill	Illinois #6	70	Piqua	30	Blend F-3	3	2% Allbond + 1% Polyco 2136	87	112	100	85	> 112
142	CPM Lab Mill	Illinois #6	70	Piqua	30	Asphalt 47808	5	Bituminous Mat. Co.- slow setting emulsion	64	54	75	30	43
143	CPM Lab Mill	Illinois #6	70	Piqua	30	Asphalt 47808	10	Bituminous Mat. Co.- slow setting emulsion	67	59	76	10	30
144	CPM Lab Mill	Illinois #6	70	Piqua	30	Asphalt	5	Bituminous Mat. Co. med. setting emulsion	2	36	0	--	--
145	CPM Lab Mill	Illinois #6	70	Piqua	30	Asphalt	10	Bituminous Mat. Co. med. setting emulsion	36	48	63	2	30
146	Banner Extrusion	Illinois #6	70	Piqua	30	Blend M-9	2	Low density	75	40-110	--	--	--
147	Banner Extrusion	Illinois #6	70	Piqua	30	Blend M-9	2	Medium density	86	70	--	--	--
148	Banner Extrusion	Illinois #6	70	Piqua	30	Blend M-9	2	High density	80	72	--	--	--
149	Banner Extrusion	Illinois #6	70	Piqua	30	Blend M-9	2	High density	81	81	--	--	--
150	Banner Extrusion	Illinois #6	70	Piqua	30	Blend M-9	2	Low density	82	66	--	--	--
151	Banner Extrusion	Illinois #6	70	Piqua	30	Blend M-9	2	Low density	85	70	--	--	--
152	Banner Extrusion	Illinois #6	70	Piqua	30	Blend M-9	2	Low density	85	70	--	--	--
153	Banner Extrusion	Illinois #6	70	Piqua	30	Blend M-9	2	Medium density	89	90	--	--	--
154	Banner Extrusion	Illinois #6	70	Piqua	30	Blend M-9	2	High density	87	62	--	--	--
155	Banner Extrusion	Illinois #6	70	Piqua	30	Blend F-4	6	5% Allbond 200 + 1% M-167.01	99	110	100	98	> 112
156	Banner Extrusion	Illinois #6	70	Piqua	30	Blend F-5	2.5	1.5% Allbond 200 + 1% M-167.01	94	84	100	62	60
157	Banner Extrusion	Muskingum	62	Piqua	31	Unknown	1.5	Banner sample 10M	--	110	--	--	--
158	Banner Extrusion	Muskingum	98	--	--	Unknown	1.9	Banner sample 11M	--	88	--	--	--
159	Banner Extrusion	Muskingum	90	Piqua	7.1	Unknown	1.7	Banner sample 12M	--	73	--	--	--
160	Banner Extrusion	Muskingum	87	Piqua	11	Unknown	1.6	Banner sample 13M	--	102	--	--	--
161	CPM Lab Mill	Illinois #6	89	CaO	11	Allbond 200	5		38	24	--	--	--
162	CPM Lab Mill	Illinois #6	89	CaO	11	Allbond 200	10		0	0	--	--	--
163	CPM Lab Mill	Illinois #6	70	Piqua	30	Blend F-6	10	5% Allbond 200 + 5% asphalt 47808	92	64	91	88	> 112
164	CPM Lab Mill	Illinois #6	70	Piqua	30	Blend A-1	9	5% asphalt 47808 + 4% M-167.01	78	76	90	42	48
165	CPM Lab Mill	Illinois #6	70	Piqua	30	Blend F-1	3	Reproducibility check on Test 137	96	> 112	--	--	--
166	CPM Lab Mill	Illinois #6	100	--	--	Allbond 200	2		92	97	--	--	--

Baseline Data

The data in Table III-3 indicate that the eastern bituminous coal was superior to the others in mechanical properties. This coal retained its mechanical strength characteristics after the weatherability tests. Those values listed in Table III-3 for the eastern bituminous coal (Run No. 2) were used as the target goals.

Lignite and western subbituminous coals are susceptible to weathering as evidenced by the postweathering indexes. The cement-bound pellet from Phase II is clearly inferior to the stoker coals.

Effect of Production Technique

The characteristics of pellets produced by each of the four methods are summarized in Table III-4. These characteristics based on the laboratory standard tests are similar to those of eastern bituminous coals and superior to those of lignite and the western subbituminous coals.

The data in Table III-4 indicate that pellets produced by mill pelleting and auger extrusion have comparable mechanical strength characteristics. The mechanical strength characteristics of the disc pellets and briquets are clearly inferior. Disc pellets, however, exhibit a good PDI compared to their compression strength. This characteristic is attributed to the spherical shape, which means there are no corners to be broken. The disc pellets, however, have relatively low weatherability. The high porosity of these pellets allows water to penetrate them readily, dissolving any water soluble binder and creating fractures during freezing. The briquets could not be readily procured and thus extensive evaluation could not be made.

TABLE III-4. COMPARISON OF TEST RESULTS BY PRODUCTION TECHNIQUE

Test No.	Production Technique[(a)]	Binder Loading, percent	PDI	Compression Strength, N *
82	Pelleting - CPM	1	96	498
136	Auger extrusion - Banner	1	92	449
112	Briquetting - Evergreen	1	60	124.5
71	Disc pelletizing - Mars	5	99	267

(a) All tests have been formulated as follows:

70 percent coal
30 percent limestone
Methylcellulose binder

* 1 lb = 4.448 N

Effect of Binder

The most desirable binders are those that can produce pellets with physical properties similar to conventional eastern bituminous coals and yet be relatively inexpensive. Since the binder can contribute to as much as 20 percent of the cost of producing a limestone/coal fuel pellet with a Ca/S ratio of 3.5, economics were considered in binder selection.

Inorganics. Six inorganic binders were tested. With these binders, the amount of limestone affected the mechanical strength, with higher limestone additives producing stronger pellets. The calcium appears to present an active attachment site for the binders. None of the pellets produced with these binders were as strong as the cement-bound pellet. Because of this, and a feeling that inorganics add to the ash content and would inhibit combustion, no additional inorganic binders were tested.

Naturally Occurring Organics. The distinction between naturally occurring and processed organics is somewhat arbitrary. Naturally occurring substances there were limited to materials like starches and asphalts that need minimal additional processing and/or waste materials such as lignin or ligno sulfonates that are readily available. Due to the availability and low cost of these materials and the potential for enhanced combustion, the Phase II effort had focused heavily in this area. The best binder investigated in this category was a slow setting asphalt emulsion supplied by Bituminous Material Co. Pellets with this binder showed a PDI of 64, a compression strength of 240 N, and a WI of 75. This represents an improvement over the cement bound pellets but does not meet the larger goals. Relatively high (5-10 percent) binder loadings are required to produce these pellets. No other binder in this category produced pellets worthy of further consideration.

Processed Organics. Included in this category are synthetics such as methycellulose and further processed natural organics such as Allbond 200, a gelatanized cornstarch. These products offer the optimum potential for strength, weatherability, and combustion enhancement. Many of these materials do in fact produce pellets with the desired properties. The major drawbacks to this category for a commercial application are cost and availability. For example, methyl cellulose, at today's prices, might add as much as $40 to the cost of 910 Kg of pellets. The Allbond 200 binder, with a strength of 30 nt, a PDI of 78, and a WI of 98, while adding only $5.50 Mg ($5/ton) to the cost of pellets, was the most promising. This binder is 20 percent water soluble so there is some concern about long-term weatherability.

Combustion Characterization. The standardized laboratory tests provided relatively quick comparison of the mechanical strength characteristics of a wide variety of pellet formulations produced using different techniques. To complement this effort, small-scale tests were conducted to determine the combustion characteristics (sulfur capture and reactivity) of various formulations of limestone/coal pellets. Variables that were considered include:

- Ca/S ratio
- Sorbent type
- Production technique
- Binder type and concentration
- Catalysts or other additives.

A tubular, fixed-bed reactor that could be operated to 1300 C was selected for these tests.

Fixed-Bed Reactor Experiments. The tubular fixed-bed reactor provides a relatively fast method of evaluating a matrix of variables while minimizing fuel preparation costs. The more promising formulations can then be evaluated on a larger scale.

Fixed-Bed Reactor. Figure III-2 is a drawing of the fixed-bed reactor test facility. This facility has the following features to simulate fixed-bed burning and provide for collection of data of interest;

- High-temperature (1300 C) operation
- Controlled temperature set point
- Controlled air input
- Small charge-batch operation
- Analysis of off-gases
- Easily collectible ash
- Rapid quenching of the combustion reactions
- No wall effects.

The fixed bed reactor consists of a tubular electrical resistance furnace capable of heating the quartz reactor tube to 1300 C. Furnace temperatures can be controlled by varying the electric power input. Primary combustion air is introduced at the bottom of the bed. A porous, stainless steel distributor plate, located 50 mm inside the furnace hot zone, supports the fuel bed and provides for air distribution. Test-bed depths of 50 to 300 mm are possible, and the small quantity (50 to 300 grams) of fuel required minimizes fuel preparation costs. Secondary air is preheated and introduced above the bed by a helical coil that is heated by the furnace. Both air flows are metered and controlled between 0 and .0005 m^3/sec (0 and 1 cfm) by rotameters. Rapid introduction of inert gas

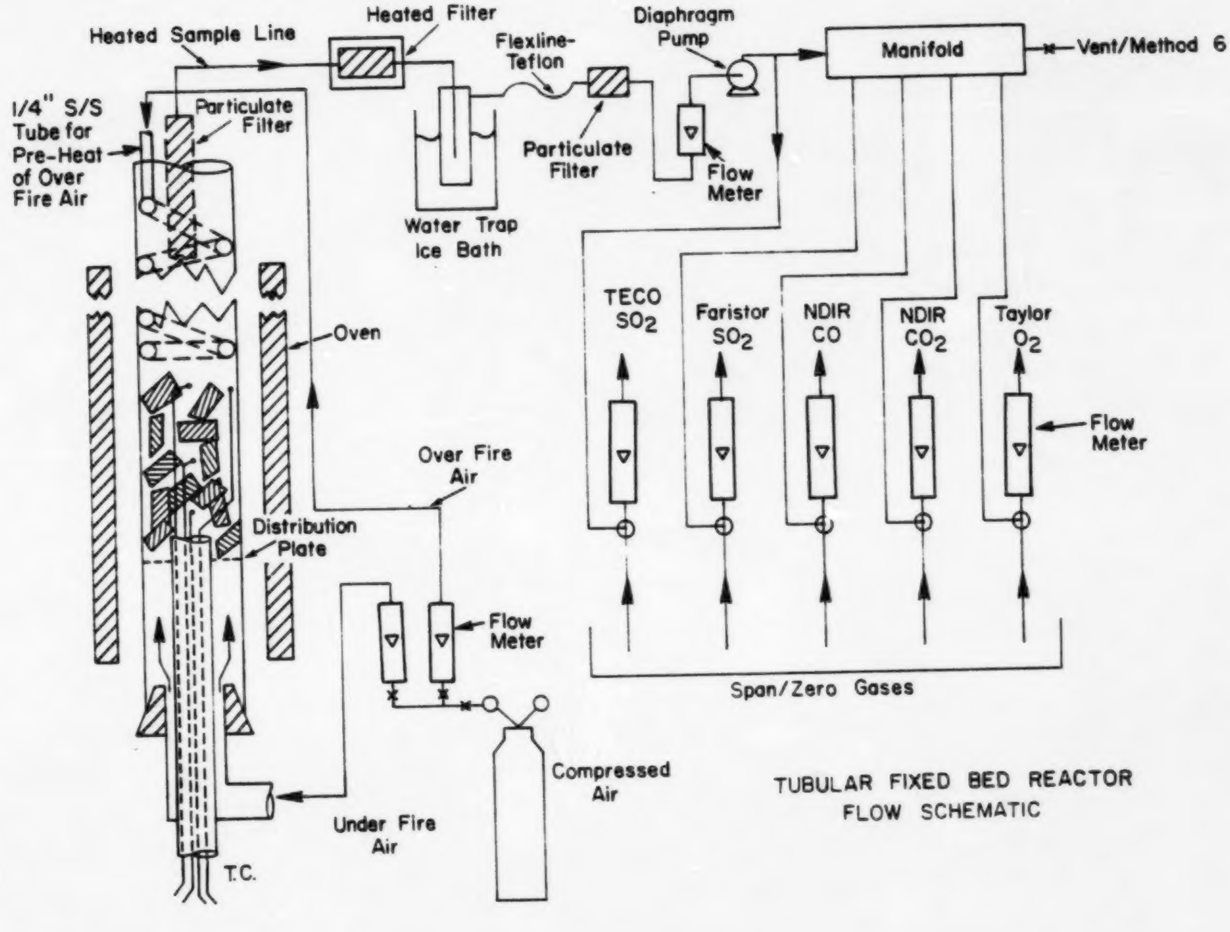
Heated Sample Line
Heated Filter
Flexline-Teflon
Diaphragm Pump
Manifold
Vent/Method 6
1/4" S/S Tube for Pre-Heat of Over Fire Air
Particulate Filter
Particulate Filter
Flow Meter
Water Trap Ice Bath
Oven
TECO SO_2
Faristor SO_2
NDIR CO
NDIR CO_2
Taylor O_2
Flow Meter
Over Fire Air
Distribution Plate
Flow Meter
Span/Zero Gases
Compressed Air
Under Fire Air
T.C.
TUBULAR FIXED BED REACTOR FLOW SCHEMATIC

FIGURE III-2. FIXED-BED REACTOR

(N_2, CO_2, or argon) can quench the combustion reactions at any time. Temperatures can be monitored at any chosen point in or above the bed by thermocouples introduced through holes provided in the distributor plate.

A probe inserted in the reactor tube exit withdraws samples of the flue gas through a conventional stack sampling train for analysis. The sample is continuously analyzed by the following equipment:

- Taylor paramagnetic analyzer for oxygen
- Beckman NDIR analyzer for CO_2 and CO
- Faristor analyzer for SO_2
- TECO pulse fluorescence analyzer for SO_2.

The output from the analytical instruments, as well as all thermocouples, is recorded on a data acquisition system for later processing by computer.

The fixed-bed reactor also provides ash samples with a clearly defined history for chemical and metallographic analysis. Wet chemical analyses for SO_2 and H_2S are made for selected runs using the EPA Method 6.

Experimental Procedure. After systematically investigating different modes of operation for the fixed-bed, the following experimental procedure was developed, based on the most consistent set of runs:

1. Preheat the furnace to the selected temperature.
2. Load the reactor tube with the selected fuel charge.
3. Connect the air lines, establish flow rates, and place thermocouples.
4. Insert the charged reactor tube into the heated furnace.
5. Place the sample probe in the outlet.

The coal ignites in the preheated furnace. The run is continued until the CO_2 and SO_2 instruments return to zero indicating the combustion reactions are complete. This typically takes about 30 minutes. When combustion is complete, the reactor tube is removed from the furnace and allowed to cool. The residue is then collected, weighed, and analyzed for carbon, sulfur, ash, and moisture content. From these data, the mass of carbon and sulfur remaining in the residue is determined. The tape from the data acquisition system containing the flue gas analysis is input to produces concentration-versus-time profiles of O_2, CO_2, CO, and SO_2 as well as temperature-time profiles. Maximum, minimum, and average values are also determined. Using trapezoidal integration of these profiles, the computer then determines the mass of carbon and sulfur contained in the flue gas. Mass balances are completed by comparing the carbon and sulfur contents in the ash and flue gas to those in the fuel charge, as determined by chemical analysis of a sample of the input fuel. Because of the small fuel charge and the pellet compositional variation, errors of closure in these balances of 10 percent or higher might be anticipated.

Forty-three runs with 50 percent limestone pellets (cement bound) were made to shake down the equipment and fix the independent variables. During these runs, it was found that volatiles condensed at the colder, discharge end of the reactor. To avoid the consequent loss of combustible carbon, and possibly of organic sulfur compounds, the exit end of the reactor was preheated by placing it in the furnace hot zone while keeping the fuel bed outside the hot zone. The results of these shakedown tests suggested that the 50/50 pellets could be tested satisfactorily in a 75-mm deep bed at 1050 C using 0.0002 m^3/sec underfire air and 0.00006 m^3/sec overfire air. Table III-5 shows the results of four repeat runs (44-47) made following this procedure. These runs showed excellent reproducibility with a variance of less than 10 percent in all items except the maximum SO_2 concentration. The maximum (peak) SO_2 concentration is highly dependent on the response of the instrument and has little effect on the total mass of SO_2 found by integration of the SO_2-time curve.

The 75-mm deep bed of pellets used in the preliminary tests required a charge of 55 grams of pellets, which contained about 27 grams of coal. When work was started with pellets containing 70 and 80 percent coal, a decision had to be made as to whether the bed depth or coal charge would be maintained constant. If the same coal charge was used, primary air would bypass through the relatively thin bed. Therefore, the bed depth was kept at 75 mm approximately. This resulted in increasing the quantity of coal in the tests with 70/30 pellets to approximately 38 grams, a quantity also used for runs with 80/20 pellets.

Eleven runs were made in this manner, Tests 48-58 of Table III-6. At this point, data analysis began to indicate that only 72-82 percent of the

TABLE III-5. REPRODUCIBILITY SERIES WITH 50/50 PELLETS, FURNACE TEMPERATURE 1040 C, WITH 33% OVERFIRE AIR

Run D	44	45	46	47	Average
Percent C Accounted					
Flue gas	98.5	88.6	93.4	92.6	93.3 ± 4.1
Total	99.0	89.2	93.9	93.3	93.9 ± 4.0
Percent S accounted					
Flue gas	17.5	12.3	17.8	18.1	16.4 ± 2.8
Total	92.1	86.9	97.3	93.5	92.5 ± 4.3
Run time	19.78	18.00	17.85	19.92	18.89 ± 1.11
Max SO_2	2646	1878	2213	2942	2420 ± 469

fuel sulfur was being accounted for. It was also noted that the Faristor SO_2 analyzer was malfunctioning, possibly because of H_2S poisoning. Since these effects were not observed previously, a series of tests (59-69) were made to check these results and to determine the effect of the increased coal charge. These runs indicated that the increase in coal was contributing in part to the sulfur-balance problems. During this period (Run 65), the TECO SO_2 analyzer was added to the sampling system. Corrections for interference by other stack gas constituents were found to be minimal and easily handled by the computer. The SO_2 curves produced by the Faristor and the TECO analyzers have some marked differences. The TECO data frequently show a higher peak value. This is probably due to a faster response time. Of more interest is a TECO drop near to zero during the period of low oxygen. This dip, which is more severe at higher coal charges, is felt to represent a shift from SO_2 formation as less oxygen becomes available. The Faristor, which responds to H_2S, shows no dip. However, sensitivity is severely degraded by prolonged exposure to H_2S.

TABLE III-6. FIXED-BED EXPERIMENT RUNS

Run No.	Fuel No.	Fuel Type	Fuel Charge, grams	Run Time, min	Distribution						SO_3 Max, ppm
					Flue Gas		Ash		Total		
					% S	% C	% S	% C	% S	% C	
48	29	50/50 Cement (CPM)	77	23	10.96	88.72	62.84	1.45	73.80	90.15	2017
49	30	60/40 Cement (CPM)	64	25	11.03	88.72	65.23	1.14	76.26	89.86	2347
50	31	70/30 Cement (CPM)	55	27	11.41	91.4	60.9	2.26	72.3	93.66	2263
51	32	80/20 Cement (CPM)	48	26	19.97	88.22	61.38	0.23	81.35	88.45	2148
52	34	CaO (at limestone 70/30 ratio)	48	24	7.05	89.76	87.05	0.96	94.10	90.72	728
53	37	70/30 Fredonia (CPM)(a)	55	30	12.86	87.80	68.49	1.70	81.35	89.50	1567
54	38	70/30 Baseline (CPM)	55	25	22.07	83.22	71.38	1.29	93.45	84.51	4013
55	39	70/30 Howard Limestone (CPM)	55	25	13.74	80.47	76.71	1.91	90.45	82.38	2864
56	71	70/30 5% Methocel (Disc)	55	22	24.72	86.40	71.20	1.81	95.92	88.21	3844
57	82	70/30 5% Methocel (CPM)	55	28	15.26	74.23	66.75	2.20	82.01	76.43	2145
58	76	70/30 5% Dowell (CPM)	55	30	20.10	89.87	75.0	2.35	95.10	92.22	2947
59	32	80/20 Cement (CPM)	48	27	22.64	87.40	62.18	0.75	84.82	88.15	3635
60	34	CaO (at limestone 70/30)(CPM)	48	29	10.43	91.19	78.40	1.61	88.83	92.80	1170
61	37	70/30 Fredonia (CPM)	55	28	25.93	87.76	62.08	1.32	88.01	89.09	4449
64	5	50/50 Cement (CPM WJ)	11	23	16.69	23.15	92.27	0.56	68.96	83.71	2628
65	82	70/30 5% Methocel (CPM)	55	25	25.91	71.17	64.46	0.05	90.37	71.22	4036
67	5	50/50 Cement (CPM WJ)	55	20	16.85	86.20	80.33	0.72	97.18	86.92	1808
68	31	70/30 Cement (CPM)	55	27	15.69	89.55	70.50	0.07	86.19	89.63	2860
69	37	70/30 Fredonia (CPM)	55	29	17.31	87.28	58.32	0.40	75.03	87.68	2170
70	52	70/30 Epsom Salt (CPM)(a)	41	25	15.82	93.31	68.93	0.25	84.75	93.56	2888
71	53	70/30 Magnesium Sands (CPM)	41	23	20.21	84.04	73.17	0.58	93.38	84.62	3630
72	54	70/30 Magnesium Hydroxide (CPM)	41	28	17.18	93.05	67.00	0.49	84.18	93.54	3248
73	112	70/30 1% Methocel (Briquet)	41	36	19.38	102.93	72.10	0.78	91.48	103.71	3234
74	113	70/30 Cement + Bentonite (Briquet)		51	18.69	105.68	66.42	2.90	85.11	108.58	2172
75	118	70/30 Cement + Latex (Banner)	41	29	14.18	96.70	73.31	0.83	87.49	97.53	2669
76	119	70/30 1% Methocel (Banner)	41	30	15.52	104.74	76.83	1.25	92.34	105.99	1634
77	128	70/30 0.1% NaCl (CPM)	41	25	25.33	84.05	63.73	0.19	89.06	84.24	2398
78	130	70/30 0.1% Fe_2O_3 (CPM)	41	26	18.68	83.75	62.60	0.34	81.28	83.79	1032
79	31	70/30 Cement (1500 F)	41	25	24.82	89.83	74.07	2.09	98.88	91.92	2500
80	31	70/30 Cement (1900 F)	41	21	23.45(b)	89.29	64.01	1.87	87.46	91.16	2789(b)
81	126	70/30 5% Allbond	41	28	17.23(b)	82.67	63.19	1.50	80.42	84.17	2562(b)
82	127	70/30 1% Allbond	41	26	26.92(b)	91.79	60.27	1.89	87.19	93.68	3193(b)
83	132	94/6 Coal/CaO	41	24	45.02(b)	80.22	51.89	1.56	96.91	81.78	4311(b)
84	133	70/30 + 1.27 CaO	41	21	29.82(b)	89.39	79.10	2.24	108.92	92.18	3190(b)
86	157	Banner 10M-30% Limestone	49	34	24.9(b)	97.5	58.4	0.8	83.3	98.3	2989(b)
87	158	Banner 11M-Muskingum Coal	30	34	54.3(b)	96.0	1.0	0.1	55.3	96.1	2704(b)
88	159	Banner 12M-7% Limestone	33	38	55.9(b)	88.3	7.9	0.2	63.8	88.5	3664(b)
89	160	Banner 13M-11% Limestone	35	30	53.8(b)	93.4	14.5	0.4	68.3	93.8	2056(b)

(a) Changed Faristor analyzer cell.

(b) Teco data.

In light of these findings, it was felt that the decision to run at 1040 C to produce the "real world" conditions more closely using the higher coal charge, may have been an error. Runs 79 and 80 were made with 41 grams (28 grams of coal) of 70/30 cement bound pellets at 820 and 1040 C, respectively. The data show excellent agreement of the TECO and Faristor instruments at 820 C. Further, the profiles are essentially identical. At 1040 C, the TECO indicates a severe drop in SO_2 concentration but nearly the same dosage as at 820 C. The Faristor value is low at 1040 C, one half the value at 820 C. The differences in Method 6 data, which implies more sulfur capture at the higher temperature, are not understood.

Except for Runs 48-51, the sulfur balance is not exceedingly low. But it is always low, never high as might be expected with normal random fluctuations. This suggests that sulfur capture as determined by the fixed-bed reactor tests may not be accurate in absolute terms. However, the generally constant overall sulfur balance is reason to believe that these tests rank the various formulations correctly and thus satisfy their objective.

The TECO and Faristor comparisons indicated that a 28-gram coal charge and 820 C furnace temperature, or possibly more secondary air, would be desirable to eliminate problems with H_2S formation. However, to conform with the previous work, the remaining runs were made at 1040 C. It is interesting to note that with different charges of the same fuel, run times were essentially the same. Furthermore, variability in the sulfur balance comes more from the ash than the flue gas composition. For these reasons, it is felt that comparisons of runs at these conditions are valid.

Discussion of Experimental Results

Table III-6 summarizes the data of Runs 48-89 from the fixed-bed reactor experiments. As previously discussed, Runs 1 through 43 were for checkout purposes and provide little direct information on the evaluation of pellets. The results of reproducibility runs (44-47) were shown in Table III-5. The effect of pellet formulation variables and system operating temperature on sulfur capture and reactivity are discussed below.

Ca/S Ratio. The effect of Ca/S ratio was examined by making cement-bound pellets in the CPM lab mill with various levels of Piqua limestone. Table III-7 gives the results of these experiments.

TABLE III-7. THE EFFECT OF Ca/S RATIO ON SULFUR CAPTURE

Run	Fuel	Limestone/ Coal	Sulfur[(a)] Capture, percent	Reactivity (burn time) minutes	Approximate Ca/S Ratio
48	29	1.0	89	23	8
49	30	0.67	89	25	6
50	31	0.43	89	27	3.5
68	31	0.43	84	27	3.5
51	32	0.25	80	26	2
59	32	0.25	78	27	2

(a) Based on sulfur found in flue gas.

These results indicate that the Ca/S ratio (as reflected by the limestone/coal ratio) has only a small effect on sulfur capture at limestone/coal ratios at or above 0.43 (Ca/S = 3-4). At a limestone/coal ratio of 0.25 (20 percent limestone, Ca/S = 1.7-2.3), the sulfur capture begins to drop noticeably.

The limestone/coal ratio may have a slight effect on reactivity. Pellets with the higher limestone content appear to burn slightly faster. Because of the higher ash content at higher limestone levels, an opposite result was anticipated. Though lime is known to catalyze some gasification and combustion reactions, the levels present here (20 percent) should swamp any concentration effect. Perhaps this effect is due to the higher CO_2 values within the pellet from the calcining limestone and the surface reaction $C + CO_2 \rightarrow 2\ CO$ taking place.

Type of Sorbent. Piqua, Fredonia, and Howard limestones, as well as "basic lime", (a precipitated $CaCO_3$ of very small particle size), were compared at a limestone/coal ratio of 0.43 (Ca/S - 3-9) in cement-bound CPM pellets. Table III-8 gives the results of these tests.

TABLE III-8. THE EFFECT OF SORBENT ON SULFUR CAPTURE

Run	Fuel	Type of Sorbent	Sulfur Capture, percent	Reactivity (burn time), minutes
50	31	Piqua	88.6	27
53	37	Fredonia	87.1	30
61	37	Fredonia	74.1	28
69	37	Fredonia	82.7	29
54	38	Basic Lime	77.9	25
55	39	Howard	86.3	25

These results show that "basic lime" is the poorest sorbent. The three limestones appear about equal, with some indication that Fredonia limestone is slightly inferior. These results are also contrary to what was anticipated. The "basic lime" was included since it was the smallest particle size available and it was believed that more finely divided $CaCO_3$ would prove to be a better sorbent. Perhaps the precipitation process reduces the reactivity of this material.

The "basic lime" and Howard limestone pellets show the highest reactivity, and the Fredonia limestone the lowest reactivity. The reasons for this are unexplained.

Calcium Oxide. Calcium oxide and Piqua limestone were compared at a Ca/S ratio of 3 to 4 in cement bound CPM pellets, as shown in Table III-9.

TABLE III-9. COMPARISON OF THE EFFECT OF LIMESTONE AND LIME ON SULFUR CAPTURE

Run	Fuel	Sorbent	Sulfur Capture, percent	Reactivity, Burn Time, minutes	Approximate Ca/S
50	31	Limestone	88.6	27	3.5
68	31	Limestone	84.3	27	3.5
52	34	CaO	93.9	24	3.5
60	34	CaO	89.6	29	3.5
83	132	CaO	55.0	24	2.0
84	133	Limestone and CaO	70.2	21	4.0

As expected, CaO is the superior sorbent. The limestone must be calcined before it can react with the sulfur while the CaO can react immediately. Any sulfur released prior to this calcining cannot be captured by limestone but could be captured with CaO. This leads to the speculation that a small addition of CaO to the limestone might significantly improve the sulfur capture. This is not supported by the one test conducted with this combination, where capture was poorer that with limestone alone. Additionally, however, the significant reduction in sulfur capture in Run 83 is surprising. Further work is needed to investigate lower Ca/S ratios using CaO and CaO-limestone mixtures.

Under the test conditions, the substitution of CaO for limestone does not appear to alter reactivity, but this conclusion is weak in view of the widely different burn times obtained with pellets containing CaO.

Binder

Binders were compared with CPM pellets at a limestone/coal ratio of 0.43 using Piqua limestone. Table III-10 gives the results of fixed-bed reactor experiments.

TABLE III-10. THE EFFECT OF BINDER TYPE ON SULFUR CAPTURE

Run	Fuel	Binder	Sulfur Capture, percent	Reactivity Burn Time, minutes	Peak Reactor, temperature, C
50	31	Cement	88.6	27	1184
68	31	Cement	84.3	27	1173
57	82	Methylcellulose	84.7	28	1347
65	82	Methylcellulose	79.6	25	1178
58	76	Dowell Latex	79.9	30	1152
70	52	Epsom Salts	84.2	25	1130
71	53	Mag Sands	80.9	23	1170
72	54	Mg (OH)	82.7	28	1095
81	126	Allbond 200	82.8	28	1120

The cement binder appears most favorable for sulfur capture and the organic binders appear slightly inferior to the inorganic binders. The poorer performance of organic binders might be caused by increased pellet temperature caused by combustion of the binder, or the volatility of these organic binders may drive off additional sulfur. Also, the organic binders were used at 5 percent concentration, which may be higher than necessary for pellet strength and durability. At lower concentrations, the organic binders might capture sulfur better.

The Epsom Salts and "Magnesium Sand" binders, which were believed to have some catalytic properties, produced the most reactive pellets in terms of run time, and the Dowell Latex the least reactive pellet. The Allbond 200 cornstarch pellets were similar to cement-bound pellets. Because of two rather different results in replicate runs, the position of the methylcellulose pellets is uncertain, but may be approximately the same as the cement-bound pellets.

The peak temperature reached in the reactor does not correlate with the run time, which is unexpected. The peak temperatures were similar, with the exception of one run with methylcellulose pellets, which reached a peak temperature 182 C higher than the average of the other runs.

Pellet Production Method. Pellets with a limestone/coal ratio of 0.43 using Piqua limestone and methylcellulose binder were produced by each of the four production methods. Table III-11 gives the results of the fixed-bed reactor experiments using these pellets.

TABLE III-11. THE EFFECT OF PRODUCTION METHOD ON SULFUR CAPTURE

Run	Fuel	Method	Sulfur Capture, percent	Reactivity (burn time), minutes	Density[a], grams/cc
56[b]	71	Pelletizing	75.3	22	0.79
57[b]	82	Mill pelletizing	84.7	28	1.39
65[b]	82	Mill pelletizing	79.6	25	1.39
73	112	Briquet	80.0	36	1.26
76	119	Extrusion	84.5	30	0.85

(a) Determined by displacement.

(b) These runs were made with a 55-gram fuel charge, whereas only 41 grams were used in the other two runs listed.

Except for the extruded pellets, sulfur capture increased as pellet density increased. This is because the higher density produces a more tortuous path and lower diffusion rate for the escaping sulfur. Since excess calcium is present, the increase in contact should permit the kinetically controlled reaction to go further towards completion. The high performance of the extruded pellets, in these terms, is anomalous.

Reactivity, as measured by burn time, does not correlate well with the pellet density either, as shown in Table III-12.

TABLE III-12. THE EFFECT OF PRODUCTION TECHNIQUE ON REACTIVITY

	Ranking		
Pellet Type	Density	Sulfur Capture	Reactivity
Mill pelleting	1 (high)	2	2
Briquetting	2	3	4 (low)
Extrusion	3	1 (high)	3
Disc pelletizing	4 (low)	4 (low)	1 (high)

Lower-density pellets should be more receptive to diffusion of air into and combustion products out of the pellet, thereby promoting combustion. The low-density, disc-agglomerated pellets support this premise by being the most reactive. However, the second most reactive pellet is the CPM pellet which has the highest density. Evidently sulfur capture and reactivity are not related to pellet density or porosity in any simple way.

Additives. The addition of 0.12 percent NaCl or Fe_2O_3 to cement-bound pellets with a Piqua limestone/coal ratio of 0.43 was expected to enhance sulfur capture or, in the case of Fe_2O_3, possibly enhance burning rate. Table III-13 shows the results of these tests.

TABLE III-13. THE EFFECT OF ADDITIVES ON SULFUR CAPTURE

Run	Fuel	Additive	Sulfur Capture, percent	Reactivity (Burn Time), minutes
77	128	0.1% NaCl	73.6	25
78	130	0.1% Fe_2O_3	80.3	26
80	31	None	76.5	21
50(a)	31	None	88.6	27
68(a)	31	None	84.3	27

(a) These runs were made with a 55-gram fuel charge, whereas only 41 grams were used with the other three runs listed.

Neither additive appears to be beneficial, although the comparisons are clouded by the noted change in the fuel charged to the reactor.

Conclusions from Fixed Bed Reactor Study

The data from the fixed bed reactor tests showed few effects of formulation on reactivity. Often, the effects that were observed were opposite of those expected. This might indicate an insensitivity of the test equipment and procedure to actual reactivity.

Bearing this in mind, the conclusions reached from this study are:

- Ca/S ratio is relatively unimportant at values above 3-4. Sulfur capture is only slightly lower at a Ca/S ratio of 2.
- Three limestones gave comparable sulfur capture with only the precipitated "basic-lime" inferior.
- CaO is a superior sorbent to limestone. A small amount of CaO in conjunction with limestone might be expected to improve sulfur capture, but this effect was not observed.
- Use of organic binders instead of inorganic substances results in slightly lower sulfur capture. This disadvantage might be reduced at lower binder concentrations.
- Sulfur capture increased with pellet density when comparing production methods with the exception of the anomalous extruded pellets. The pellet mill produces highest density and highest sulfur capture.
- NaCl and Fe_2O_3 additives (0.12 percent) did not improve sulfur capture or reactivity.
- The effect of the variables on pellet reactivity, as evidenced by the burning time, were not clearly distinguished. Some differences were observed.

SECTION 4

PROCESS VARIABLES SELECTION

A mathematical modeling analysis, in combination with a series of experimental studies, was performed to develop a more comprehensive understanding of the processes that influence the burning of the coal/limestone pellets and control sulfur capture. The purpose of the experimental studies was to provide physical and chemical rate constants for the model, and to provide a basis for assessing model reliability. The main objectives of the modeling studies were to predict burning rates and sulfur capture as a function of pellet properties such as size, composition, and physical structure under different combustion conditions. Knowledge of how these parameters affect pellet performance is important for the development of optimum pellets for specific boiler applications.

The mathematical model described here is a preliminary model with a number of simplifying assumptions incorporated into it. An important purpose of this effort was to demonstrate how modeling can be practically and usefully employed to understand how coal/limestone pellets behave and how to improve their performance. The basic structure of this preliminary model can be expanded to include either additional processes or refined mechanisms to increase its accuracy.

In the model, the pellet's cylindrical geometry is represented by an equivalent sphere having the same surface-to-volume ratio. The burning of the pellet is represented by the shrinking core model developed by Wen and co-workers.(III-3 to III-6) It is based on a burning reaction zone that penetrates into the pellet and is supported by oxygen that diffuses through the ash layer surrounding the burning core. SO_2, formed at the burning interface between the unburned core and ash, is assumed to diffuse out through the ash layer where it is captured by the $CaCO_3$ in the limestone. The calcination process is represented by the reaction

$$CaCO_3 \rightarrow CaO + CO_2$$

and sulfur capture by the reaction

$$CaO + SO_2 + 1/2\ O_2 \rightarrow CaSO_4\ .$$

SO_2 that does not react with the CaO while diffusing to the outer surface of the ash layer is considered to be released from the pellet. The model, in its present form, neglects factors such as heat transfer, devolatilization of the coal, the reaction between CO_2 and carbon forming CO, and solid-state reactions. These mechanisms can be incorporated into extended versions of the present model as appropriate.

The experimental studies associated with the modeling effort were performed using the fixed-bed reactor described in detail in section 4. These experiments involved heating pellets in the fixed-bed reactor in a flowing air stream for various periods of time corresponding to different levels of fuel consumption in the pellets. The combustion gases exiting from the reactor were analyzed continuously for SO_2, CO, and O_2 to follow the kinetic rates of the combustion and SO_2-release processes. Burned pellets were recovered, weighed, analyzed chemically, and subjected to examination by metallographic techniques, scanning electron microscopy, and X-ray diffraction. Some limitations, however, exist in accurately applying some of these data to the model because of uncertainties in the fixed-bed reactor experiments. These difficulties can be eliminated in future work by using the model developed here as a guide for designing the experiments.

Further details on both the fixed-bed reactor experiments and the model are presented below.

PELLET DETAILS

Two different pellet compositions were used in these studies: 70 wt. percent coal/30 wt. percent limestone and 50 wt. percent limestone. These pellets were produced at Battelle using a California pellet mill. In addition to the coal and limestone, the pellets also contained corn starch and latex at levels equivalent to 2 wt. percent and 1 wt. percent, respectively, of the weight of coal plus limestone. The latex contained 50 wt. percent solids. The pellets were cylindrical in shape with a 12.5 mm diameter. The ends of the pellets had a fracture texture with a variable overall length of approximately 12 mm. Variability in the end conditions and lengths of the pellets may have been responsible for some of the variations noted in the experimental results. For comparison purposes, some information is also included on the Banner and Alley Cassetty pellets used in the steam-plant demonstration experiments performed at Battelle in November 1979.

Information on densities and porosities for typical pellets is summarized in Table III-14. The density values were calculated from measured volumes and weights of typical pellets. Porosities were calculated using densities for the solid coal, solid limestone, corn starch, and latex of 1.21, 2.60, 1.53 and 0.92 g/cm^3, respectively. The Alley Cassetty pellet ran about 8.5 percent less dense than the Battelle 70/30 pellet, while the Banner pellet was over 12 percent less dense.

Results of chemical analyses on the coal used to prepare the Battelle pellets and on typical pellets are given in Table III-15. Calcium-to-sulfur ratios and the percentage of total sulfur occurring as organic sulfur for the Battelle pellets were:

Pellet Composition	Calcium/Sulfur Ratio, g-moles Ca/g-moles S	Organic Sulfur, percent
50/50	5.04	58.15
70/30	3.14	51.43

Total sulfur occurring as organic sulfur in the raw coal was about 51.74 percent corresponding closely to the result of the 70/30 analysis.

FIXED BED REACTOR EXPERIMENTS

The fixed-bed reactor experiments were conducted mainly with the Battelle 50/50 and 70/30 pellets with the exception of several runs with pellets of only coal and only limestone. Each experiment involved three pellets that were rapidly introduced into the high temperature zone of the furnace via the quartz tube using an open wire support designed for minimum contact with the pellets. Thermocouples attached to the wire cage were used to determine pellet temperatures. At the end of a preselected burn time the air flow passing through the quartz tube was changed to argon

TABLE III-14. TYPICAL PELLET DENSITIES AND POROSITIES

Pellet No.	Pellet Source	Pellet Composition	Density, g/cm^3	Porosity, percent
70	Battelle	50 w/o coal/50 w/o limestone	1.50	9
76	Battelle	70 w/o coal/30 w/o limestone	1.41	2
30	Battelle	100% coal	1.18	2.5
16	Battelle	100% limestone	1.84	29
200	Alley-Cassetty	70 w/o coal/30 w/o limestone	1.29	10
202	Banner	70 w/o coal/30 w/o limestone	1.24	15

TABLE III-15. SUMMARY OF CHEMICAL ANALYSES ON RAW COAL AND PELLETS

Pellet No.	Pellet Source	Pellet Composition	Chemical Composition, w/o								
			C	Ca	CO_3	Fe	Ash	H_2O	Total Sulfur	Organic Sulfur	Pyritic Sulfur
--	--	Raw coal*	59.5	0.67	--	3.7	15.6	9.77	4.02	2.08	1.79
79	Battelle	100 w/o coal	63.0	0.50	1.03	1.99	12.7	3.1	4.5	2.36	1.97
80	Battelle	70 w/o coal/30 w/o limestone	46.4	11.0	20.1	1.43	29.0	2.0	2.8	1.44	1.25
81	Battelle	50 w/o coal/50 w/o limestone	39.4	17.0	29.7	1.34	37.8	1.6	2.7	1.57	1.04
205	Banner	70 w/o coal/30 w/o limestone	45.4	10.1	17.7	2.53	32.4	2.0	2.8	1.45	1.22
206	Alley-Cassety	70 w/o coal/30 w/o limestone	46.6	10.8	17.4	1.22	26.5	2.1	2.7	1.63	1.10
18	Battelle	100 w/o limestone	11.4	31.0	53.7	--	51.0	8.3	--	--	--

* Analysis of Illinois No. 6 coal used to produce Battelle pellets.

to quench the combustion, and the pellets were removed from the high-temperature zone. All pellet experiments were performed with the furnace set at 1040 C. Along with thermocouple temperature, the outputs from the CO_2, O_2, CO, and SO_2 analysers monitoring the combustion gases from the fixed-bed reactor were recorded continuously. A total flow rate of 0.00012 m^3/sec was used in the reactor with 0.00002 m^3/sec of this total added above the pellets as over-fire air. The intention was to maintain high excess air to convert any H_2S released from the pellets to SO_2, which would be detected by both the Faristor and TECO analyzers to give a complete accounting of sulfur release. H_2S is not detected by the TECO analyzer but does produce a spurious response with the Faristor. After each experiment, each pellet was weighed and selected samples were analyzed chemically or sectioned for metallographic examination, scanning electron microscopy, and X-ray diffraction.

Experimental Results

Weight of the pellets is given in Table III-16 with the chemical analyses for selected burned pellets presented in Table III-17. For several cases where pellets were not completely burned, values are given in the two tables for both the ash and the unburned core. The postheating weights for the limestone pellets missing from Table III-16 could not be determined because the pellets exploded when heated and could not be completely recovered.

Analyses of the exhaust gas from the fixed-bed reactor are summarized in Figures III-3, III-4, and III-5. CO_2 release from the limestone pellets, shown in Figure III-3, was somewhat erratic, which may be associated with the explosion of one of the pellets, shown in Figures III-4 and III-5. Most of the SO_2 release occurred within the first 5 minutes, while oxygen consumption and CO_2 production continued for significantly longer times. Some of the sulfur released from the pellets into the gas stream could be present as H_2S. Earlier experiments with a number of pellets in the fixed-bed reactor(Runs 86-89) showed H_2S levels ranging from about 6 to 10 percent of the SO_2. Use of only three pellets and of high excess air was intended to convert all H_2S to SO_2, but this has not been confirmed experimentally. Since the TECO monitor detects only SO_2, any sulfur present as H_2S would not be detected and higher sulfur retention by the pellets would be indicated.

TABLE III-16. SUMMARY OF FIXED-BED REACTOR EXPERIMENTS PERFORMED IN SUPPORT OF THE MODELING STUDIES

Pellet No.	Pellet Composition	Pellet Batch	Run No.	Burn Time, Min.	Original Pellet Weight, g	Pellet Weight After Heating, g		
						Total	Ash	Unburned Core
1	Limestone	169	109	43(a)	3.2630	1.7405	--	--
2	"	"	"	"	3.2750	1.6178	--	--
3	"	"	"	"	3.2650	--	--	--
4	"	"	110	31(a)	2.4990	1.2874	--	--
5	"	"	"	"	3.3905	--	--	--
6	"	"	"	"	2.5205	1.3747	--	--
7	"	"	111	18	2.7619	1.5483	--	--
8	"	"	"	"	3.1688	--	--	--
9	"	"	"	"	3.0329	1.6205	--	--
10	"	"	112	12	3.1518	1.5681	--	--
11	"	"	"	"	3.0487	1.6400	--	--
12	"	"	"	"	3.2448	--	--	--
13	"	"	113	6	2.7385	1.7543	--	--
14	"	"	"	"	2.9415	1.5212	--	--
15	"	"	"	"	2.8381	1.5844	--	--
19	Coal	172	94	(a)	1.7275	--	--	--
20	"	"	"	(a)	2.2102	--	--	--
21	"	"	"	(a)	1.7402	--	--	--
22	"	"	95	(a)	1.9568	--	--	--
23	"	"	"	(a)	2.1032	--	--	--
24	"	"	"	(a)	1.7939	--	--	--
25	"	"	96	5	1.8690	--	--	--
26	"	"	"	"	1.9036	--	--	--
27	"	"	"	"	2.0847	0.7600	--	--
37	70/30	173	97	20	2.5113	0.6475	--	--
38	"	"	"	"	2.2216	0.5752	--	--
39	"	"	"	"	2.3316	0.6186	--	--
40	"	"	98	5	2.3100	0.9694	--	--

TABLE III-16. (Continued)

Pellet No.	Pellet Composition	Pellet Batch	Run No.	Burn Time, Min.	Original Pellet Weight, g	Pellet Weight After Heating, g		
						Total	Ash	Unburned Core
41	70/30	173	98	5	2.2035	0.8876	--	--
42	"	"	"	"	2.2364	0.8750	0.1605	0.7145
43	"	"	99	11	2.0811	0.5505	--	--
44	"	"	"	"	2.2428	0.6603	--	--
45	"	"	"	"	2.3287	0.6352	0.4436	0.1916
46	"	"	100	15	2.1567	0.5746	--	--
47	"	"	"	"	2.2779	0.6243	--	--
48	"	"	"	"	2.0071	0.5470	--	0.0000
49	"	"	101	20	2.2786	0.5770	--	--
50	"	"	"	"	1.9107	0.5163	--	--
51	"	"	"	"	2.1246	0.5877	--	0.0000
52	"	"	102	10	2.5570	0.8559	0.3799	0.4760
53	"	"	"	"	2.0349	0.6354	0.3603	0.2751
54	"	"	"	"	2.2760	0.6709	0.1949	0.4760
73	"	"	103[(b)]	10	2.3062	0.7422	0.3929	0.3493
74	"	"	"	"	2.2079	0.6549	0.4507	0.2042
75	"		"	"	1.9507	0.5856	0.3771	0.2085
55	50/50	174	104	22[(a)]	2.4193	0.7814	--	--
56	"	"	"	"	2.6733	0.5788	--	--
57	"	"	"	"	2.5346	0.8129	--	--
58	"	"	105	4	2.0642	0.9466	--	--
59	"	"	"	"	2.2296	0.9544	--	--
60	"	"	"	"	2.4874	1.0345	0.2996	0.7349
61	"	"	106	6	2.7737	1.0768	--	--
62	"	"	"	"	2.2662	0.8120	--	--
63	"	"	"	"	2.5910	0.9820	0.5280	0.4540
64	"	"	107	12	2.3511	0.8388	--	--
65	"	"	"	"	2.4552	0.8590	--	--
66	"	"	"	"	2.4155	0.8133	0.7774	0.0359
67	"	"	108	14	2.4564	0.8515	--	--
68	"	"	"	"	2.6856	0.8950	--	--
69	"	"	"	"	2.7084	0.8763	--	0.0000

(a) Denotes complete combustion or reaction as determined by gas analyzers.

(b) Experiment No. 103 was performed with the three pellets located side-by-side in the quartz reactor tube.

TABLE III-17. RESULTS FROM CHEMICAL ANALYSES OF PELLETS FROM FIXED-BED REACTOR EXPERIMENTS

Pellet No.	Pellet Composition	Type of Sample	Chemical Composition, 2.C/2.C.								
			C	Ca	CO_3	Fe	Ash	H_2O	Total Sulfur	Organic Sulfur	Pyritic Sulfur
1	Limestone	Total pellet	0.2	60.2	1.89	--	99.3	(a)	--	--	--
6	"	"	0.1	60.6	0.81	--	99.7	(a)	--	--	--
9	"	"	0.1	60.2	0.54	--	99.5	(a)	--	--	--
10	"	"	1.5	56.9	7.33	--	93.5	(a)	--	--	--
15	"	"	0.6	59.9	2.71	--	97.5	(a)	--	--	--
40	70/30	"	35.0	22.70	3.02	3.23	64.20	0.1	4.30	3.73	0.13
42	"	Ash	13.8	32.1	--	--	84.0	<0.1	4.6	--	--
--	"	Unburned core	46.3	20.8	--	--	57.1	<0.1	3.9	--	--
45	"	Ash	1.2	42.9	--	--	*	<0.1	5.5	--	--
--	"	Unburned core	39.0	24.7	--	--	66.0	<0.1	4.4	--	--
48	"	Total pellet	0.7	34.5	--	--	98.9	<0.1	6.2	--	--
51	"	"	0.2	35.5	--	--	98.9	<0.1	6.0	--	--
52	"	Ash	8.8	36.1	--	--	97.2	--	6.4	--	--
--	--	Unburned core	46.0	20.2	--	--	60.8	--	4.2	--	--
73	70/30	Ash	6.0	35.0	--	--	99.1	--	6.7	--	--
--	"	Unburned core	46.3	20.5	--	--	61.3	--	4.8	--	--
57	50/50	Total pellet	0.2	45.0	--	--	98.5	<0.1	3.9	--	--
60	"	Ash	8.0	37.4	--	--	91.0	0.3	4.6	--	--
--	--	Unburned core	27.7	31.5	--	--	72.6	<0.1	3.1	--	--
63	50/50	Ash	5.0	34.2	--	--	97.7	0.1	4.6	--	--
--	--	Unburned core	30.2	16.5	--	--	68.6	<0.1	3.9	--	--
66	50/50	Ash	0.6	34.0	--	--	99.4	0.1	4.6	--	--
--	--	Unburned core	26.9	--	--	--	--	--	3.4	--	--
69	50/50	Total pellet	0.4	37.5	--	--	98.0	<0.1	4.5	--	--
61	"	Ash	9.4	42.7	7.43	2.94	90.7	0.2	3.9	2.67	0.07
--	--	Unburned core	27.8	32.3	7.82	2.19	69.6	0.2	2.8	1.87	0.48

(a) Indicates that sample gained weight during analysis and value could not be determined.

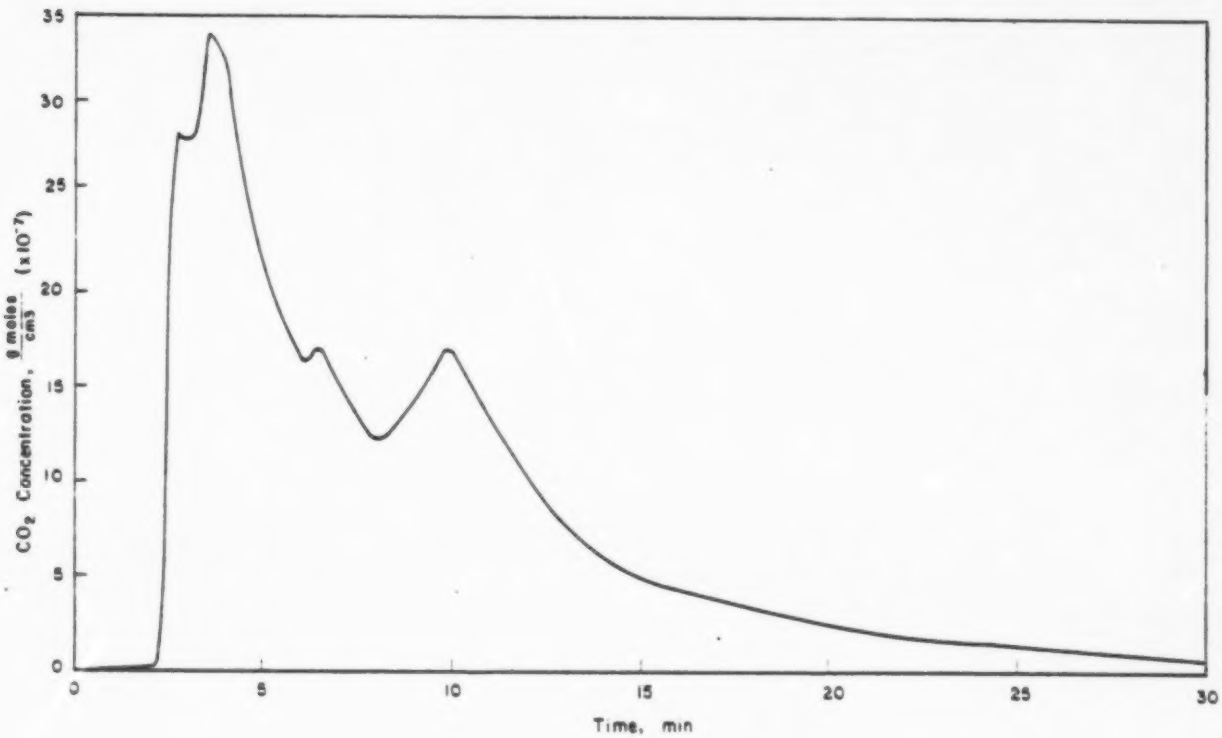

FIGURE III-3. CO_2 CONCENTRATION MEASURED IN THE GAS STREAM FROM THE FIXED-BED REACTOR FOR THE LIMESTONE PELLETS IN RUN 110

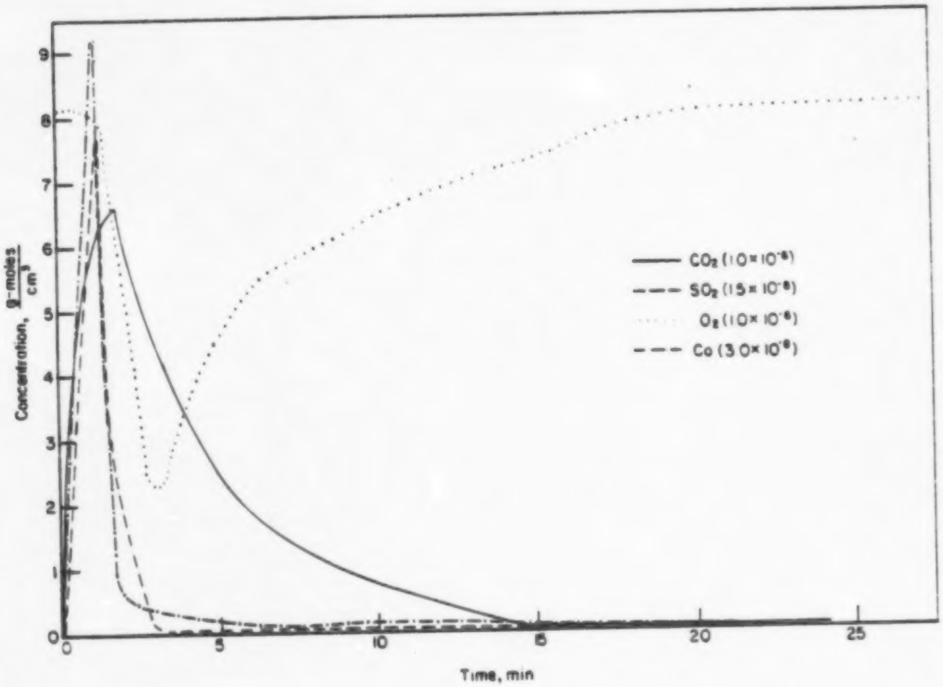

FIGURE III-4. CONCENTRATIONS OF CO_2, SO_2, O_2, AND CO MEASURED IN GAS STREAM FROM THE FIXED-BED REACTOR FOR THE 50 WEIGHT PERCENT COAL/50 WEIGHT PERCENT LIMESTONE PELLETS IN RUN 104

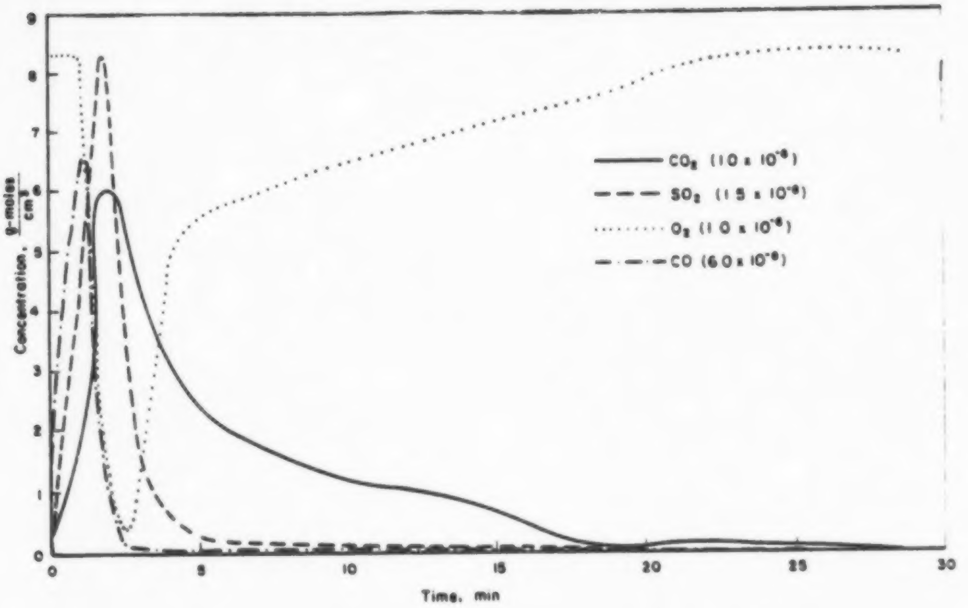

FIGURE III-5. CONCENTRATIONS OF CO_2, SO_2, O_2, AND CO MEASURED IN GAS STREAM FROM THE FIXED-BED REACTOR FOR THE 70 WEIGHT PERCENT COAL/30 WEIGHT PERCENT LIMESTONE PELLETS IN RUN 101

Measurements were made to determine the time response characteristics of the CO_2 and the SO_2 gas analyzers. Sampling lines from the fixed-bed reactor to the gas analyzers introduce a response delay and the finite volume of the detector cell in the instruments along with other factors can retard instrument response. Response measurements were made by separately introducing SO_2 and CO_2 into the fixed-bed reactor and recording the output of the respective instruments as they followed the rise and decay of the concentrations when the gas flows were switched on and off. The response data were analyzed using the following differential equation to approximate response time:

$$\frac{dC_m}{dt} = \frac{f}{V_m} \frac{R(t)}{F} - \frac{f}{V_m} C_m$$

where

C_m = concentration measured by analyzer, moles/cm^3
V_m = effective volume of sensor in analyzer, cm^3
f = flow rate through analyzer, cm^3/sec
F = flow rate through fixed-bed reactor, cm^3/sec
$R(t)$ = release rate, moles/sec
t = time, sec.

For the instrument response measurements, R(t) was either a finite constant, R_o, or 0, and the above equation could be integrated to give

$$C_m = \frac{R_o}{F} \left(1 - e^{-\frac{f}{V_m} t}\right)$$

when the detected gas was switched on or

$$C_m = \frac{R_o}{F} e^{-\frac{f}{V_m} t}$$

when the gas was switched off after having achieved steady state. Response parameters determined for the O_2 and SO_2 analyzers are summarized in Table III-18. The difference in the CO_2 analyzer response parameters between increasing and decreasing transients indicates the inadequacy of the response equation.

Release rates were calculated for Runs 101 and 104 using the differential form of the response equation

TABLE III-18. RESPONSE PARAMETERS FOR GAS ANALYZERS

Analyzer	Analyzer Flow Rate,(a) cm^3/sec	Delay Time, sec	Response Parameter, Increasing Release	$f/Vm, sec^{-1}$ Decreasing Release
• Beckman CO_2	1.52	36	0.0764	0.0501
• TECO SO_2	8.10	19.6	0.0367	0.0367
• Faristor SO_2	8.44	17	0.0223	0.0223

(a) Flow rate based on a pressure of 29.54 in. Hg.

$$R(t) = \frac{FV_m}{f} \left(\frac{dC_m}{dt} + \frac{f}{V_m} C_m \right) \text{, moles/sec}$$

with the analyzer concentration curves and their derivatives, and the response parameters from Table III-18. The results of the calculations, which are based on a flow-rate, F, of 0.0006 m^3/sec are presented in Figures III-6 and III-7. In general, the response of the analyzers followed the release rates with only a slight lag. So for the experiments reported here, it was acceptable to use the concentrations from the analyzers without response corrections.

Results from the gas analyzer measurements are presented in Table III-19 in terms of total O_2 consumption and CO_2, CO and SO_2 release. In the table, parentheses designate values corrected for instrument responses that show no significant differences when compared with the results obtained by integrating the concentration curves. The total CO_2 observed in Run 110 seems to be twice as high as would be anticipated from stoichiometric considerations. The data from Table III-19 for the coal/limestone pellets are compared in Table III-20. In general, about 10 percent of the observed CO_2 released would be expected to come from calcination of the limestone. The amount of CO observed is small, running only about 1 to 2 percent of the CO_2. Figures III-4 and III-5 both show that the major CO release, like the SO_2, occurs during the first 3 minutes after heating begins and does not continue at an appreciable rate for longer times as does CO_2.

Thermocouple measurements for Run 101, which involved 70/30 pellets, are given in Figure III-8. Here it is seen that the maximum pellet surface temperature runs about 60 C higher than the furnace temperature because of the heat released by combustion of the pellets.

PELLET CHARACTERIZATION STUDIES

Unburned and burned pellets were sectioned metallographically and examined microscopically by scanning electron microscopy and by X-ray diffraction. Typical longitudinal cross sections of 50/50 pellets are presented in Figure III-9 which shows an unburned pellet and two

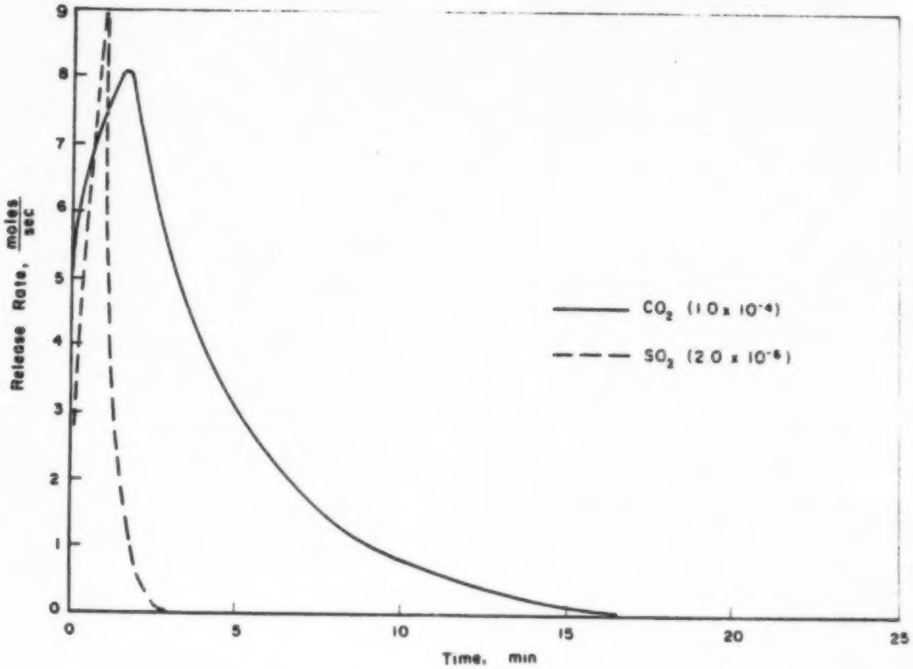

FIGURE III-6. RELEASE RATES FOR CO_2 AND SO_2 FROM 50 WEIGHT PERCENT COAL/50 WEIGHT PERCENT LIMESTONE PELLETS DURING RUN 104.

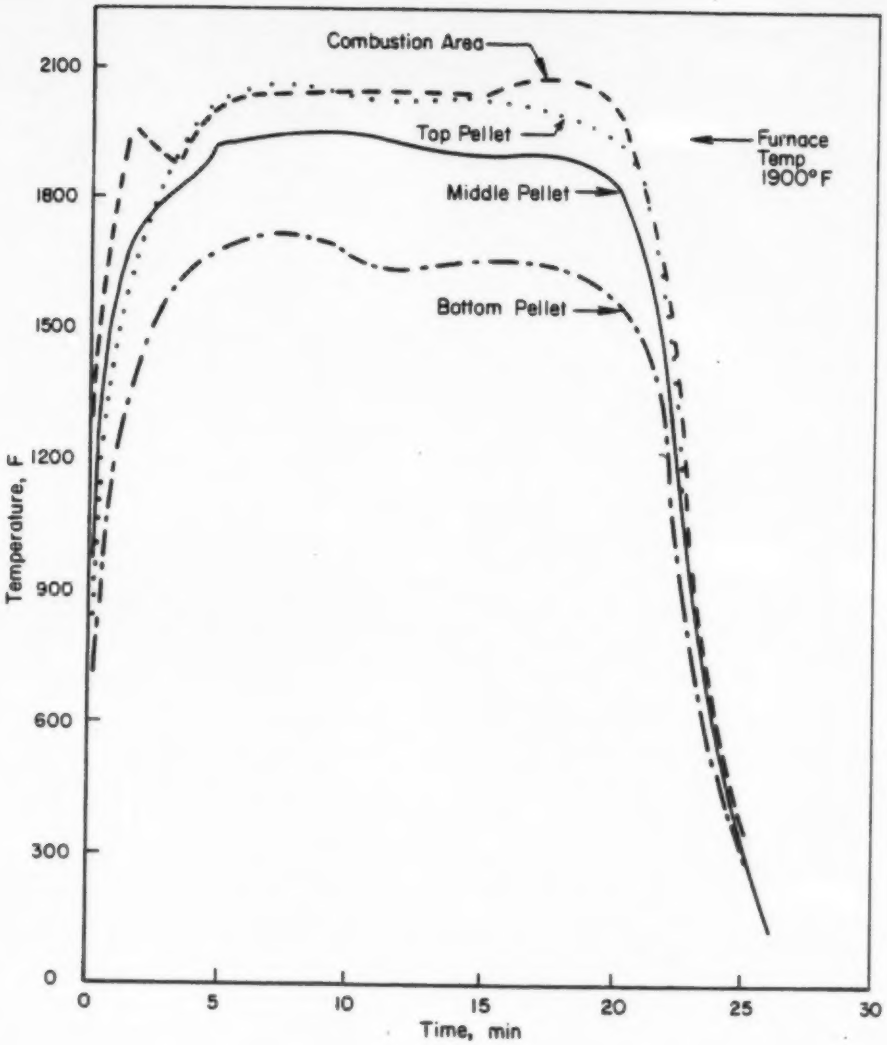

FIGURE III-8. THERMOCOUPLE MEASUREMENTS FOR FIXED BED REACTOR RUN 101 WITH 70 WEIGHT PERCENT COAL/30 WEIGHT PERCENT LIMESTONE PELLETS

Preceding page blank

Reproduced from best available copy.

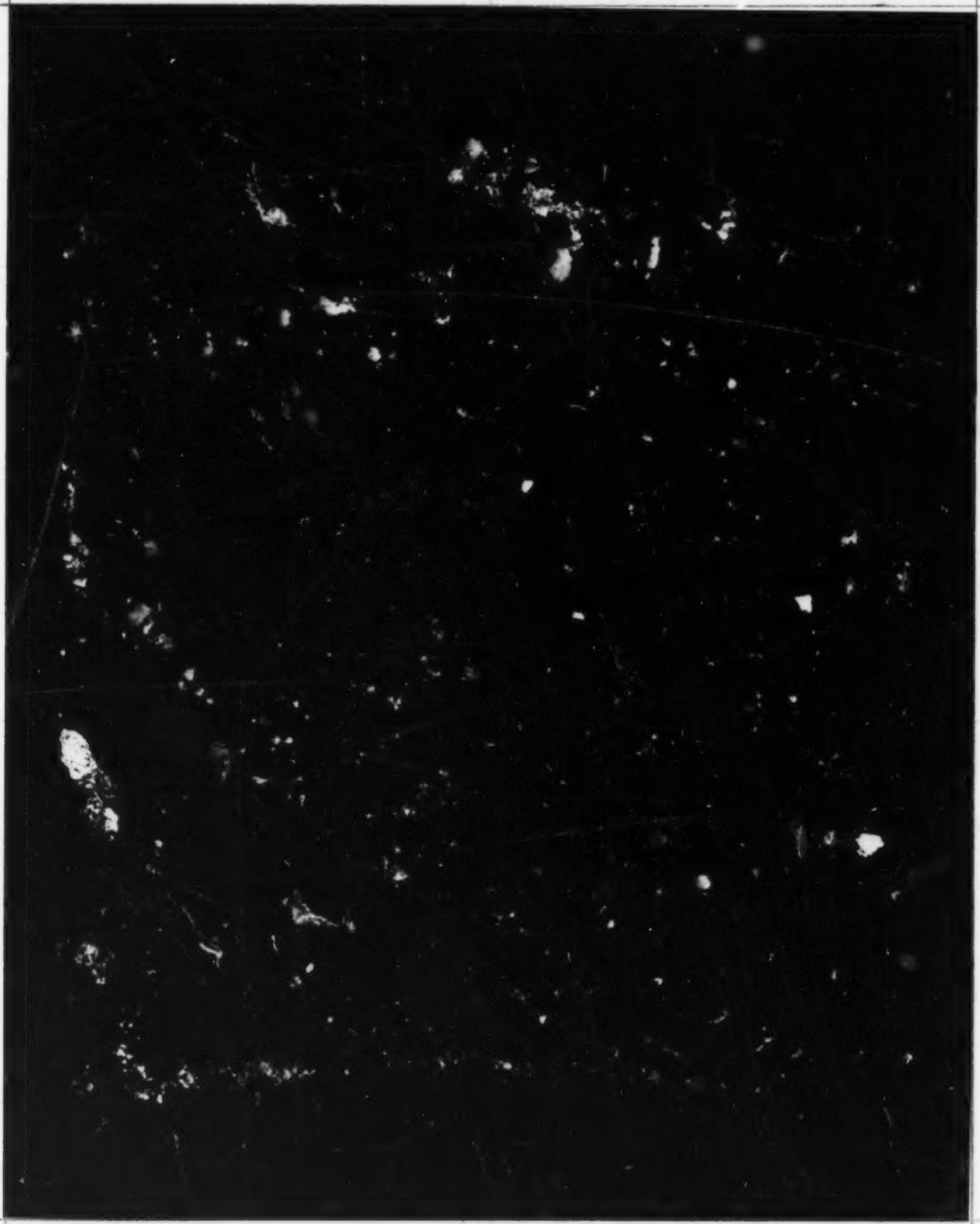

(9J665)

(a) Pellet 72

Unburned Pellet

FIGURE III-9. METALLOGRAPHIC CROSS SECTIONS OF 50 WEIGHT PERCENT COAL/50 WEIGHT PERCENT LIMESTONE PELLETS AS A FUNCTION OF BURNING TIME

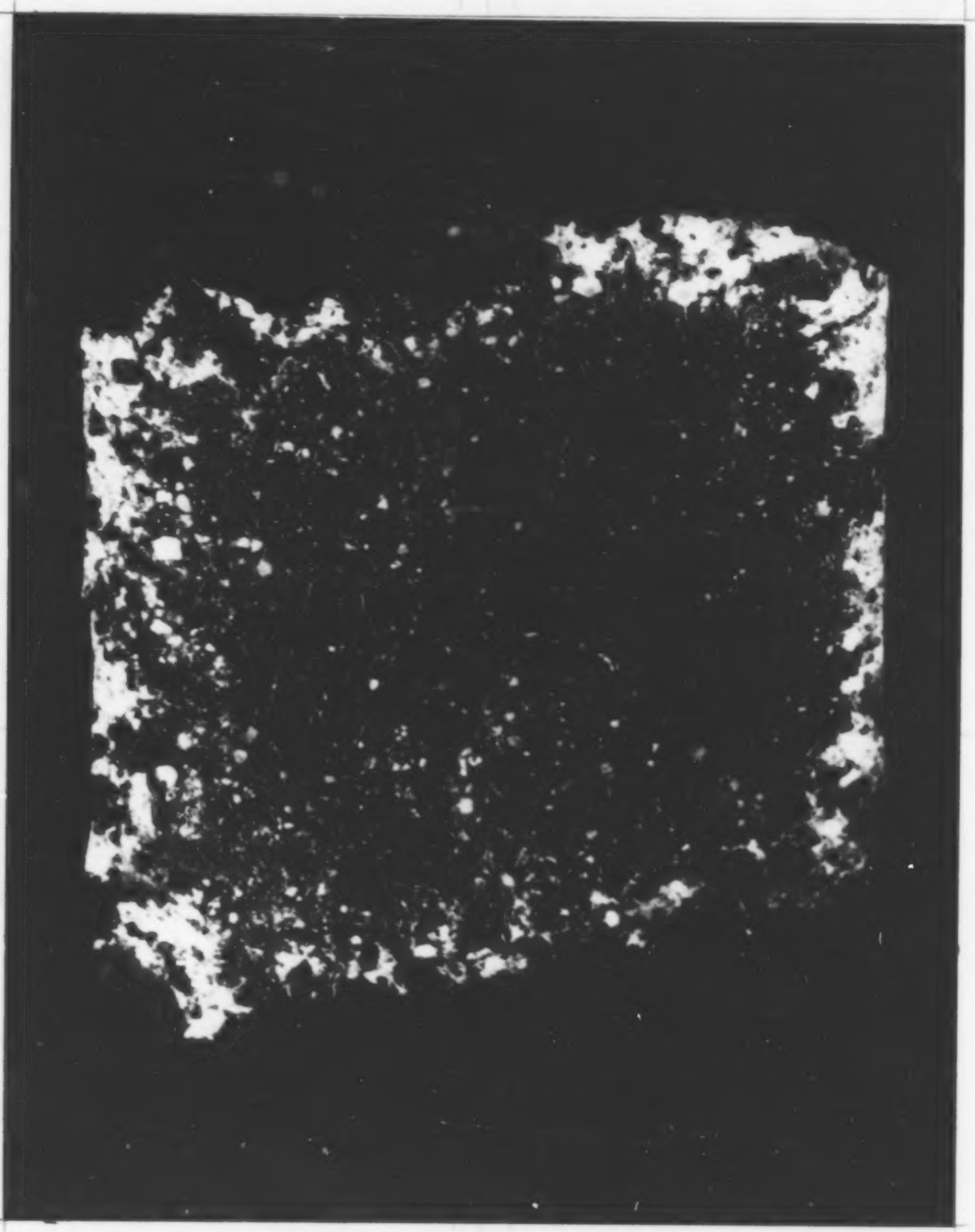

(9J666)

(b) Pellet 59

4-Minute Burning Time

FIGURE III-9. (CONTINUED)

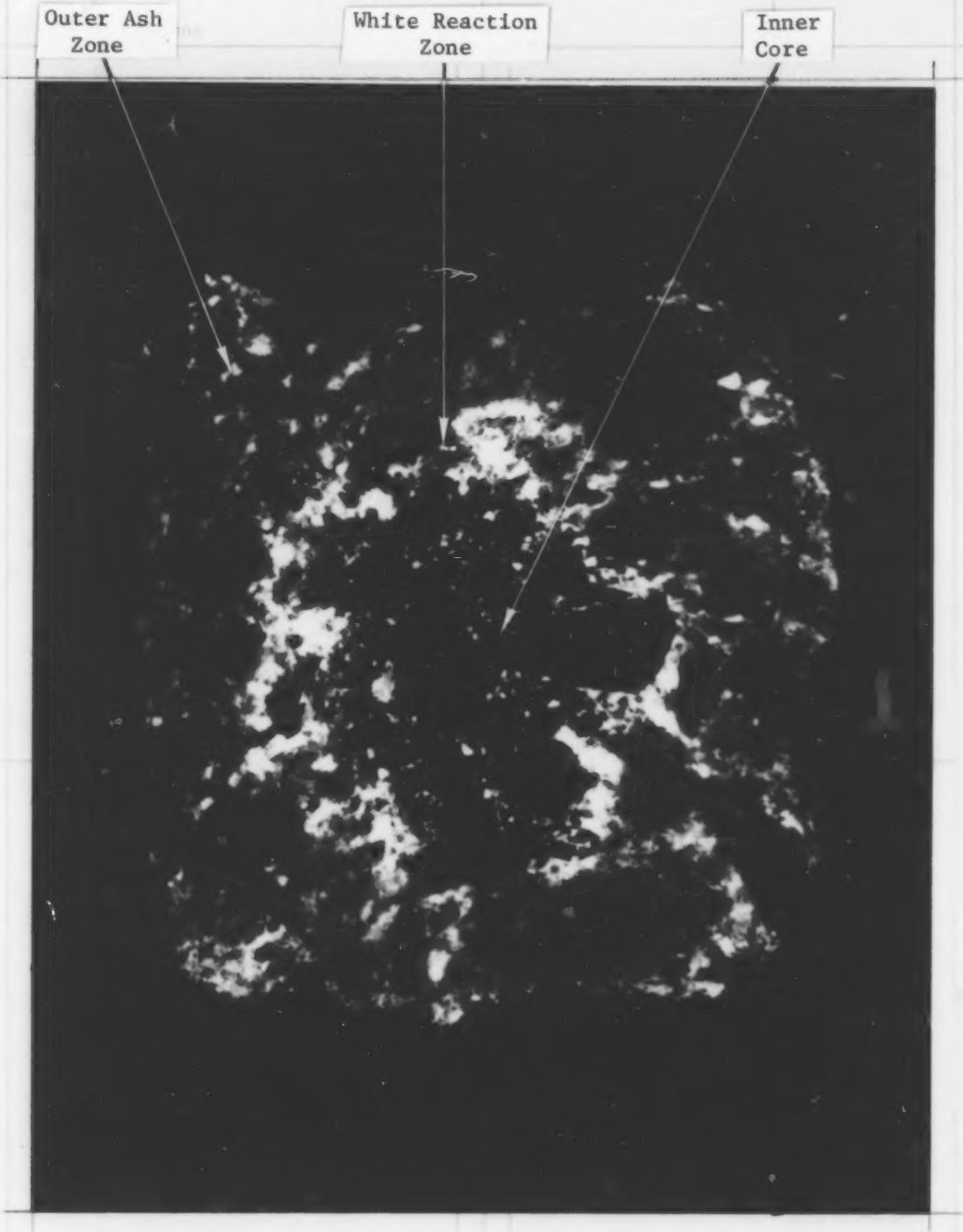
Outer Ash Zone
White Reaction Zone
Inner Core

(9J668)

(c) Pellet 65

12-Minute Burning Time

FIGURE III-9. (CONTINUED)

TABLE III-19. RESULTS FROM GAS-ANALYZER MEASUREMENTS(a)

Run No.	Pellet Composition	O_2 Consumed, Moles	CO Released, Moles	CO_2 Released, Moles	SO_2 Released,(b) Moles
110	Limestone	-	-	1.67×10^{-1}	-
		-	-	(1.60×10^{-1})	-
104	50 w/o Coal/ 50 w/o Limestone	2.49×10^{-1}	2.79×10^{-3}	2.27×10^{-1}	8.02×10^{-4}
		-	-	(2.26×10^{-1})	(8.83×10^{-4})
101	70 w/o Coal/ 30 w/o Limestone	3.18×10^{-1}	4.25×10^{-3}	2.17×10^{-1}	1.70×10^{-3}
		-	-	(2.05×10^{-1})	(1.73×10^{-3})

(a) Values in parentheses corrected for instrument response. All other values were obtained directly from concentration curves.

(b) Based on measurements from TECO Pulsed Fluorescence Analyzer.

TABLE III-20. COMPARISON OF GAS-ANALYZER MEASUREMENTS FOR COAL/LIMESTONE PELLETS

	Run 104 (50 w/o Coal/ 50 w/o Limestone)	Run 101 (70 w/o Coal/ 30 w/o Limestone)
• Percent Sulfur Released as SO_2	13.8	31.3
• Percent Carbon in Pellets Measured by Gas Analysis[(a)]	80	84
• Percent CO_2 Occurring as CO	1.2	2.0
• Ratio of O_2 Consumed to Coal Carbon Present in Pellets, Moles O_2/moles Coal Carbon	1.0	1.3

(a)Run 104 is based on 0.250 moles of carbon from coal and 0.038 moles of carbon from limestone in the three pellets. Run 101 based on 0.244 moles of carbon from coal and 0.019 moles of carbon from the limestone in the three pellets.

partially burned pellets. The unburned central zone or core is surrounded by a white halo, which is in turn surrounded by porous ash. The unburned central core shows evidence of this porosity, presumably from devolatilization of the coal.

Scanning Electron Microscopy

Photomicrographs and elemental X-ray maps of a typical area in an unburned 50/50 pellet (Pellet 72 in Figure 7) are presented in Figure III-10. The distribution of calcium, sulfur, iron, magnesium, aluminum, and silicon in the unburned pellets is shown in the X-ray maps. These maps show sulfur dispersed throughout the coal but strongly associated with the iron, probably as pyrites. Iron is also associated with magnesium, aluminum, and silicon. Calcium is seen surrounding the iron-containing particle and interdispersed between the coal particles.

Figures III-11, III-12, and III-13 show the scanning electron micrograph and X-ray maps for the three different zones shown in Figure III-9 for Pellet 65, which was burned in the fixed-bed reactor for 12 minutes. The results for the outer ash zone are presented in Figure III-11. The 50X photomicrographs show that sulfur is associated primarily with the regions containing calcium and small levels of magnesium. The photomicrographs in Figure III-12 for the white region again indicate high porosity, with the sulfur dispersed throughout the material that contains high levels of calcium.

Results for the unburned inner core, depicted in Figure III-13, indicate that some of the coal is still intact. However, there is evidence of porosity formation, which is probably associated with partial devolatization of part of the coal. There is also evidence, as can be seen by comparing the X-ray maps for calcium, sulfur, and iron, that sulfur may pass from the pyrites into the surrounding calcium by a solid-state reaction mechanism.

Further information on the chemical structure of the constituents in the pellets was obtained by X-ray diffraction.

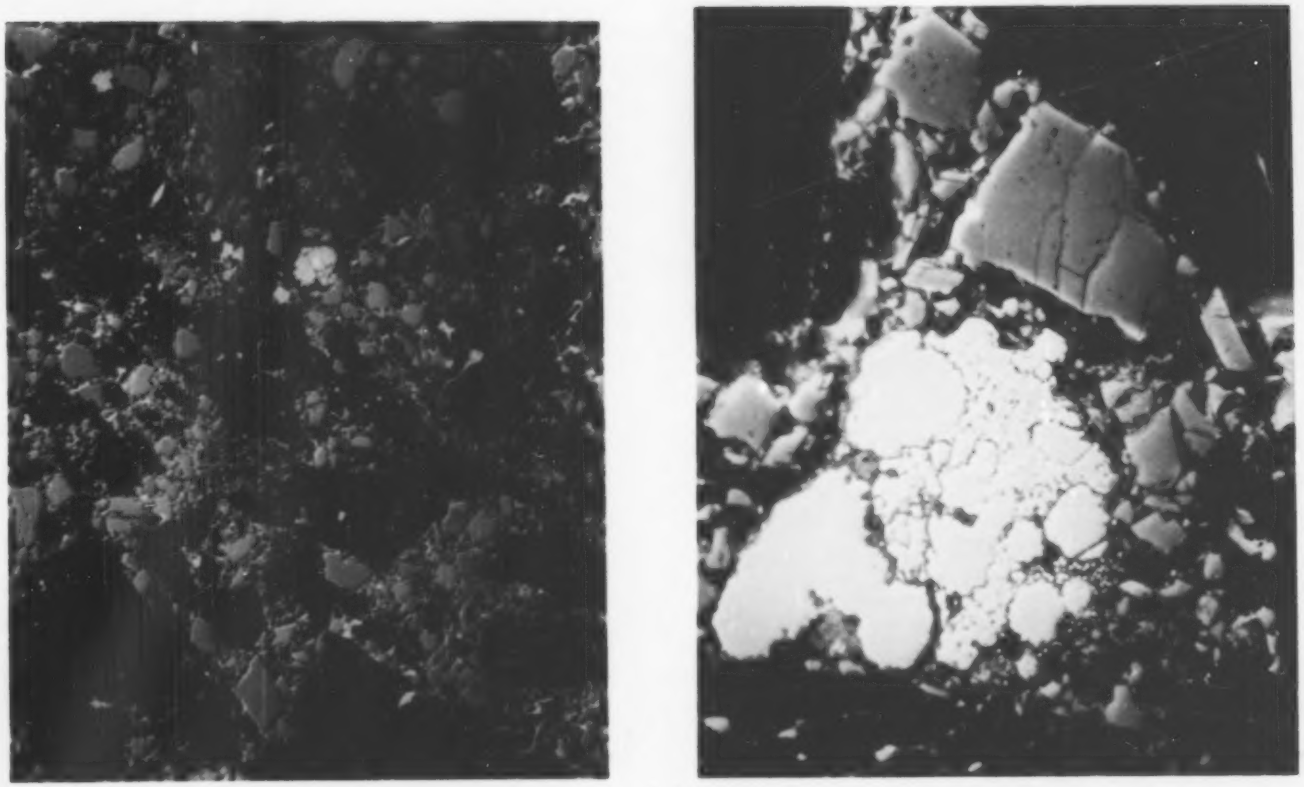

(a)

50X Photomicrograph 500X Photomicrograph

FIGURE III-10. SCANNING ELECTRON MICROGRAPHS AND ELEMENTAL X-RAY MAPS FOR UNBURNED 50 WEIGHT PERCENT COAL/50 WEIGHT PERCENT LIMESTONE PELLET (PELLET 72)

Reproduced from
best available copy.

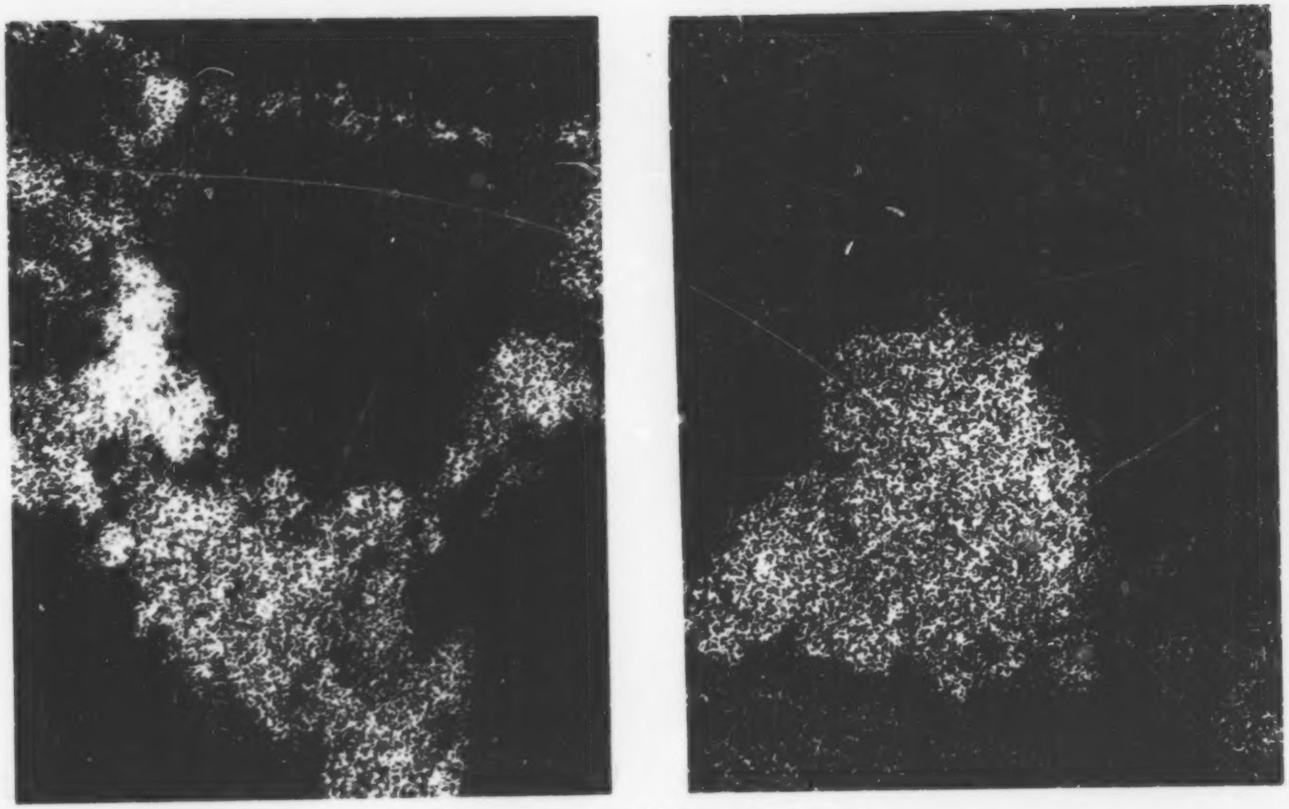

(b)

500X Calcium X-Ray Map

500X Sulfur X-Ray Map

FIGURE III-10. (CONTINUED)

Reproduced from best available copy.

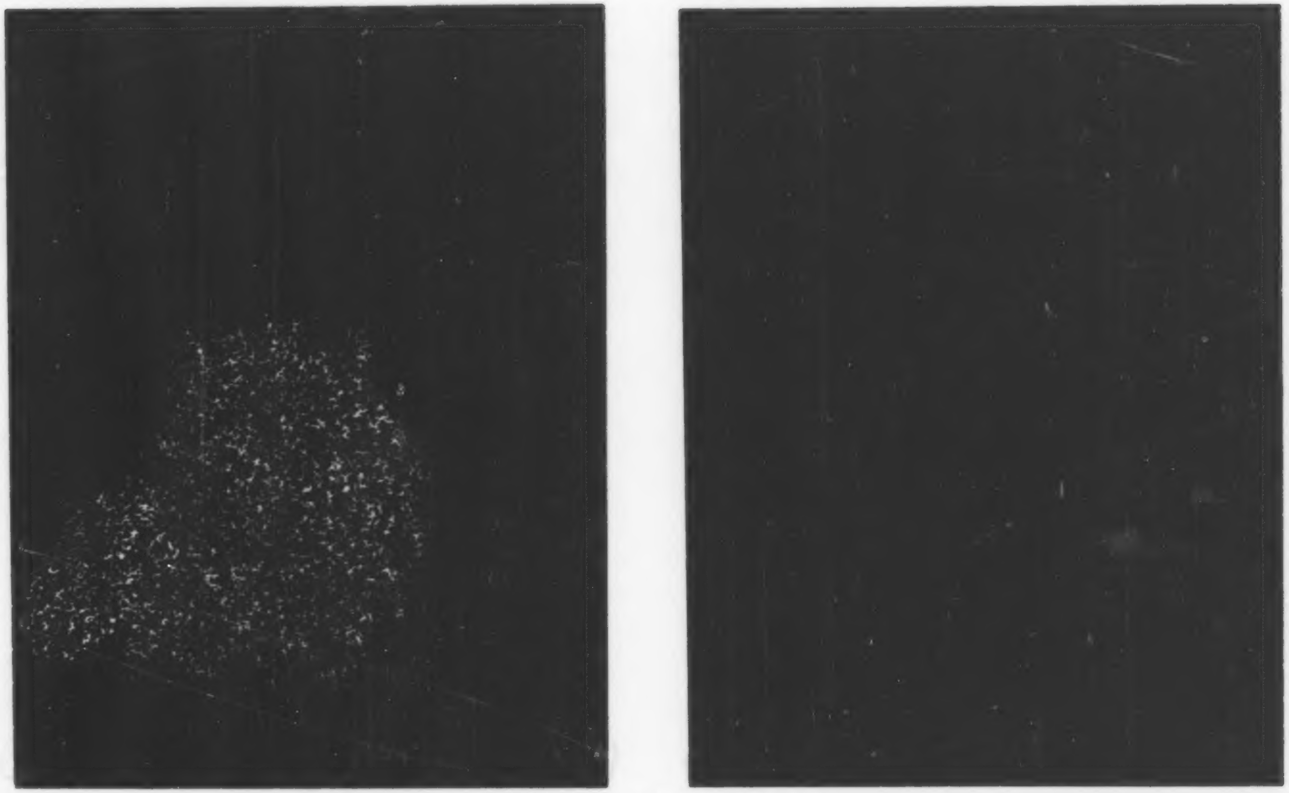

(c)

500X Iron X-Ray Map

500X Magnesium X-Ray Map

FIGURE III-10. (CONTINUED)

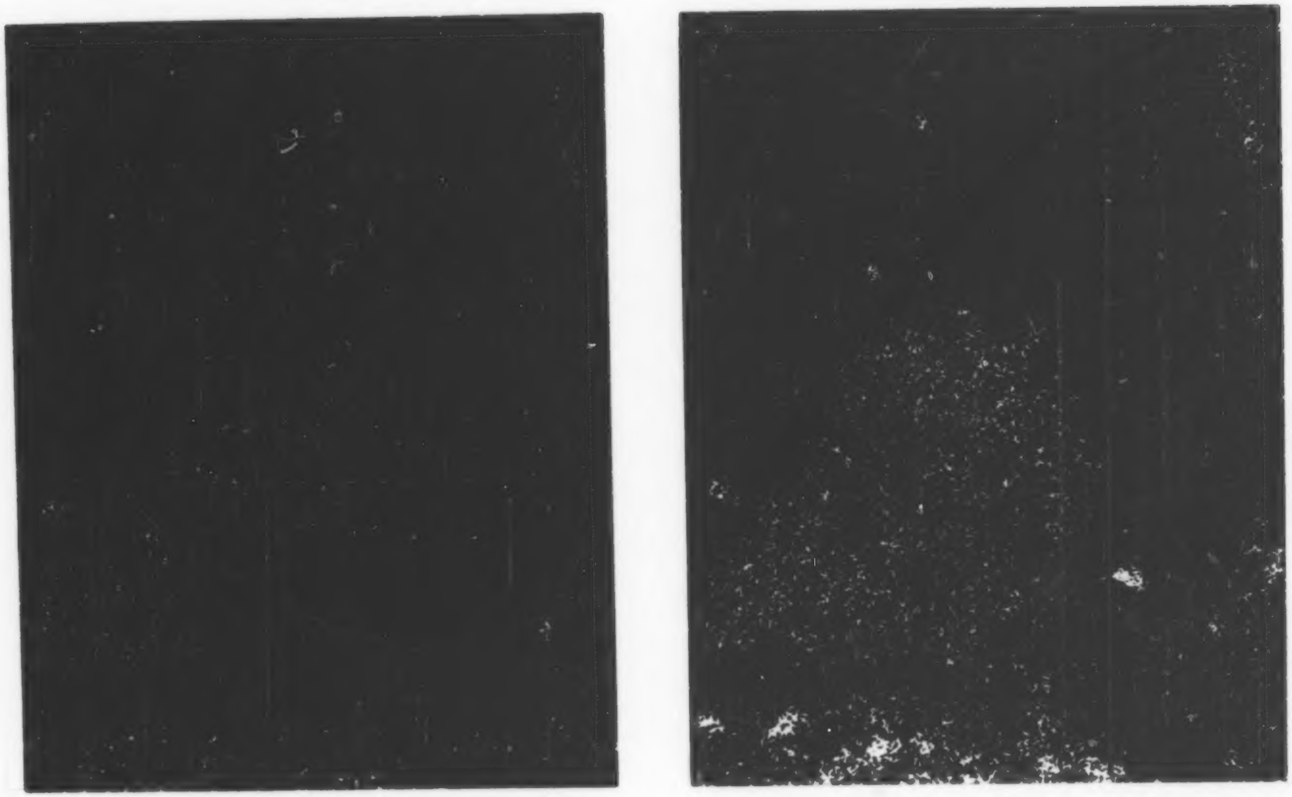

(d)

500X Aluminum X-Ray Map

500X Silicon X-Ray Map

FIGURE III-10. (CONTINUED)

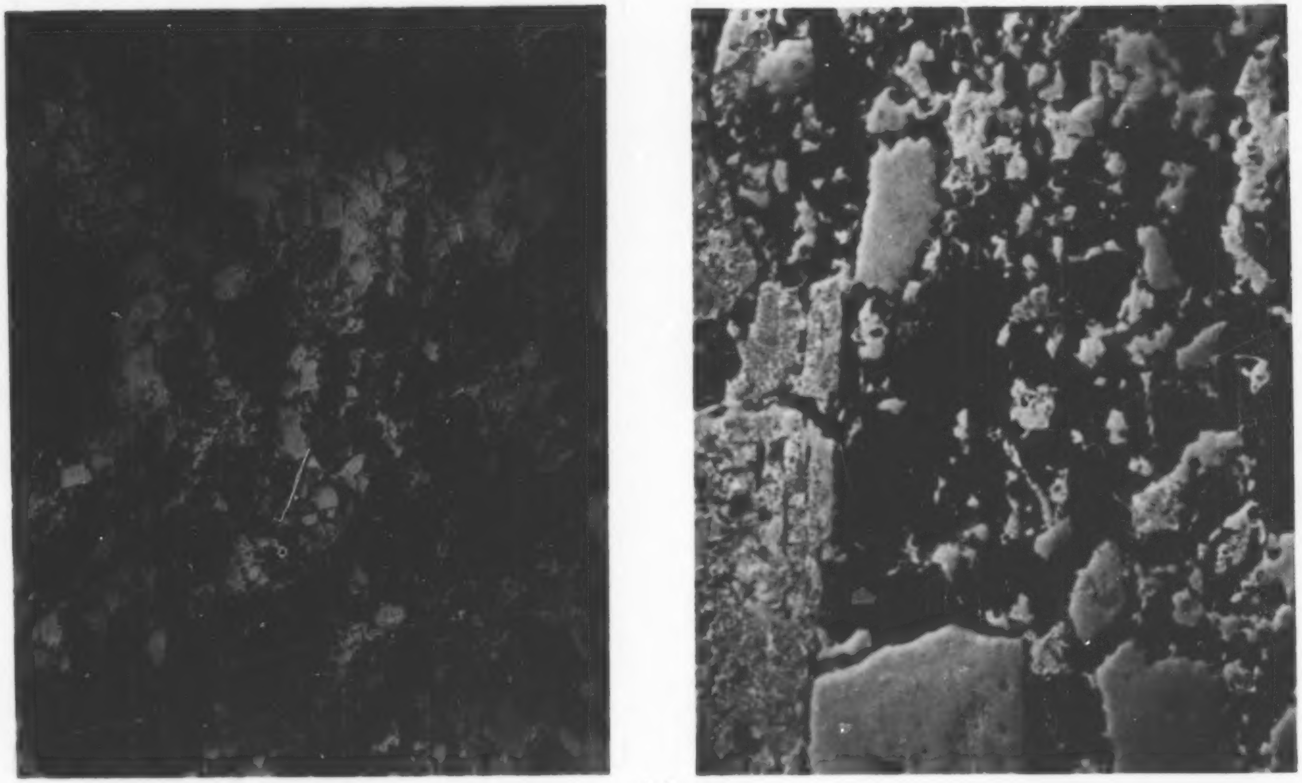

(a)

50X Photomicrograph

500X Photomicrograph

FIGURE III-11. SCANNING ELECTRON MICROGRAPHS AND ELEMENTAL X-RAY MAPS FOR OUTER ASH ZONE IN 50 WEIGHT PERCENT COAL/50 WEIGHT PERCENT LIMESTONE PELLET (PELLET 65) BURNED FOR 12 MINUTES IN THE FIXED-BED REACTOR

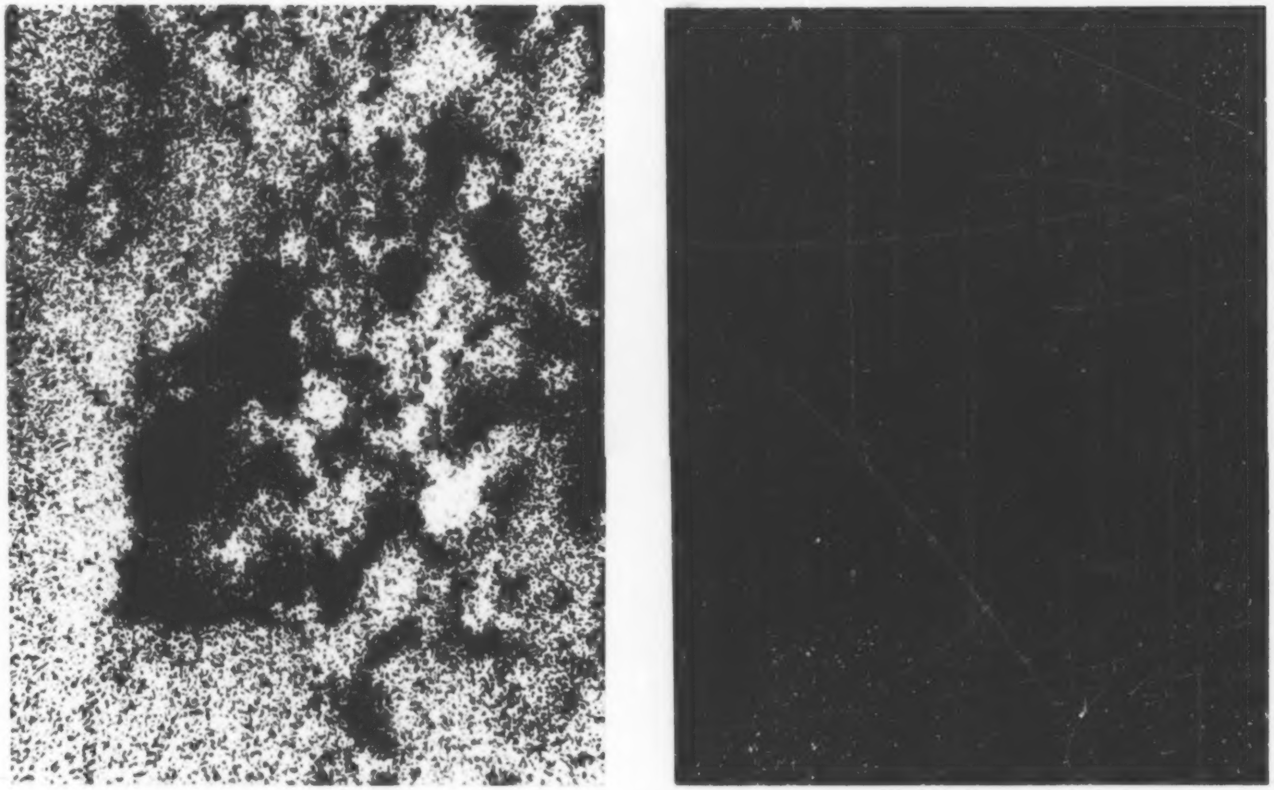

(b)

500X Calcium X-Ray Map 500X Sulfur X-Ray Map

FIGURE III-11. (CONTINUED)

Reproduced from
best available copy.

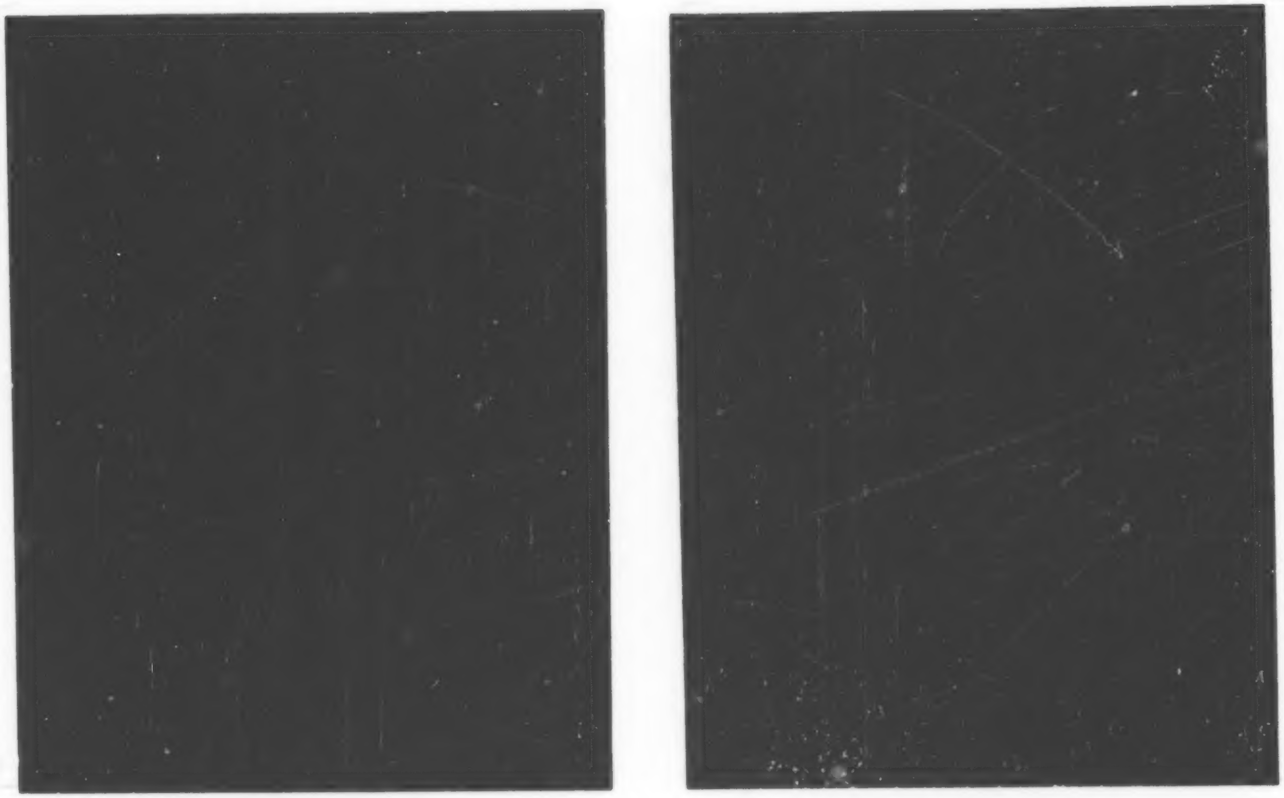

(c)

500X Iron X-Ray Map 500X Magnesium X-Ray Map

FIGURE III-11. (CONTINUED)

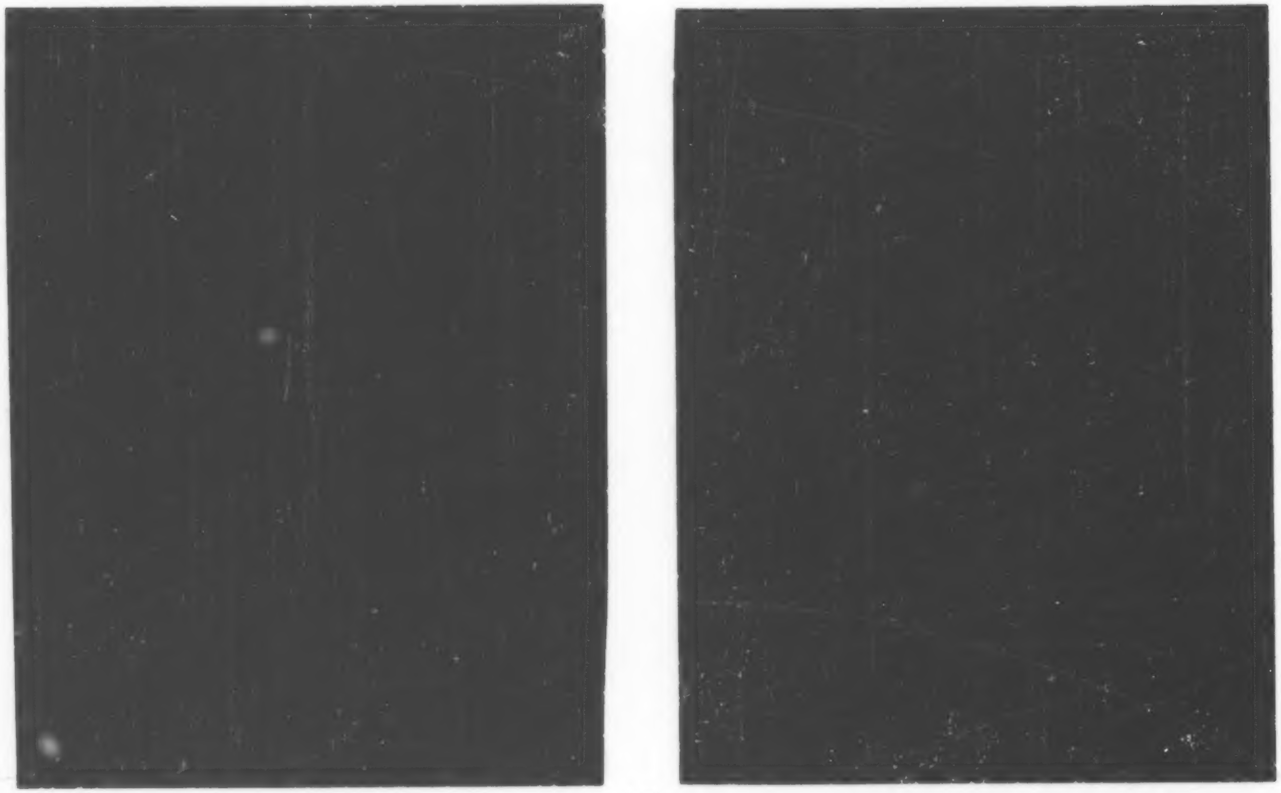

(d)

500X Aluminum X-Ray Map 500X Silicon X-Ray Map

FIGURE III-11. (CONTINUED)

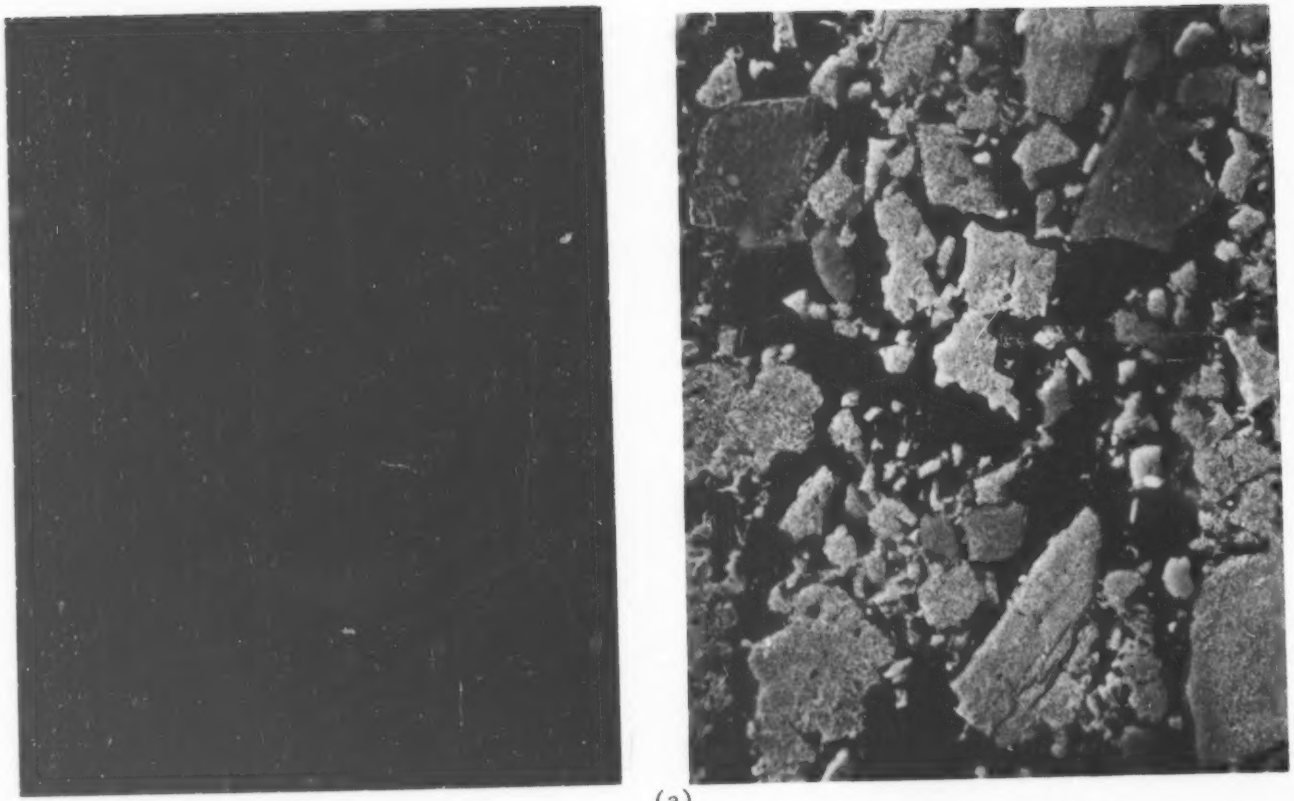

(a)

500X Chlorine X-Ray Map

500X Photomicrograph

FIGURE III-12. SCANNING ELECTRON MICROGRAPHS AND ELEMENTAL X-RAY MAPS FOR WHITE REACTION ZONE IN 50 WEIGHT PERCENT COAL/50 WEIGHT PERCENT LIMESTONE PELLET (PELLET 65) BURNED FOR 12 MINUTES IN THE FIXED-BED REACTOR

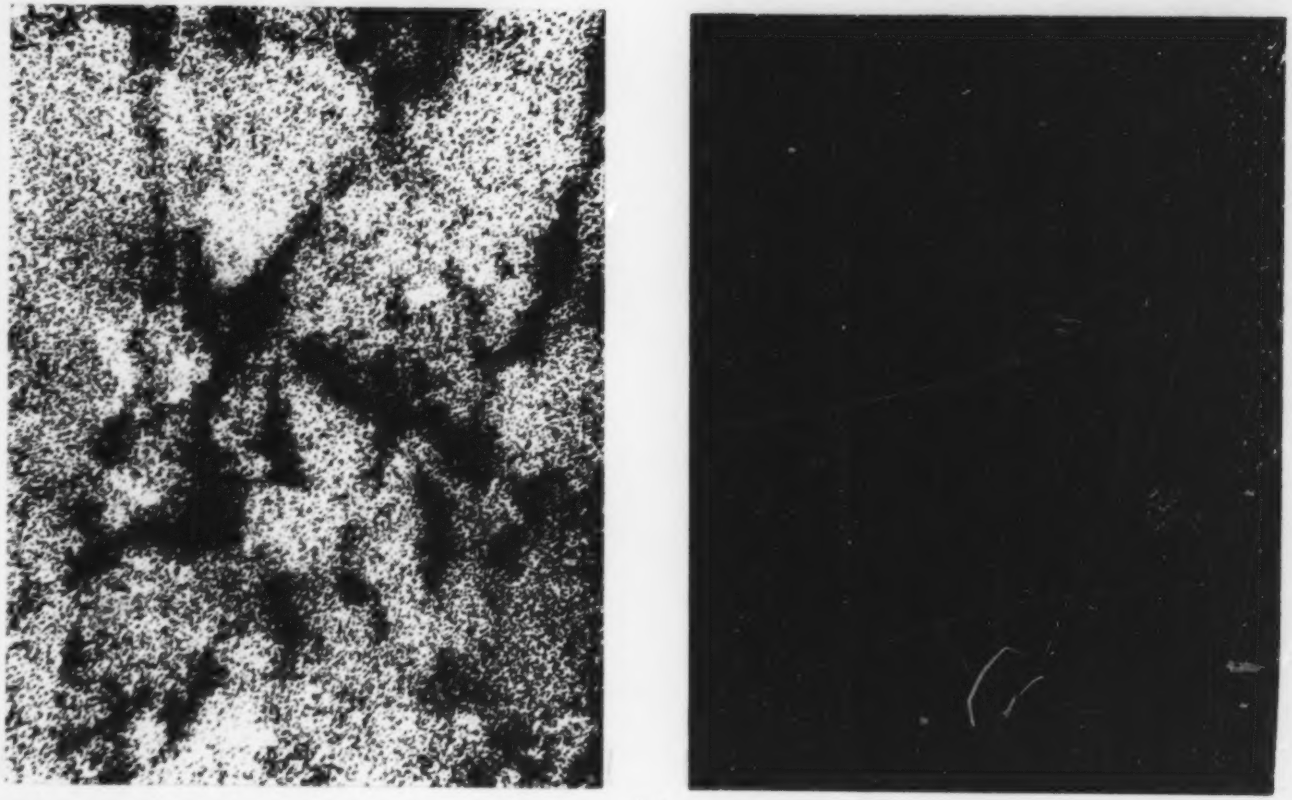

(b)

500X Calcium X-Ray Map

500X Sulfur X-Ray Map

FIGURE III-12. (CONTINUED)

Reproduced from
best available copy.

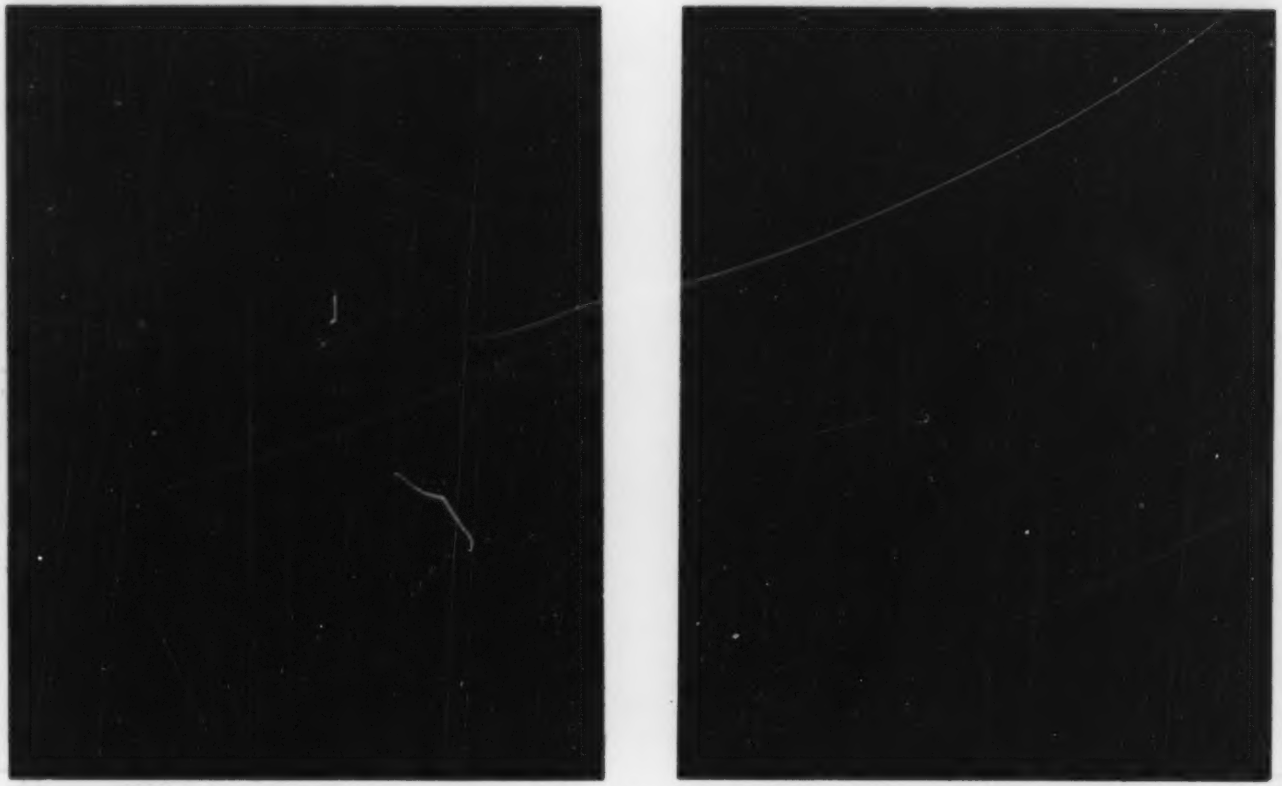

(c)

500X Iron X-Ray Map 500X Magnesium X-Ray Map

FIGURE III-12. (CONTINUED)

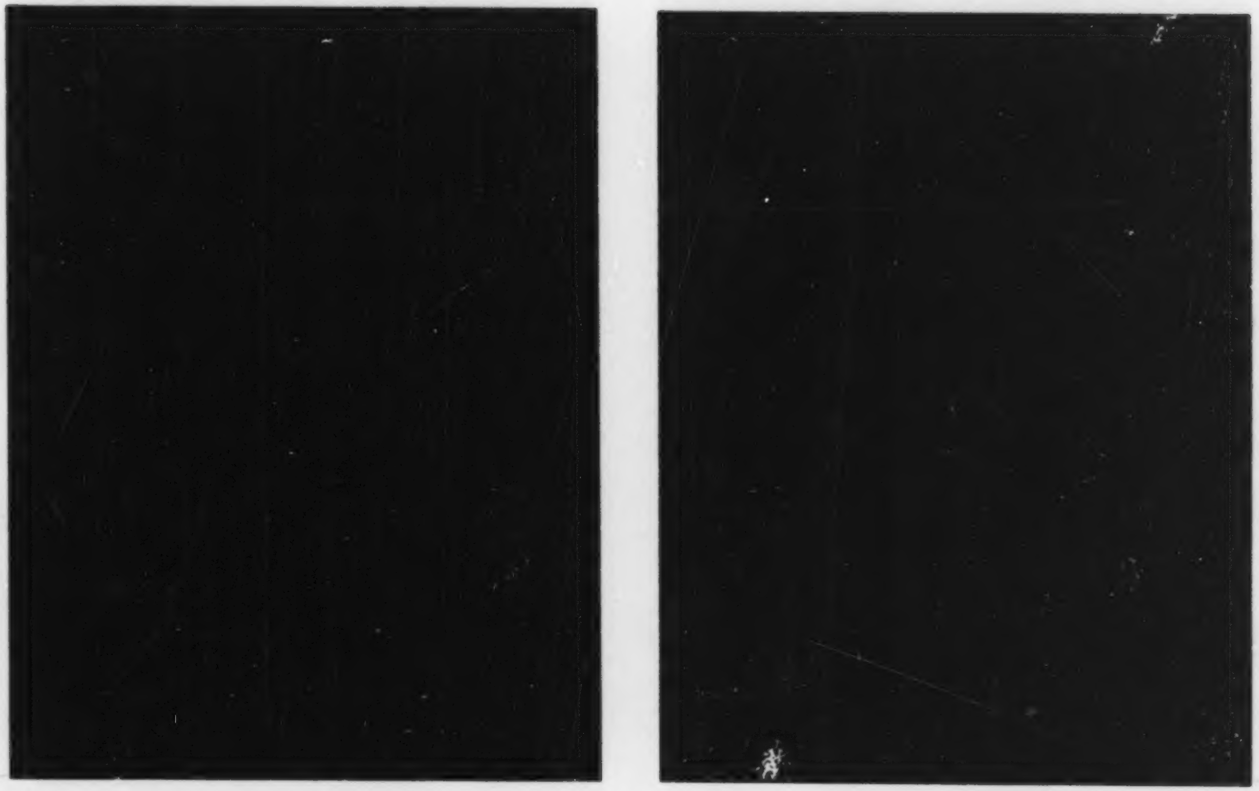

(d)

500X Aluminum X-Ray Map 500X Silicon X-Ray Map

FIGURE III-12. (CONTINUED)

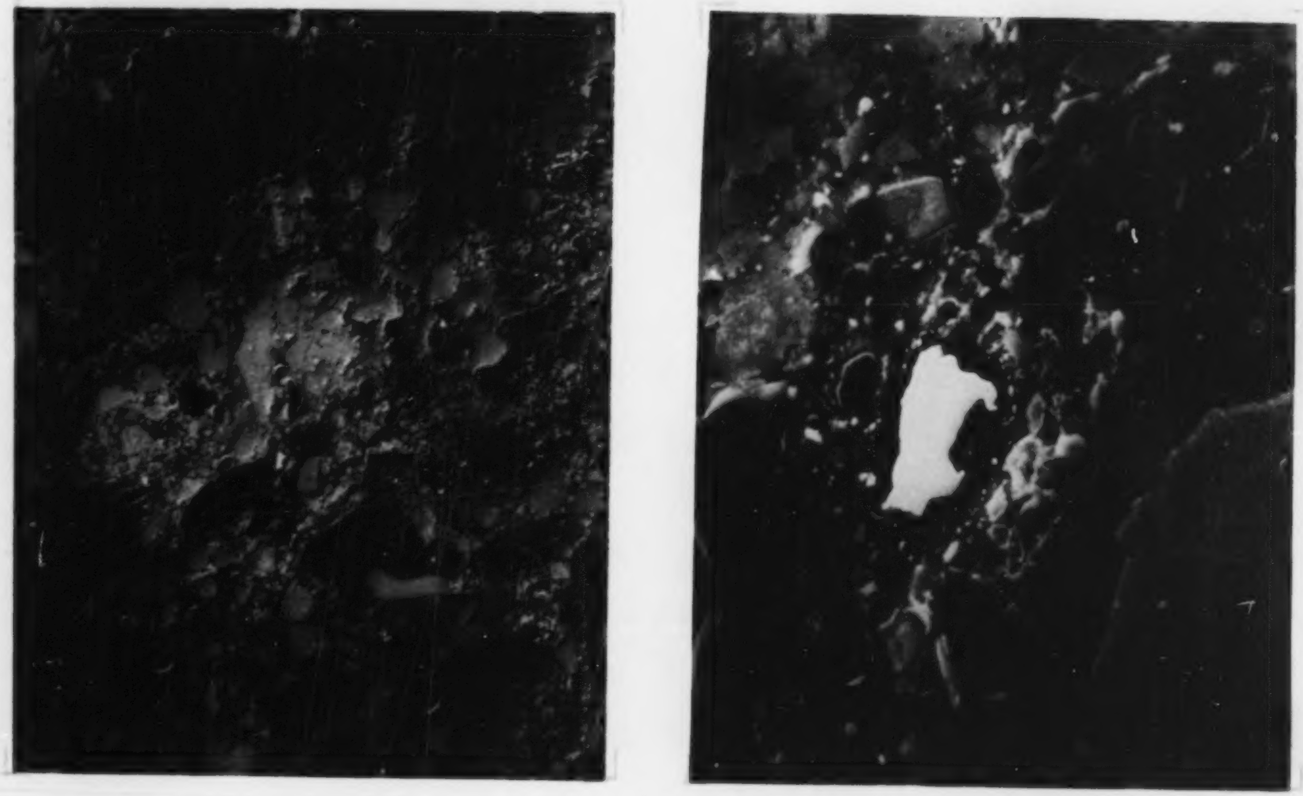

(a)

50X Photomicrograph 500X Photomicrograph

FIGURE III-13. SCANNING ELECTRON MICROGRAPHS AND ELEMENTAL X-RAY MAPS FOR INNER CORE IN 50 WEIGHT PERCENT COAL/50 WEIGHT PERCENT LIMESTONE PELLET (PELLET 65) BURNED FOR 12 MINUTES IN THE FIXED-BED REACTOR

Reproduced from best available copy.

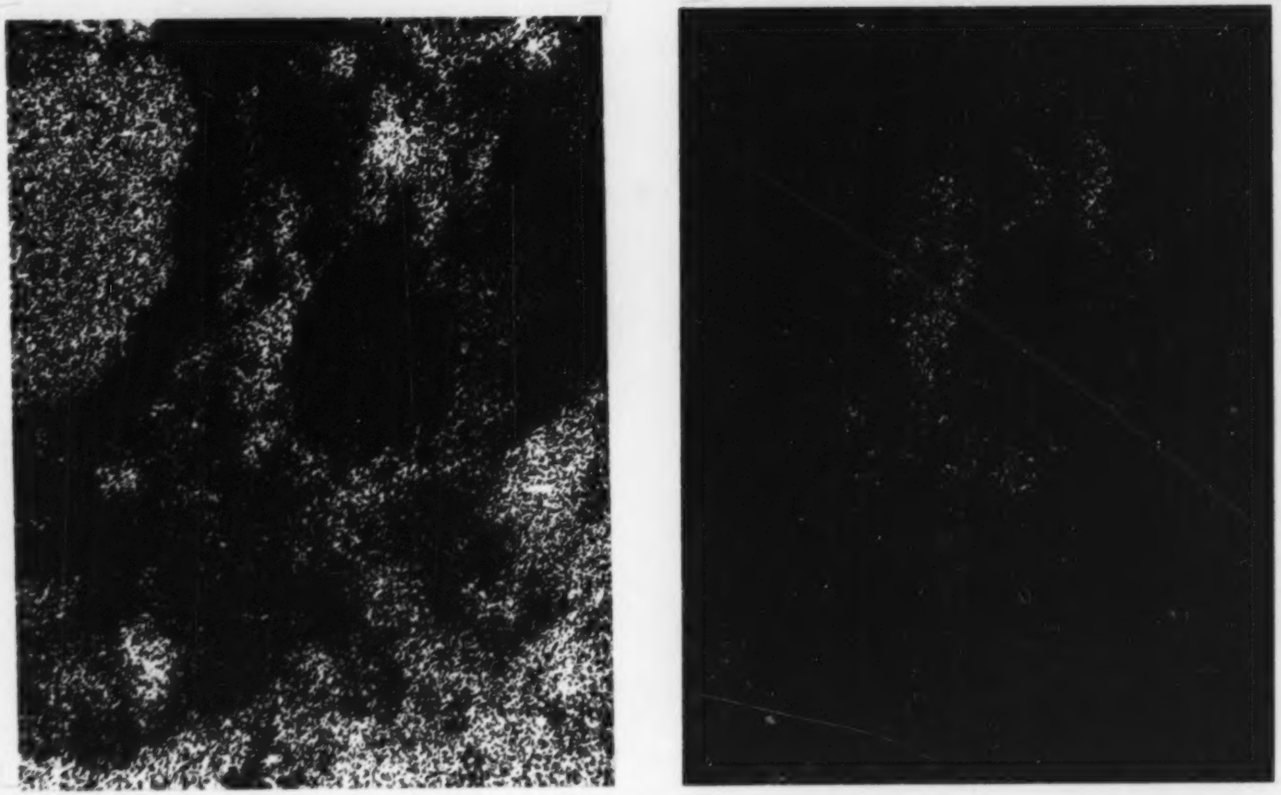

(b)

500X Calcium X-Ray Map

500X Sulfur X-Ray Map

FIGURE III-13. (CONTINUED)

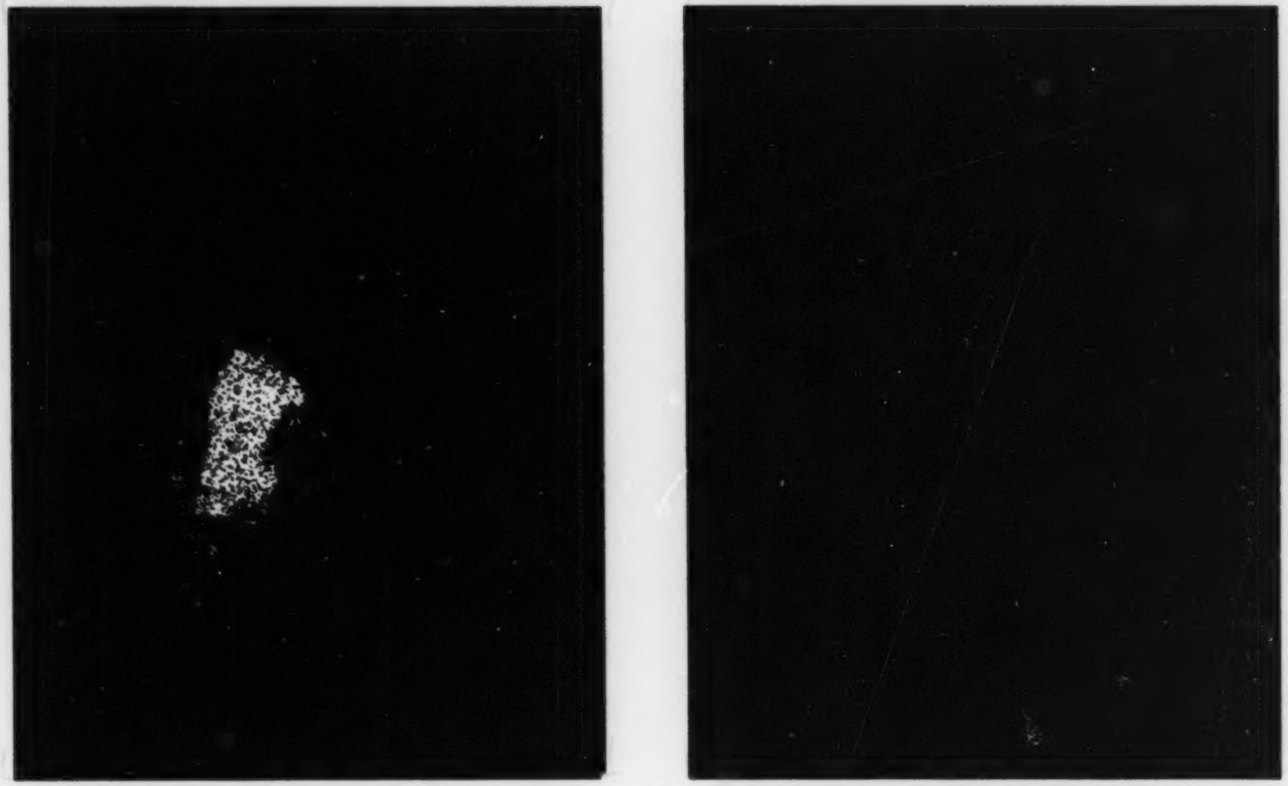

(c)

500X Iron X-Ray Map

500X Magnesium X-Ray Map

FIGURE III-13. (CONTINUED)

(d)

500X Aluminum X-Ray Map

500X Silicon X-Ray Map

FIGURE III-13. (CONTINUED)

X-Ray Diffraction

The X-ray diffraction measurements are summarized in Figures III-14 through III-17 for a coal pellet (Pellet 36), a limestone pellet (Pellet 17), an unburned 70/30 pellet (Pellet 78), and a 70/30 pellet (Pellet 37) that was burned for 20 minutes in the fixed-bed reactor. A peak analysis was performed only for Pellet 37. The identified compounds in the burned pellet were CaO, $CaSO_4$ (anhydrite), $Ca(OH)_2$, MgO, and $CaFeO_2$, indicating that the predominant sulfur containing compound is $CaSO_4$.

Further use of x-ray diffraction techniques should be quite valuable for studying the kinetics of the solid-state reactions in the coal/limestone pellets, although the relative insensitivity of x-ray diffraction will be troublesome.

Description of Mathematical Model

The pellet burning and sulfur capture model is based on a spherical approximation represented by the three coupled partial differential equations given below. The O_2 concentration distribution in the spherical pellet is given by

$$D_1 \left(\frac{\partial^2 C_1}{\partial r^2} + \frac{2}{r} \frac{\partial C_1}{\partial r} \right) - k_s' C_3 C_4 \sqrt{C_1} = \varepsilon \frac{\partial C_1}{\partial t} \tag{1}$$

with the SO_2 concentration given by

$$D_3 \left(\frac{\partial^2 C_3}{\partial r^2} + \frac{2}{r} \frac{\partial C_3}{\partial r} \right) - k_s' C_3 C_4 \sqrt{C_1} = \varepsilon \frac{\partial C_3}{\partial t} \tag{2}$$

and the CaO concentration distribution by

$$\frac{\partial C_4}{\partial t} = - k_s' C_3 C_4 \sqrt{C_1} \quad . \tag{3}$$

where

C_1 = O_2 concentration, moles/cm^3
C_3 = SO_2 concentration, moles/cm^3
C_4 = CaO concentration, moles/cm^3
D_1 = Effective diffusion coefficient for O_2 in pore structure, cm^2/sec
D_3 = Effective diffusion coefficient for SO_2 in pore structure, cm^2/sec

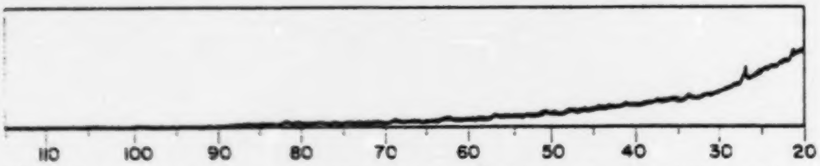

FIGURE III-14. Cu K_α RADIATION SCATTER OF UNBURNED COAL

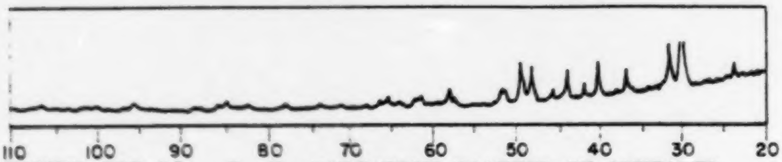

FUGIRE III-15. Cu K_α RADIATION SCATTER OF UNHEATED LIMESTONE

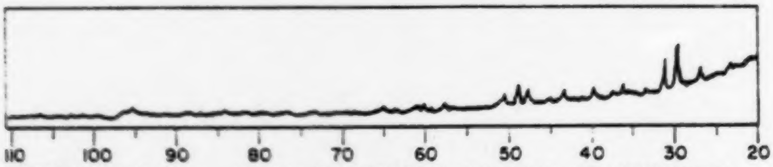

FIGURE III-16. Cu K_α RADIATION SCATTER OF UNBURNED 70/30 MIXTURE

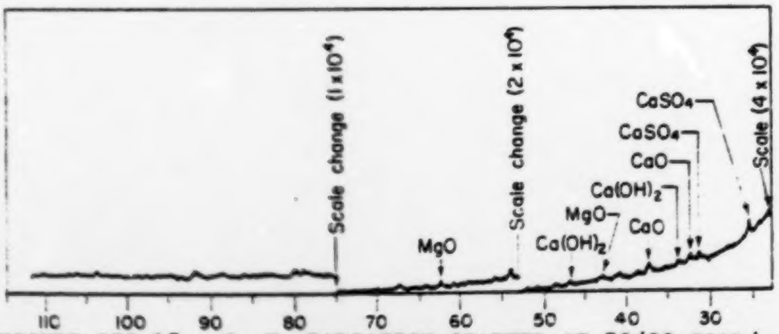

FIGURE III-17. Cu K_α RADIATION SCATTER OF 70/30 COAL/ LIMESTONE BURNED PELLET. MAJOR IDENTIFIED CONSTITUENTS CaO (LIME), $CaSO_4$ (ANHYDRITE)

k_s' = SO_2 capture rate constant, $cm^{9/2}/mole^{3/2}\cdot sec$

ε = pellet porosity.

The mechanism for the SO_2-CaO reaction is based on the work of Wen and Assciates.(III-11, III-12) The initial conditions assumed are

1. $C_1(r,o) = C_1^\circ$ $\quad r=R$
   $= o$ $\quad o \leq r < R$
2. $C_3(r,o) = o$ $\quad o \leq r \leq R$
3. $C_4(r,o) = C_4^\circ$ $\quad o \leq r \leq R$

where R is the radius of the sphere. The boundary conditions are:

1. At the surface of the pellet, r=R

$$C_1(R,t) = C_1^\circ$$
$$C_3(R,t) = o$$

2. At the surface of the combustion zone in the pellet (the moving boundary) the conditions are:

$$D_1 \left(\frac{\partial C_1}{\partial r}\right)_{r_c,t} = -k_s C_1(r_c,t) C_2(r_c,t)$$

$$D_3 \left(\frac{\partial C_3}{\partial r}\right)_{r_c,t} = -f_3 k_s C_1(r_c,t) C_2(r_c,t) \quad .$$

The latter equation gives the production rate of SO_2 at the moving boundary where

$r_c = r_c(t)$ = instantaneous radius of moving boundary, cm

k_s = burning rate constant, $cm^4/moles\cdot sec$.

f_3 = weight fraction of sulfur in solid.

The moving boundary position is determined by the expression

$$C_2(r_c,t) \frac{dr_c}{dt} = -D_1 \left(\frac{\partial C_1}{\partial r}\right)_{r_c,t}$$

with $r_c(o) = R$.

A numerical computer analysis was developed to solve the above system of equations. Details on development of the numerical procedures are given in Appendix A along with a brief description of the computer program and its input format.

The model contains several assumptions that may limit its accuracy. These assumptions are:

- Heat-transfer effects and internal heat generation are negligible
- The rather simple chemical mechanisms assumed in the model are adequate
- The calcination reaction is instananeous
- Use of a spherical geometry is adequate to simulate the pellets which are cylindrical in shape.

Of the four major assumptions, the one neglecting heat transfer is probably the most critical. All these assumptions can be refined, however, by further extensions of the present model.

To facilitate the preliminary analysis of data from the fixed-bed reactor experiments, a simplified version of the above model was derived. The simplified model is based on the assumptions that:

- The steady-state approximation is valid
- The change in the CaO content due to sulfur capture is negligible
- The oxygen dependency of the SO_2 capture reaction can be represented by an average constant O_2 concentration.

The burning rate constant, k, is expressed as

$$k,\ \text{cm/sec} = \alpha k_s \quad .$$

SO_2 capture and mass transport in the pellet are represented by

$$\frac{d^2C_3}{dr^2} + \frac{2}{r}\frac{dC_3}{dr} = \frac{K}{D_3} C_3$$

with the boundary conditions

$$C_3 = C_3^\circ \text{ at } r = R$$

and

$$D_3 \left(\frac{dC_3}{dr}\right)_{r_c} = -\beta k C_1$$

where

K = SO_2 capture rate constant, sec^{-1}

β = stoichiometric coefficient, $\frac{\text{moles S}}{\text{moles } O_2}$

O_2 consumption is represented by

$$\frac{d^2C_1}{dr^2} + \frac{2}{r}\frac{dC_1}{dr} = o \qquad r_c<r<R$$

with

$$C_1 = C_1^\circ \text{ at } r = R$$

and

$$D_1 \left(\frac{dC_1}{dr}\right)_{r_c} = kC_1 \text{ at } r = r_c \quad .$$

The velocity of the moving boundary is given by

$$-D_1 \left(\frac{dC_1}{dr}\right)_r = \alpha \frac{dr_c}{dt}$$

where

$\alpha = a\ C_s$

a = stoichiometric coefficient, moles O_2/moles C_s

C_s = concentration of solid combustible, moles C_s/cm^3.

The above equations can be solved to give the burning time

$$t\text{,sec} = \left(\frac{\alpha R}{kC_1^\circ} + \frac{\alpha R^2}{6D_1C_1^\circ}\right) - \frac{\alpha R}{kC_1^\circ}\left(\frac{r_c}{R}\right) - \frac{\alpha R^2}{2D_1C_1^\circ}\left(\frac{r_c}{R}\right)^2 + \frac{\alpha R^2}{3D_1C_o}\left(\frac{r_c}{R}\right)^3 \quad , \quad (4)$$

the oxygen consumption rate

$$U = \frac{4\pi D_1C_1^\circ}{\left(1 + \frac{D_1}{kr_c}\right)\frac{1}{r_c} - \frac{1}{R}} \text{, moles/sec} \quad , \qquad (5)$$

and the sulfur release rate from the pellet

$$W = 4\pi R^2 D_3 \left[\frac{2\delta_1}{R}\sqrt{\frac{K}{D_3}}\ e^{-\sqrt{\frac{K}{D_3}}\,t} - C_3^\circ\left(\sqrt{\frac{K}{D_3}} - \frac{1}{R}\right)\right] \text{, moles/sec} \quad (6)$$

with

$$\delta_1 = \frac{RC_3^\circ\left(\sqrt{\frac{K}{D_3}} - \frac{1}{r_c}\right) e^{-\sqrt{\frac{K}{D_3}}\,R}\, e^{\sqrt{\frac{K}{D_3}}\,r_c} + \frac{r_c\beta k}{D_3}\,\delta_2}{\left(\sqrt{\frac{K}{D_3}} - \frac{1}{r_c}\right) e^{-2\sqrt{\frac{K}{D_3}}\,R}\, e^{\sqrt{\frac{K}{D_3}}\,r_c} + \left(\sqrt{\frac{K}{D_3}} + \frac{1}{r_c}\right) e^{-\sqrt{\frac{K}{D_3}}\,r_c}}$$

$$\delta_2 = \frac{C_1^\circ D_1}{kr_c^{\,2}\left[\left(1 + \frac{D_1}{kr_c}\right)\frac{1}{r_c} - \frac{1}{R}\right]}$$

$C_3 = C_3^\circ$ at $r = R$ for $t \geq o$.

A program based on the above equations was written for a Hewlett-Packard 9825A calculator for use in analyzing data from the fixed-bed reactor experiments. Details on the application of the simplified model to the experiments are covered in the following section.

MODELING ANALYSIS OF PELLET COMBUSTION DATA

Results of the chemical analyses on the burned pellets from the fixed-bed reactor experiments are summarized in Tables III-21 and III-22. These results are also presented in Figures III-18 and III-19 for better visualization of the data. Data scatter is quite high and as a result the curves in these figures were drawn subjectively. The burning rate for the 50/50 pellets appears to be faster than for the 70/30 pellets, which is consistent with the gas-analyzer data from Runs 101 and 104. However, the chemical-analysis data indicate that sulfur retention is higher with the 70/30 pellets, which would not be expected since the 50/50 pellets contain more limestone. Nor is this in agreement with the gas-analyzer data, which showed the 50/50 pellets retain more sulfur than the 70/30 pellets (see Table III-20). The reason for this inconsistency is not understood at this time.

TABLE III-21. SUMMARY OF RESULTS OF THE CHEMICAL ANALYSES ON 50 W/O COAL/50 W/O LIMESTONE PELLETS FROM FIXED-BED REACTOR EXPERIMENTS

Burn Time, Min.	Pellet No.	Pellet Weight Loss, %	Sulfur Retained,[a] %	Carbon Burned,[a] %
0	81	0	100	0
4	60	58.4	63.5	72.9
6	63	62.1	71.1	81.0
6	61	61.2	--	--
12	66	66.3	67.1	98.2
14	69	67.7	64.3	99.6
22	57	67.9	55.5	99.8

(a) Based on the use of the ash content as a constant reference for calculations.

TABLE III-22. SUMMARY OF RESULTS OF THE CHEMICAL ANALYSES ON 70 W/O COAL/30 W/O LIMESTONE PELLETS FROM FIXED-BED REACTOR EXPERIMENTS

Burn Time, Min.	Pellet No.	Pellet Weight Loss, %	Sulfur Retained, %	Carbon Burned,(a) %
0	80	0	100	0
5	42	60.9	67.3	59.4
5	40	58.0	69.4	65.9
10	52	66.5	69.7	76.1
10	73	67.8	74.0	80.8
11	45	72.7	--	--
15	48	72.7	64.9	99.6
20	51	72.3	62.8	99.9

(a) Based on the use of the ash content as a constant reference for calculations.

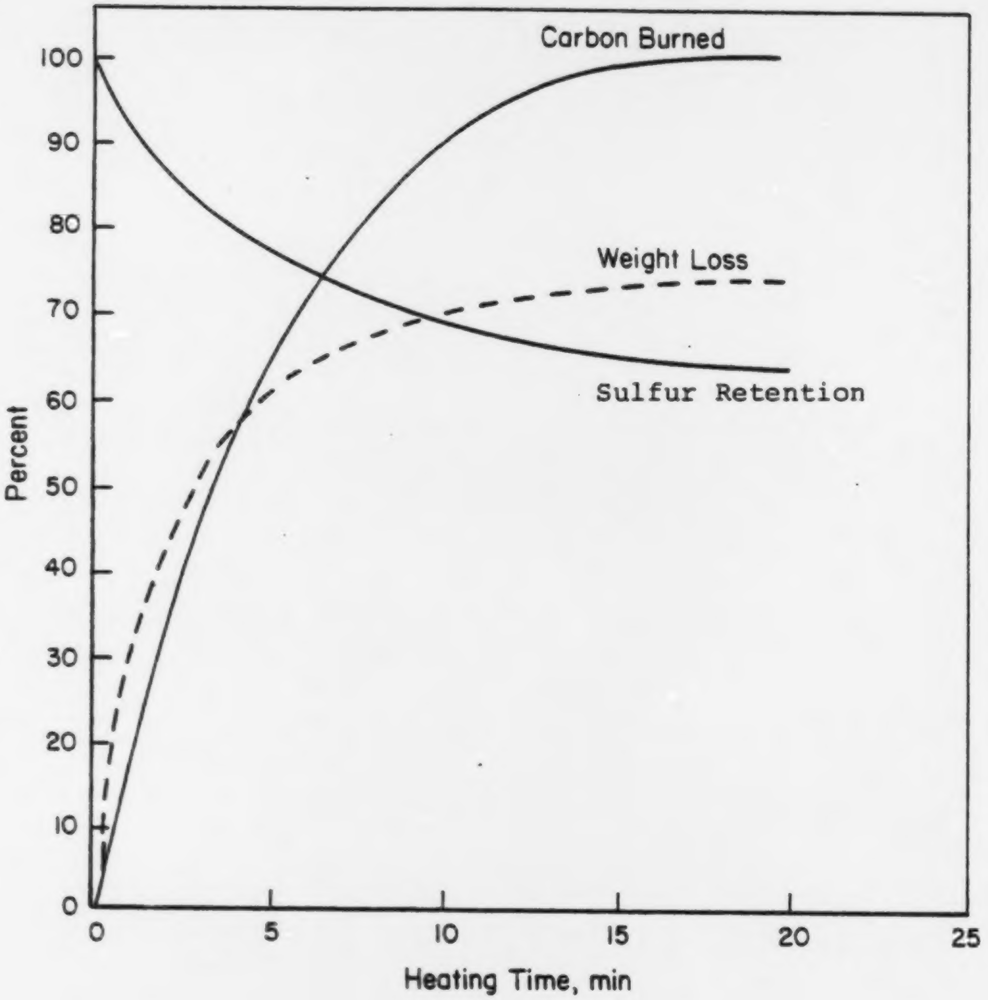

FIGURE III-18. SUMMARY OF RESULTS OF THE CHEMICAL ANALYSES ON 50 WEIGHT PERCENT COAL/ 50 WEIGHT PERCENT LIMESTONE PELLETS FROM FIXED BED REACTOR EXPERIMENTS

(Data from Table 8)

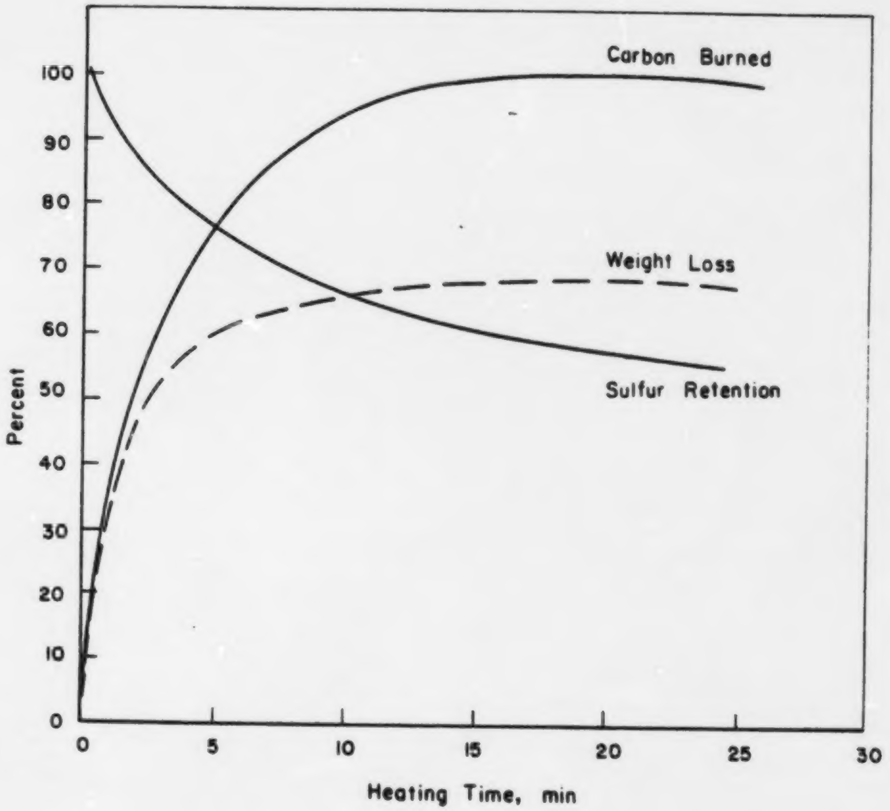

FIGURE III-19. SUMMARY OF RESULTS OF THE CHEMICAL ANALYSES ON 70 WEIGHT PERCENT COAL/ 30 WEIGHT PERCENT LIMESTONE PELLETS FROM FIXED BED REACTOR EXPERIMENTS

(Data from Table 9)

The chemical analysis data and dimensional measurements for the limestone pellets heated in the fixed-bed reactor are given in Table III-23. The data show a decrease in pellet diameter with heating and indicate that calcination is nearly complete within 6 minutes. This is not consistent with the gas-analyzer data, which show significant release of CO_2 after 6 minutes. This difference and the fact that the analyzer data gave a higher integrated CO_2 release value are also unexplained at this time.

Determination of Rate Constants

Burning rate data from the metallographic measurements on 50/50 pellets are presented in Table III-24. The 70/30 pellets disintegrated to the extent that it was not possible to obtain similar data. The data from Table III-24 were correlated with the burning-rate expression given by Equation (5) for the simplified model. A calculated burning velocity curve based on the derived constants is shown in Figure III-20 along with a curve calculated for the 70/30 pellet based on a burning time of 20 minutes. The calculations are based on an effective spherical pellet radius, R, equal to 0.635 cm, the radius of a sphere having the same surface-to-volume ratio as a right circular cylinder with a diameter and height of 12.7 mm. Temperature was assumed to be 1040 C. Assuming appropriate physical constants, the values of the burning rate constant and the diffusion coefficient for oxygen diffusion in the ash were calculated. Using the same burning-rate constant, the analysis was also repeated to determine the oxygen diffusion coefficient for the 70/30 pellet. The results were then incorporated into the simplified SO_2 release equation, Equation (6), with the value of K, the SO_2 capture rate constant, selected to give the levels of sulfur capture determined by the gas analyzer results. The values of the constants used in the calculations and the results are given in Table III-25. It was impossible to obtain a valid SO_2 capture rate for the 70/30 pellet that corresponded to 68.7 percent sulfur retention by the pellet. For a range of reasonable variables, the model predicts a sulfur capture in excess of 80 percent, just under that calculated for the 50/50 pellet. The model is extremely sensitive to the values of the constants, and small uncertainties in the data can produce large variations in the

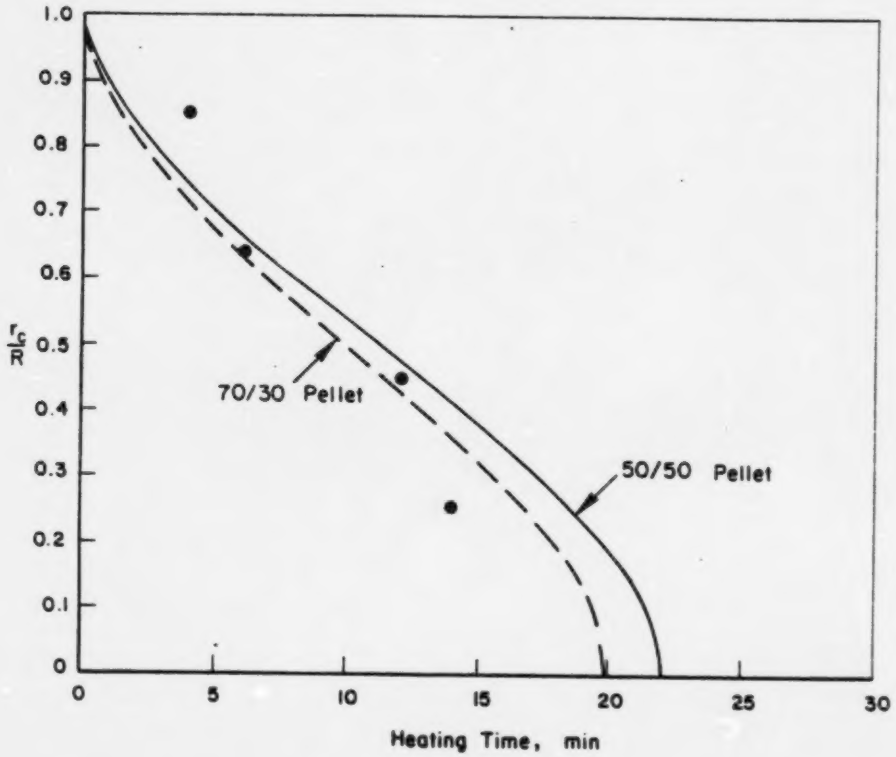

FIGURE III-20. UNBURNED CORE RADIUS AS A FUNCTION OF BURNING TIME CALCULATED USING SIMPLIFIED MODEL (Data Points Represent Measurements on 50/50 Pellets)

TABLE III-23. SUMMARY OF CHEMICAL ANALYSES AND PHYSICAL MEASUREMENTS ON THE LIMESTONE PELLETS FROM THE FIXED-BED REACTOR EXPERIMENTS

Pellet No.	Heating Time, Min.	Pellet Diameter After Heating, In.	Weight Change[(a)] %	Total CO_2 Released, %
17	0	0.506	0	0
14	6	0.501	48.3	95.7
11	12	0.494	46.2	88.4
7	18	0.498	43.9	99.1
4	31	0.496	47.4	98.7

(a) The weight change for complete calcination of $CaCO_3$ would be 44 percent.

TABLE III-24. SUMMARY OF BURNING RATE MEASUREMENTS FOR 50 W/O COAL/50 W/O LIMESTONE PELLETS BASED ON METALLOGRAPHIC STUDIES

Pellet No.	Burning Time, Min.	Relative Burning Interface Radius, r_c/R
72	0	1
59	4	0.75
62	6	0.64
65	12	0.44
68	14	0.25
56	22	0

TABLE III-25. SUMMARY OF CALCULATIONS USING SIMPLIFIED MODEL

	50 w/o Coal/50 w/o Limestone Pellet	70 w/o Coal/30 w/o Limestone Pellet
Constants		
R,cm	0.635	0.635
Temperature, °F	1900	1900
C_1^o, moles O_2/cm^3	1.84×10^{-6}	1.84×10^{-6}
C_3^o, moles SO_2/cm^3	0	0
α, moles O_2/cm^3	6.11×10^{-2}	6.74×10^{-2}
β	2.07×10^{-2}	1.83×10^{-2}
ε, (ash porosity)	0.66	0.73
Derived Rate Coefficients		
K, cm/sec	3.5×10^2	3.5×10^2 (b)
K, sec^{-1}	2.6×10^1 (a)	(c)
D_1, cm^2/sec	1.77	2.17
D_2, cm^2/sec	1.17	1.43

(a) Based on a sulfur retention of 86.2%.

(b) Assumed value.

(c) Would not correlate with the measured sulfur retention of 68.7%.

results. The relation of diffusion rates to porosity was determined using the effective diffusion constants for the 50/50 and 70/30 pellets and the relationship

$$D_e = \varepsilon^n D_t$$

where D_e is the effective diffusion coefficient, ε is the porosity, and D_t is the true diffusion coefficient. For oxygen diffusion, n was determined as 2.28 with the true diffusion coefficient for oxygen equal to 4.5 cm^2/sec. The value for n corresponds to those observed by Wen and Chuang(III-8) for coal ash. The true value of the diffusion coefficient for O_2 seems somewhat high but may indicate higher temperatures in the pellets, possibly nearer 1470 C. The value of K also matches very closely with values reported by Field, et al.(III-9) The value of K for the 50/50 case is considerably smaller than would be anticipated from the results of Wen, et al (III-11, III-12) with pure limestone. This may not be unreasonable, though because of the presence of the coal ash and other impurities in combination with the limestone in the pellets.

Using the derived data for the 50/50 pellet in Equation (6), the SO_2 release rate and the concentration of SO_2 as it would be measured by the TECO analyzer was calculated. These results (Figure III-21) show the same characteristics as the actual experimental curves, however, experimental response times initially seem to lag behind the calculated response. This may be due to heat-transfer effects, which are discussed below. Oxygen consumption calculated from Equation (5) for the 50/50 and 70/30 pellet compositions is presented in Figure III-22.

To illustrate the predictive capabilities of the simplified model, calculations shown in Figures III-23 and III-24 were made to estimate sulfur retention and burning time as a function of pellet diameter, and burning time as a function of temperature for a 50/50 pellet. The burning rate constant used for the calculations in Figure III-24 was

$$k = C_1^\circ A\, T\, e^{-\frac{17,967}{T}} \ \text{cm/sec}$$

where the temperature dependency was based on the work of Field, et al.(7) In the above equation, A was determined to be 1.3×10^{11} using the rate constant

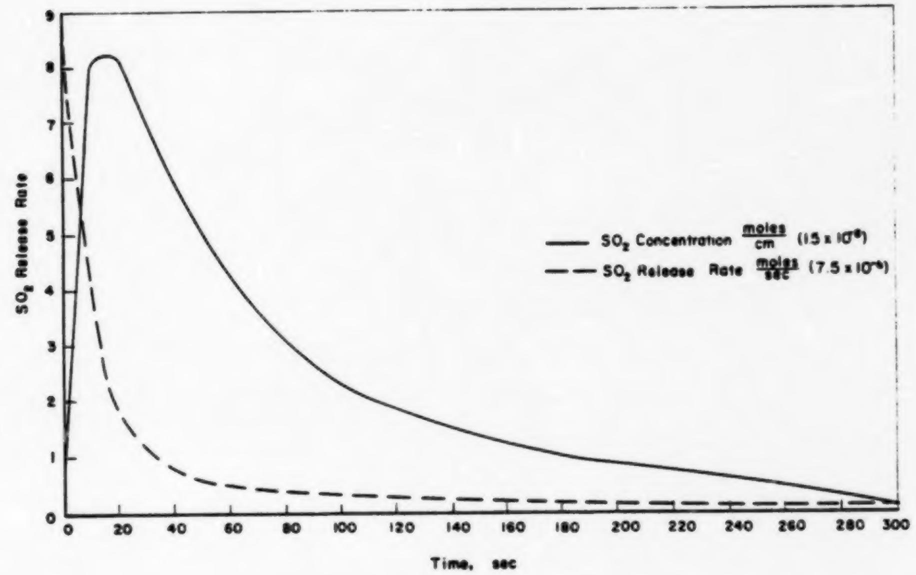

FIGURE III-21. SO$_2$ RELEASE RATE AND CALCULATED TECO ANALYZERS BASED ON THE SIMPLIFIED MODEL (EQUATION 7) FOR 50 WEIGHT PERCENT COAL/50 WEIGHT PERCENT LIMESTONE PELLET

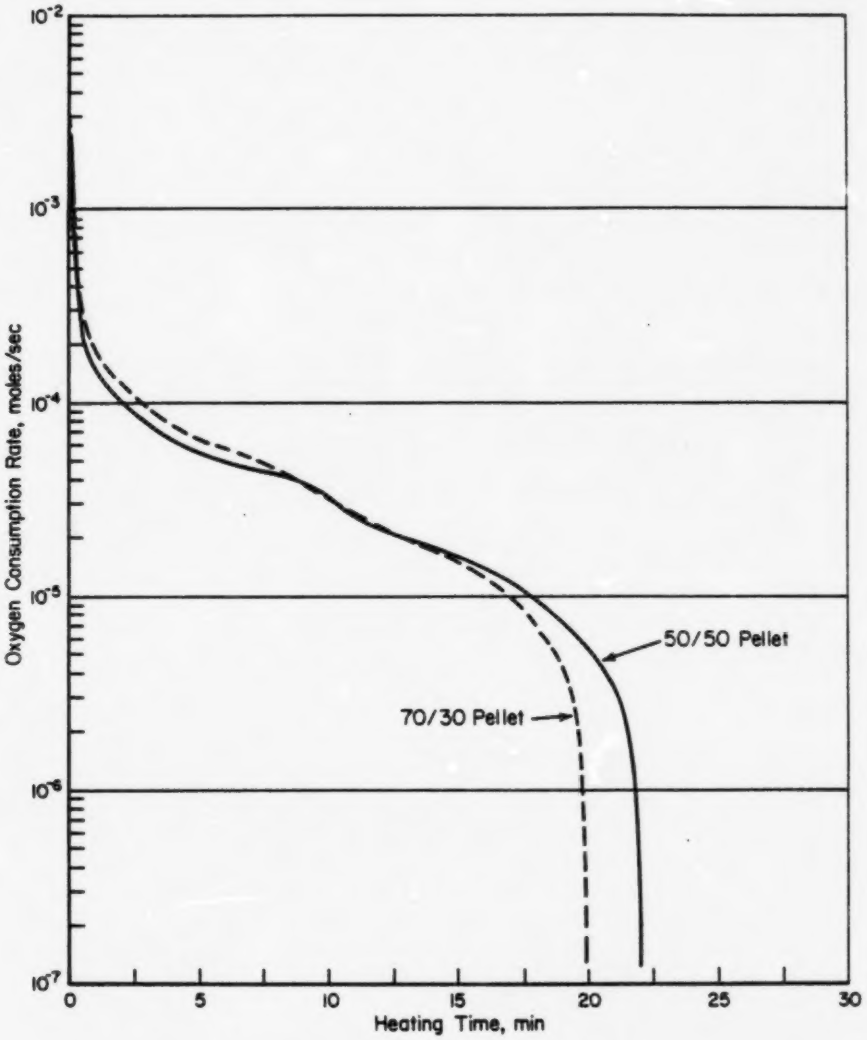

FIGURE III-22. OXYGEN CONSUMPTION RATES CALCULATED USING SIMPLIFIED MOEDL

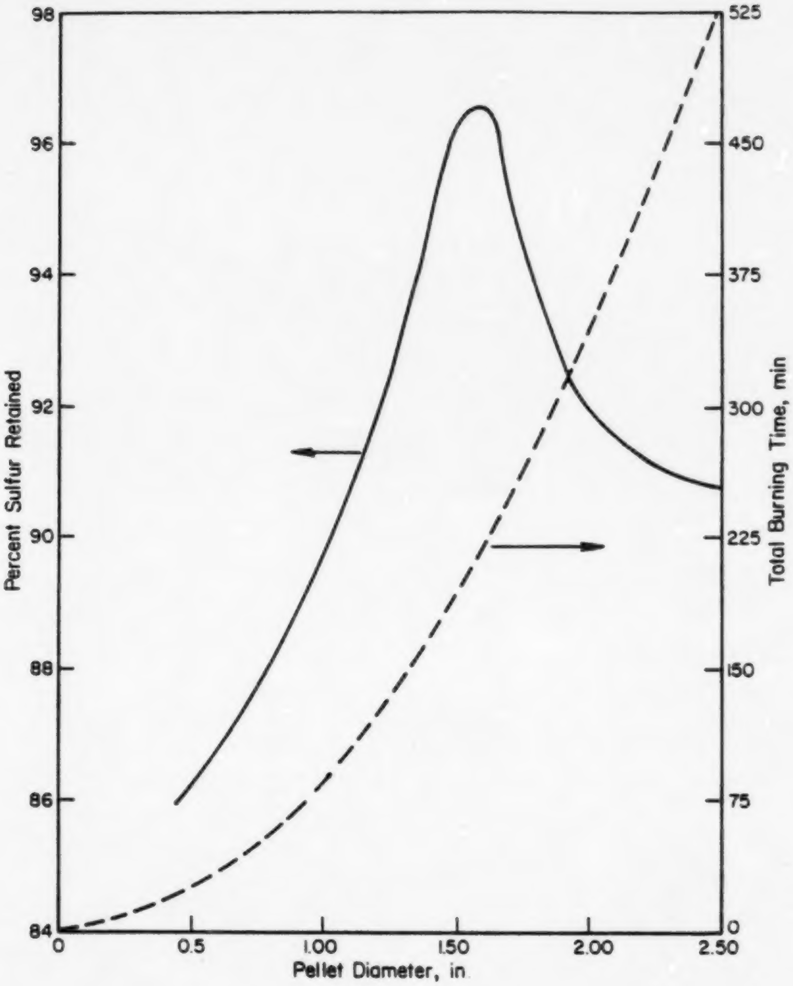

FIGURE III-23. SULFUR RETENTION AND BURNING TIME FOR 50 WEIGHT PERCENT COAL/50 WEIGHT PERCENT LIMESTONE PELLET CALCULATED AS A FUNCTION OF PELLET DIAMETER USING THE SIMPLIFIED MODEL

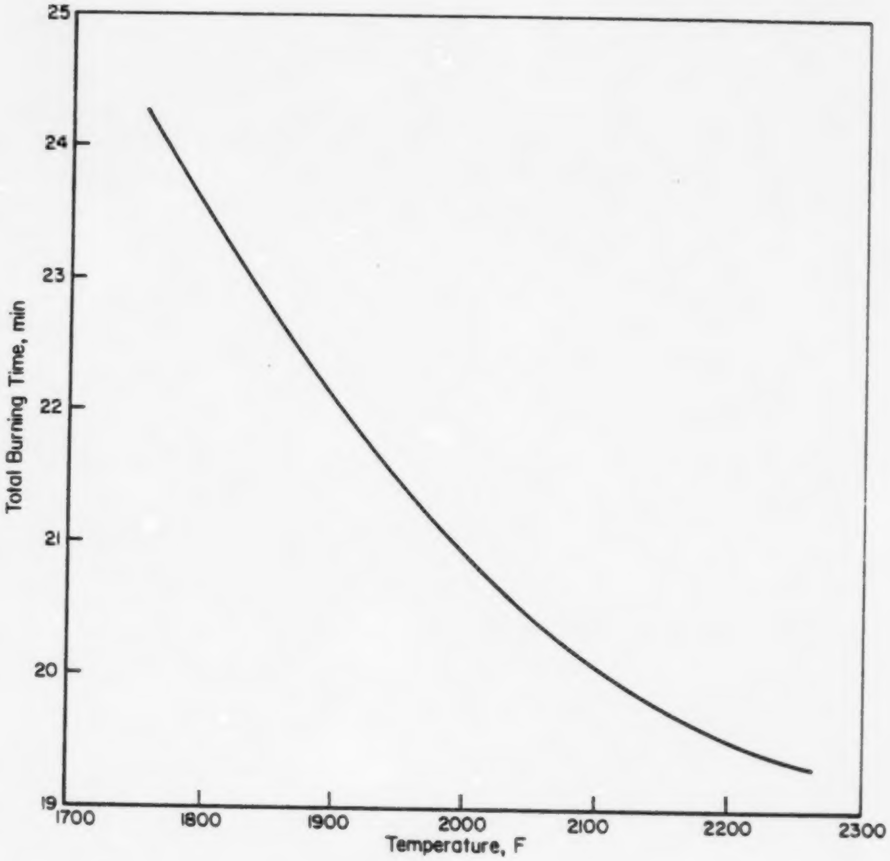

FIGURE III-24. BURNING TIME FOR 50 WEIGHT PERCENT COAL/ 50 WEIGHT PERCENT LIMESTONE PELLET CALCULATED AS A FUNCTION OF TEMPERATURE USING THE SIMPLIFIED MODEL

determined for the 50/50 pellet assuming a temperature of 1040 C. T is the temperature in °K and C_1° is the oxygen concentration, as previously defined. The temperature dependency of the burning rate constant is very approximate and should be accurately determined through more detailed experiments than those reported here, if definitive conclusions are to be drawn about the performance characteristics of the pellets. An interesting conclusion from Figure III-23 is that there is an optimum diameter for sulfur retention. Sulfur retention reaches a maximum of about 96 percent for a pellet diameter of about 38 mm. A more detailed model or actual experiments may change this conclusion, but the effect of size and geometry probably merits further attention.

Transient Heat-Transfer Analysis

A simple transient heat-transfer analysis based on a treatment by Heisler(III-13) was performed to assess the effects of thermal lag on pellet combustion and SO_2 release. The results of the heat-transfer analysis are presented in Figures III-25 and III-26 for the 50/50 and 70/30 pellets, respectively. The calculations assumed a spherical pellet with a radius of 0.635 cm at an initial temperature of 21 C which is instantaneously introduced into a furnace at 1040 C. The surface temperatures of the two pellets respond at the same rate, with the center temperature of the 70/30 pellet lagging slightly behind that of the 50/50 pellet because of its lower thermal conductivity. The surface temperature of both compositions reached the furnace temperature in just over 1 minute, while the centers of the pellets required about 2-1/2 minutes to attain the furnace temperature of 1040 C. Heat generated by pellet combustion could increase the temperatures more rapidly and significantly increase the pellet temperatures over the furnace temperature while endothermic reactions, such as calcination of the limestone and devoletilization of the coal, will delay the temperature rise. A more detailed heat-transfer analysis would be required to examine these effects. The simplified analysis does indicate that initial heating effects could play an important role in pellet burning and SO_2 release. These effects are probably responsible for the deviation between the model prediction of SO_2 and the experimental gas-analyzer data. One of the next refinements in the model should be to include heat-transfer effects.

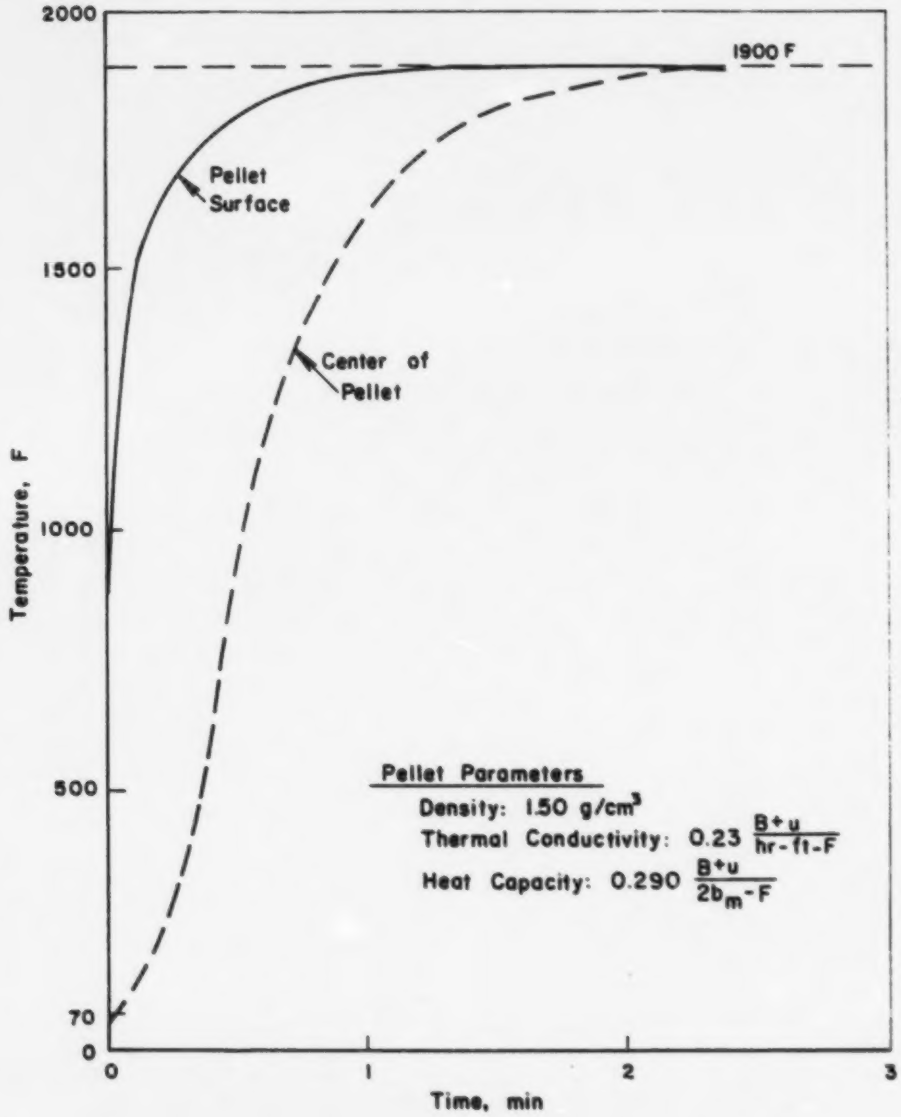

FIGURE III-25. TRANSIENT HEAT TRANSFER CALCULATIONS FOR A 70 WEIGHT PERCENT COAL/30 WEIGHT PERCENT LIMESTONE 13.7 MM DIAMETER SPHERICAL PELLET

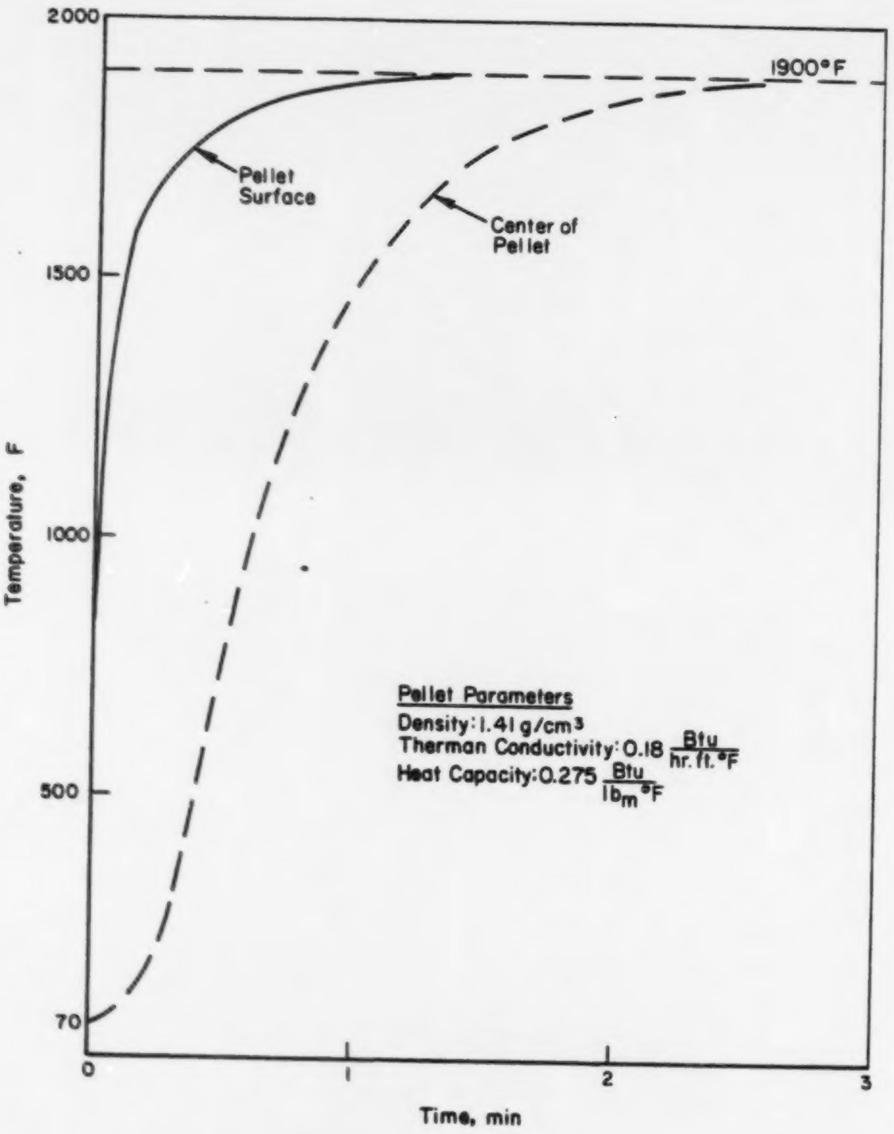

FIGURE III-26. TRANSIENT HEAT TRANSFER CALCULATIONS FOR A 50 WEIGHT PERCENT COAL/50 WEIGHT PERCENT 13.7 MM DIAMETER LIMESTONE SPHERICAL PELLET

Detailed Modeling Calculations

For economic reasons, computer calculations using the more detailed model were limited. Improvements still need to be made in the numerical analysis to decrease the computational time. An example of a calculation using the program is shown in Figures III-27 through III-32 for a 70/30 pellet at 1040 C. The following constants were employed in the calculations:

$$k_s = 3.5 \times 10^4 \frac{\text{cm}}{\left(\frac{\text{moles}}{\text{cm}^3}\right)\cdot\text{sec}}$$

$$k_s' = 4.5 \times 10^6 \frac{\text{cm}^{9/2}}{\text{moles}^{3/2}\cdot\text{sec}}$$

$C_4^\circ = 4.2 \times 10^{-3}$ moles C_a/cm^3

$C_1^\circ = 1.84 \times 10^{-6}$ moles O_2/cm^3

$C_5^\circ = 1.2 \times 10^{-2}$ moles S/cm^3

$C_2 = 1.0 \times 10^{-1}$ moles coal/cm^3

$f_3 = 1.19 \times 10^{-2}$

$D_1 = 2.17\ \text{cm}^2/\text{sec}$

$D_3 = 1.43\ \text{cm}^2/\text{sec}$

$R = 0.635$ cm

$\varepsilon = 1$

The curves for both SO_2 and O_2 appear to correspond roughly with the experimental measurements in Figures III-5 and III-7. Longer time calculations are needed, however, to accurately determine the validity of the model. The results obtained to date do indicate that extension of the model to include heat transfer and the effects of coal devolatilization would be appropriate.

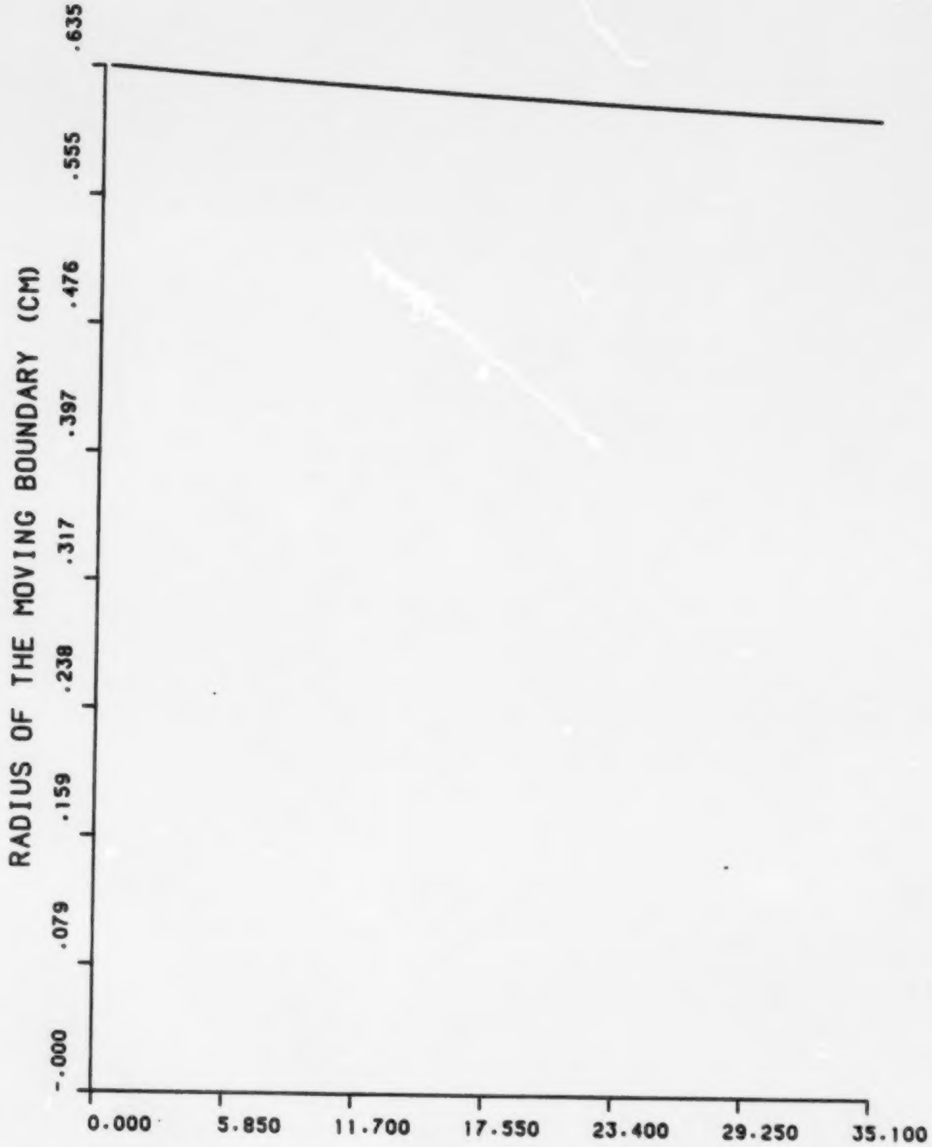

FIGURE III-27. CALCULATED COMBUSTION RATE FOR 70 WEIGHT PERCENT COAL/30 WEIGHT PERCENT LIMESTONE PELLET

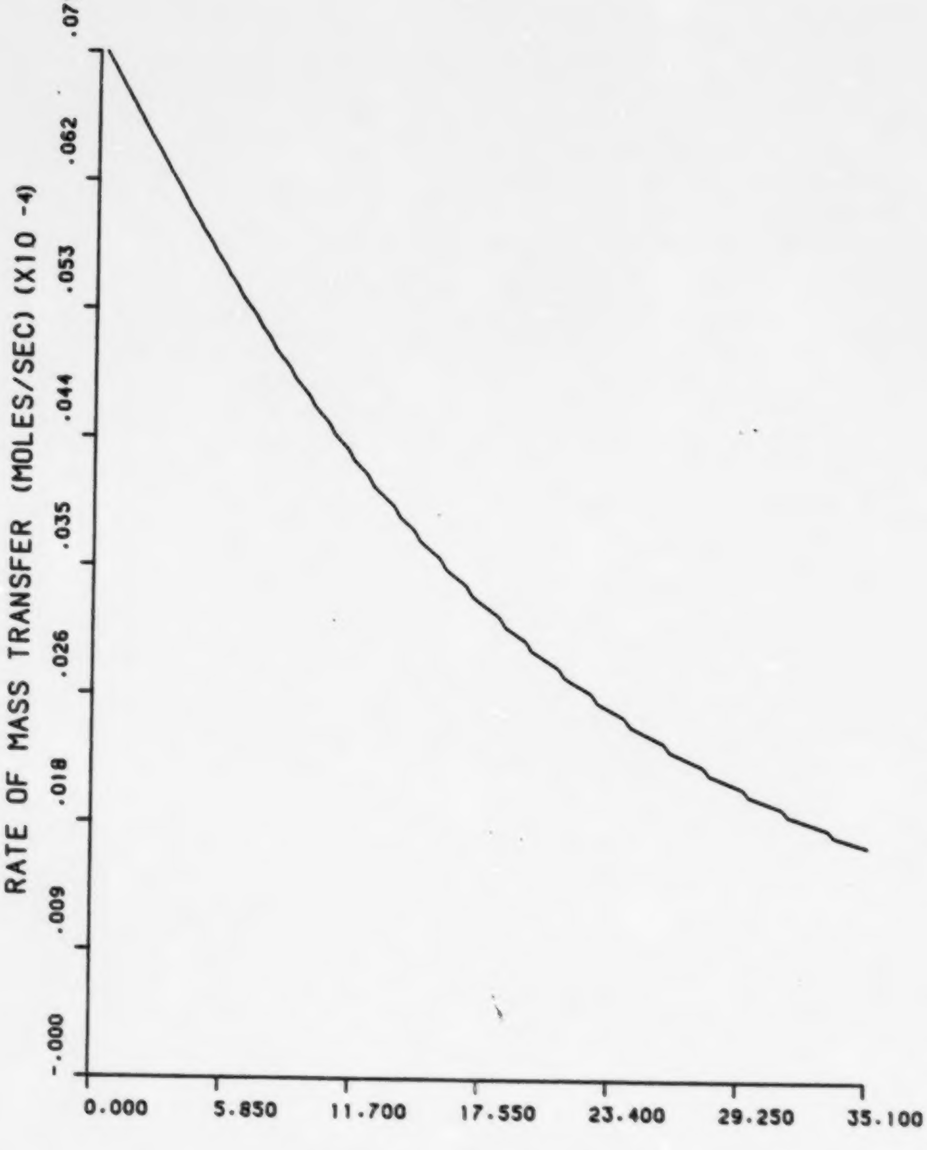

Time of Combustion (sec)

FIGURE III-28. CALCULATED SO_2 RELEASE RATE FOR 70 WEIGHT PERCENT COAL/30 WEIGHT PERCENT LIMESTONE PELLET

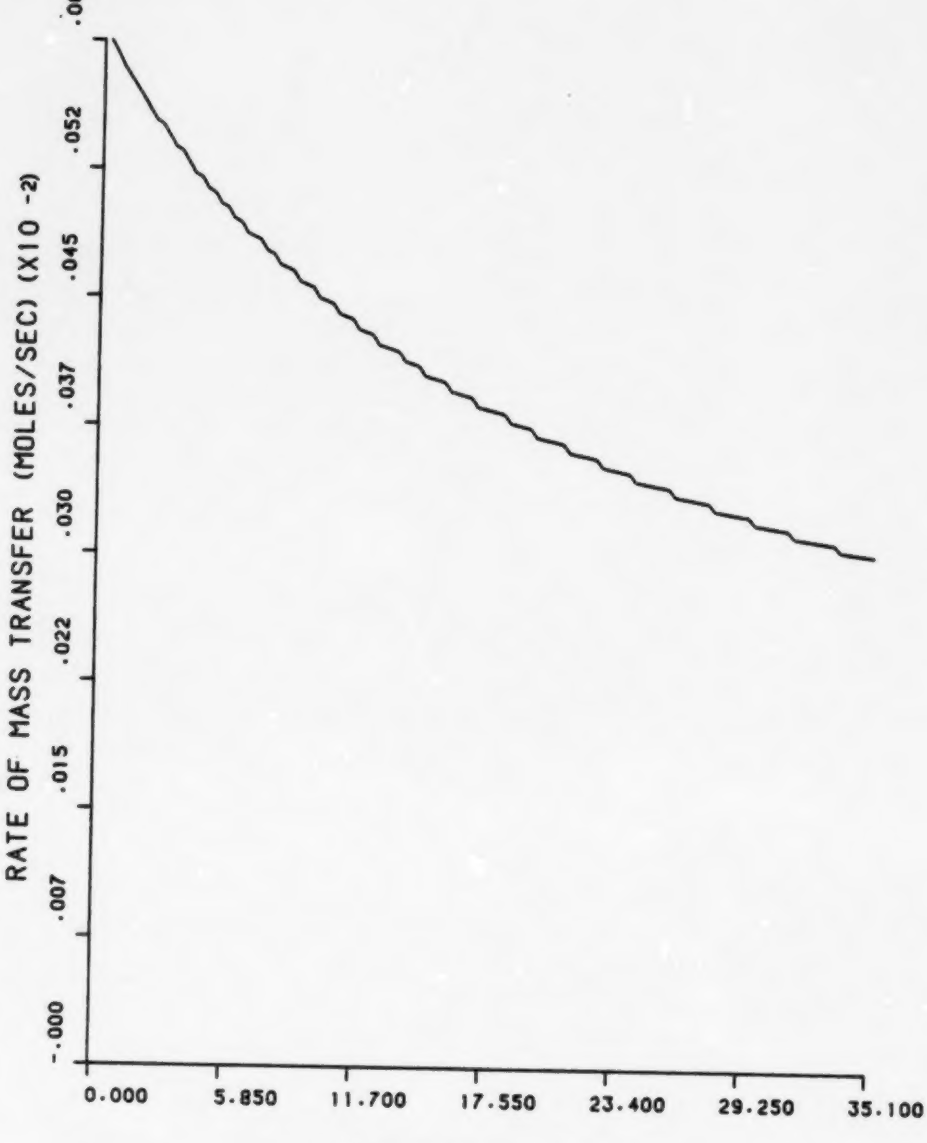

FIGURE III-29. CALCULATED O_2 CONSUMPTION RATE FOR 70 WEIGHT PERCENT COAL/30 WEIGHT PERCENT LIMESTONE PELLET

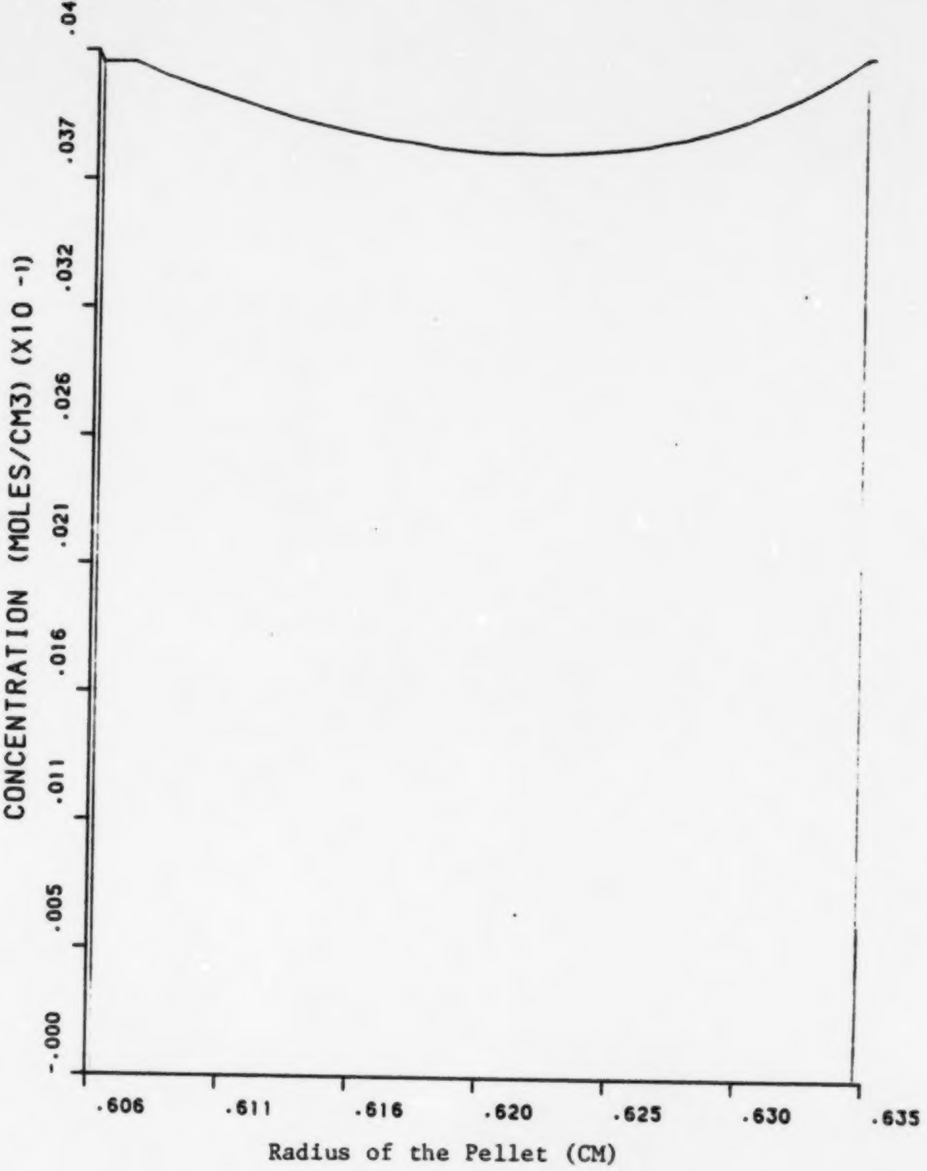

FIGURE III-30. CALCULATED CaO DISTRIBUTION AT 35.10 SEC IN 70 WEIGHT PERCENT COAL/30 WEIGHT PERCENT LIMESTONE PELLET

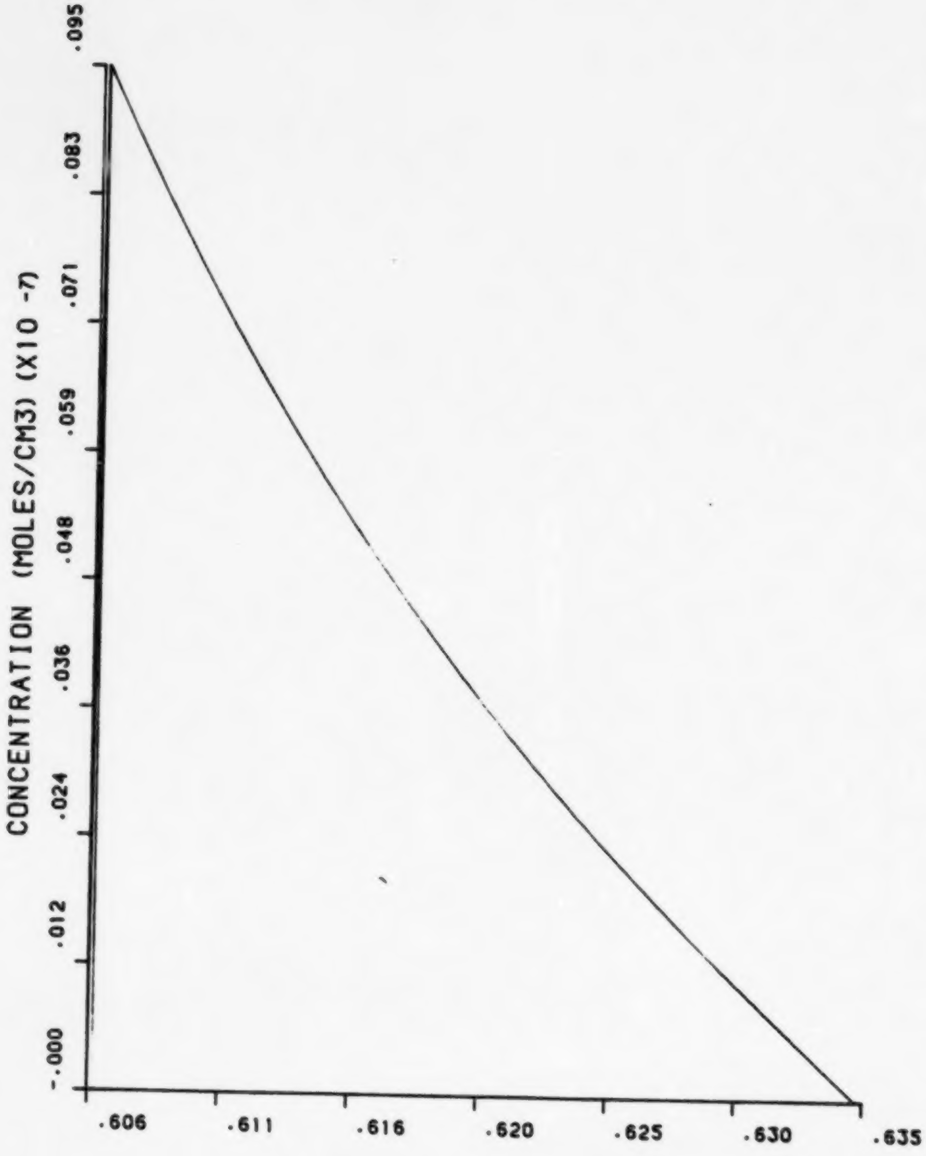

Radius of the Pellet (CM)

FIGURE III-31. CALCULATED SO_2 DISTRIBUTION AT 35.10 SEC IN 70 WEIGHT PERCENT COAL/30 WEIGHT PERCENT LIMESTONE PELLET

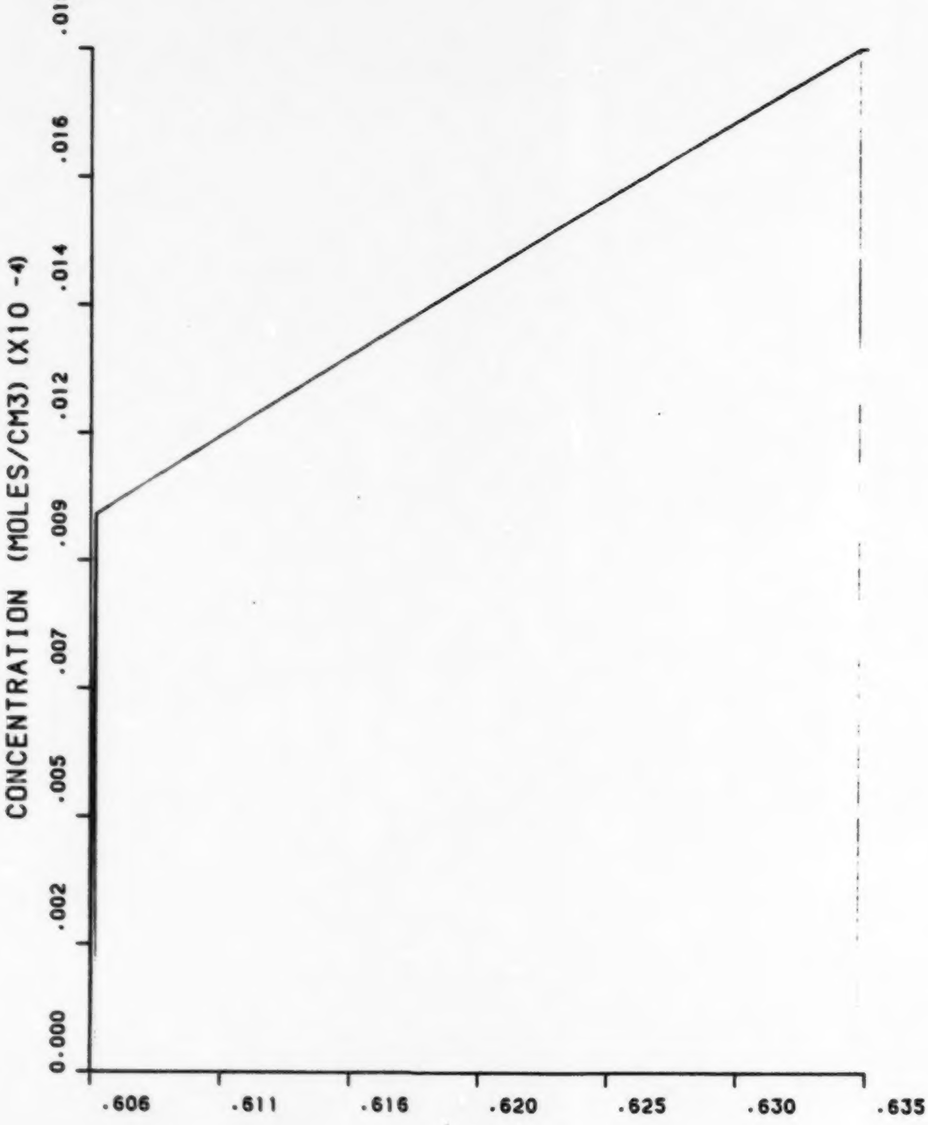

Radius of the Pellet (CM)

FIGURE III-32. CALCULATED O_2 DISTRIBUTION AT 35.10 SEC FOR 70 WEIGHT PERCENT COAL/30 WEIGHT PERCENT LIMESTONE PELLET

MODELING AND CHARACTERIZATION
SUMMARY AND CONCLUSIONS

The results of the preliminary modeling analysis and the pellet characterization studies described suggest that further study and optimization of coal/limestone pellets for sulfur capture offers potential benefits.

The simplified model developed for correlation of the experimental data approximates some of the performance characteristics of the pellets. For the range of calcium/sulfur ratios considered, the model indicates a weak dependency on this ratio, which is in line with observations. Also, the model predicts an optimum pellet size for maximum sulfur retention. This possibility should be given further attention.

Scanning electron microscopy and X-ray diffraction analysis are powerful tools for the study of the solid-state reactions in pellets. Results show that the captured sulfur in the burned pellets is tied up predominantly as $CaSO_4$. There is evidence that the sulfur may react directly with the limestone by solid-state processes that do not involve formation of SO_2.

Recomendations for further studies are:

- The present model should be extended to include heat-transfer effects, calcination, coal devolatilization, and solid-state reactions.
- Detailed experimental measurements should be made to determine SO_2-capture and burning rate constants as a function of temperature.
- Further information on the pore and ash structure of the pellets and its influence on the mass transport processes should be identified.
- The pellet burning model should be coupled with models of different boiler combustion systems to predict the interaction between pellet parameters and systems operating conditions.

SECTION III-5

LABORATORY EVALUATION

The promising pellet formulations identified during the mechanical strength and fixed-bed reactor experiments were evaluated in the model spreader-stoker boiler. This evaluation was based on gaseous emissions (primarily SO_2) and visual observations of the fuel bed. In addition, 18 Mg of the most promising pellet formulation were fired in the Battelle steamplant stoker. Criteria pollutants, visual observations, and ash analyses were used in these evaluations. Both facilities have been described in Parts I and II of this report.

MODEL SPREADER EXPERIMENTS

To supplement the fixed-bed reactor experiments, the model spreader-stoker boiler was used to evaluate the more promising pellet formulations. Compared to the fixed-bed reactor, the model spreader provides an improved simulation of the operation of an industrial stoker boiler and thus evaluates the fuel pellet more realistically.

Table III-26 presents the results of these experiments. In these experiments, the effect of Ca/S ratio (3.5 and 7), the four pellet production techniques, and binder type (cement and methylcellulose) were investigated. Additionally, for comparison, experiments were conducted with medium-S Kentucky coal, Illinois No. 6 coal, and the 50/50 pellets produced during Phase II. Prior to experimentation, the sampling system and procedures were modified to minimize any reactions that may occur in the sampling system.

TABLE III-26. MODEL-SPREADER STUDIES

Run No.	Fuel	Fuel Size, mm	Ca/S Ratio (Approx.)	Average SO_2,(a) ppm	Predicted SO_2, ppm	Average Stack Temp, C	Average Excess Air, percent	Average Sulfur Retention, percent	O_2, percent	CO_2, percent	CO, ppm
MS-20(b)	100/50 CPM pellets (Latex)	12.5 x 19	4	1370	3840	295	100	64	10.7	9.7	42
MS-31	50/50 CPM pellets (cement)	Ditto	7	1100	4020	340	100	73	11.0	10	55
MS-32	50/50 CPM pellets (cement)	Ditto	7	1040	3700	350	140	72	11.5 - 15.0	5.9 - 8.0	--
MS-33	70/30 CPM pellets (cement)	Ditto	3.5	1220	3700	360	110	67	10.0 - 13.8	NA	--
MS-34	Medium S Kentucky	--	0	1050	900	--	120	-15	9.5 - 19	8.2 - 10	150
MS-35	Illinois #6 Coal	--	0	4120	3700	340	95	-11	8.0 - 12.7	8.4 - 10.8	100
MS-36	50/50 CPM pellets (cement)	12.5 x 19	7	1240	3700	300	120	67	13.5	8.5	300
MS-37	Illinois #6 Coal	--	0	3700	3700	325	100	0	10.6	9.2	100
MS-38	70/30 CPM pellets (methocel)	12.5 x 19	3.5	1480	3700	335	90	60	9.5 x 11.5	8.0 - 11.2	150
MS-39	70/30 briquets (methocel)	12.5 x 25	3.5	1780	3700	365	80	52	8.2 - 9.8	10.8 - 11.6	85
MS-40	70/30 disc pellets (methocel)	12.5 dia	3.5	--	--	--	--	--	--	--	--
MS-41	70/30 extrusion (methocel)	--	3.5	1370	3700	375	60	63	7.4 - 9.2	10.8 - 12.6	90
MS-42	70/30 CPM pellets (methocel)	12.5 x 19	3.5	1260 (1220)(c)	3700	345	75	67	8.4 -10.2	10.4 - 12	50

(a) Normalized to 3 percent O_2.

(b) 1978 data.

(c) By Method 6.

Sampling System

The sampling system was a modification of that used during the Phase II experiments. An in-stack filter was used upstream of the water trap and the water trap was coupled as close to the stack as physically possible. Figure III-33 is a schematic of the modified sampling system.

Modifications were made to minimize the presence of water (especially water with calcium-laden particulates) in the sampling system that could remove SO_2. Provisions were also made to span the instruments by injecting calibration gases through the entire sampling system before, during, and after the experiments. This procedure indicated no loss of SO_2 in the sampling train at any time during the experiment.

A comparison of the model-spreader pellet data from the Phase III experiments with those from Phase I indicate that sulfur capture was not as great (about 10 to 15 percent lower) for the Phase III experiments. This small reduction may be attributed to the improved sampling system where precautions were taken to minimize sulfur capture in the sampling line. Because of the difficulty in obtaining a representative sample, sulfur retention based on SO_2 emission levels could not be verified from a sulfur analysis of the bed ash.

Ca/S Ratio

The fixed-bed reactor experiments indicated that the Ca/S ratio had little or no effect on sulfur capture for Ca/S ratios greater than 3.5. The model spreader data presented in Table III-26 confirm this observation. Visual observations indicated, as expected, that the pellets with less limestone (Ca/S = 3.5) burned more uniformly and rapidly than those with more limestone (Ca/S = 7).

Production Technique

Pellets using the same formulation consisting of Illinois No. 6 coal, limestone (Ca/S = 3.5), and methylcellulose binder, were prepared by the following production techniques:

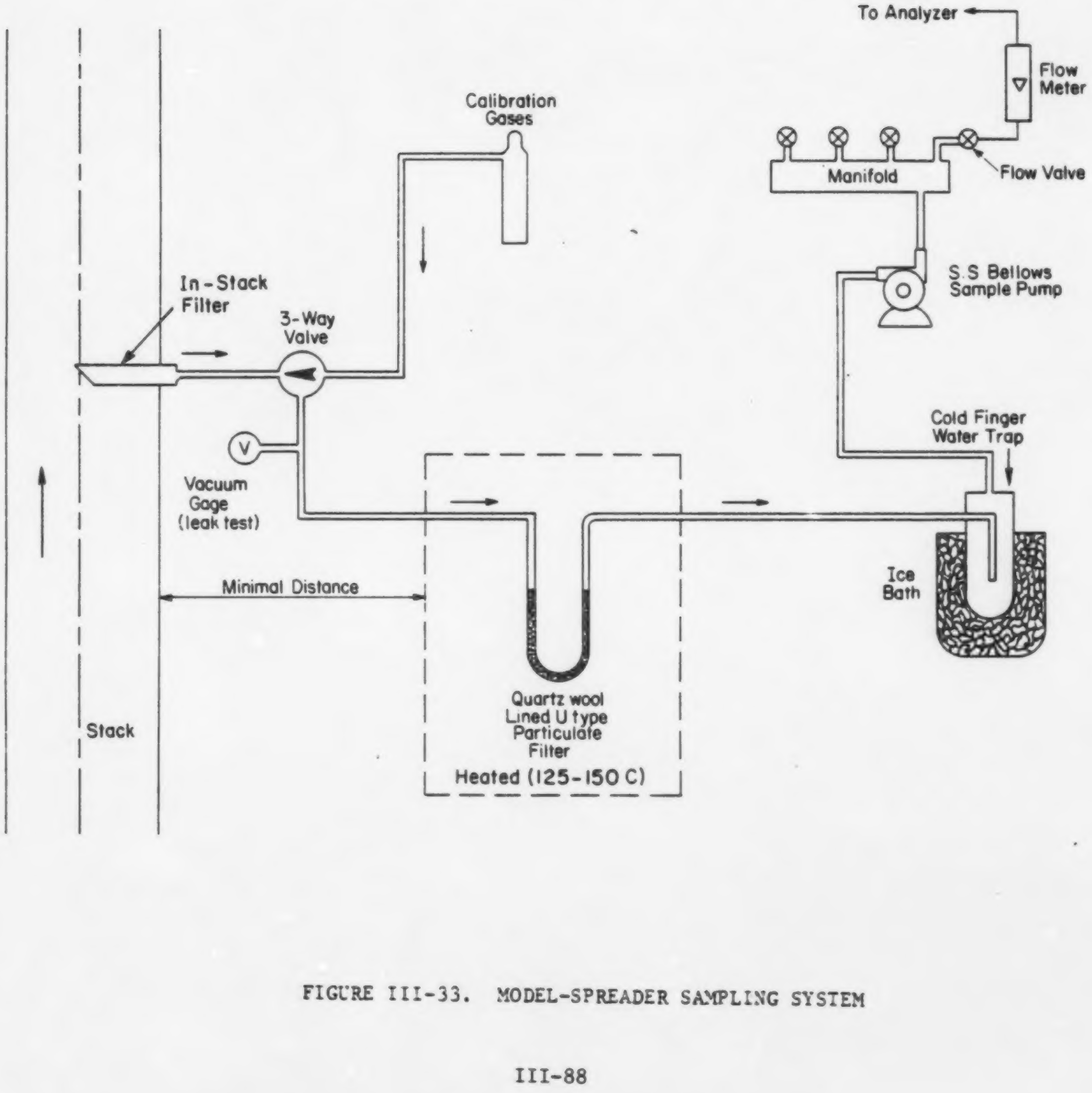
To Analyzer
Flow Meter
Calibration Gases
Manifold
Flow Valve
S.S Bellows Sample Pump
In-Stack Filter
3-Way Valve
V
Vacuum Gage (leak test)
Cold Finger Water Trap
Ice Bath
Minimal Distance
Quartz wool Lined U type Particulate Filter
Heated (125-150 C)
Stack

FIGURE III-33. MODEL-SPREADER SAMPLING SYSTEM

- Pellet mill (prepared by Battelle staff)
- Auger extrusion (prepared by Banner Industries)
- Disc agglomeration (prepared by Mars Mineral Corporation)
- Briquets (prepared by Evergreen Company).

The pellet-mill and auger-extruded pellets burned satisfactorily, having sulfur captures of 67 and 63 percent, respectively. The auger extruded pellets were observed to burn more uniformly than the pellet mill pellets perhaps because they were more porous (~1.0 g/cc compared to ~1.9 g/cc).

The briquetted formulations burned satisfactorily and showed relatively low sulfur retention (52 percent) -- a surprising and unexplained result. The disc agglomerated pellets were entirely unsatisfactory when fired in the model spreader. These pellets disintegrated in the combustion zone producing excessive amounts (greater than 50 percent) of fines. Such fines matted the bed causing nonuniform air distribution. Fuel-bed conditions degraded so rapidly that meaningful data could not be obtained.

Binder Type

Comparison of sulfur retention data of the auger-extruded and mill-pellets made with organic (methylcellulose) and inorganic (cement) binders indicated no significant difference. The binders are used in very small quantities (less than 4 percent) and do not have any catalytic effects. As a result, it appears that the type of binder does not significantly effect the combustion behavior of the pellet providing the physical properties of the pellet are retained. Cement-bound pellets with satisfactory physical properties could not be made by the disc agglomeration and briquetting methods.

STEAMPLANT STOKER DEMONSTRATION

Eighteen Mg of the limestone coal fuel pellets with a Ca/S molal ratio of approximately 3.5 were fired in the steamplant boiler. Two types of pellets were used--a lower density of (0.9 to 1.2 g/cc) pellet produced by Banner Industries using auger extrusion and a higher density pellet (~1.4 g/cc) produced by Alley-Cassetty Coal Company using a pellet mill. Both types of pellets were fired under a variety of boiler conditions. Evaluations were based on visual observations, criteria pollutants, and ash analyses.

PELLET PREPARATION AND PROPERTIES

Throughout Phase III, efforts were made to identify companies that could provide tonnage quantities of pellets to our specifications at no more than $1100/Mg, excluding grinding and raw material costs. Table III-27 identifies candidate tolling firms. Of these, only Banner Industries and Alley-Cassetty Coal Company could meet the criteria. Neither had on-sight grinding capabilities. The Illinois No. 6 coal was pulverized by Battelle and shipped with the necessary Piqua limestone and binders to the respective preparation sites.

Allbond 200 cornstarch and M-167 latex emulsion were used as binders, although this combination was not evaluated in the model spreader. These binders were readily available, while the methylcellulose binder previously used could not be procured in sufficient quantities in time for the demonstration. In addition, the mechanical-strength characterization tests and fixed-bed reactor experiments indicated that the Allbond and methylcellulose bound pellets were comparable.

The resulting pellet formulation (dry basis) consisted of:

67 percent Illinois No. 6 coal
30 percent Piqua limestone
2 percent Allbond 200 binder
1 percent M-167 latex binder.

These pellets were cylindrical, about 13 mm in diameter and 25- to 75-mm long. Table III-28 gives the proximate and ultimate analyses and also the ash-fusion temperature (initial deformation) for these pellets. Table III-29 gives the mineral analysis of the ash.

TABLE III-27. POTENTIAL TOLLING COMPANIES FOR LARGE QUANTITIES OF PELLETS(a)

Company	Location
Pro-Serve	Memphis TN
Stott Briquet & Carbon	Superior WI
Pelle Tech Corp.	Fontana CA
Pittsburgh Pacific Processing (Incomet/ Inco)	Pittsburgh PA
Alley Cassetey	Morgantown KY
Banner Industries	Bruceville IN
Helena Chemical Co.	Des Moines IA
Bethlehem Steel Corp. (Homer Research Labs)	Bethlehem PA
Mars Mineral Corp.	Valencia PA

(a) Based on Assumption I: material is preground elsewhere; and Assumption II: the tolling firm is now in business and has facilities, so that only some additional new equipment and modifications are required.

TABLE III-28. ULTIMATE, PROXIMATE, AND ASH-FUSION TEMPERATURE ANALYSES FOR LIMESTONE/COAL FUEL PELLET Ca/S = 3.5

Proximate Analysis (As received), %										Ash-Fusion Temperature, C	
										Initial Deformation	
Volatiles	Fixed Carbon	Moisture	Ash	C	H	N	S	O (difference)	Heating Value, KJ/g	Reducing	Oxidizing
42.9	21.8	2.15	33.2	47.0	3.2	.9	2.9	10.5	18.6	1500+	1500+

TABLE III-29. MINERAL ANALYSIS OF ASH

Compound	Percent Weight
Silica, SiO_2	14.20
Alumina, Al_2O_3	5.42
Titania, TiO_2	0.24
Ferric oxide, Fe_2O_3	7.10
Lime, CaO	51.88
Magnesia, MgO	6.94
Potassium oxide, K_2O	0.55
Sodium oxide, Na_2O	0.42
Sulfur trioxide, SO_3	10.77
Phos. pentoxide, P_2O_5	0.09
Strontium oxide, SrO	0.00
Barium oxide, BaO	0.01
Manganese oxide, Mn_3O_4	0.06
Undetermined	2.32
	100.00

The high CaO in the ash of the treated coal preclude the usual procedures for evaluating ash characteristics, which are limited to about 20 percent CaO. The excess CaO above that which will react with the other ash constituents, principally with SiO_2, to form a low-viscosity slag, provides a matrix of solid CaO particles. Thus, in the ASTM cone fusion determination, this matrix retains the original shape of the cone, probably even at temperatures above 1650 C, which explains the anomalous data on the "fusion temperature" of the ash.

The high CaO content physically interferes with flow of the fluid slag that would result with a smaller addition of CaO. For example, if the CaO content of typical Illinois No. 6 coal ash were increased to only 20 percent on a normalized basis, the resulting fluxed coal ash would have a viscosity of only 10 poise at 1430 C, comparable to that of castor oil at room temperature. With 60.7 percent CaO, the ash will behave as a solid rather than a liquid because of all the unreacted CaO.

The pellets remained sufficiently intact during storage and handling that an acceptable pellet was fed into the boiler. However, it was observed that some pellets softened during exposure to rain. Weatherability tests on these pellets were rerun showing approximately the same characteristics previously observed, i.e., no softening. It appears that the weatherability test used during pellet development has some limitations and that pellets will require some undercover storage or further formulation refinement for weatherproofing.

EXPERIMENTAL PROCEDURES

Experimental procedures were similar to those of Phase II experiments with modification of on-line gaseous monitoring. Gases from the combustion of pelletized coal were sampled as follows. First, a representative gas sample was continuously removed from the boiler outlet by placing a "rake" in the center of the first and second cyclone via an access port. Figure III-34 shows the relative location of the rake, boiler outlet, and cyclones. The sample port holes along the length of the

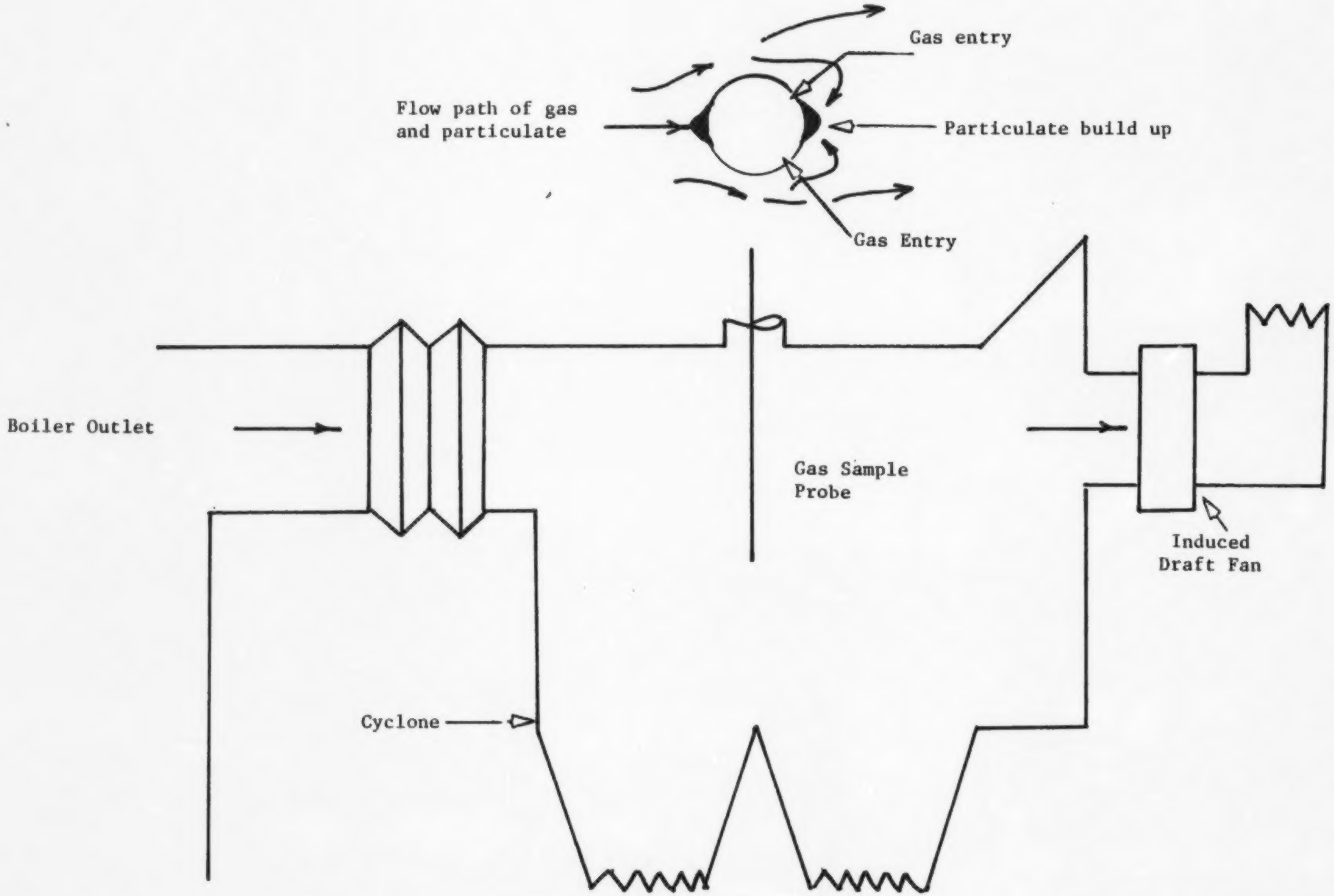
Gas entry
Flow path of gas and particulate
Particulate build up
Gas Entry
Boiler Outlet
Gas Sample Probe
Induced Draft Fan
Cyclone

FIGURE III-34. LOCATION AND ORIENTATION OF GAS SAMPLE PROBE

rake were located and sized to draw an equal amount of gas through each hole. The holes were also located to minimize interference by particulates, as seen in Figure III-34.

A heated filter maintained at approximately 150 C to avoid water condensation was located immediately downstream of the sample probe to remove particulates. The gas was passed through a wet ice trap to remove excessive moisture and then transported to the on-line monitors through a 6-mm diameter teflon line. An additional fiber glass filter was placed in the sample line just before the sample pump to remove any extraneous material that may have passed through the particulate/condensate trap.

Relatively high sample rates were maintained to insure fast response and short residence times.

All instruments were checked for operational condition before and after use by using nitrogen for a zero response gas and an appropriate certified span gas to set the gain for each of the individual monitors.

EXPERIMENTAL RESULTS

Checkout Runs

Prior to the demonstration test, the fuel pellets were fired for 10 hours to determine the necessary stoker adjustments and to establish a range of operating conditions.

The limestone/coal pellets were fired without any adjustment to the stoker mechanism, previously set for a low-sulfur Ohio stoker coal. The stoker feed mechanism distributed the pellets uniformly over the grate. This was unexpected since the pellets were all approximately the same size. It was observed, however, that approximately 50 percent of the pellets broke randomly into smaller pieces providing a reasonably good size distribution.

a. Phase II/Phase III Pellet Comparison. Pellets fired in the Phase III study were significantly superior to those fired in the Phase II steamplant runs. They burned more readily at lower excess air rates, provided improved boiler response (shallower bed), ignited more readily, and generated lower CO and smoke levels. These improvements are attributed to the fact that the Phase III fuel had a higher heating value, contained an organic (rather than inorganic binder), contained less ash, and exhibited superior mechanical strength. However, sulfur retention was not as high with the Phase III pellets.

b. Stoker Coal/Phase III Pellet Comparison. Phase III pellets appeared to burn equally as well as the low-sulfur Ohio coal that is normally fired in the Battelle steamplant boiler. The boiler appeared to be as responsive to the load and could be operated at comparable excess air levels. Table III-30 compares these two fuels. Emissions are corrected to 3 percent O_2.

c. Effect of Operating Parameters on Sulfur Retention. Because it was not the intent of the checkout runs to characterize the emissions for a variety of boiler operating conditions nor was it possible with the limited supply of fuel pellets, only limited amounts of data were collected in the checkout runs.

Sulfur retention was observed to decrease for increasing load as indicated below for relatively constant excess air (about 80 percent).

Boiler Load, percent full load	Sulfur Retention, percent	Bed Temperature, C
0.64	50	1315
0.80	48	1405
0.85	47	1425

The bed temperatures were measured with an optical pyrometer sighted on the combustion zone at the top surface of the bed. Sulfur retention varies with bed temperature. However, this observation must be tempered as the combustion conditions were not closely controlled throughout these tests.

TABLE III-30. COMPARISON OF EMISSIONS FROM COMBUSTION OF A LOW SULFUR COAL AND LIMESTONE/COAL PELLET

Coal Type	Smoke Opacity, percent	CO	NO	Fuel N Converted, percent	SO_2	Fuel S Emitted, percent
Low-S coal	10	70	480	18	540	90
Fuel pellet	20	400	310	20	1800	45

and the observed temperature measurement may not be a good indication of the actual bed temperature.

At a low-load condition, the excess O_2 was varied from 9.5 percent to 16 percent with no significant change in the SO_2 retention (46 to 50 percent). Bed depths were also varied from 76 to 152 mm. SO_2 retention increased somewhat with deeper beds. The increased retention was attributed to the lower bed temperatures measured for the deeper beds.

Demonstration Test

During the limestone/coal fuel pellet demonstration, the pellet feed rate was maintained at approximately 1360 Kg/hr for a boiler load of 80 percent. Tables III-31, III-32, III-33, and III-34 summarize the results of this test.

a. Sulfur Capture. As indicated in Table III-31, sulfur capture was 45 percent during the demonstration test. This sulfur retention is less than that observed for the model spreader and fixed-bed reactor experiments firing pellets of similar formulations. Additionally, as previously discussed, a 75 percent sulfur retention was achieved when firing a cement-bound pellet with a Ca/S ratio of 7 in the steamplant during Phase II. The greater sulfur retention of these other experiments is attributed to the lower bed temperatures, which seldom exceeded 1260 C. The bed temperatures in the Phase III steamplant demonstration were seldom less than 1370 C and ran as high as 1455 C. Additionally, with a pulsating ash discharge stoker, the fuel bed is violently disturbed. Ash can be recirculated back into the hot zone. Thus, if sulfur is retained in the ash at a lower bed temperature, it may be released when the ash is exposed to a higher temperature.

The average SO_2 emission level of 1600 ppm during the Method 5 test was verified by the Method 6 wet-chemistry technique. (Wet chemistry gave an SO_2 emission level of 1590 ppm.) In addition, as indicated in Table III-34, the sulfur balance based on the fuel pellet analysis, the SO_2 emission and the sulfur content in the bottom ash (Table III-33) was complete.

TABLE III-31. EMISSION DATA SUMMARY FOR FUEL PELLET DEMONSTRATION

Load, %	O_2, %	CO_2, %	CO, %	NO, %	SO_2, %	Smoke Opacity, %	CO at 3% O_2, ppm	NO at 3% O_2, ppm		Fuel N Converted, %	SO_2 at 3% O_2, ppm		Fuel S Emitted, %	Particulates, ng/J
								Computed	Measured		Computed	Measured		
80	8.4	10.5	300	310	1600	20	420	2250	440	20	4100	2250	55	258

TABLE III-32. ANALYSIS OF METHOD 5 FILTER CATCH (Weight Percent)

Ash	C	Ca	CO_3	Fe	Total S
81	19	11	—	4	54

TABLE III-33. ANALYSIS OF GRATE DISCHARGE (Weight Percent)

Ash	C	Ca	CO_3	Fe	Total S
97.7	1.8	36.5	0.7	5.8	3.9

TABLE III-34. SULFUR BALANCE

Computed Fuel S In, $lb/10^6$ Btu	Emitted as SO_2, $lb/10^6$ Btu	Sulfur Retained in Bed Ash as SO_2, $lb/10^6$ Btu
7.4 (3182 ng/J)	4.1 (1763 ng/J)	3.3 (1419 ng/J)

b. CO Levels. CO levels from pellet firing were relatively high compared to those from the firing of conventional stoker coals which are usually <100 ppm. These higher CO levels may be related to the nature of the fuel bed and to the fact that the overfire air flow rate was decreased during the pellet tests. Higher CO levels have been observed in other pellet firings. Because of the compactness of the pellet and the limited access of air into it, the capture process first involves the formation of calcium sulfide via

$$2CaO + FeS_2 \xrightarrow{C} FeO + CO,$$

which can account for part of this increase in CO.

Another possible explanation for the higher CO levels was that the overfire air rate was significantly decreased during pellet firing. In the Battelle boiler the overfire air jets are only 254 mm above the grate. With the increased bed depth from pellet firing, the overfire air jets would have impinged upon the fuel bed if the normal flow rate were maintained. The impingement would increase ash carryover, increasing particulate loadings.

c. Particulate Loading. The Battelle steamplant boiler facility has a mechanical collector to control particulates. Depending on the ash and sulfur content of the coal, the experiments in Phase II showed that particulate loadings varied between 86 and 258 ng/J (0.2 and 0.6 lb/10^6 Btu). Generally, for low S, low ash coals, particulate loadings were less than 129 ng/J (0.3 lb/10^6 Btu).

The particulate loading from the firing of the fuel pellet was 258 ng/J (0.6 lb/10^6 Btu). This loading was not unusually high for a spreader stoker firing a 33-percent-ash coal. This loading should be significantly less for a chain-grate stoker. The smoke opacity was only 20 percent, which would appear low for a particulate loading of 258 ng/J if the fly ash collected was from conventional stoker coal. However, the fly ash from pellet firing is about 50 percent more dense and considerably more coarse than from conventional coals. For equivalent mass loadings, optical density varies inversely with particle size and density. Thus, the apparent discrepancy between smoke opacity and particulate loading is explained partially by laws of optics. As indicated in Table III-32, about 19 percent of the fly ash was carbon, a negligible carbon loss.

d. Grate Discharge. Table III-34 shows that the unburned carbon content in the grate discharge was less than 2 percent. This indicates that the fuel pellets were burned essentially to completion. Analysis indicates that Ca and SO_4 were present and could have combined with water to form a solid mass. Some minor plugging problems were experienced in the ash-disposal system when steam was used to control dusting during transport of the ash.

SUMMARY

The steamplant demonstration indicated the limestone/coal fuel pellet could be fired in an acceptable manner without modifying the facility. During the demonstration, sulfur capture levels that would make the fuel pellet a viable SO_2 control were not achieved. The data suggest that improved SO_2 retention could be realized if bed temperature could be reduced to below 1315 C, perhaps with flue gas recirculation. In addition, a quiescent fuel bed in a stoker boiler may increase the sulfur retention in the bed and should reduce particulate emissions.

SECTION III-6

LIMESTONE/COAL FUEL PELLET PROCESS COST SUMMARY

Table III-35 summarizes an economic analysis of the limestone/coal pellet process. This analysis considers costs related to raw materials, utilities, labor, and capital, including profit, interest, and income tax. It indicates a process cost of approximately \$15.40/Mg (\$14/ton) of pellets in addition to the cost of the high sulfur coal. Increased costs of firing the boiler are not considered. As an example of such costs, because of the high ash content of the pellet, ash handling and disposal costs would be higher than for the low-ash conventional coals.

The estimated cost of \$15.40/Mg of pellets above the price of the raw coal is based on the best available data. The cost may vary depending on the type of system used and whether the process may be integrated into a physical coal cleaning preparation plant. This cost is for a product with a heating value of 18.6 KJ/g (8000 Btu/lb) and thus adds about \$0.95 per 10^9 joules (\$1 per million Btu) for SO_2 control. It indicates that the limestone/coal pellet is cost competitive with other control strategies.

BASIC ASSUMPTIONS

The following assumptions were used in the analysis.

- Mine-mouth operation
- Limestone and coal ground to 60 to 100 mesh
- Pellet composition:

  65 percent high sulfur coal
  32 percent limestone
  2 percent pregelenized cornstarch
  1 percent latex emulsion

- Plant capacity of 54.4 Mg/hr (60 tons/hr).

TABLE III-35. SUMMARY OF LIMESTONE/COAL PELLETIZING PROCESS COSTS

Basis: 60 tons per hour product with 65 percent coal, 32 percent limestone, 3 percent binder
23 hours per day, 330 days per year
1380 tons per day, 455,400 tons per year of product

Fixed plant investment	$2,790,000
Working capital	80,000
Interest during construction	250,000
	$3,120,000

Item	Annual Costs, Dollar	Per Ton Product, Dollars
Raw Materials		
Limestone 18 tons/hr, 136,620 tons/year at $8/ton delivered	$1,092,960	2.4
Pregelatin cornstarch, 9100 tons/year at $20/ton delivered	1,138,500	3.0
Latex emulsion, 1.2 ton/hr, 9100 ton/year at $150/ton delivered		
Utilities		
Process water 12 tons/hr (48 gpm) 21.9 MM gallon/year at $0.2/M gal	4,400	0.01
Fuel oil 32 MMBtu/hr, 243 trillion Btu/yr of $3/MMBtu	728,600	1.60
Power 75 percent of 1917 KW or 1440 KW at $0.035/KW-hr	382,500	0.84
Diesel fuel 5 gph, 37,950 gallon/year at $0.80/gal	22,800	0.06
Labor Related		
Direct labor -- 7 operators @ $8/hr plus 25 percent payroll burden ($10/hr total); staffed 365 days/yr	613,200	1.30
Supervision -- 15 percent of direct labor	91,980	.20
Overhead — 50 percent of direct labor and supervision	306,500	.70
Capital Related		
Maintenance — 6 percent of fixed plant investment	167,400	0.37
Special pelletizer maintenance at $0.30/ton plus $0.55/ton die and rollers	387,100	0.85
Front-end loader maintenance at $0.22/hr per machine	3,300	0.01
Taxes and insurance -- 1.5 percent of fixed plant investment	41,850	0.09
Depreciation -- 11 year, straight line on fixed plant investment	250,000	0.56
Profit, interest, income tax -- 30 percent of total employed capital	936,000	2.05
TOTAL	$6,167,100	~$14.00

The pellet composition was based on the results of the pellet development effort.

PROCESS FLOWSHEET

The economic analysis was based on the process flowsheet presented in Figure III-35. In this process

- Coal is taken from a pile instead of directly from an existing mine operation conveyor
- Limestone is delivered to a pile by truck
- Portland cement is delivered directly to a bin from a truck by pneumatic feeding system suggested by Jeffrey Manufacturing Company
- Relatively long inclined conveyors from the coal and limestone piles are assumed. Costs would be about 35 percent less for horizontal conveyors combined with bucket elevators.
- A paddle-type mixer, as suggested by California Pellet Mill, is used
- California Pellet Mill pelletizers and dryers are costed.

A California Pellet Mill was used in the analysis since cost information was available. However, pellets can be produced by an extruder at perhaps a lower cost. Specifications for processing equipment are given in Table III-36.

SOURCES OF INFORMATION

Information on equipment included in the flowsheet was obtained from the following sources:

Front-end loaders — Caterpillar Tractor
Conveyors/elevators -- Jeffrey Manufacturing
Storage bins -- Butler Manufacturing
Feeders — Jeffrey Manufacturing
Solids mixer — Rapids Machinery
Pelletizers -- California Pellet Mill
Coolers — California Pellet Mill

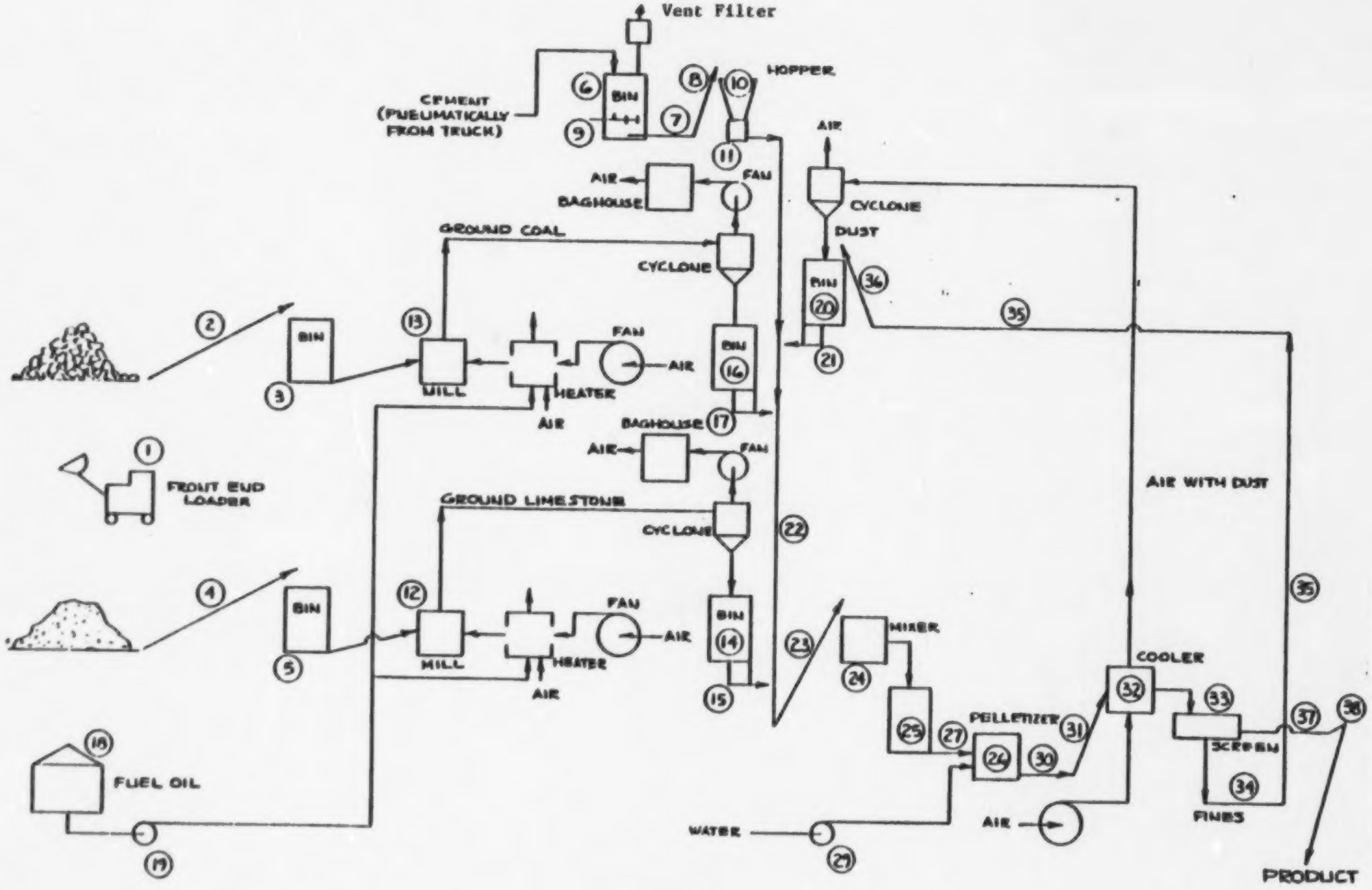
Vent Filter
CEMENT (PNEUMATICALLY FROM TRUCK)
BIN
6
9
7
8
10
HOPPER
11
AIR
AIR
FAN
BAGHOUSE
CYCLONE
DUST
GROUND COAL
CYCLONE
2
BIN
13
FAN
AIR
BIN
16
BIN
20
36
35
21
3
MILL
HEATER
AIR
BAGHOUSE
17
1
AIR
FAN
FRONT END LOADER
AIR WITH DUST
GROUND LIMESTONE
CYCLONE
22
4
BIN
12
FAN
AIR
BIN
14
35
23
MIXER
24
5
MILL
HEATER
AIR
15
25
COOLER
32
33
27
PELLETIZER
31
26
30
37
38
18
FUEL OIL
SCREEN
34
WATER
29
AIR
FINES
19
PRODUCT

FIGURE III-35. COAL/LIMESTONE/CEMENT PELLETIZING PROCESS FLOWSHEET

TABLE III-36. COAL/LIMESTONE/CEMENT PELLETIZING PROCESS

Capacity: 60 tons per hour

Feed Storage and Handling Section

1. Front-end loaders
2. Coal conveyer from pile to bin. 45.7-m long, 9.1-m elevation, 36.3 Mg/hr, with hopper, feeder, tresses, walkway, 3.7 KW motor
3. Coal storage bin, 47.7 m^3 (2.74-m dia x 7.3 m), 1 hour
4. Limestone conveyer from pile to bin. 30.5-m long, 9.1-m elevation, 18.1 Mg/hr, with hopper, feeder, tresses, walkway, 2.2 KW motor
5. Limestone storage bin. 47.7 m^3 (2.74-m dia x 7.3 m)
6. Portland Cement storage bin. 60.9 m^3 (3.7-m dia x 4.4 m) with bin vent filter and auxiliaries
7. Cement screw auger from bin; 4.6 m, 228.6 m screw, with motor 1.1 KW, 316 SS, 5.4 Mg/hr
8. Cement elevator to feed hopper; 6.1-m elevation, 5.4 Mg/hr, 1.5 KW
9. Cement bin agitator with 1.5 KW motor
10. Cement feed hopper; 5.7 m^3
11. Cement feeder; 5.4 Mg/hr

Coal and Limestone Grinding Section

12. Limestone air-swept mill with drying from 12 to 1%, moisture, 18.1 Mg/hr (for Hardgrove 70), with hot air heater, cyclone, valve, baghouse, motors, conveyers to crusher
13. Coal air-swept mill with drying from 12 to 1% moisture, 36.3 Mg/hr (for Hardgrove 55) with hot air heater, cyclone, valve, baghouse, motors, feeder conveyers to crusher
14. Ground limestone storage bin; 47.7 m^3 (2.74-m dia x 7.3 m)
15. Ground limestone feeder to mixer, 18.1 Mg/hr
16. Ground coal storage bin; 47.7 m^3 (2.74-m dia x 7.3 m)
17. Ground coal feeder to mixer, 36.3 Mg/hr
18. Fuel oil tank, 76,000 liters, 3-1/2 days
19. Fuel oil pump, 19 lpm

Mixer Section

20. Recycle fines storage bin, 47.7 m^3 (2.74-m dia x 7.3 m)
21. Recycle fines feeder
22. Feed conveyer to mixer from bins; 61.0-m belt, 12.2-m long, 59.9 Mg/hr
23. Feed elevator to mixer; 14 x 8, 9.1-m elevation, 59.9 Mg/hr
24. Mixer, continuous paddle; 1.06 x 3.65 x 1.37 m, 2.66 m^3 max, with 44.7 KW motor drive
25. Mix surge hopper, 47.7 m^3 (2.74-m dia x 7.3 m)

Pelletizer Section

26. California Pellet Mill, 13.6 Mg/hr, 23 hours/day, with motors, starters, feeders, magnet separator, dies, mixer (15 sec), oil pump
27. Conveyers from mix surge hopper feeder to pelletizers, 3 m, 14.85 Mg/hr
28. Conveyers from mix surge hopper feeder to pelletizers, 6 m, 14.85 Mg/hr
29. Water pump, 190 lpm, 450 KPa

Cooling Section

30. Conveyers from pelletizers to coolers, 3 m, 14.85 Mg/hr
31. Elevators from pelletizers to coolers, 6-m elevation, 29.7 Mg/hr, .3 x .15 m
32. Pellet coolers from 90 C to 40 C, 11.6 m double door with belts, with 980 m^3/m

Screening and Product Discharge

33. Screens, 30 Mg/hr, 10% fines with suspension, motor 1.5 KW, starter
34. Recycle fines pickup conveyer, 7.6 m, 2.7 Mg/hr, .75 K motor
35. Recycle fines conveyer to bin, 18.2 m, 5.4 Mg/hr, 1.1 KW motor
36. Recycle fines elevator to bin, 9.1 elevation, 5.4 Mg/hr, 1.5 KW motor
37. Product pickup conveyer, 7.6 m, 27 Mg/hr, 1.1 KW motor
38. Product conveyer inclined with swivel spout, 12.8-m elevation, 45.8 long, 54 Mg/hr, 6 KW motor, walkway

Screens -- California Pellet Mill (Rotex)
Other -- Guthrie
Factors for installation costs -- Guthrie
Pulverizers -- a paper "Estimated Cost, Beneficiation, and Applications of Ultrafine Coal Pulverization" by Foo, DeCarlo, Jamgochian, and Foster. Presented at 1978 ASME Winter Annual Meeting.

CAPITAL COST ESTIMATES

Capital cost estimates were based on mine-mouth operation for a plant of 60 ton/hr capacity and are summarized in Table III-37.

COMPARISON TO OTHER CONTROL STRATEGIES

The limestone/coal fuel pellet is an attractive control for two major reasons:

(1) No major modification of the stoker boiler facility is required to fire the pellets

(2) The cost of \$15.40/Mg is competitive with other control strategies such as used flue gas scrubbers or low sulfur coals.

The steamplant experiments indicate that neither the stoker boiler facility nor its operation will require major modification to fire fuel pellets. The pellets burn similarly to a lower heating value coal. In contrast, the addition of a flue gas scrubber is a major facility modification and increases system maintenance.

Cost comparisons of the various types of control strategies are difficult to interpret, primarily because of different sets of basic assumptions and different reference points. However, the pellet process costs of \$15.40/Mg or \$0.95 per 10^9 joules (\$1 per million Btu) are competitive with flue gas scrubbers. Foley(III-14) indicated costs of between \$22 and \$33/Mg (\$20 and \$30/ton) of coal for the gas scrubber for small to medium-sized industrial boilers based on 1973 figures.

TABLE III-37. CAPITAL COST ESTIMATES

Process Sections	Installed Cost, Thousands of Dollars
Feed storage and handling	220
Coal and limestone grinding	1,200
Mixer	90
Pelletizer	710
Cooling	220
Screening and product discharge	180
	2,620
Offsites	
Site preparation: at 2% of $2,620,000	52
Industrial buildings: at 2% of $2,620,000	52
Miscellaneous utilities: (substations, wells, etc.) at 1% of $2,620,000	26
Auxiliary facilities: (scales, etc.) at 0.5% of $2,620,000	13
Offsite piping: (water, air, oil) at 1.0% of $2,620,000	26
TOTAL (OFFSITE)	169
TOTAL FIXED PLANT INVESTMENT	2,790

Working Capital	Thousand Dollars
Raw material inventories	Negligible
Product inventories	ditto
Spare equipment and tools at 2% of fixed plant investment	56
Miscellaneous cash	34
TOTAL	80

Interest During Construction	Thousand Dollars
9% of fixed plant investment (1-1/2-year construction period)	250

Operating Requirements

	Connected Power Load, KW	Direct Labor, Men per Shift
Feed storage and handling	10	2
Coal and limestone grinding	898	1
Mixing	52	1
Pelletizing	82	1-1/2
Drying	123	1/2
Screening and product discharge	13	1
TOTAL	1917	7

Mason, et al(III-15) reported flue gas scrubber costs of about \$22/Mg (\$20/ton) for larger industrial boilers based on 1978 figures. Additionally, the cost differential between high- and low-sulfur coals is approaching \$22/Mg and should increase as the availability of low-sulfur coals decreases. Another point to consider is that the limestone/coal pellet concept can be applied to waste coal fines, a readily available and inexpensive source of fuel.

REFERENCES

III-1. Komarek. Chem. Eng., 74 (25): 154, 1967.

III-2. Perry, Robert H. and Cecil H. Chilton. Chemical Engineer's Handbook. 5th Ed., McGraw-Hill.

III-3. Wen, C. Y. Noncatalytic Heterogeneous Solid Fluid Reaction Models. Ind. Eng. Chem., 60 (9): 34, 1968.

III-4. Wen, C. Y. and S. C. Wang. Thermal and Diffusional Effects in Noncatalytic Solid Reactions. Ind. Eng. Chem., 62 (8): 31, 1970.

III-5. Ishida, M. and C. Y. Wen. Comparison of Zone Reaction Model and Unreacted-Core Shrinking Model in Solid-Gas Reactions - I. Isothermal Analysis. Chem. Eng. Sci., 26: 1031, 1971.

III-6. Ishida, M. and C. Y. Wen. Comparison of Zone Reaction Model and Unreacted-Core Shrinking Model in Solid-Gas Reactions - II. Non-Isothermal Analysis. Chem. Eng. Sci., 26: 1043, 1971.

III-7. Ishida, M. and C. Y. Wen. Effectiveness Factors and Instability in Solid-Gas Reactions. Chem. Eng. Sci., 23: 125, 1968.

III-8. Wen, C. Y. and T. Z. Chuang. Entrained-Bed Coal Gasification Modelling. Interim Report. U.S. Department of Energy Report FE-2274-T1, 1978.

III-9. Field, M. A., D. W. Gill, B. B. Morgan, and P.G.W. Hawksley. Combustion of Pulverized Coal. The British Coal Utilization Research Association, Leatherhead, England, 1967.

III-10. Mulcahy, M.F.R. and I. W. Smith. Kinetics of Combustion of Pulverized Fuel: A Review of Theory and Experiment. Rev. Pure and Appl. Chem., 19: 81, 1969.

III-11. Wen, C. Y. and M. Ishida. Reaction Rate of Sulfur Dioxide with Particles Containing Calcium Oxide. Environ. Sci. Technol., 7: 703, 1973.

III-12. Kito, M. and C. Y. Wen. Analysis of SO_2-Limestone Reaction Systems: Part II. Simulation. AIChE Symposium Series No. 147, Vol. 71, 119, 1975.

III-13. Heisler, M. P. Temperature Charts for Inducation and Constant-Temperature Heating. Trans. ASME, 69: 227, 1947.

III-14. Foley, G. J., et al. Control of SO_x Emissions from Industrial Combustion. Proceedings of First Annual AIChE Southwestern Ohio Conference on Energy and the Environment, Oxford, Ohio, October 25-26, 1974.

III-15. Mason, et al. Operating History and Present Status of the General Motors Double Alkali SO_2 Control System. Proceedings Symposium on Flue Gas Desulfurization -- Volume II, Las Vegas, Nevada, March, 1979.